**NTNU – Trondheim**
Norwegian University of
Science and Technology

# Estimation and Computation of Ice-Resistance for Ship Hulls

Ingvill Bryn Thorsen

Marine Technology (2 year)
Submission date: June 2012
Supervisor: Bernt Johan Leira, IMT

Norwegian University of Science and Technology
Department of Marine Technology

Master Thesis, Spring 2012

for

Stud. Techn. Ingvill Bryn Thorsen

# Estimation and Computation of Ice-Resistance for Ship Hulls

## *Estimering og beregning av is-motstand for skips skrog*

The presence of sea ice is a main factor in relation to hindering of operations in Arctic areas. Sea ice is a complex material and induces high pressures when being in contact with ships or structures. To understand how the ice force is developed and is acting, the ice physics and ice mechanics have to be studied.

Different models for estimation of ice-induced resistance on ship hulls are given in the literature. These models are to be reviewed in the present thesis, and comparison between the different models is to be made. Furthermore, the modeling of local ice-structure interaction is to be considered.

As the result of a project which was managed by DnV, *Ice Load and Monitoring (*ILM), which was supported by the Norwegian Research Council, a large amount of measurements from the coast-guard vessel Svalbard was obtained.

The purpose of the present work is to consider how these measurements can be applied for the purpose of estimating ice resistance. This will be of use e.g. in order to estimate the additional transportation costs associated with operation in arctic as compared to non-arctic areas.

The following subjects are to be examined:

1. Different types of sea ice and their mechanical/physical properties are to be described. Furthermore, models for calculation of ice-induced resistance as well as local loading on ship hulls are to be reviewed and summarized. The various parameters which enter the different models are to be listed and their effects on the ship resistance are to be studied.

2. The monitoring system and the relevant parameters with respect to ice-loading are to be described for the coast-guard vessel Svalbard. The procedure which is applied for computation of the ice-induced resistance based on the measurements is to be described.

3. A systematic comparison between estimated and calculated ice resistance is to be made for a selected set of time intervals with relatively stationary conditions. A statistical analysis of the ratio between the estimated and calculated resistance is to be included as part of this comparison.

The work scope may prove to be larger than initially anticipated. Subject to approval from the supervisor, topics may be deleted from the list above or reduced in extent.

In the thesis the candidate shall present his personal contribution to the resolution of problems within the scope of the thesis work.

Theories and conclusions should be based on mathematical derivations and/or logic reasoning identifying the various steps in the deduction.

The candidate should utilise the existing possibilities for obtaining relevant literature.

The thesis should be organised in a rational manner to give a clear exposition of results, assessments, and conclusions. The text should be brief and to the point, with a clear language. Telegraphic language should be avoided.

The thesis shall contain the following elements: A text defining the scope, preface, list of contents, summary, main body of thesis, conclusions with recommendations for further work, list of symbols and acronyms, references and (optional) appendices. All figures, tables and equations shall be numbered.

The supervisor may require that the candidate, in an early stage of the work, presents a written plan for the completion of the work. The plan should include a budget for the use of computer and laboratory resources which will be charged to the department. Overruns shall be reported to the supervisor.

The original contribution of the candidate and material taken from other sources shall be clearly defined. Work from other sources shall be properly referenced using an acknowledged referencing system.

The thesis shall be submitted in 3 copies:

- Signed by the candidate
- The text defining the scope included
- In bound volume(s)

- Drawings and/or computer prints which cannot be bound should be organised in a separate folder.

Supervisor: Professor Bernt J. Leira

Deadline: June 6th 2012

Trondheim, January 16th, 2012

Bernt J. Leira

## Preface

This is my Master thesis in Marine technology written in spring 2012 at NTNU. The thesis has been challenging and interesting. I have learned a lot about the behaviour of ice, ice resistance and statistics. In addition my skills in MATLAB have been significantly improved.

I will like to thank my supervisor, Professor Bernt J. Leira, who has formulated my master thesis and given me guidance along the way. I will also like to thank PhD student Abdillah Suyuthi that has given me valuable assistance. Information about Keinonen's method was obtained with good help from my professor in the course "Ice 2"Kaj Riska and Janne Valkonnen from DNV. The MTS librarians have also been to great help finding relevant literature.

Trondheim, June 10, 2012

Ingvill Bryn Thorsen

## Abstract

The oil price continues to increase while oil companies search for oil in new areas. There is assumed that 25% of the world's hydrocarbons are located in the arctic area. Operating in these areas will be a huge challenge due to extreme low temperatures and ice condition

Today one can predict with good accuracy how a ship will manage in different ice condition. Research on ship operating in ice the last decades has resulted in many different formulas for predicting ice resistance on a ship hull. Analytical and numerical methods are developed to estimate the resistance working on the ship hull under different ice conditions. Model test will still be the most accurate prediction, but the other methods may give you some guidelines on what to expect.

This thesis contain a theoretically study of ice physics and mechanics. The formation and development of sea ice has been reviewed.

The Ice Load Monitoring system tested on the Norwegian coast guard vessel KV Svalbard is described. Three different analytical ice resistance calculation methods are described. The three methods are Lindqvist (1989), Keinonen et al. (1996) and Riska et al. (1997).

Data obtained from the Ice Load Monitoring system are used to estimate the full scale ice resistance on KV Svalbard. The three analytical methods are calculated with KV Svalbard as a reference ship to be able to compare with the full scale measurements. MATLAB is used for the calculations.

# Table of Contents

# List of Figures

## List of Tables

# Nomenclature

| Symbol | Description/definition |
|---|---|
| B | Breadth |
| D,T | Draught |
| E | Young's modulus |
| $P_{max}$ | Max propulsion power |
| g | Gravity constant |
| $h_{ice}$, $h_i$ | Ice thickness |
| $L_{bow}$ | Length of bow section |
| $L_{par}$ | Length of parallel sides |
| $L_{pp}$ | Length between perpendiculars |
| L | Length of ship |
| $R_{tot}$ | Total resistance |
| $R_c$ | Crushing resistance |
| $R_b$ | Breaking by bending resistance |
| $R_s$ | Submergence resistance |
| $R_{ice}$, $R_i$ | Total ice resistance |
| $R_{ow}$ | Open water resistance |
| v | Velocity |
| $v_{increased}$ | Velocity over 1 m/s (Keinonen's method) |
| ψ | Flare angle (In formulas) |
| $y_n$ | Flare angle (In figure) |
| y | Frame angle |
| α | Waterline entrance angle |
| φ | Stem angle |
| $\varphi_b$ | Buttock angle |
| $\sigma_f$, $\sigma_b$ | Flexural strength |
| v | Poisson`s ratio |
| μ | Friction coefficient |
| $l_w$ | Length of waterline segment |
| $F_v$ | Vertical force acting on the ice |
| $\rho_w$ | Density of saltwater |
| $\rho_i$. $\rho_{ice}$ | Density of ice |
| $F_{si}$ | Size factor |
| $F_{sh}$ | Shape factor |
| $F_i$ | Ice factor |
| $C_s$ | Salinity coefficient (Saline=1, Brackish=0,85 Fresh water=0,75) |
| $C_h$, $C_{hull}$ | Hull condition factor (Inertia coating=1, Bare steel=1,33) |
| t | Temperature |

| Symbol | Description/definition |
|---|---|
| $\Delta k$ | Change of kinetic energy |
| $k_f$ | Final kinetic energy |
| $k_i$ | Initial kinetic energy |
| $w_{net}$ | Work done by the force |
| $w_{thrust}$ | Work done by thrust |
| m, M | Mass of ship |
| $F_{resistance}$ | Resistance force |
| $\sigma$ | Standard deviation |
| $\mu$ | mean value |
| $\kappa_i$ | Thermal conductivity |
| $L_f$ | Latent heat from fusion |
| $T_b$ | Temperature at bottom of ice sheet |
| $T_a$ | Temperature at top of ice sheet |
| $t_{freeze}$ | total freezing time |
| $v_b$ | Brine volume |
| $v_a$ | Relative air volume |
| $d_{EM}$ | Distance from EM system to sea water |
| $d_{Altimeter}$ | Distance from EM system to top of ice sheet |
| Riska ratio | Ratio between resistance estimated from measurements and resistance estimated from Riska's formulation |
| Lindqvist ratio | Ratio between resistance estimated from measurements and resistance estimated from Lindqvist's formulation |
| Keinonen ratio | Ratio between resistance estimated from measurements and resistance estimated from Keinonen's formulation |
| $R_{riska}$ | Resistance estimated from Riska's formulation |
| $R_{Lindqvist}$ | Resistance estimated from Lindqvist's formulation |
| $R_{Keinonen}$ | Resistance estimated from Keinonen's formulation |
| SSE | Sum of squares due to error |
| SSR | Sum of squares at the regression |
| SST | Total sum of squares |
| $R^2$ | Coefficient of determination |
| $w_i$ | Weight of point i |
| $y_i$ | Data value |
| $\hat{y}_i$ | Estimated value |
| $r_{adj}$ | Adjusted residuals |
| $r_i$ | Least squared residuals |
| k | Tuning constant |
| s | Robust variance |
| X | Predictor matrix |

| Symbol | Description/definition |
|---|---|
| u | Adjusted residuals |
| MAD | Median absolute deviation |
| MSE | Mean square error |
| RMSE | Root mean square |
| $P_{riska}$ | Average value of Riska ratio |
| $P_{Lindqvist}$ | Average value of Lindqvist ratio |
| $P_{Keinonen}$ | Average value of Keinonen ratio |
| $Surface_{RiskaRatio}$ | Equation for fitted surface to Riska ratio |
| $Surface_{LindqvistRatio}$ | Equation for fitted surface to Lindqvist ratio |
| $Surface_{KeinonenRatio}$ | Equation for fitted surface to Keinonen ratio |

# 1 Introduction

The Arctic area contains approximately 25% of the world's hydrocarbons. Due to the global warming it is possible to operate in larger parts of the year. There is expected a growth of oil and gas activities in the Arctic region, hence there will be important to require good design of ice going ships. Operations in ice will need good planning and ice strengthen vessels that are able to operate in extreme weather and ice conditions.

Years of experience and testing has led to several different classifications systems for ship in ice that contain information on what kind of requirement different ships have in ice. The forces acting on a ship in ice had been studied in decades and many different methods to predict the ice resistance on a ship hull is presented.

The best way to measure the ice resistance on new ship hull design is still model tests, which has improved a great deal the last years. The downside of this method is the high costs and it is time consuming. In this thesis three different analytical methods will be presented. These are all at best semi empirical and should only be used for guidelines, not replace model tests. The analytical methods are compared with estimated resistance from full scale trials with the coastguard vessel KV Svalbard.

## 1.1 Previous work

A lot of research has been done on the ship-ice interaction, in this thesis there will be presented three analytical methods for calculating ice resistance on ships.

A master thesis written by Torstein Skår (2011), *Ice induced resistance of ship hulls,* has investigated the analytical formulations of Riska et al. and Lindqvist. These methods where compared with estimated resistance from full scale measurements. In this thesis a third analytical method, Keinonens method, will be reviewed and compared with the other two.

Torstein Skår used KV Svalbard as reference ship when calculating the ice resistance. The same ship will be used in this thesis. Some information regarding KV Svalbard and the ice properties has been updated, such as the flexural strength and the waterline entrance angle.

Torstein Skår developed a MATLAB program to select relevant data from the raw material and to do statistical calculations. This MATLAB program have been modified by the author and used in this thesis.

# 2 Ice covered areas

Ice covered areas are located mostly in the northern or southern latitudes but can also be found in low latitude areas like the Caspian Sea, Sea of Azov or the Bohai Bay. Countries that have ice covered harbours parts of the year must be able to run the shipping activity year around. To operate in ice hull strengthen ships specialized for ice impact are needed. In some cases ice breaker support is needed, ice breakers are supposed to handle all ice conditions.

## 2.1 The Arctic Ocean

The definition of the arctic area is many. Some of them are:

- The tree line
- 60 degrees north
- Sea ice cover
- Arctic circle

The Arctic Ocean is to great interest for many countries, approximately 25% of the world oil and gas reservoir are located in this area. This is one of the reasons for the increased activities in the area. As the global warming continues and the amount of ice decreases the season with activities can be extended. In addition there will be possible to use the sea routes along the edges of the Arctic, shown on figure 2-2 which will shorten the time of days in shipping considerably. Because of the difficult environment and the remote location only limited oil and gas areas are explored.

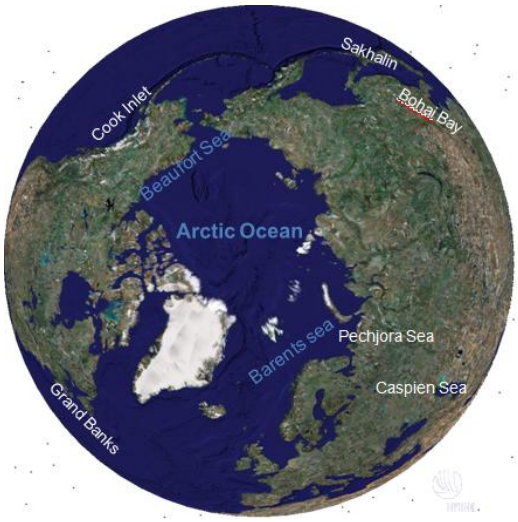


Figure 2-1: Arctic Ocean [3]

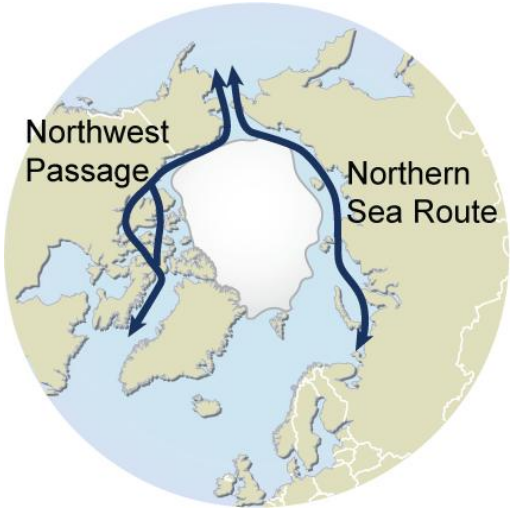


Figure 2-2: Northern sea route and Northwest Passage [1]

## 2.2 The Baltic

In the Baltic year around operations require ice strengthen ships and ice breakers due to seasonal ice cover. The connection to the ocean is narrow which result in little exchange of ocean water between the Baltic and North Sea. Because of this the Baltic is less saline than the ocean. The Baltic is the most active sea area for navigation in ice. The experience from the Baltic is of interest worldwide. The Finnish-Swedish Ice Class rules are developed for the Baltic area and classify different types of ships after their performance in ice. The strength of ship hull and machinery is mostly designed based on experience.

## 2.3 Differences in operating areas

In the design process of an ice going ship there are several functional requirements that needs to be determined. One of the requirements is to define the area where the ship will be operating. The Arctic area contains multiyear ice which is an important parameter to take into account in the design phase. In the Baltic there will be no multiyear ice since the ice will melt away every season. Also the salinity of the Baltic area will be lower due to the low circulation from the North Sea.

# 3 Formation and structure of sea ice

This chapter is based on information from mainly based on [15], [16], [21] and [22]. Sea ice is a complex mixture of solid ice, brine cells, air and solid salt. The properties of sea ice are variable and are dependent on several factors.

## 3.1 The molecular structure of ice

The ice crystals consist of hydrogen bonds between water molecules and have a tetrahedral geometry. The figure below illustrates the atomic structure of ice.

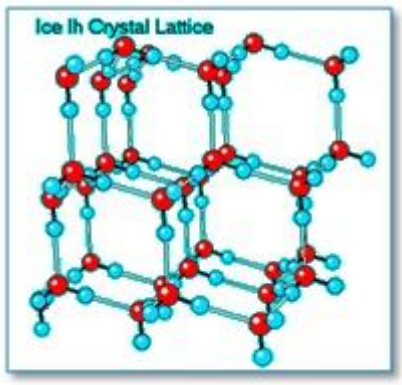


Figure 3-1: Molecular structure of ice [16]

When all possible bonds on the H2O molecular unit have been made you have an ideal perfect crystal of ice which is difficult to deform. However this is not the case in practice. Numerous point-defects exists where a hydrogen bonding is broken and converted to a non-bonded oxygen contact with two proton or no proton at all. The ice structure changes as a function of temperature, salinity, imperfections and pressure. The molecules in ice can be arranged in a number of different crystalline structures. When the ice structure changes due to e.g. temperature, the ice strength is also changed.

## 3.2 Ice formation and growth

Tiny plates of pure ice will form when surface water reaches the freezing point. A newly formed ice sheet will increase in thickness if water on its lower surface freezes. Hence heat must be removed from the water for the thickness to increase. This happened when the air above the ice is colder than the water below the ice. The heat is removed due to conduction through the ice from water to air. In very cold temperatures, thin ice sheet will grow fast in thickness to a certain point. The rate of growth slows down as the ice thickens.

Depending on its compactness, snow cover is an efficient heat insulator. When a layer of soft and fluffy snow is covering the ice sheet the rate of ice growth will drastically slow down. Ice

will form first in shallow water because of the relatively small depth of water that has to be cooled.

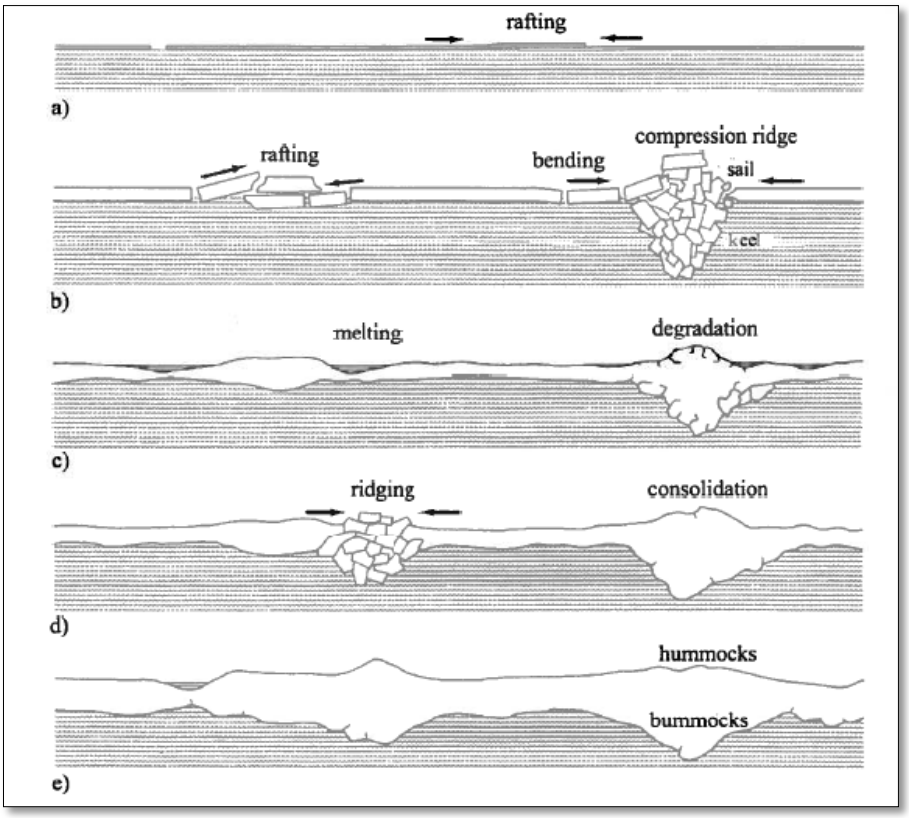


Figure 3-2: Development of an ice cover. [15]

The figure 3-2 above shows stepwise how ice forms from young ice in early winter to first-year ice in mid-winter/early spring. Then there will be melting and degradation of second-year ice in late summer before more ridging and consolidation of second-year ice during its second winter. In the end you have mature multi-year ice. [16]

As the ice move and grows it is created different zones of sea ice. Figure 3-3 illustrates the different ice zones. The ice is mainly classified and categorized depending on the distance from land and the age of the ice. As the figure shows there are two main zones, the fast ice zone and the pack ice zone. The fast ice zone is close to the shore where the ice is stationary and unbroken due to support of the outer island or grounded ridge zone. In steep coastlines without islands, this zone is negligible. In the pack ice zone the ice cover is broken and moving. In the transition zone the coastline effect is felt.

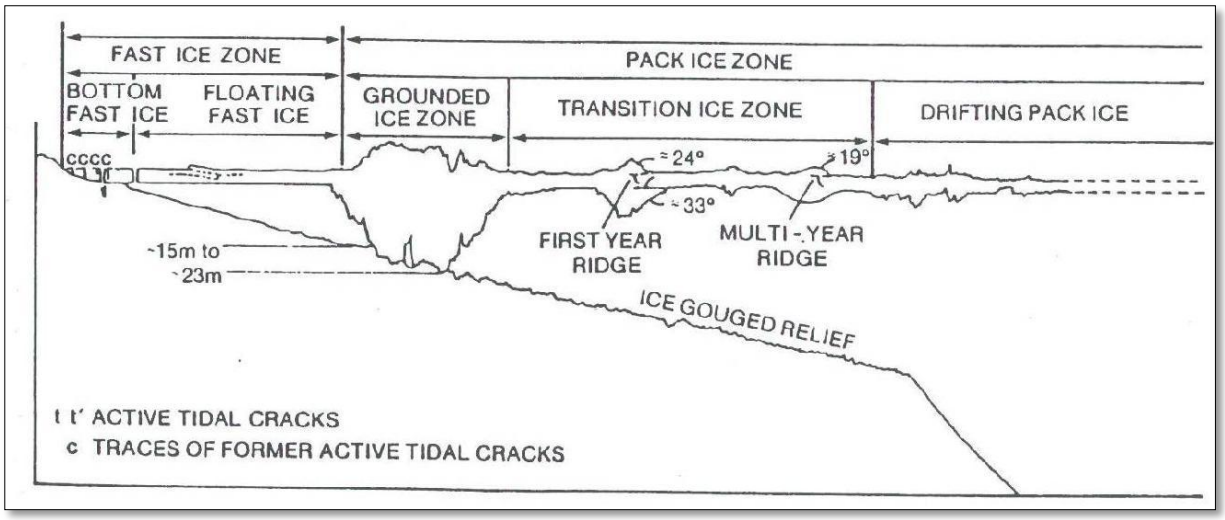


Figure 3-3: The different zones in a sea ice cover [15]

## 3.3 The different types of ice

**New ice:** General term for newly formed ice.

**Young ice:** Ice in transition between new ice and first year ice. The thickness is 10-30 cm.

**First year ice:** Sea ice from more than one year`s growth, developing from young ice. The thickness is typically 30cm-2m. Level when undeformed, but where ridges and hummocks occur, it is rough and sharp.

**Old ice:** Ice that have survived at least one melting season.

**Multi-year ice:** Old ice that has survived at least two melting seasons. Hummocks and ridges are smooth and the ice is almost salt-free.

**Frazil ice:** Consolidation of ice crystals of water, represent the first stage of sea ice growth. Give the sea an oily appearance.

**Nilas ice:** Frazil ice frozen at the surface under calm conditions has a matt surface and is up to 10cm in thickness. Nilas ice will easily bend under action of waves, swells or pressure.

**Grease ice:** Accumulations of frazil ice prevented from freezing together by wave influence. Behaves in a viscous fluid- like manner, and does not form distinct ice floes.

**Pancake ice:** Circular pieces of newly formed ice from 30cm-3m diameter. The rims are raised due to wave interaction.

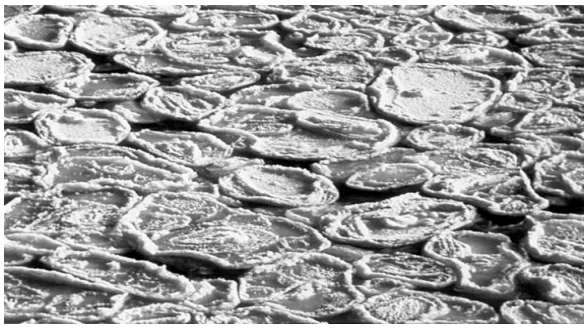

Figure 3-4: Pancake ice [3]

**Hummocks:** A hill of ice that is less salty than pressure ridges. Hummocks are formed by broken ice which has been forced upwards by pressure. They are also much stronger per unit of thickness than ridges. Hummocks melt around zero degrees and are always the last type of sea ice to melt.

**Ice floe:** When a solid ice sheet cracks ice floes are formed. They are flat and have a thickness of more than 1 meter and are typically larger than 20 meter across the floe.

Figure 3-5: Ice Floes [3]

**Rafted ice:** When two floes are pressed together in such a way that one over-ridges the other the layers freeze together and form rated ice. Rafted ice is most common in new and young ice. Rafting plays an important role in increasing the thickness, in early stages of ice development the ice thickness doubles where rafting occurs.
**Level ice:** Sea ice which is not affected by any deformations.

**Brash ice:** Rounded ice pieces having a diameter around 30cm. Normal in ship channels made by ice breakers. The brash ice layer can be quite thick; it is common that a channel with brash ice can be more than 1 m thick.

**Fast ice:** Sea ice which remain fast along the coast, over shoals, or between grounded icebergs. Fast ice may be more than one year old.

**Ridges:** Ridges are categorized by their mode of formation; shear or compression. When two sheets of ice are driven towards each other and form a wall of broken ice, it is called compression ridge. Compression ridges have a keel underwater below sea level and the pile on the surface is called sail as figure 3-7 shows. Shear ridges can form from compression ridges if the relative movement changes or from relative movement of two ice sheet. Shear ridges can be many kilometres long and the walls are nearly vertical consisting of finely pulverized ice.


Figure 3-6: Ridge [12]

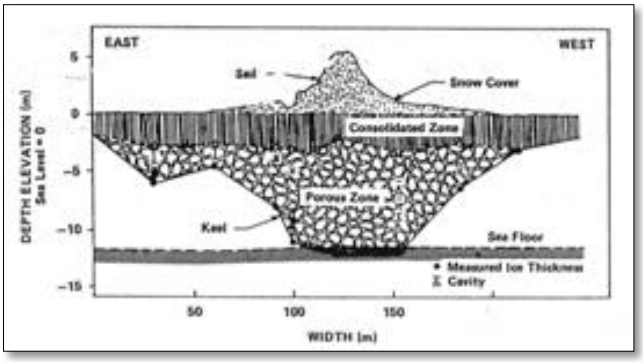


Figure 3-7: Ridge with keel under the surface and sail above. [5]

## 3.4 Physical and mechanical properties of level ice

This section will review some relevant physical and mechanical properties. Most of the information is found from [22]. Physical properties that will be reviewed are ice thickness, salinity, density and brine volume. The mechanical properties reviewed are flexural strength, Poisson's ratio and friction.

### 3.4.1 Ice thickness

The thickness of ice is an important parameter when calculating the ice resistance on a ship. The bearing capacity of ice, the way the ice will fail and the ship speed in ice is highly dependent on the ice thickness. The ice resistance on a ship or ice loads on an offshore structure increases significantly with increasing ice thickness.

From the Stefan's equation the maximum expected thickness in level ice can be calculated assuming $h_i$=0 at t=0:

$$h_i = \sqrt{\frac{2\kappa_i}{\rho_{ice} L_f}[T_b - T_a] t_{freeze}} \qquad \text{Eq. 3-1}$$

where:
$h_i$ = the thickness of the ice
$\kappa_i$ = is the thermal conductivity
$\rho_{ice}$ = the density of ice
$L_f$ = latent heat from fusion
$T_b$ = temperature at bottom of ice sheet
$T_a$ = temperature at top of ice sheet
$t_{freeze}$ = total freezing time

For derivation of this equation see [22]

Due to some simplifications done during the derivation of the equation the ice thickness will be over predicted, to compensate for this a factor less than one is commonly multiplies with the equation.

### 3.4.2 Temperature of ice

Brine volume and ice thickness are dependent on the temperature. In the analytical methods there is only Keinonen´s method that has the temperature as an input parameter. Figure 3-8 below shows how the ice resistance varies over the temperature. With decreasing temperature the ice resistance increase. The method assumes no ice resistance at zero degrees.

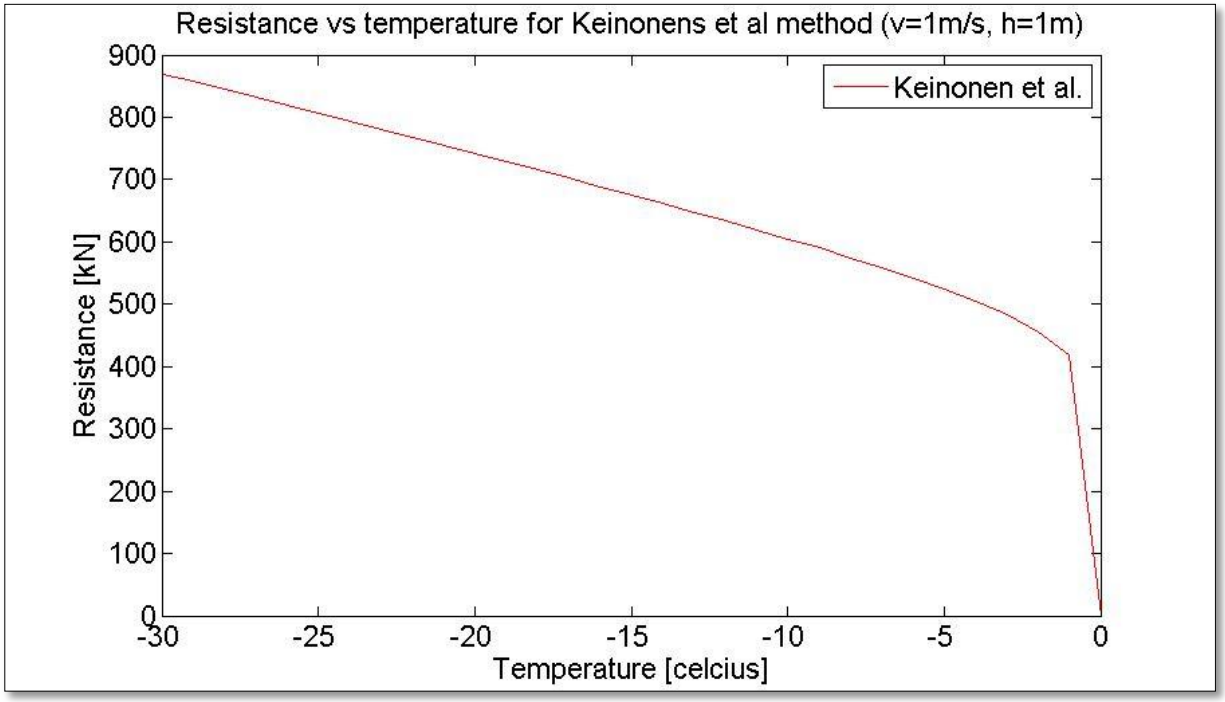


Figure 3-8: Temperature plotted against resistance for Keinonen's method.

### 3.4.3 Salinity and density of ice

Salinity of the ice depends on the age of the ice, density and ice thickness. The figure below describes the density as a function of temperature at different salinities. It shows that when the salinity is increased it gets more temperature dependent. This is due to brine cells in the ice which is sensitive to temperature changes. The resistance of submersion is influenced by the density of ice.

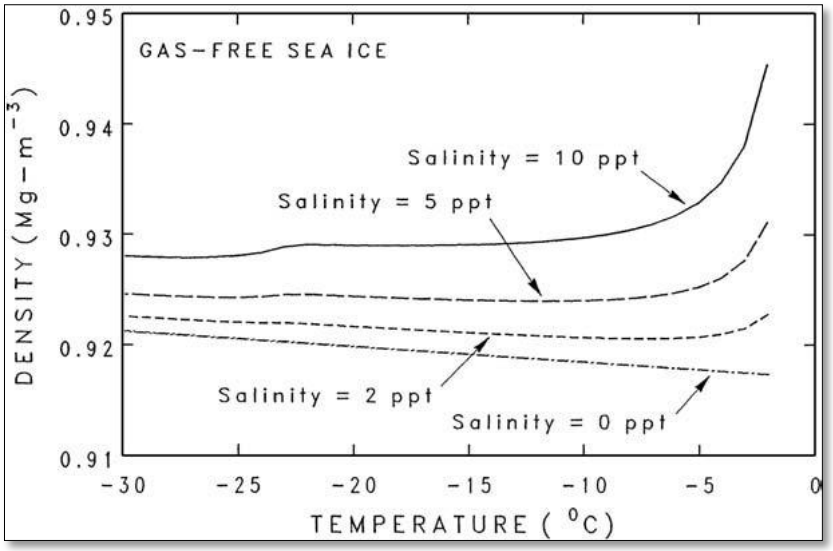


Figure 3-9: Density as a function of temperatures for different salinities.

There is proposed a relationship between the ice thickness and salinity:

$$S_i[ppt] = 4{,}606 + \frac{91{,}603}{h_i[cm]} \qquad \text{Eq. 3-2}$$

Where $S_i$ is the average salinity of the ice sheet in parts per thousand and $h_i$ is the ice thickness. Here it is assumed that there is no variation in salinity through the depth of the ice sheet. For second year ice and multiyear ice the salinity will be lower since the majority of the salt has been drained from the ice.

Ice salinity has usually been expressed in parts per thousand (ppt) or gram of salt per kilo of seawater. Recently this is changed and ice salinity is now measured in practical salinity units (psu). This definition is complex, but more accurate. In this thesis parts per thousand will be used. The salinity varies in most cases with the depth of the ice sheet. Through the winter the salt within the ice will migrate down through the ice.

The exact freezing point of sea water depends on seawater brine contents but is approximately -1,8 degrees. In arctic sea water the salinity varies generally between 30 ppt and 34 ppt during winter months. In the summer months the salinity decreases because of melting and river run-of. The range is then typically 25-30 ppt. The ice has typically a salinity of 2-4 ppt.

### 3.4.4 Friction coefficient

In every problem with an ice-structure interaction the friction is an important component. The friction depends on several parameters. Some of them are ice temperature, surface roughness and relative velocity.

### 3.4.5 Brine volume in ice

When ice crystals are formed the water in their immediate vicinity becomes a little saltier since the salt is not a part of the initial crystals. The saltier water starts to sink and more crystal will form. When the crystals starts to freeze together, small pockets called brine cells will exist among the groups of crystals.
If the ice freezes slowly there will be less brine cells than if the ice freezes fast. In this case, the ice freezes slowly and more of the remaining brine will sink to the water underneath. The content of brine cells in sea ice is measured as brine volume

Brine volume of sea ice is related to the strength of the ice. A lot of investigation has shown that with decreasing brine volume the strength of the ice increases. The brine volume is a function of salinity and temperature of ice. To calculate the brine volume it is common to use Assur`s brine volume table. From the values of this table there are also derived three equations which can be used to calculate the brine volume in a temperature range of -0,5$^{o}$C to -22,9$^{o}$C [4].

$$v_b = S\left(\frac{52.56}{|T|} - 2.28\right) \quad \text{for} \quad -0.5^{o} \leq \mathrm{T} \leq -2.6^{o} \qquad \text{Eq. 3-3}$$

$$v_b = S\left(\frac{45.917}{|T|} + 0.93\right) \quad \text{for} \quad -2.6^{o} \leq \mathrm{T} \leq -8.2^{o} \qquad \text{Eq. 3-4}$$

$$v_b = S\left(\frac{43.795}{|T|} - 1.189\right) \quad \text{for} \quad -8.2^{o} \leq \mathrm{T} \leq -22.9^{o} \qquad \text{Eq. 3-5}$$

Where $v_b$ is the brine volume in parts per thousand, T is the ice temperature and S is the salinity of the ice. A simplified calculation for the whole temperature range may also be used (-0.5$^{o}$ to -22.9$^{o}$ )

$$v_b = S\left(\frac{49.185}{|T|} + 0.532\right) \quad \text{for} \quad -0.5^{o} \leq \mathrm{T} \leq -22.9^{o} \qquad \text{Eq. 3-6}$$

This equation is less accurate but provides a reasonable estimate of the brine volume and will be used in the calculations for this thesis.

**Total porosity of ice**

In some cases there can be useful to know the amount of gas in the ice. The air volume can be important in some cases i.e. when the brine drainage has occurred. This is more relevant for older ice. The total porosity of ice can be expressed as:

$$v_T = v_b + v_a \qquad \text{Eq. 3-7}$$

Where $v_a$ is the relative air volume.

### 3.4.6 Flexural strength

The information on flexural strength is taken from [21]. Flexural strength or bending strength is a measure of how a material resists bending before failure. For an ice going ship the ice usually fails in bending so the flexural strength is important. The parameters that influence the flexural strength have a wide variability which leads to a wide range for the measured flexural strength. Several investigators have measured the flexural strength and the range in fresh water ice is 0.2 MPa to 3.0 MPa and from 0.1 MPa to 1.5 MPa for sea ice.

The interaction mechanism between an ice shelf and a structure is complex. There are many parameters you need to take into account such as friction, buoyancy, drag, non-uniform stress states and inertial effects. Ice is in nature a complex material, it is inhomogeneous, anisotropic and elasto-viscoplastic material which makes the flexural strength hard to measure. Hence, simplified assumptions regarding the ice material are required in order to interpreter the test results. Numerous experiments have been conducted in order to determine the flexural strength. Examples on test methods are:

- Cantilever beam test: Cut the ice to form three sides of a beam, the fourth side is uncut and connected to the ice sheet. An increasing vertical load is applied to the beams free end until it breaks at the root of the beam.

- Simple beam test (three or four point bending test): The beam is completely cut free and loaded at three or four point equidistant such that the centre load is parallel to, but opposed to, the load at the ends of the beam. This test is often performed in laboratories on smaller samples.

In both tests there is assumed that the ice in the beam is perfectly elastic and homogenous.

Flexural strength for first year sea can be expressed as:

$$\sigma_b = 1.76 * e^{-5.88*\sqrt{v_b}} \quad \text{Eq. 3-8}$$

where $v_b$ is the brine volume.

The flexural strength decreases with increasing brine volume as the figure 3-10 below shows.

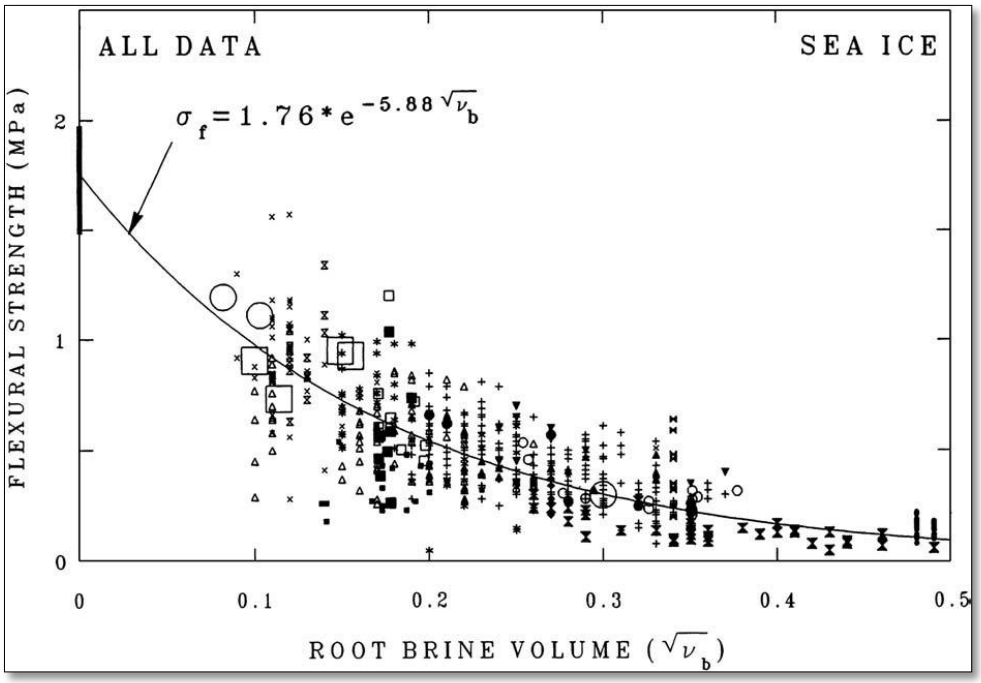


Figure 3-10: Flexural strength as a function of the square root of the brine volume [22]

Figure 3-11 shows how the flexural strength varies with ice thickness and temperature. This graph is calculated from MATLAB by using the equation 3-8. This graph is later used to find the flexural strength in the calculations, this is described in section 3.5.

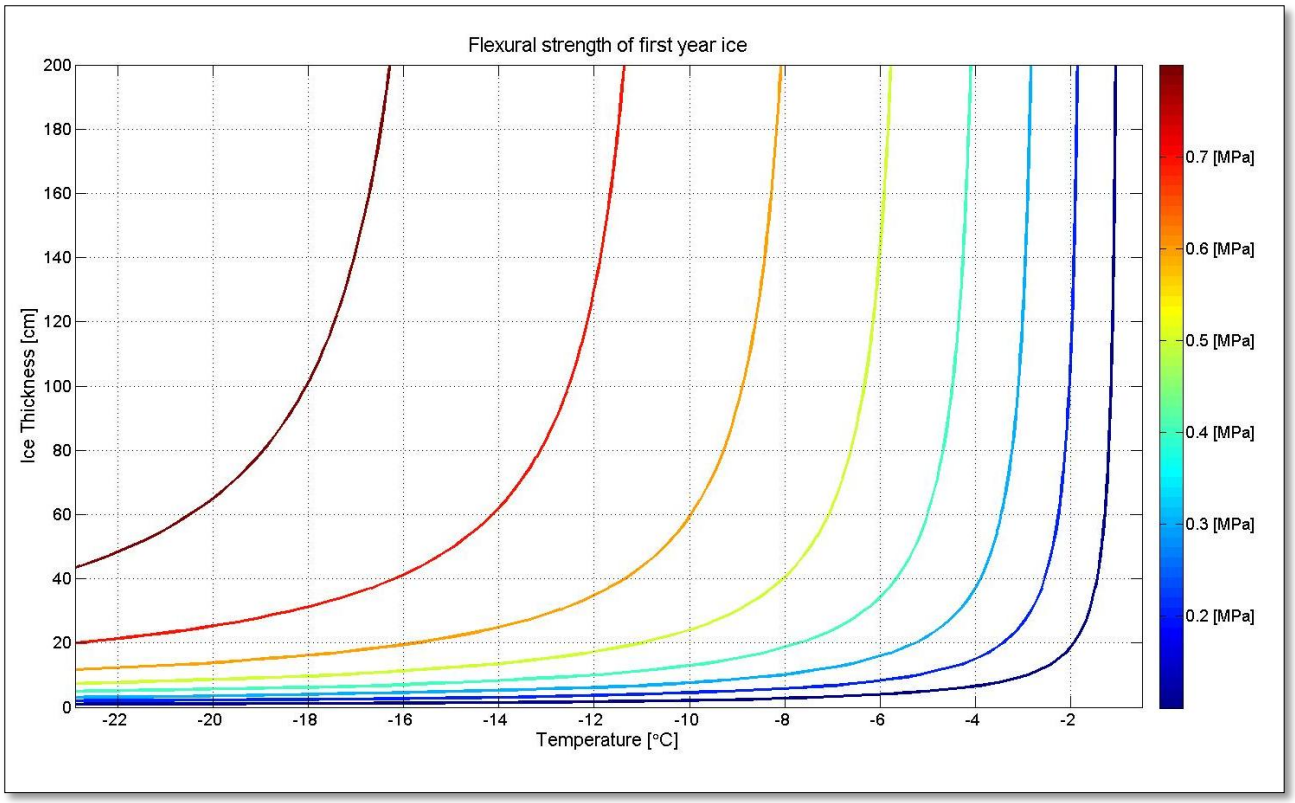


Figure 3-11: Flexural strength plotted against ice thickness and temperature.

### 3.4.7 Compression ice

This property has been extensively studied for sea ice. Ice often fails in compression ice. Observations of both large and small-scale ice failures show that failure in compression often occurs. Some examples are when pressure ridges forms or when sea ice is crushing against an offshore structure. Below is a picture showing a ship in compressive ice which illustrates the huge forces compression ice causes on the ship.

Figure 3-12: Ship in compression ice in the Baltic Sea [24]

### 3.4.8 Elastic modulus for ice

The ratio of the stress to the strain is called the Elastic modulus, E. Several reviews have been done to determine the elastic modulus. Figure 3-13 is a series of test performed by Langleben and Pounder (1963). The elastic modulus increases linearly as a function of the brine volume.

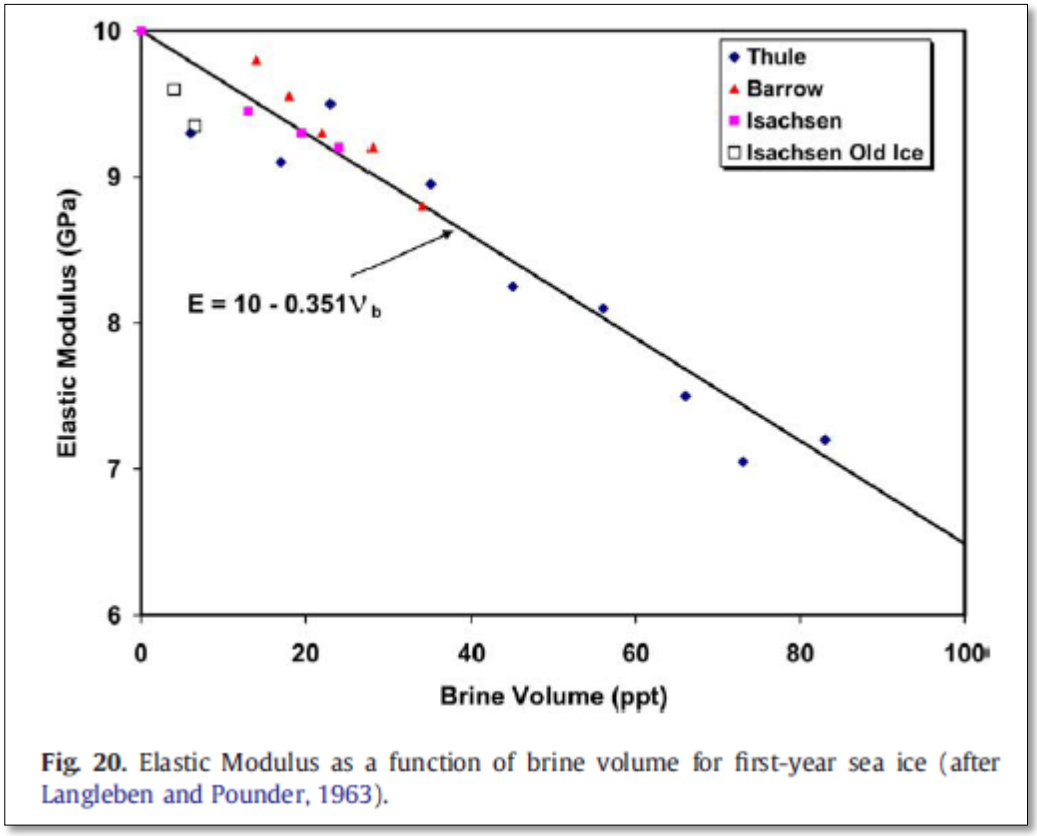


Fig. 20. Elastic Modulus as a function of brine volume for first-year sea ice (after Langleben and Pounder, 1963).

Figure 3-13: Elastic modulus as a function of brine volume for first year ice. [22]

The elastic modulus from this test results can be expressed:

$$E = 10 - 0.0351 * v_b \qquad \text{Eq. 3-9}$$

where $v_b$ is the brine volume.

## 3.5 Input values used for calculations

The input values used in the calculations for this thesis is represented below:

$T = -10^o$

$\sigma_b = 650\ [Mpa]$

$E = 9 * 10^9 [Pa]$

$v = 0.33$

$\rho_{salt\ water} = 1025\left[\frac{kg}{m^3}\right]$

$\rho_{ice} = 900\left[\frac{kg}{m^3}\right]$

Keinonen´s method for calculating the ice resistance is the only analytical method depending on the temperature of ice. From the table in appendix E some of the temperatures during the full scale test with KV Svalbard are given. This temperature varies from 4 degrees to minus 15 degrees Celsius. Here it is done a simplification and a temperature at minus 10 degrees is chosen for the calculations.

From figure 3-11 the flexural strength can be found. Between 1 to 2 meters ice thickness the flexural strength varies from 635 Kpa to 665 Kpa for a temperature at$-10^o$. The average of 650 KPa is used here.

The brine volume is calculated from equation 3-6 and from equation 3-9 the young's modulus for ice is found to be 9*10^9.

# 4 Ice breakers

Icebreakers support other vessels in ice and should be able to operate in all kinds of ice conditions. When bulk carriers, gas carriers or large tanker operate in ice infested water they often need support of an ice breaker to clear the shipping channels. Icebreakers also come to rescue if ships get stuck in ice.

## 4.1 KV Svalbard

KV Svalbard is a Norwegian coast guard vessel that operates in Arctic ice conditions. The vessel has the DNV class notation POLAR-10. This class requires the ship to break ice of 1.0 m level thickness in polar areas. KV Svalbard can also break through thicker ice in short distances. Some of the main data on KV Svalbard is listed in the table below.

Figure 4-1: The Norwegian coast guard vessel KV Svalbard. [11]

| **Main data KV Svalbard** | | | |
|---|---|---|---|
| Ice class | DNV POLAR-10 ICEBREAKER | | |
| Propulsion | 2xAzipod | | |
| Displacement | | 6375 | [ ton ] |
| Beam: | B | 19.1 | [ m ] |
| Draught: | D | 6.5 | [ m ] |
| Length: | L | 103 | [ m ] |
| Length between perpendiculars | Lpp | 89 | [ m ] |
| Max propulsion power | Pmax | 10 | [MW] |
| | | | |
| Stem angle at the waterline | $\varphi$ | 33° | [Degrees] |
| Average buttock angle at waterline in bow region | $\varphi_b$ | 30° | [Degrees] |
| Average flare angle at the waterline in the bow region | $\Psi$ | 32° | [Degrees] |
| Average waterline entrance angle near the stem | $\alpha$ | 59° | [Degrees] |
| Flexural strength of ice | $\sigma_F$ | 400 | [kPa] |
| Dynamic friction coefficient | $\mu$ | 0,15 | [-] |

Table 4-1: Main data for KV Svalbard. [10]

## 4.2 Challenges in ice covered areas:

When operating in ice covered areas there are many challenges in such extreme climate and increased risks. The consequence of an accident may be more serious in the arctic due to remoteness. The equipment on the vessel must tolerate extremely low temperatures and icing. The darkness in the wintertime requires good view from the bridge and good light.

## 4.3 Ice load monitoring system (ILM)

DNV has in cooperation with different partners developed an ice load monitoring system to get better information about the ice conditions along the route and the actual load on the hull. The ILM equipment has been tested as a prototype on the icebreaker KV Svalbard. The ILM system provides real time information about the ice thickness and the ice condition. Information about the system is taken from [8].

The system exists of the following parts:

1. **Fibre optic strain sensors:**

The applied fibre optic strain sensors are installed on girders and stiffeners to measure the shear strain at the frames, i.e. actual ice loads. The sensors have a high sampling rate and sensitivity.

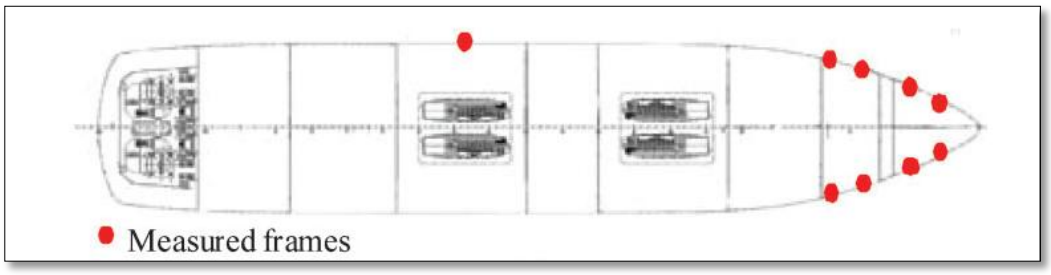


Figure 4-2: Strain sensors [8]

2. **Electromagnetic ice thickness measurements [26]:**

To measure the ice thickness two instruments are used:

1. Electromagnetic (EM) system: This is used to measure the electrical conductivity structure of the underground. The conductivity of ice (0-50 mS/m) is very low compared to the conductivity in sea water (2400-2800 mS/m). The influence of ice will be negligible and a magnetic field will be induced in the sea water by the EM instrument. This EM field is sensed by the EM instrument installed on KV Svalbard. From the strength of the induced EM field, which is directly related to the conductivity and distance to the EM instrument, the distance to the water surface is calculated. Figure 4-3 shows how the system is installed on the vessel.

2. Sonic altimeter or laser: An altimeter measures the distance to the top of the ice sheet and the ice thickness can be calculated.

When these two measurements are obtained the ice thickness will be the difference between them:

$$h_i = d_{EM} - d_{Altimeter} \quad \text{Eq. 4-1}$$

$d_{EM}$=distance from EM system to sea water
$d_{Altimeter}$=distance from EM to top of ice sheet

One weakness in the EM ice thickness measurements is that ridge keels will be underestimated since they consist of both unconsolidated ice and water. Snow cover can also cause a problem since the instrument is unable to distinguish between ice and snow. In undisturbed level ice the measurements have good accuracy, but if disturbance occur the accuracy will drop.

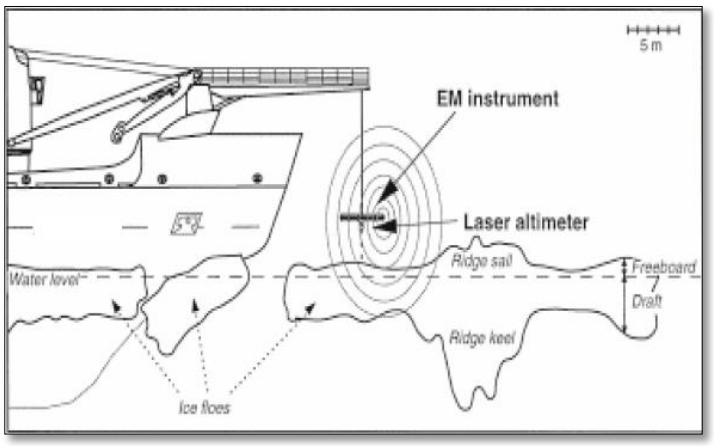


Figure 4-3: Electromagnetic ice thickness measurement equipment. [13]

3. **Meteorological and satellite data**
   The Norwegian Meteorological Institute and satellite images where used to gain information about the ice conditions. This data will be applied to an electronic chart, and will be very useful to find the best possible route.

4. **Information update**
   It is important that the information obtained is continuously updated so other vessels operating along the same route can use the information.

**5. Display on the bridge**

A screen connected to the ILM system is placed on the bridge so the personnel can display the stress level estimated. The instant values and statistical values are available.

# 5 Ice resistance calculation methods

## 5.1 Ice resistance

The total resistance on a ship in ice is assumed to be the sum of open water resistance and ice resistance even if this assumption is inaccurate. When superimposing, the cross coupling between ice and hydrodynamic forces are ignored. Since the open water resistance is very small relative to the ice resistance this does not lead to significant errors. The total resistance can then be expressed as [2]:

$$R_{TOTi} = R_i + R_{ow} \qquad \text{Eq. 5-1}$$

The ice resistance on a ship is in some analytical methods based on regression on full scale and model scale data, where the resistance is assumed linear with ship speed. In this thesis only first year ice is accounted for in the calculations.

Ship performance is usually not based on the worst encountered condition, but rather on an average ice condition. Of all ice performance the basic case is sailing in level ice. A ship hull that has good performance in level ice is usually good in other ice condition as well. In this thesis level ice is therefore used when calculating the ice resistance.

In figure 5-1 the resistance for a ship over a period of time is represented. The resistance is split into different components and the most commonly average forces used in some of the analytical methods are:

- Forces from breaking the ice
- Forces from submerging the broken ice
- Forces from friction along the ship hull
- Hydrodynamic forces

The largest force of these is the breaking force and account for approximately 50 per cent of the resistance in lower speeds. As the picture shows it is only the waterline at the bow that is breaking the ice. Figure 5-2 shows how the Ice force acting on the ship hull varies with time.

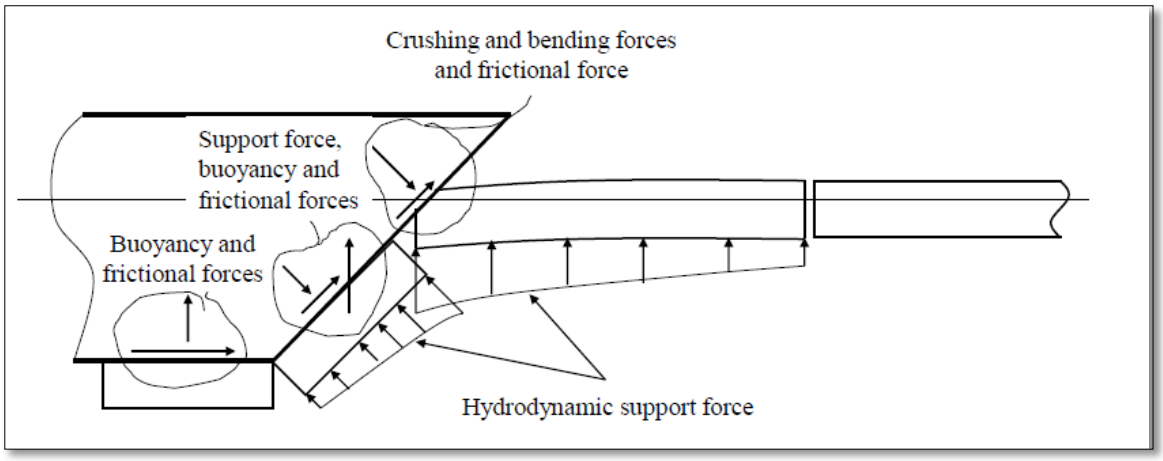


Figure 5-1: Forces acting on ship-ice impact. [15]

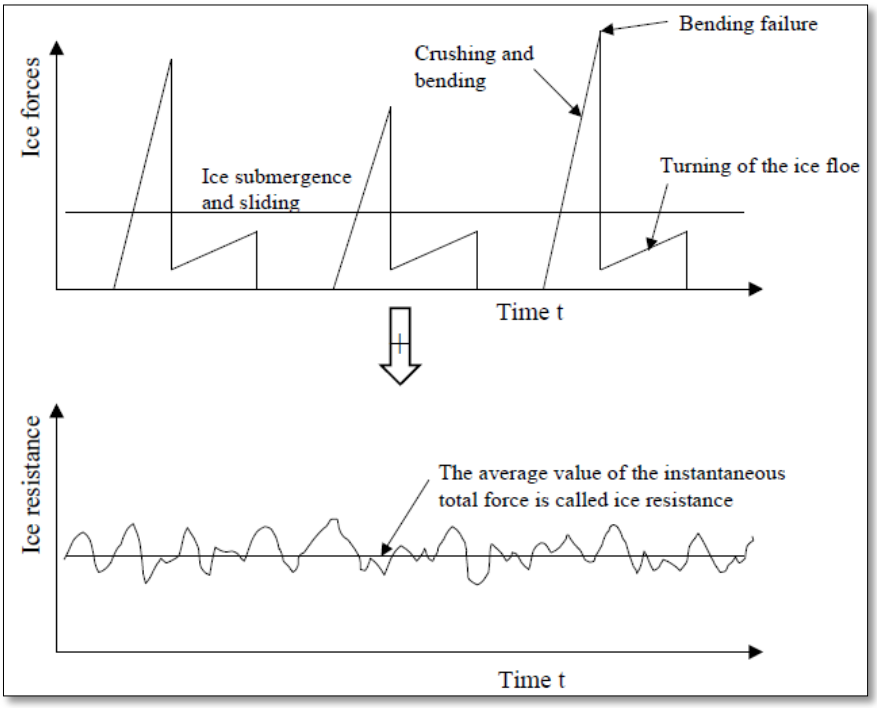


Figure 5-2: Ice forces versus time. [15]

## 5.2 Ship angles

The analytical methods use the definitions of ship hull angles as shown on figure 5-3. The angle between the waterline and bow is the stem angle, $\phi$. The waterline entrance angle, $\alpha$, is the angle between the waterline and longitudinal axis of the ship. The frame angle is $\gamma$, and flare angle is denoted $\gamma_n$ or $\psi$ in formulas. The length of the waterline segment is $l_w$.

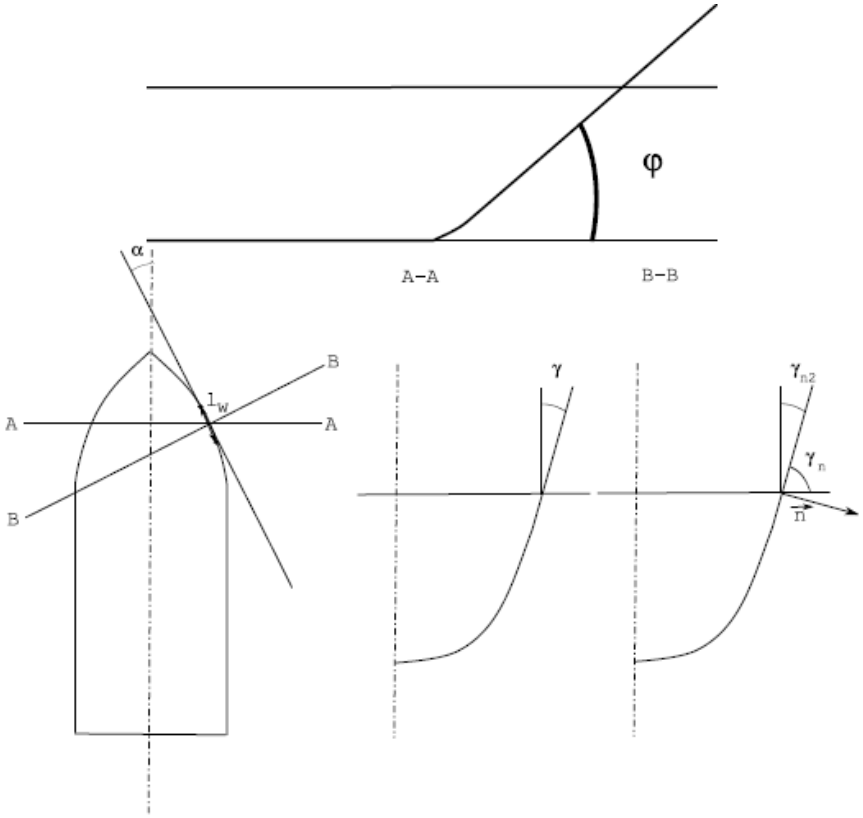


Figure 5-3: Definitions of angles. [11]

## 5.3 Empirical methods

From experience you can estimate the resistance. This method can be good if the new design is close to a design that is already tested. Today many new design is tested to optimize the travelling in ice, so this method is not may not be very good.

## 5.4 Model test

Model testing is another approach to calculate ice resistance. The development of model ice and testing techniques has shown good results in model testing. The drawback in this method is the time-consuming testing and the high costs.

## 5.5 Analytical methods

In this thesis three analytical methods will be presented and compared. Analytical methods are not reliable but the reliability will increase as knowledge of the ice physics advances. The analytical methods can give a good indication on the ship resistance in ice.

### 5.5.1 Lindqvist

The information from this method is taken from [9]. In 1989 Gustav Lindqvist presented a method for calculation of ice resistance. Parameters included in the method are main dimensions, hull form, ice thickness, friction and ice strength. Breaking, submersion and speed dependence are the main resistance component used in this method. To simplify and make the calculations shorter the ice breaker is approximated with flat surface. The method are intended to be a tool in the design process which can help deciding which hull to use and not a substitute for model testing.

**Crushing at the stern**

An icebreaker with a sharp bow crushes the ice. The force is not big enough to cause the ice to break into bending mode at the stem. The reason for that might be that the ice is undamaged at the stem and it is easier to bend the ice when it is already many cracks more aft at the ship. Another reason can be due to the different geometry there is greater bending failure force at the stem than further aft.

It is difficult to measure the crushing force so an estimate is done by rational approximation. The vertical force acting on the ice estimated as:

$$F_v=0.5\cdot\sigma_f\cdot h_i^2 \qquad \text{Eq. 5-2}$$

Where:

$\sigma_f =$ bending strength of the ice
$h_i$=Ice thickness

The crushing resistance can be derived while analysing the crushing process and use geometrical considerations as:

$$R_C=F_v\cdot\frac{\tan\psi+\mu\cdot\frac{\cos\phi}{\cos\psi}}{1-\mu\cdot\frac{\sin\phi}{\cos\psi}} \qquad \text{Eq. 5-3}$$

Where:

$\psi=\arctan\cdot\frac{\tan\phi}{\sin\alpha}$
$\mu$=Friction coefficient
$\phi$=Stem angle
$\alpha$=Waterline entrance angle

**Breaking by bending**

This is the final failure mode of the ice and happens as mentioned at a distance aft of the stem. The ship hits a sharp edge of the ice sheet and crushes the ice until shearing failure occurs. The shearing failure takes place close to the contact point, and the crushing continue with an increasing contact area. When the force transmitted through the contact area is big enough it will cause bending failure. Bending failure can be expressed as:

$$R_B = \frac{27}{64} \cdot \sigma_f \cdot B \cdot \frac{h_{ice}}{\sqrt{\frac{E}{12(1-v^2)g\rho_w}}} \frac{\tan\psi + \mu \cdot \cos\phi}{\cos\psi \sin\alpha} \cdot \left(1 + \frac{1}{\cos\psi}\right) \quad \text{Eq. 5-4}$$

Where:

$h_{ice}$ = Ice thickness
$E$ = Youngs modulus
$v$ = Poissons ratio
$\sigma_f$ = Flexural strength
B=Breadth of ship
$\rho_w$ = Density of sea water

For calculations in detail see [9].

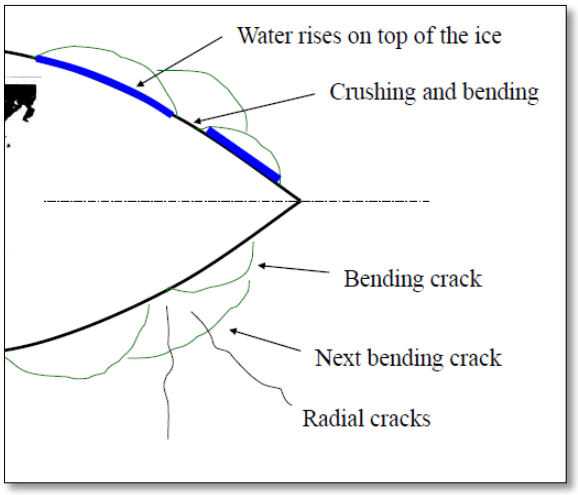


Figure 5-4: Breaking by bending [15]

**Submersion**

The submersion resistance exists of two components, the loss of potential energy and the frictional resistance. In level ice the ship hull will almost be completely covered in ice, since ice is lighter than water it is lifted against the ship hull. The resistance will then be directly

from the normal force acting on the hull and indirectly through friction. When the friction component is calculated, it is made an assumption that the bow is completely covered in ice and the bottom is covered in ice 70% of the ship length. The resistance from the normal force is calculated trough the potential energy and the total submergence resistance become:

$$R_S=(\rho_w-\rho_i)\cdot g\cdot h_{tot}\cdot B\cdot K \qquad \text{Eq. 5-5}$$

$$K=\left\{T\cdot\frac{B+T}{B+2T}+\mu\cdot\left[\left(0{,}7\cdot L-\frac{T}{\tan\phi}-\frac{B}{4\cdot\tan\alpha}\right)+T\cdot\cos\phi\cdot\cos\psi\cdot\sqrt{\frac{1}{\sin^2\phi}+\frac{1}{\tan^2\alpha}}\right]\right\} \qquad \text{Eq. 5-6}$$

Where $\rho_i$ is the density of ice and $h_{tot}$ is the total ice and snow thickness.

Derivations of equation see [9].

**Speed**

This component is more uncertain than the others. From research it seems that the resistance increase almost linearly with the speed. Empirical constants are used to obtain the total ice resistance which can be expressed:

$$R_i = (R_C+R_B)\cdot\left(1+\frac{1{,}4\cdot v}{\sqrt{g\cdot h_i}}\right)+R_S\cdot\left(1+\frac{9{,}4\cdot v}{\sqrt{g\cdot L}}\right) \qquad \text{Eq. 5-7}$$

To make the term dimensionless it is assumed that the breaking resistance is proportional to the speed divided by the square root of ice thickness multiplied by the gravity constant. And in the same way the submersion resistance is proportional to speed divided by the square root of the length of the ship multiplied with the gravity constant.

### 5.5.2 Riska et al.

Riska`s resistance calculations are based on a set of empirical coefficients. These coefficients are derived from many full scale tests of different ships. All test where located in the Baltic area. The main resistance is expressed as:

$$R_T=R_{openwater}+R_{ice} \qquad \text{Eq. 5-8}$$

The open water contribution is assumed to be known. The ice resistance is then expressed as:

$$R_i=C_1+C_2v \qquad \text{Eq. 5-9}$$

Where:

$$C_1=f_1\frac{1}{\frac{2T}{B}+1}BL_{par}h_i+(1+0{,}0021\phi)\cdot(f_2Bh_i^2+f_4BL_{bow}h_i)$$

$$C_2=(1+0{,}063\phi)\cdot\left(g_1\cdot h_i^{1,5}+g_3\cdot B\cdot h_i\right)+g_3\cdot h_i\cdot\left(1+1{,}2\frac{T}{B}\right)\cdot\frac{B^2}{\sqrt{L}}$$

L, B and T are respectively length, breadth and draught. V is vessel speed, $h_i$ is ice thickness and $\phi$ is the stem angle in degrees. $L_{par}$ and $L_{bow}$ are the length of the parallel side section and length of the bow respectively. This formulation assumes a linear relationship between vessel speed and ice thickness, the same as Lindqvist. Riska does not normalize the velocity which Lindqvist does.

The empirical coefficients used in the formulas are given in table 5-1.

| Constants | Value |
|---|---|
| $f_1$ | 0,23 kN/m$^3$ |
| $f_2$ | 4,58 kN/m$^3$ |
| $f_3$ | 1,47 kN/m$^3$ |
| $f_4$ | 0,29 kN/m$^3$ |

| Constants | Value |
|---|---|
| $g_1$ | 18,9 kN/(m/s*m$^{1,5}$) |
| $g_2$ | 0,67 kN/(m/s*m$^{2,0}$) |
| $g_3$ | 1,55 kN/(m/s*m$^{2,5}$) |

Table 5-1: Empirical coefficients

### 5.5.3 Keinonen et al.

Information about this method is taken mainly from [6] and [7]. This method is based on trials of icebreaker performance in ice at 1 m/s. The total icebreaking resistance data at 1m/s where analysed, and from this there were developed resistance models for 1 m/s icebreaking speed for each hull form family of ice breakers. The model where based on ship dimension, ship angles, hull condition, ice and snow thickness, flexural strength, salinity of the water body and surface temperature.

The ice resistance is expressed as:

$$R_i = 0{,}015 \cdot (F_{si} \times F_{sh} \times F_i) \quad \text{Eq. 5-10}$$

$F_{si} = Size\ factor$
$F_{sh} = Shape\ factor$
$F_i = Ice\ factor$

$$F_{si} = C_s \times C_h \times B^{0,7} \times L^{0,2} \times T^{0,1} \quad \text{Eq. 5-11}$$

where L is length of ship perpendicular, B is breadth of ship and T is the draught. $C_s$ is the Salinity coefficient and $C_h$ is the hull condition coefficient.

$\mathrm{C_s} = 1{,}0$ for saline, $0{,}85$ for brackish and $0{,}75$ for fresh water conditions
$\mathrm{C_h} = 1{,}0$ for inertia coating and $1{,}33$ for bare steel

According to Keinonen et al. ship resistance is proportional to a combination of the size factor, shape factor and ice factor. For different hull forms, the shape and ice factors are slightly different. Below are the equations for chined hulls and rounded hulls.

1. Rounded hull:

$$F_{sh}(ro) = (1 + 0{,}0018 \times (90 - \psi)^{1,6}) \times (1 + 0{,}003 \times (\varphi - 5)^{1,5}) \quad \text{Eq. 5-12}$$

$$F_i(ro) = (1 - 0{,}0083 \times (t + 30)) \times \left(0{,}63 + (0{,}00074 \times \sigma_f)\right) \times H^{1,5} \quad \text{Eq. 5-13}$$

2. Chined hull:

$$F_{sh}(ch) = (1 + 0{,}0018 \times (90 - \psi)^{1,4}) \times (1 + 0{,}004 \times (\varphi - 5)^{1,5}) \quad \text{Eq. 5-14}$$

$$F_i(ch) = (1 - 0{,}0083 \times (t + 30)) \times \left(0{,}63 + (0{,}00074 \times \sigma_f)\right) \times H^{1,25} \quad \text{Eq. 5-15}$$

Where t is the air surface or air temperature, $\psi$ is the average flare angle, $\sigma_f$ is the flexural strength of ice and $\varphi$ is the average buttock angle.

**Speed component**

Keinonen et al. also developed practical models for the increase in ice going resistance above 1m/s. The expression for total resistance of an icebreaker is:

$$R(v)_t = R(v)_{ow} + R(1\ m/s)_{ice} + R(>1\ m/s)_{ice} \qquad \text{Eq. 5-16}$$

$R(v)_t =$ total resistance at speed v m/s.
$R(v)_{ow} =$ open water resistance at speed v m/s
$R(1\ m/s)_{ice} =$ Icebreaking resistance at 1 m/s
$R(>1\ m/s)_{ice} =$ The increase in icegoing resistance abowe that at 1 m/s.

For rounded hull form icebreaker the increase in resistance for over 1 m/s speed is expressed as:

$$R(>1\ m/s)_{ice} = 0.009 * \mathrm{V_{increse}}/(\mathrm{g} * \mathrm{L_{WL}})^{0,5} * \mathrm{B}^{1,5} * \mathrm{T}^{0,5} * \mathrm{H_{ice}} * (1 + 0{,}0018 * (90 - \psi)^{1,4}) * (1 + 0{,}003 * (\phi - 5)^{1,5}) * \big(1 - 0{,}0083 * (\mathrm{t} + 30)\big) * \mathrm{C_{hull}} \qquad \text{Eq. 5-17}$$

The resistance increased over 1 m/s is assumed to be dependent on speed increase, ice thickness, vessel dimensions, generic hull form, hull condition and surface temperature. Snow density and buoyancy, which is not known, may also have some influence.

One of the things that also make Keinonen´s method different from the other is that this method is based on trials also outside the Baltic area. The formulas are based on data from different geographical regions which can influence the prediction of resistance.

# 6 Parameter study

The table below shows the different parameters that work as input in the different analytical methods. A parameter study will be done here to analyze the sensitivity of the different input parameters.

| Input parameters: | Symbol: | Keinonen | Riska | Lindqvist |
|---|---|---|---|---|
| Breadth | B | X | X | X |
| Length pp | $L_{pp}$ | X | X | X |
| Draught | T | X | X | X |
| Length par | $L_{par}$ | | X | |
| Length bow | $L_{bow}$ | | X | |
| Flexural strength | $\sigma_b$ | X | | X |
| Ice thickness | h | X | X | X |
| Stem angle | $\varphi$ | | X | X |
| Water entrance angle | $\alpha$ | | | X |
| Buttock angle | $\varphi_b$ | X | | |
| Flare angle | $\Psi$ | X | | X |
| E-modulus | E | | | X |
| Vessel speed | v | X | X | X |
| Gravity constant | g | X | | X |
| Salt water density | $\rho_{salt\ water}$ | | | X |
| Ice density | $\rho_{ice}$ | | | X |
| temperature | t | X | | |
| Poisson ratio | $\nu$ | | | X |
| Elastic modulus ice | E | | | X |
| Friction coefficient | $\mu$ | | | X |
| Salinity coefficient | C_s | X | | |
| Hull condition coefficient | C_h | X | | |
| Empirical constants | $g_1$, $g_2$, $g_3$, $g_4$, $f_1$, $f_2$, $f_3$ | | X | |

Table 6-1: Overview of which parameters that work as input for the different analytical methods.

The sensitivity is described as the ratio between calculated estimate and reference estimate for KV Svalbard. This parameter study will show the influence of different variables, but it is important to remember that when one parameter is change this can also influence other parameters.

In each graph there is a textbox describing the vessel speed and ice thickness for that case. In the report only graphs for ice thickness at 1 meter and vessel speed at 2m/s is illustrated.

However in appendix B graphs with different values of ice thickness and vessel speed are illustrated to see if these two parameters have any influence.

## 6.1 Stem angle

Figure 6-1 shows that both methods depending on the stem angle are sensitive to change, but Lindqvist changes the most. The stem angle on KV Svalbard is 33 degrees, if it is increased 30% the resistance will increase 23% with Lindqvist's method and 10,3 % with Riska's method. In the additional graphs in appendix B it is seen that the graphs behave nearly similar when ice thickness and vessel speed are changed.

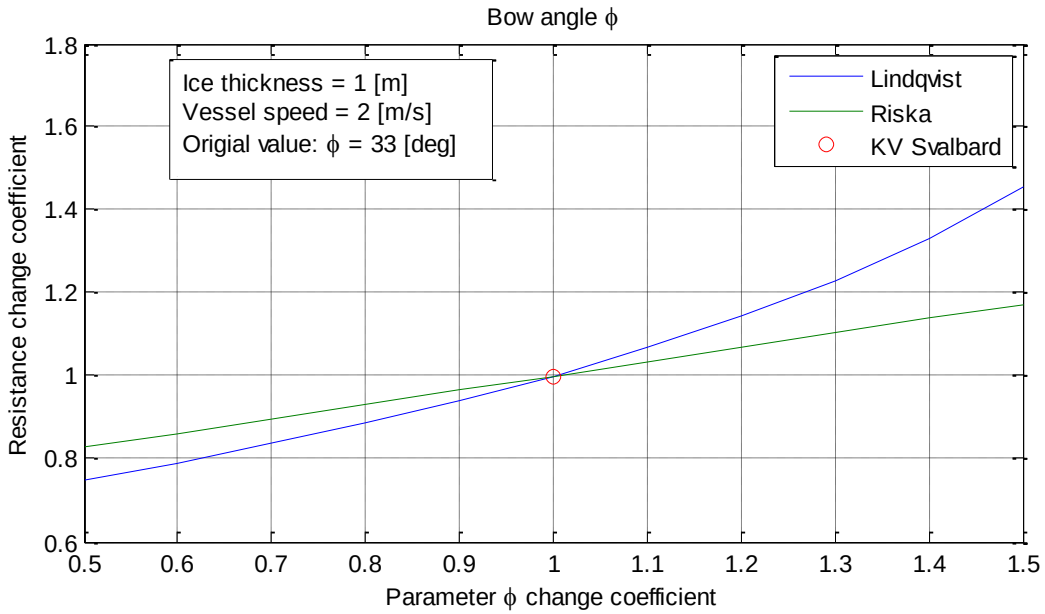


Figure 6-1: Sensitivity of stem angle.

## 6.2 Flexural strength

Riska has included all mechanical properties in the equation constants so flexural strength only work as input parameter for Lindqvist and Keinonen. Figure 6-2 shows that Lindqvist's method influences the resistance, with change in bending strength, much more than Keinonen's method. For example if the bending strength is increased with 30% Lindqvist's method the resistance is increased with 16% while with Keinonen's method the resistance is only increased with 10,5%.

From the plots in the appendix B it is illustrated that the two methods are almost similar for low speed (1m/s) and smaller ice thickness (0,5m). As the speed and ice thickness increase the gap between the two methods increase as well.

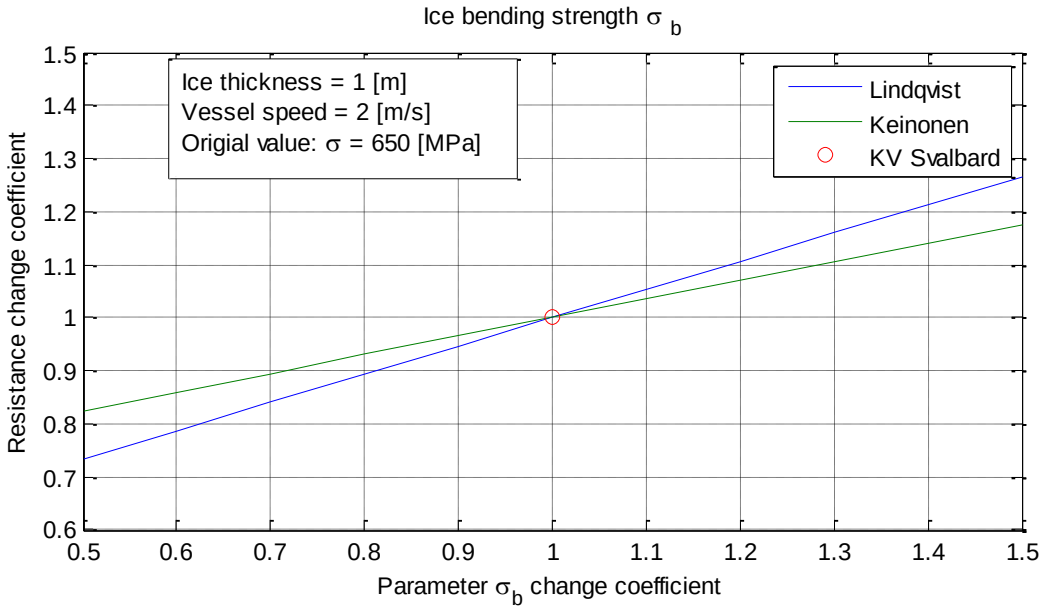


Figure 6-2: Sensitivity of change in flexural strength.

## 6.3 Temperature

Only Keinonen's method is influenced by the temperature. The figure illustrates that the ice resistance increase when the temperature decrease. From figure 6-3it is shown that with a temperature of zero degrees the ice resistance is assumed to be zero.

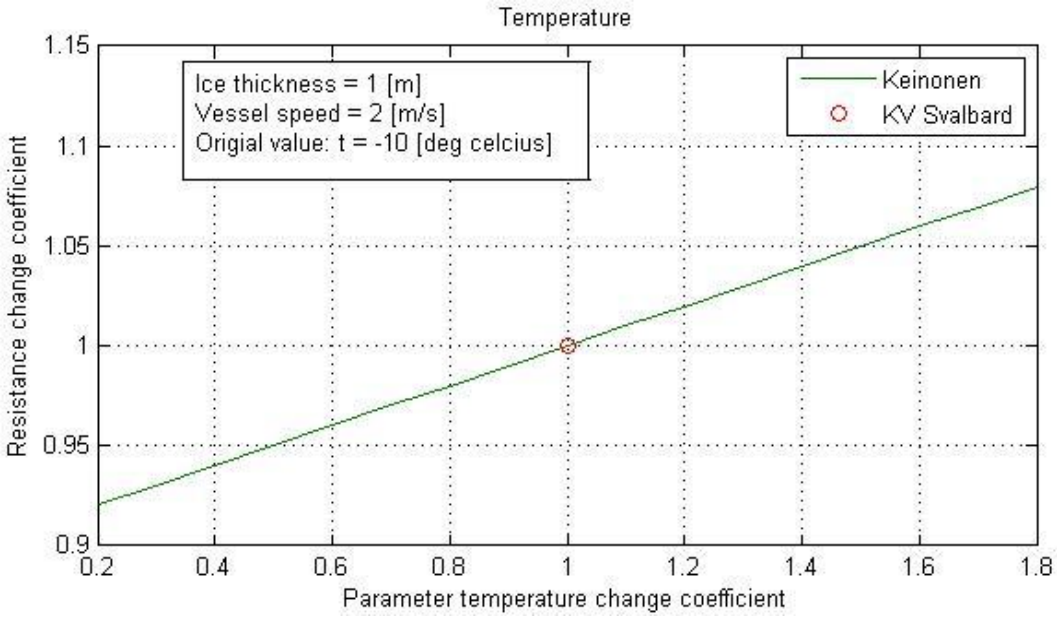


Figure 6-3: Sensitivity of change in temperature.

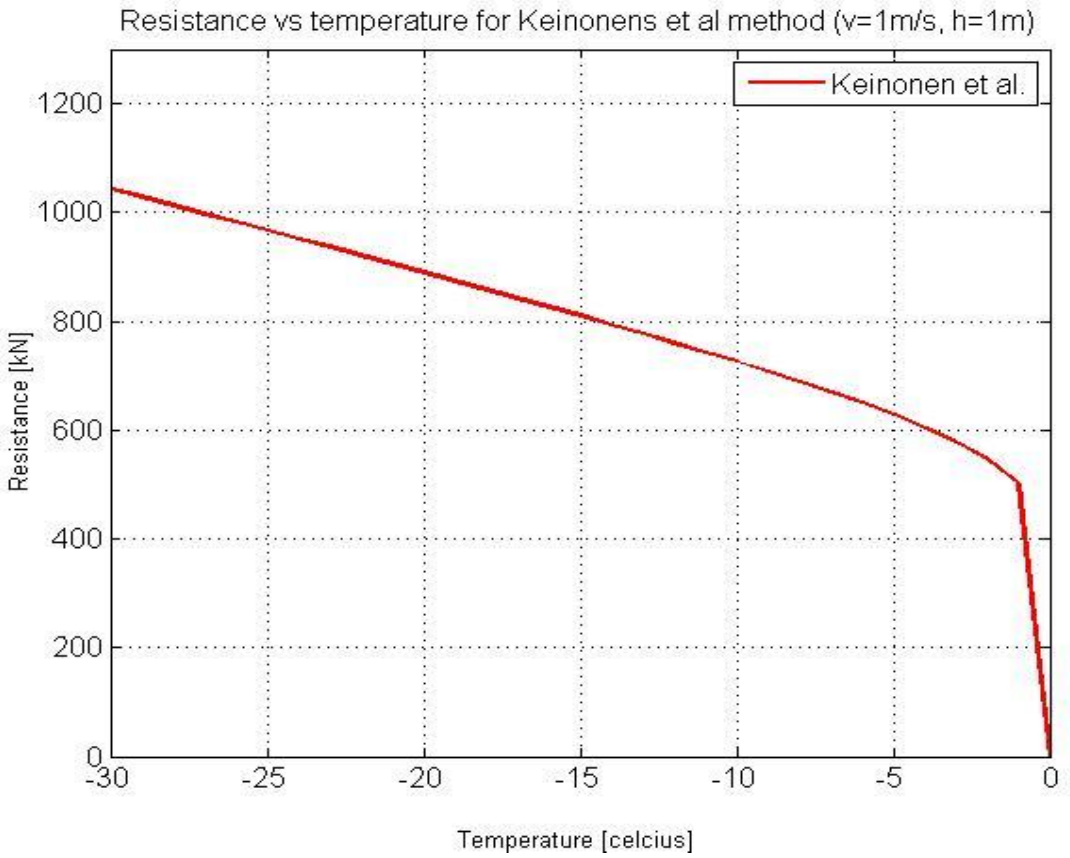


Figure 6-4: Temperature plotted against Resistance for Keinonen's method.

## 6.4 Water entrance angle

Lindqvist's method is dependent on the water entrance angle. As the graph below shows the resistance will almost not change if the angle is increased. It is more sensitive to change in resistance if the water entrance angle is decreased. This is better illustrated on figure 6-5 where it is shown that increasing the water entrance angle reduces the resistance considerably. KV Svalbard's water entrance angle is 59 degrees and should hence be a good design.

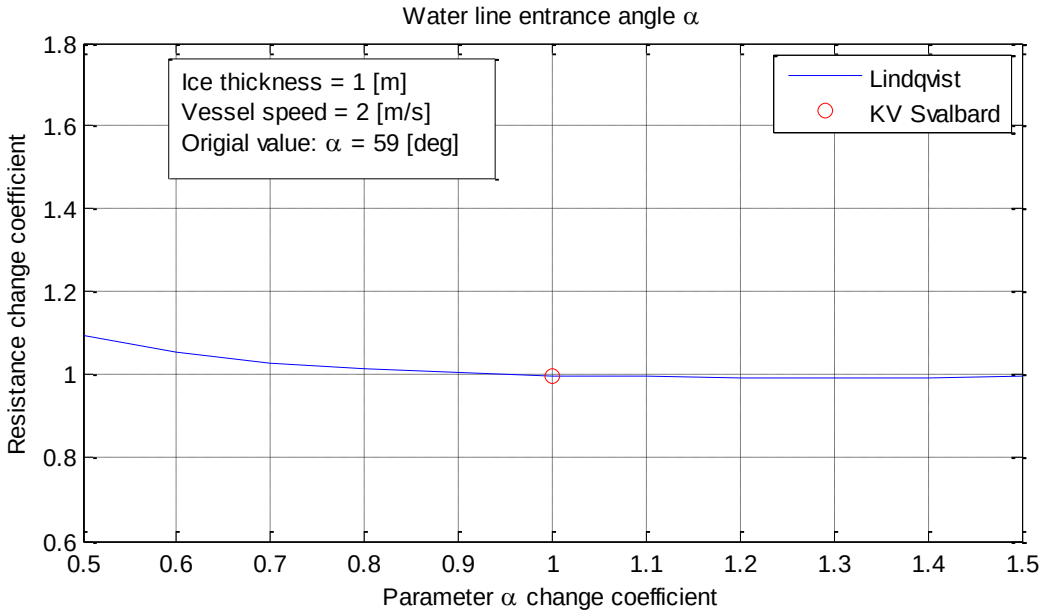


Figure 6-5: Sensitivity of waterline entrance angle.

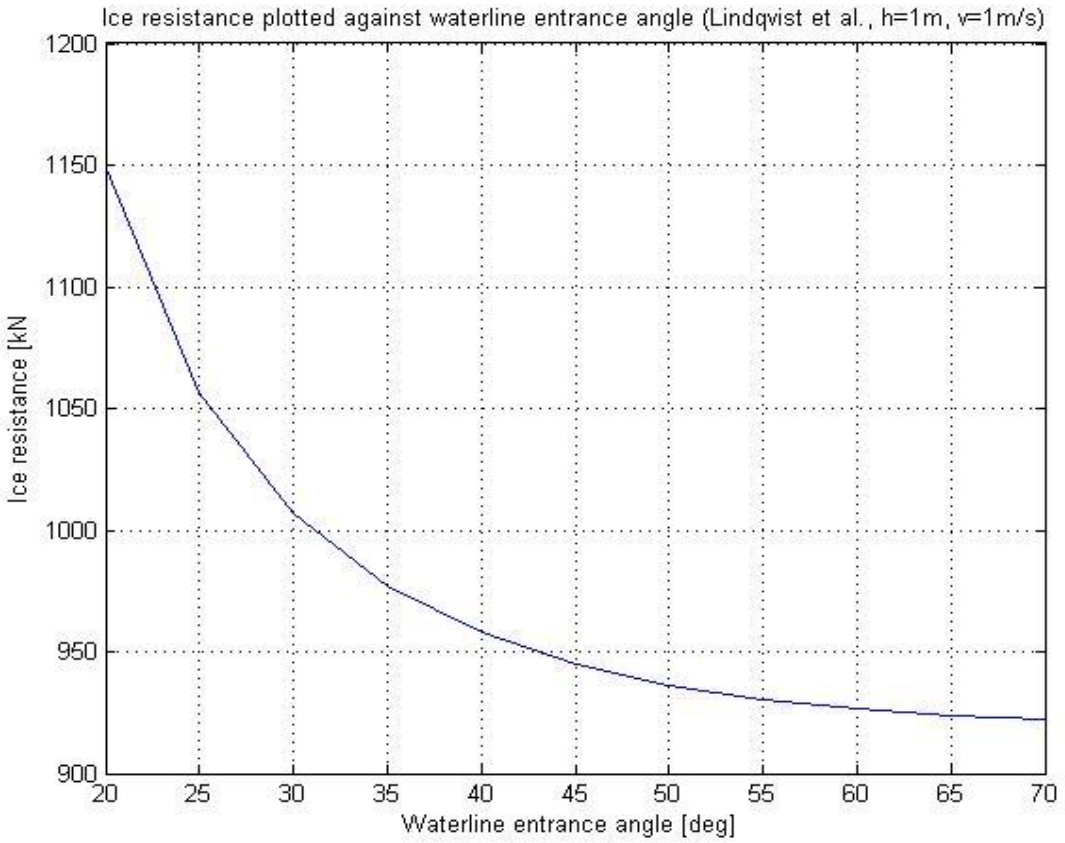


Figure 6-6: Ice resistance plotted against waterline entrance angle.

## 6.5 Friction coefficient

The friction coefficient work as one of the input parameters for Lindqvist's method. The friction coefficient varies linearly as illustrated on the graph. A 20% change in friction coefficient will lead to approximately 10% change in resistance coefficient.

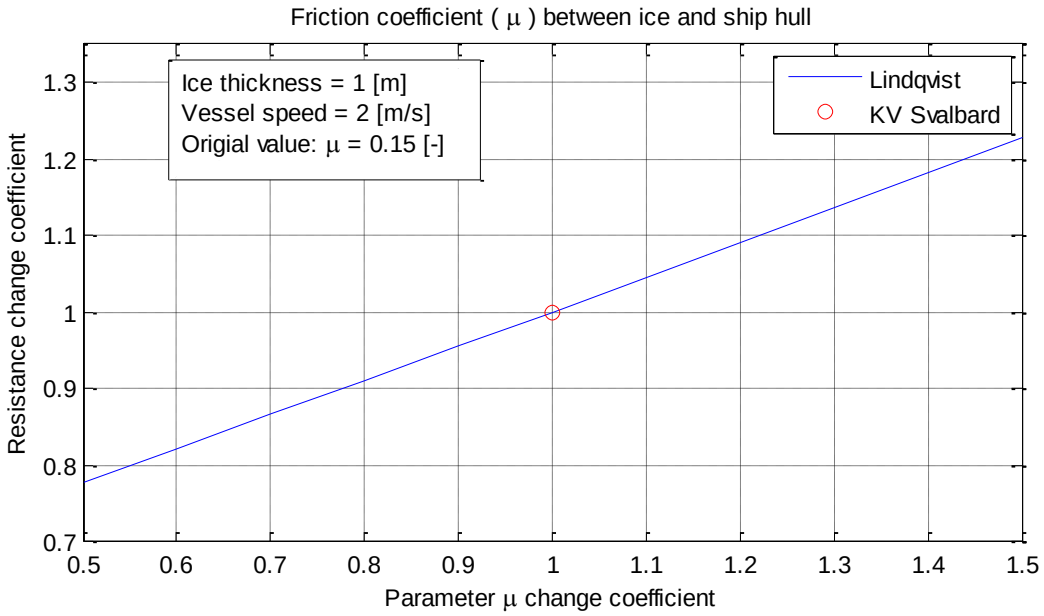


Figure 6-7: Sensitivity of friction coefficient.

## 6.6 Buttock angle

The buttock angle of KV Svalbard is 30 degrees from the figure below it is seen that the resistance will change approximately 10% when the buttock angle is changed 20%.

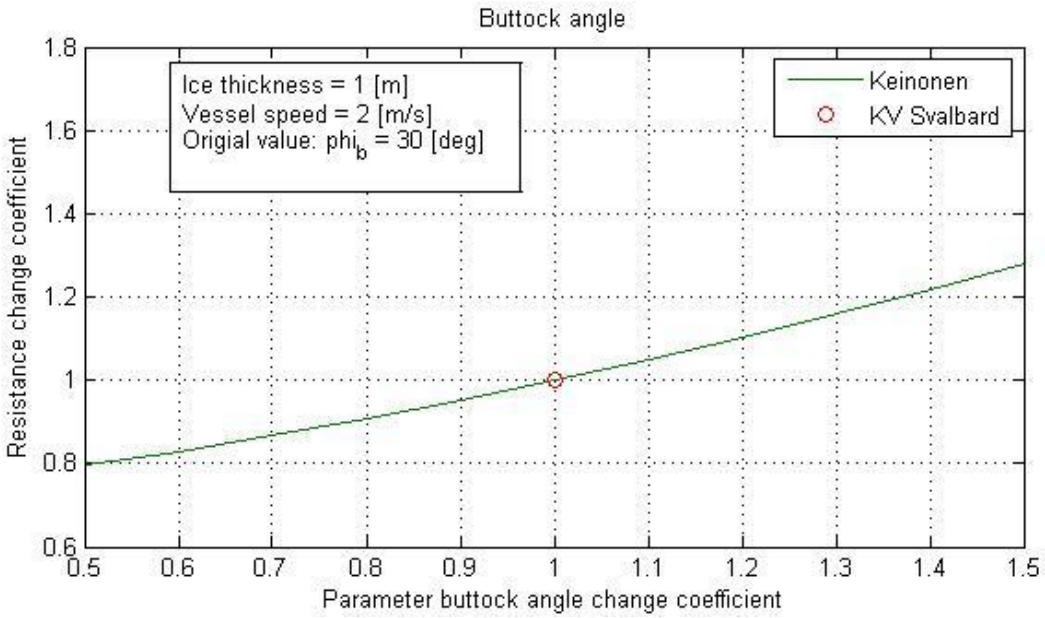


Figure 6-8: Sensitivity of buttock angle.

# 7 Open water resistance

This information is taken from [17]. Riska`s and Keinonen's method is calculated as open water resistance plus the ice resistance. To be able to compare the estimated resistance with the analytical methods the open water resistance needs to be calculated and added.

The open water resistance will be calculated for KV Svalbard in MATLAB. Data points with no ice thickness where sorted from the raw data and open water resistance where estimated in the same way as ice resistance. Ship resistance is approximately proportional to the vessel speed squared.

A least square regression has been used to predict open water resistance as a function of ship speed. To test the regressions quality 50% of the data points are chosen to the regression while the rest of the data points are used to test the goodness of the fit. From figure 7-1 it is shown that the data points used for testing the results fits the regression line well.

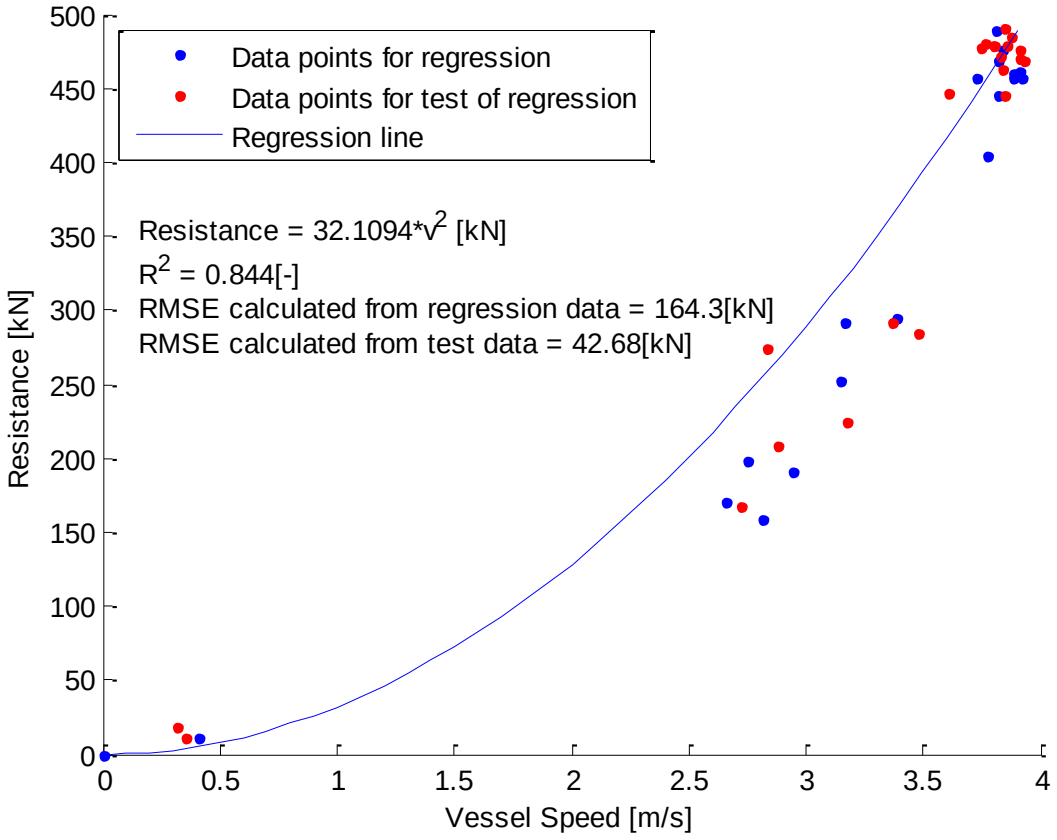


Figure 7-1: Open water resistance plotted against vessel speed.

Using this method to calculate the open water resistance is not very accurate since it is assumed no loss of energy from propeller engine to net thrust. Other things that may influence the open water resistance such as wind and waves are also not taken into account. All data points used for the calculations have approximately the same speed which also make it difficult to determine the whether the regression line below the operating speed is satisfying.

# 8 Estimation of resistance from full scale measurements

The ice load monitoring system on KV Svalbard provides the measured data needed to estimate the resistance of the ship. The procedure used is found from [19] described below. The estimated resistance from the full scale measurement will be used to evaluate the three analytical methods.

1. Conservation of energy

The law of conservation of energy is used to estimate the resistance. It states that the total amount if energy in an isolated system remains constant over time. In this case the ship and surrounding ice can be considered to be a closed system. Change in energy can only be caused by work by the system or work on the system.

2. Work-energy theorem

The work-energy theorem states that if external forces cause the kinetic energy to change then the work done by the net force is equal to the change in kinetic energy. Mathematically it can be expressed as:

$$\Delta K = K_f - K_i = W_{net} \quad \text{Eq. 8-1}$$

$\Delta K = change\ if\ kinetic\ energy$
$K_f = final\ kinetic\ energy$
$K_i = initially\ kinetic\ energy$
$W_{net} = net\ work\ done\ by\ the\ force(s)$

This energy formulation is based on Newton's second law as shown below.

$$\Delta K = W_{net} = \int_1^2 ma \cdot dt \quad \text{Eq. 8-2}$$

$$\Delta K = \frac{1}{2} m \cdot v_f^2 - \frac{1}{2} m \cdot v_i^2 = \frac{1}{2} m \cdot \left(v_f^2 - v_i^2\right) \quad \text{Eq. 8-3}$$

$m = mass\ of\ ship$
$v = velocity$

Now we have the change in kinetic energy expressed by mass and velocity at the beginning and end of the time step.

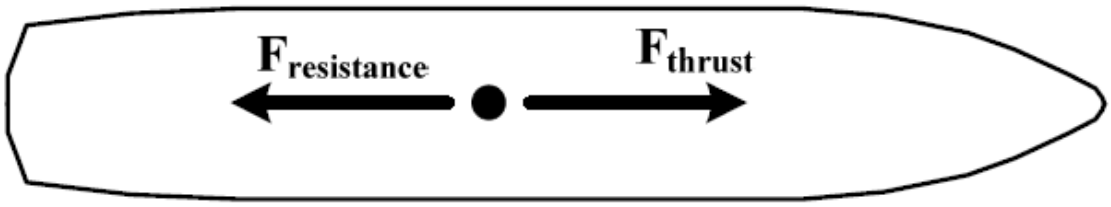


**Figure 8-1: For a specific speed, total resistance experienced by the ship needs is balanced by thrust force. [19]**

3. Propulsion work

The propeller thrust requires advanced measuring instrument and are usually not measured. Propeller thrust can also be found in model testing from the propeller curves. This information is unfortunately not available hence simplifications must be done. The power delivered to the shaft is known and can be used to give estimate of the thrust:

$$W_{thrust} = \int_{t_i}^{t_f} P\, dt \qquad \text{Eq. 8-4}$$

Where P is the power delivered. This simplification will cause a resistance larger than expected since the efficiency of the propeller is assumed to be 1, but is normally less than 1.

4. Resistance work and force

The sum of the thrust work and the kinetic energy is assumed to be equal the work done by the resistance:

$$W_{resistance} = \int_{t_i}^{t_f} P\, dt - \frac{1}{2} \cdot M\left(v_f^2 - v_i^2\right) \qquad \text{Eq. 8-5}$$

The resistance force then become:

$$F_{resistance} = \frac{dW_{resistance}}{ds} \qquad \text{Eq. 8-6}$$

# 9 Data

For two weeks KV Svalbard was out on an expedition carrying out a several projects planned by DNV (Det Norske Veritas), one of them being the Ice Load Monitoring. The relevant data for this thesis will be taken from the raw data collected from this expedition.

Torstein Skår developed an automated routine for selection of data.
Coefficient of variation is the ratio of the standard deviation to the mean:

$$Coefficient\ of\ variation(CV) = \frac{Standard\ deviation}{mean\ value} = \frac{\sigma}{|\mu|} \qquad \text{Eq. 9-1}$$

This is useful because it allows for meaningful comparison between two or more magnitudes of variations even if they have different means or different scales of measurements.

Vessel speed, vessel heading, ice thickness and propeller engine power are the variables that are analysed. In the MATLAB program Torstein Skår defined threshold values for the different variables, this can be changed in the input file. Values used in this thesis:

| Parameter | Max coefficient of variation |
|---|---|
| **Vessel speed** | 0.15 |
| **Vessel heading** | 0.4 |
| **Ice thickness** | 0.6 |
| **Propeller engine power** | 0.2 |

Table 9-1: Max coefficient of variation.

The ice thickness is allowed to vary more than the other variables due to high variation in the ice thickness.

In addition to this coefficient of variation an amount of the data points need to be removed. The ice thickness for first year level ice is approximate two meters. Some of the ice thickness data collected from the raw data is much higher than 2 meters. This data is considered as multiyear ice ridges or errors from the measurement, and therefore neglected. In the MATLAB program Torstein Skår has made an automated selection process that removes data point with an ice thickness larger than 3 meters.

# 10 Statistical calculations

The data selected from the raw data will here be analysed using statistical tools. The ratio between estimated resistance and predicted resistance from analytical methods are of interest and are hence defined as [17]:

$$\text{Riska ratio} = \frac{R_{measurements}}{R_{riska}} \quad \text{Eq. 10-1}$$

Where $R_{measurements}$ is the estimated resistance from measurements and $R_{riska}$ is the resistance calculated from Riskas method. Similar for Lindqvist and Keinonen's method the ratios are expressed:

$$\text{Lindqvist ratio} = \frac{R_{measurements}}{R_{lindqvist}} \quad \text{Eq. 10-2}$$

$$\text{Keinonen ratio} = \frac{R_{measurements}}{R_{keinonen}} \quad \text{Eq. 10-3}$$

If the ratio is larger than 1 the resistance from estimated resistance is larger than the resistance predicted from the analytical methods. The predictor variables chosen for this ratio are ice thickness and vessel speed.

## 10.1 Regression

A regression surface will be calculated for the different ratios to describe the relationship between the ratios, ship speed and ice thickness. First some information on regression and which regression method that is used to create surface fits.

Some definitions:

**Outlier:** An outlier is an observation with large residual, hence the measurement deviate much from the mean value.

**Least square estimation [20]:** A method used in regression analysis for estimating parameters by minimizing the differences between the observed response and the value predicted by the model. It is an easy method to use but it is sensitive to outliers in the data.

Regression is an important statistical tool in many fields. Regression is a statistical measure that tries to determine the strength of the relationship between one variable that is dependent and a series of other changing variables. One problem that often occurs when applying a regression is the presence of outlier or outliers in the data. Small simple mistakes can generate outliers and make serious effects of statistical interference. Least squares estimations can be destroyed, which will result in useless information for the most of the data. To improve this robust regression analysis is used when there is a large amount of outliers. One method of robust regression is described below and used in this thesis.

### 10.1.1 Robust bisquare fitting

This is an iterative weighted least squared method and the most commonly used of robust regression. The weight given to each data point depends on the distance to the fitted line. Points close to the line get full weight and points further away from the fitted line gets reduced weight. In MATLAB this is the default method for robust least square fitting,

The procedure in MATLAB [20]:

- The model is fitted by weighted least squares.

$$SSE = \sum_{i=1}^{n} w_i (y_i - \hat{y}_i)^2 \qquad \text{Eq. 10-4}$$

  Where $w_i$ are the weights which determine how much each response value influence the final parameter estimates.

- Adjusted residuals are computed given by:

$$r_{adj} = \frac{r_i}{\sqrt{1 - h_i}} \qquad \text{Eq. 10-5}$$

  Where $r_i$ is the usual least squares residuals and $h_i$ is the leverage that weight down the large residuals and hence reduces the effect of outliers.
  The leverage is given as:

$$h = (X(X^T X)^{-1} X^T) \qquad \text{Eq. 10-6}$$

where X is the predictor matrix containing all the independent variable observations.

- The adjusted residuals are standardized:

$$u = \frac{r_{adj}}{K * s} \qquad \text{Eq. 10-7}$$

Where k is a tuning constant with the value 4.685 and s is the robust variance given as:

$$s = \frac{MAD}{0.6745} \qquad \text{Eq. 10-8}$$

$MAD =$ Median Absolute Deviation

- The robust weights are computed as a function of u:

$$w_i = \begin{cases} (1 - (u_i)^2)^2 & |u_i| < 1 \\ 0 & |u_i| \geq 1 \end{cases} \qquad \text{Eq. 10-9}$$

- If the fit converge, the procedure is done, if not the next iteration step of the fitting process will be to return to the first step. Figure 10-1 compares regular line fit with robust fit with bisquare weights.

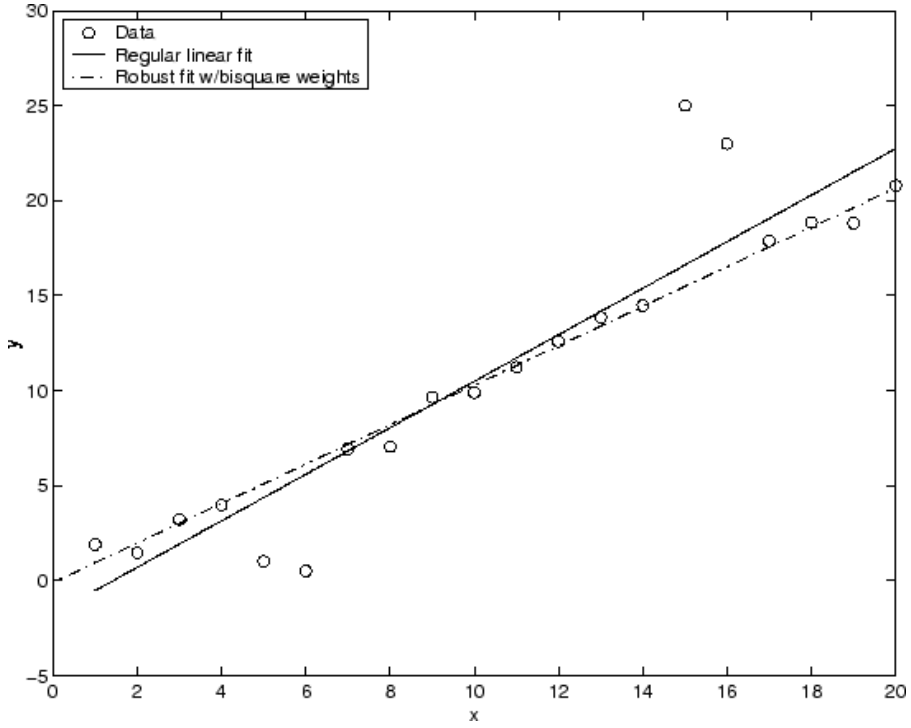


Figure 10-1: regular fit compared with robust fit.

### 10.1.2 The goodness of fitting [20]

After fitting the data with the different models, the goodness of fit should be evaluated. To assess the goodness of fit there are two methods that can be used.

- Graphical methods:
  Plotting the residuals and prediction bounds

- Numerical methods:
  Computing goodness-of-fit statistics and coefficient confidence bounds

Graphical methods allow you to view the entire data set at once while the numerical measures focus more on a particular aspect of the data, hence the graphical methods are often more beneficial. But the best will be to use both methods to determine the best fit.

**Goodness-of-fit statistics**:

- **The sum of squares due to error:**

Measurement of the difference between the fit and the measured response:

Eq. 10-10

$$SSE = \sum_{i=1}^{n} w_i (y_i - \hat{y}_i)^2$$

$w_i$= weight of point i
$y_i$= data value
$\hat{y}_i$= estimated value

A value closer to 0 indicates that the model has a smaller random error component, and that the fit will be more useful for prediction.

- **R-squared:**

Measures how successful the fit is explaining the variation of data. R-squared is defined as:

$$R^2 = \frac{SSR}{SST} = 1 - \frac{SSE}{SST}$$ Eq. 10-11

Where SSR is the sum of squares of the regression defined as:

$$SSR = \sum_{i=1}^{n} w_i (\hat{y}_i - \bar{y})^2$$ Eq. 10-12

And SST is the total sum of squares defined as:

$$SST = \sum_{i=1}^{n} w_i (y_i - \bar{y})^2$$ Eq. 10-13

The relation between the sum of squares are:

$$SST = SSR + SSE$$ Eq. 10-14

R-square is a value between zero and one. If the value is closer to one it indicates that a greater proportion of variance is accounted for by the model e.g. if R-squares is 0.90 it means that the fit explains 90.0% of the total variation of the data above average. Hence if the fit is perfect all residuals are zero and R-squared is 1.

- **Root mean squared error (RMSE):**

This is an estimation of the standard deviation of the random component in the data. RMSE is defined as:

$$RMSE = \sqrt{MSE} = \sqrt{\frac{1}{n}\sum_{i=1}^{n}(\hat{y} - y)^2} \qquad \text{Eq. 10-15}$$

where MSE is the mean square error. A value closer to 0 indicates that the model has a smaller random error component, and that the fit will be more useful for prediction.

### 10.1.3 Analyzing the residuals

The residuals from a fitted model are the difference between the predicted value and the observed value. The residuals approximate the random errors assuming the model fitted to the data is correct.

The residuals are calculated as the vertical distance from the data point of the fitted curve as figure 10-2 illustrates. When the residuals appear randomly around zero it is suggested that the data fit the model well. Figure 10-2 is an illustration on a good fit.

Good fit:

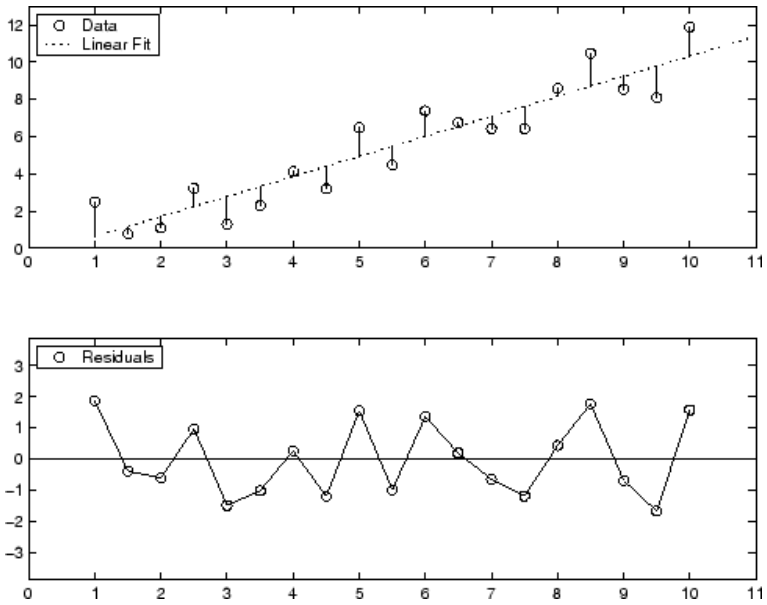


Figure 10-2: Example of good fit of residuals. [20]

When the residuals are systematically positive or negative, it indicates a poor fit. Figure 10-3 is an example of a poor fit for the data whit residuals positive for almost all data.

Poor fit:

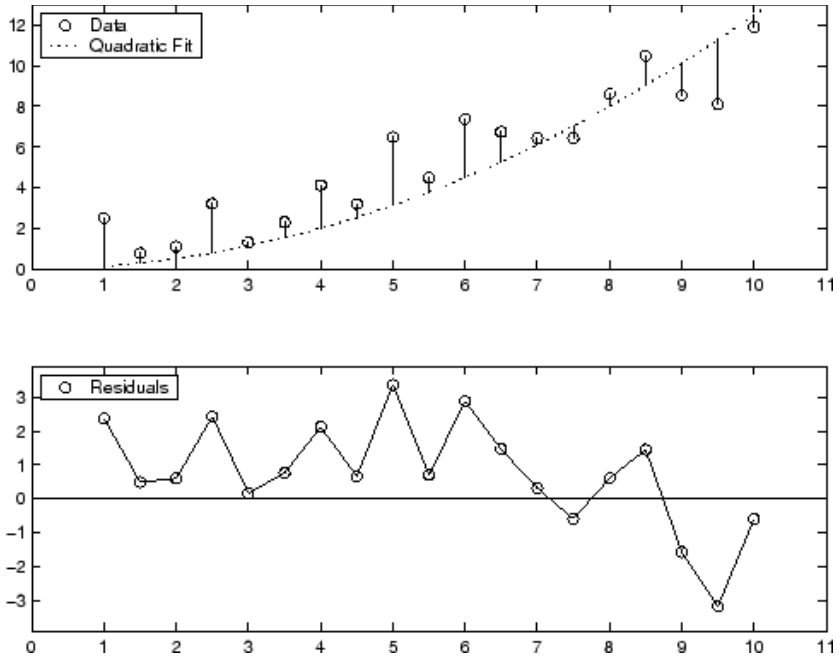


Figure 10-3: Example of poor fit of residuals.

- **Confidence bounds and prediction bounds**

Confidence bound and prediction bound defines the width of an associated interval which indicates uncertainties about the fitted coefficients, the predicted fit and the predicted observations. If the interval is very wide it is hard to say anything definite about the coefficients. The level of certainties is specified in most cases as 95%. Hence, the probability that the observation is within the lower and upper prediction bounds is 95%.

## 10.2 Surface fit

A second order surface is used to fit a surface to the different ratios. The robust bisquare method, which is described in section 10.1.1, is used. In addition to the surface fits the residual where plotted against vessel speed and ice thickness.

## 10.3 Riska

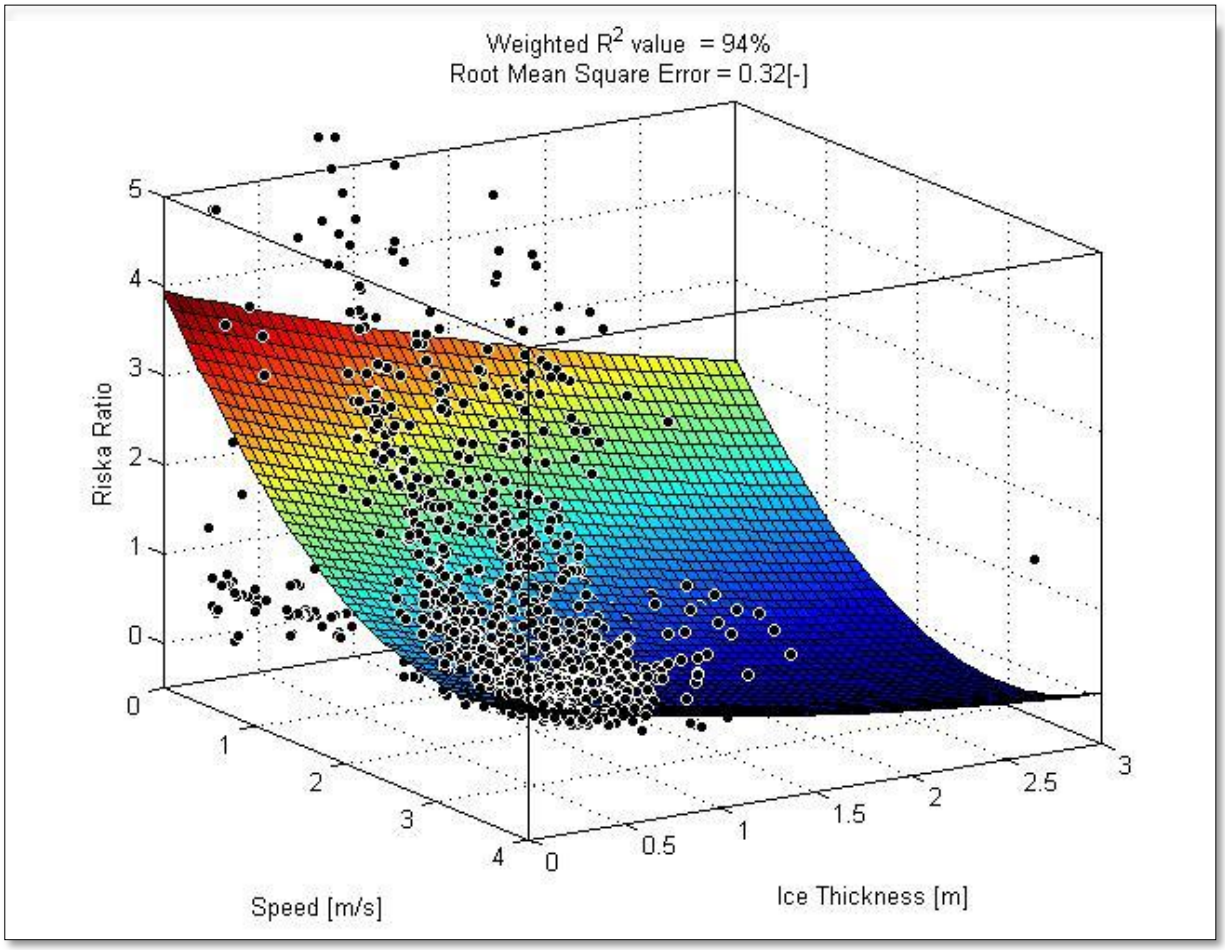


Figure 10-4: Bisquare robust fit of Riska ratio.

| | |
|---|---|
| Sum of squares due to error | 139.5915 |
| $R^2$ | 0.9382 |
| Root mean square error | 0.3212 |

Table 10-1: Goodness of fit statistics for Riska ratio.

The goodness of fit parameters are good, the R-square value indicates that almost 94% of the variance of the data is described by the model. From figure 10-4 it is obvious that this is not right for low speed, where there it is a large scatter in Riska ratio.

The equation for the fitted surface is defined as:

$$Surface_{RiskaRatio} = p_{00} + p_{10} \cdot V + p_{01} \cdot h + p_{20} \cdot V^2 + p_{11} \cdot V \cdot h + p_{02} \cdot h^2 \qquad \text{Eq. 10-16}$$

The coefficients are described in table 10-2. In addition the upper and lower values of a 95% confidence bound are given.

| Coefficient | Estimated value | Lower 95% confidence bound | Upper 95%confident bound |
|---|---|---|---|
| $P_{00}$ | 3.94 | 3.816 | 4.064 |
| $P_{10}$ | -1.893 | -1.988 | -1.798 |
| $P_{01}$ | -0.8049 | -0.9756 | -0.6342 |
| $P_{20}$ | 0.2854 | 0.2646 | 0.3061 |
| $P_{11}$ | 0.08142 | 0.02811 | 0.1347 |
| $P_{02}$ | 0.06347 | 0.008703 | 0.1182 |

Table 10-2: values for coefficients in Riska ratio surface equation 10-16 with a 95% confidence bound.

The mean value of the Riska ratio:

$$P_{Riska} = \frac{The\ sum\ of\ all\ riska\ ratios}{Total\ number\ of\ observations} = 1.043 \qquad \text{Eq. 10-17}$$

The mean value is good and predicts that Riska will slightly underestimate the resistance compared to the estimated resistance from the full scale trial. From the surface fit it is showed that the points varies much for low speeds. The Riska ratio for low speeds is very high and will contribute to increase the mean value of Riska ratio significantly.

The residual plots below illustrate the distance from each point to the fitted plane. It is seen that the points does not vary randomly around the fitted line which would indicate a good fit. One of the reasons is the huge scatter in the lower speeds compared to higher speeds. The residual plot seems to fit good for speed over 1 m/s.

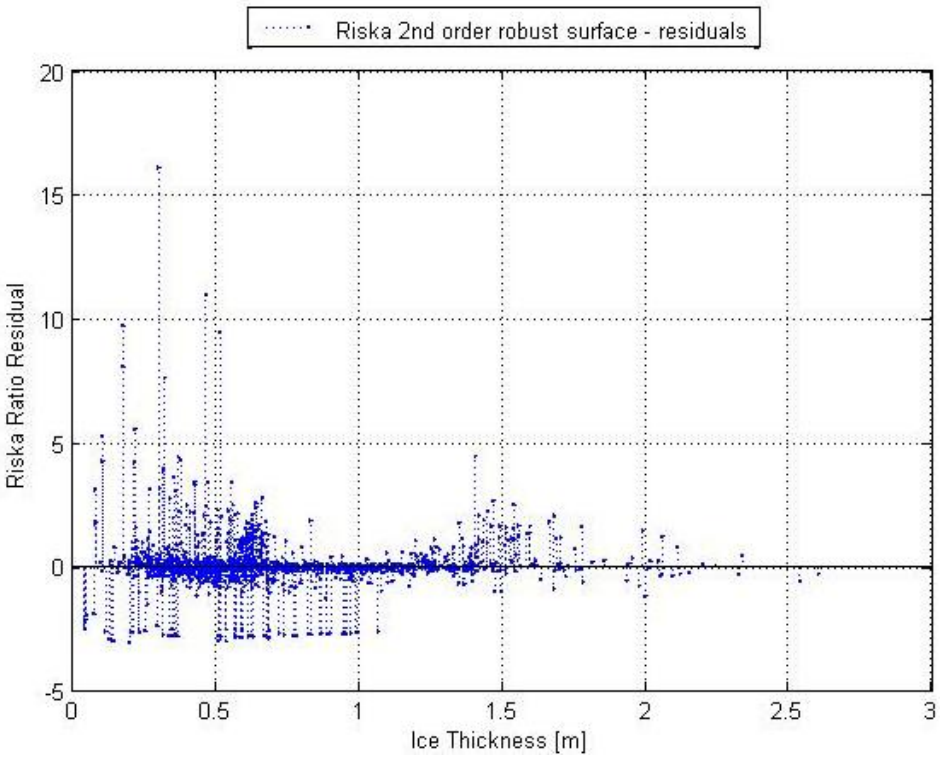


Figure 10-5: Riska ratio residuals plotted against ice thickness.

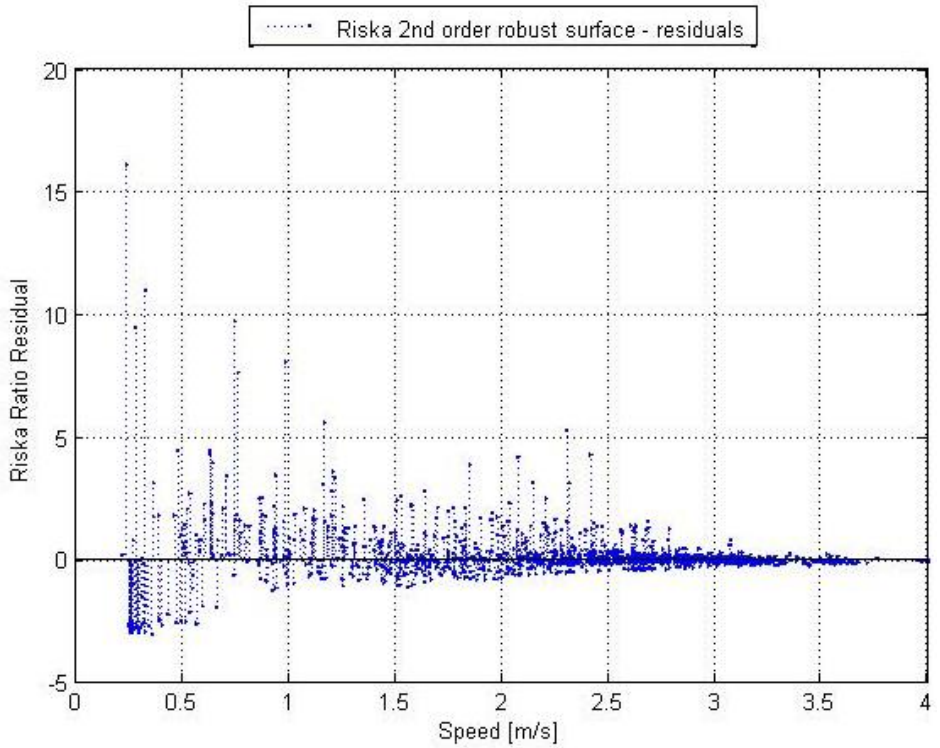


Figure 10-6: Riska ratio residuals plotted against vessel speed.

## 10.4 Lindqvist

The Lindqvist method is the only analytical method that does not include open water resistance. The results from the surface fit shows that Lindqvist`s method differs from the other two methods. If it is assumed that the open water resistance for Lindqvist's method can be super positioned in the same way as for Riska and Keinonen, the results from the surface fit will be better. Hence:

$$R_{tot} = R_{ice} + R_{ow} \qquad \text{Eq. 10-18}$$

Both results are described in the next two sections.

### 10.4.1 Without open water resistance

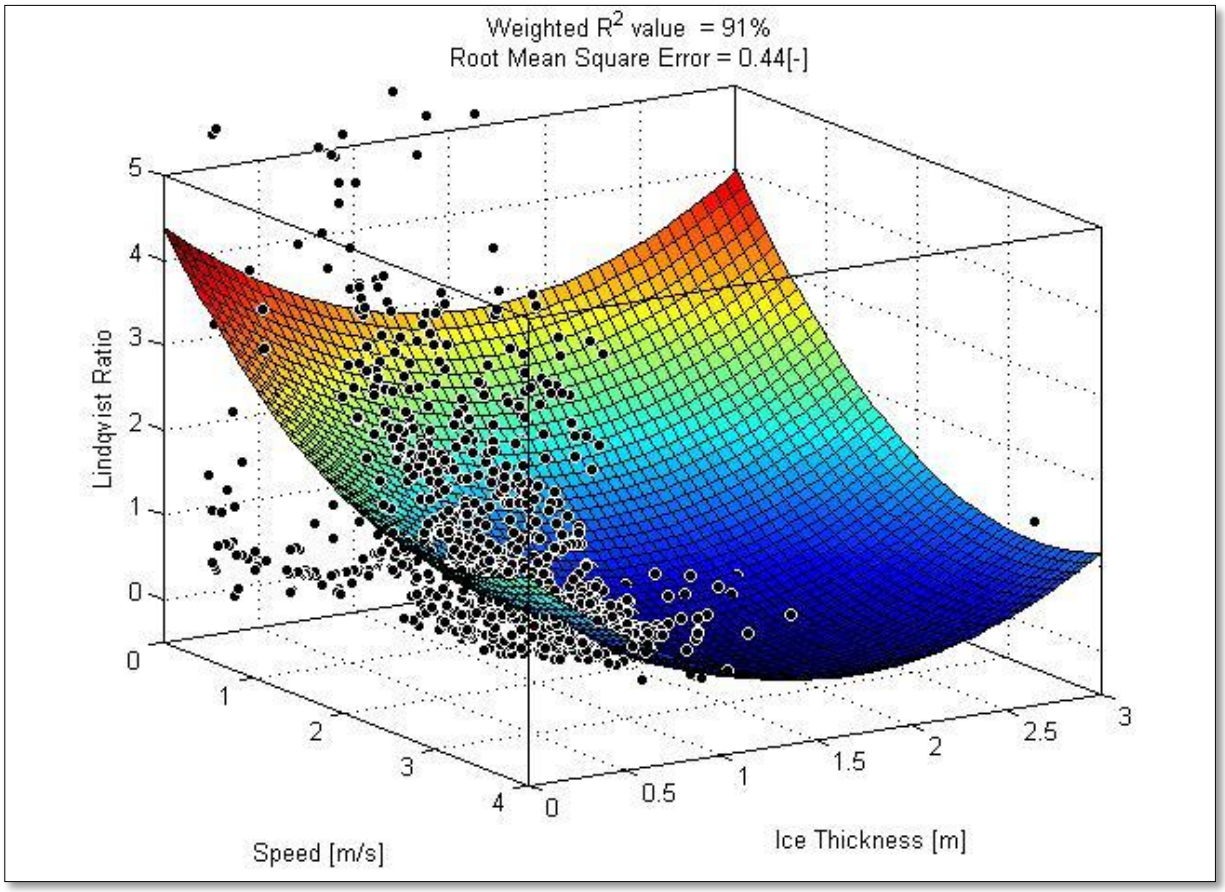


Figure 10-7: Bisquare robust fit for Lindqvist ratio

| | |
|---|---|
| Sum of squares due to error | 259.2650 |
| $R^2$ | 0.9118 |
| Root mean square error | 0.4377 |

Table 10-3: Goodness of fit statistics for Lindqvist ratio.

The goodness of fit statistic show a poorer fit for the Lindqvist ratio compared to Riska ratio.

The equation describing the surface fit is given as:

$$Surface_{LindqvistRatio} = p_{00} + p_{10} \cdot V + p_{01} \cdot h + p_{20} \cdot V^2 + p_{11} \cdot V \cdot h + p_{02} \cdot h^2 \quad \text{Eq. 10-19}$$

The constants in the equation are given in table 10-4.

| Coefficient | Estimated value | Lower 95% confidence bound | Higher 95%confident bound |
|---|---|---|---|
| $P_{00}$ | 4.403 | 4.234 | 4.572 |
| $P_{10}$ | -1.772 | -1.902 | -1.643 |
| $P_{01}$ | -1.924 | -2.157 | -1.692 |
| $P_{20}$ | 0.2897 | 0.2614 | 0.318 |
| $P_{11}$ | -0.03143 | -0.1041 | 0.04123 |
| $P_{02}$ | 0.5964 | 0.5217 | 0.671 |

Table 10-4: values for coefficients in Lindqvist ratio surface equation 10-19 with a 95% confidence bound.

The mean value of the Lindqvist ratio:

$$P_{Lindqvist} = \frac{The\ sum\ of\ all\ lindqvist\ ratios}{Total\ number\ of\ observations} = 1.21 \quad \text{Eq. 10-20}$$

The calculated mean value of the Lindqvist ratio indicates that in average the estimated resistance from measurements are higher than estimated resistance from Lindqvist's method. Hence it is unconservative to estimate the resistance with Lindqvist's method.

The residual plots are not varying randomly around the fitted line, and also here the scatter for lower speed stands out with much larger values.

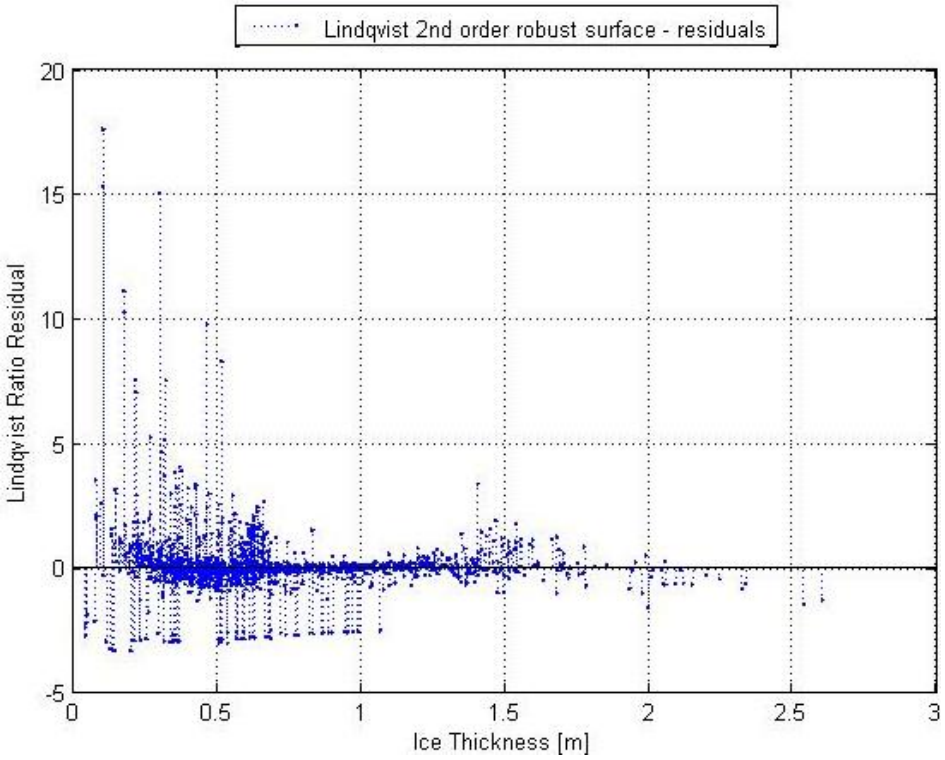


Figure 10-8: Lindqvist ratio residuals plotted against ice thickness.

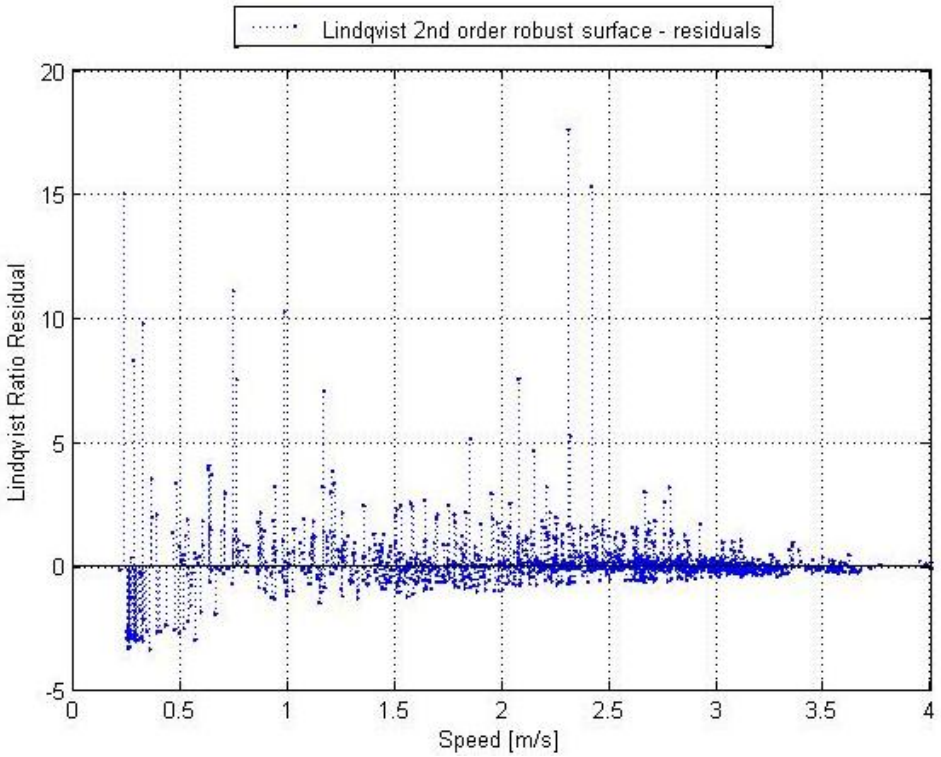


Figure 10-9: Lindqvist ratio residuals plotted against vessel speed.

### 10.4.2 Lindqvist with open water resistance

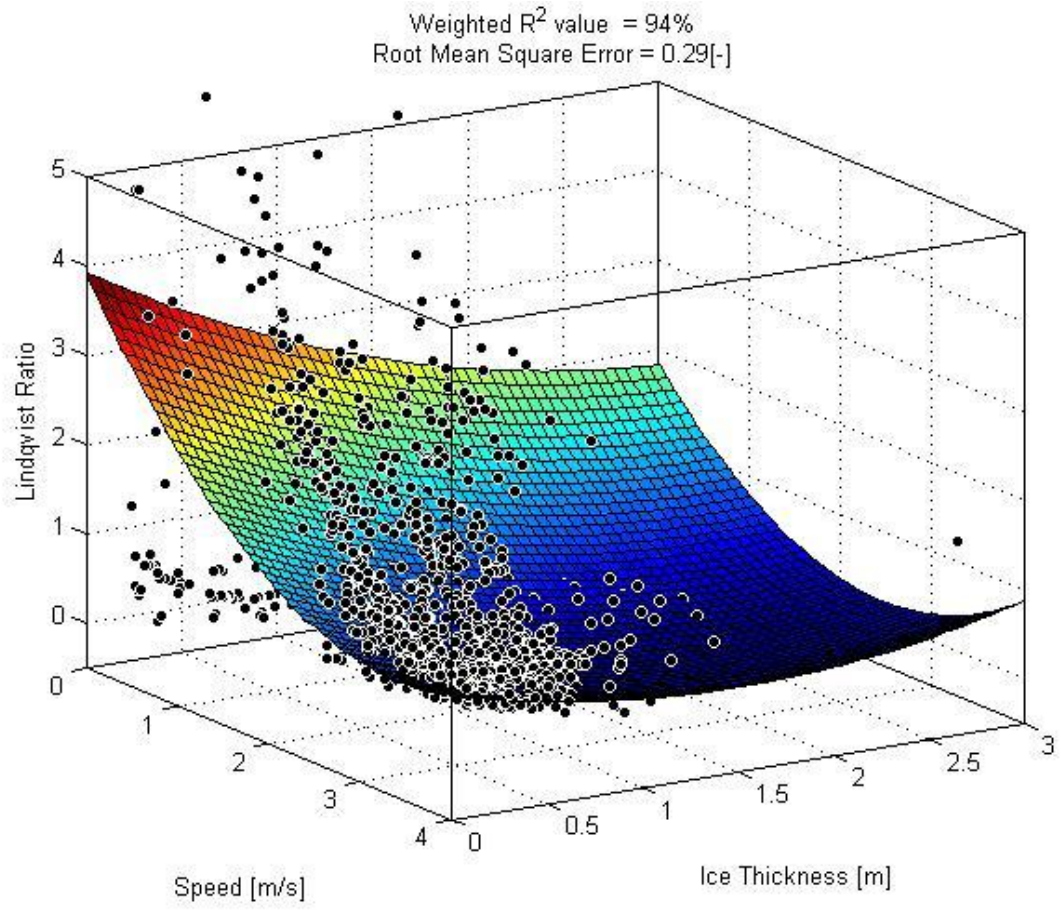


Figure 10-10: Bisquare robust fit for Lindqvist ratio with open water resistance included.

| | |
|---|---|
| Sum of squares due to error | 110.5094 |
| $R^2$ | 0.9409 |
| Root mean square error | 0.2858 |

Table 10-5: Goodnes of fit statistics for Lindqvist ratio with open water resistance included.

The goodness of fit parameters gets significantly better when open water resistance is added. And it is seen from the figure 10-10 that it is a better fit. The results are now quite similar the results for Riska ratio.

The equation describing the surface fit:

$$Surface_{LindqvistRatio} = p_{00} + p_{10} \cdot V + p_{01} \cdot h + p_{20} \cdot V^2 + p_{11} \cdot V \cdot h + p_{02} \cdot h^2 \quad \text{Eq. 10-21}$$

The coefficients are given in table 10-6.

| Coefficient | Estimated value | Lower 95% confidence bound | Higher 95%confident bound |
|---|---|---|---|
| $P_{00}$ | 3.924 | 3.814 | 4.035 |
| $P_{10}$ | -1.84 | -1.925 | -1.756 |
| $P_{01}$ | -1.278 | -1.43 | -1.126 |
| $P_{20}$ | 0.2703 | 0.2519 | 0.2888 |
| $P_{11}$ | 0.173 | 0.1256 | 0.2204 |
| $P_{02}$ | 0.1928 | 0.144 | 0.2415 |

**Table 10-6: values for coefficients in Lindqvist ratio surface equation 10-21 with a 95% confidence bound. (Included open water reistance)**

The mean value of the Lindqvist ratio after adding open water resistance:

$$P_{Lindqvist\_ow} = \frac{The\ sum\ of\ all\ lindqvist\ ratios}{Total\ number\ of\ observations} = 0.92 \qquad \text{Eq. 10-22}$$

The mean value gets now conservative. The resistance estimated from Lindqvist's method with added open water are in average slightly larger than the estimated resistance from measurements.

The residuals are here also good for speed over 1 m/s, but seem to fit poorly for the rest of the data.

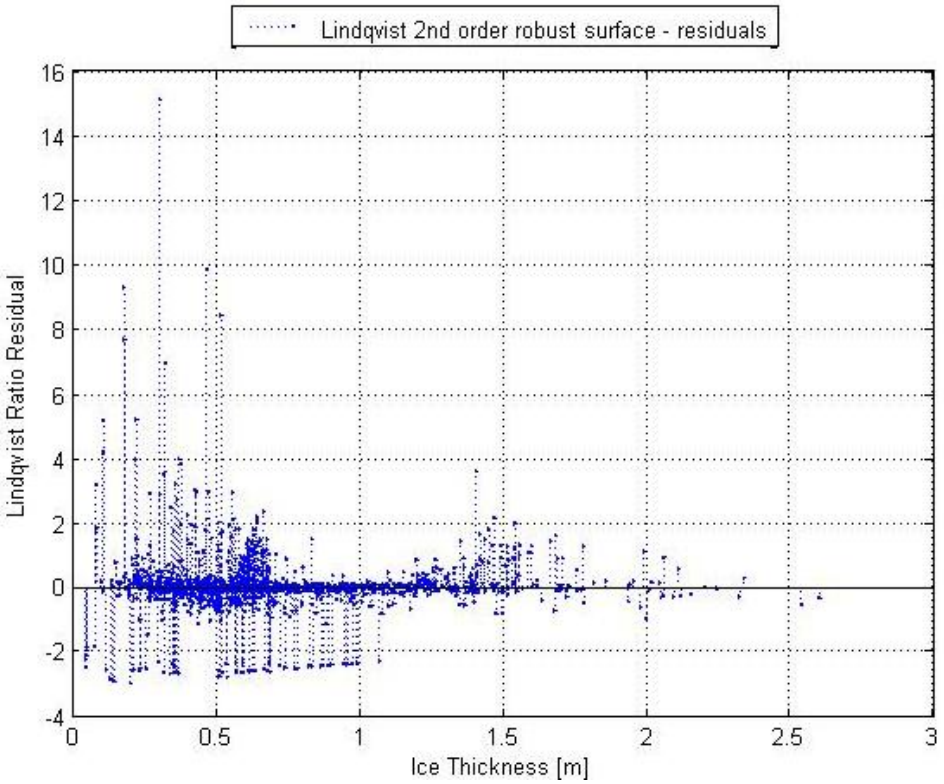
Lindqvist 2nd order robust surface - residuals
Lindqvist Ratio Residual
Ice Thickness [m]
16
14
12
10
8
6
4
2
0
-2
-4
0
0.5
1
1.5
2
2.5
3

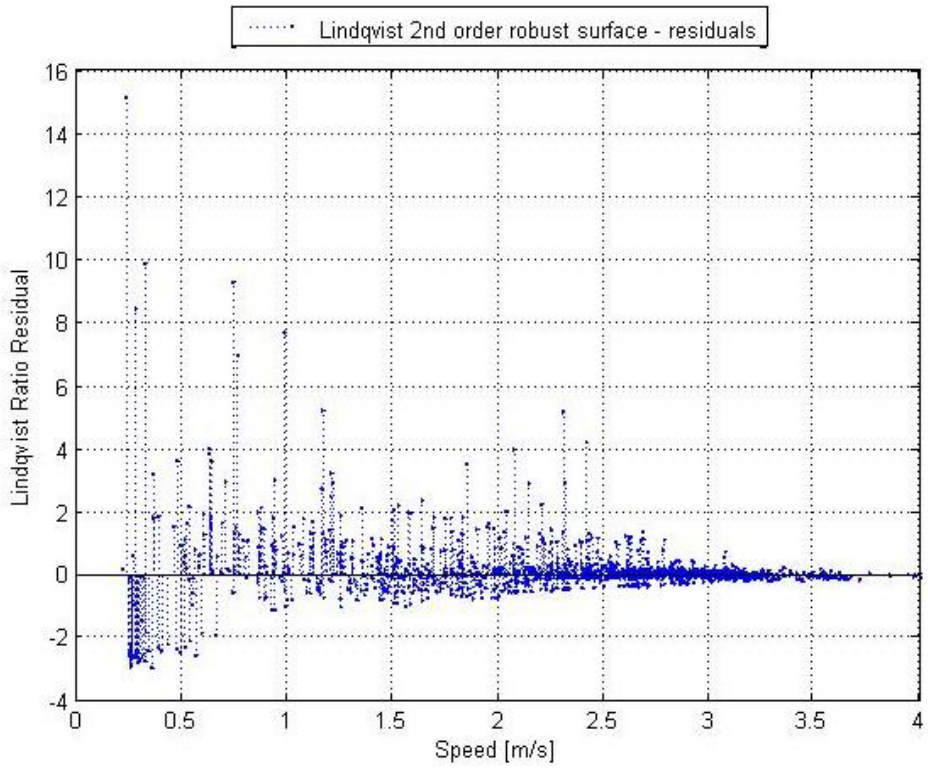
Lindqvist 2nd order robust surface - residuals
Lindqvist Ratio Residual
Speed [m/s]
16
14
12
10
8
6
4
2
0
-2
-4
0
0.5
1
1.5
2
2.5
3
3.5
4

## 10.5 Keinonen

Keinonen's method is as described in chapter 5 only valid for ship speed over 1 m/s. The surface fit of Keinonen ratio is displayed in figure 10-11.

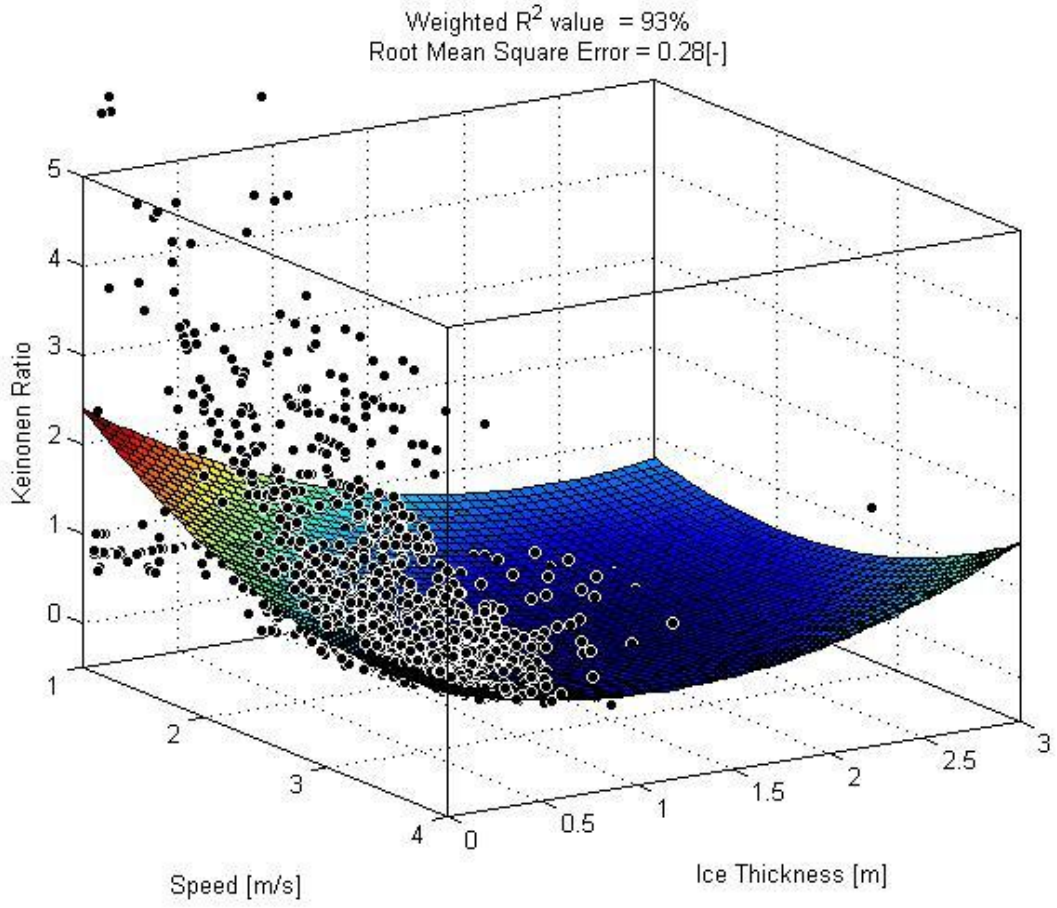


Figure 10-11: Bisquare robust fit of Keinonen ratio.

| | |
|---|---|
| Sum of squares due to error | 103.7656 |
| $R^2$ | 0.9319 |
| Root mean square error | 0.2769 |

Table 10-7: Goodness of fit statistics for Keinonen ratio.

Keinonen' surface fit get quite similar results for the goodness-of-fit statistics as the other two analytical methods.

The equation describing the surface fit for Keinonen's method is:

$$Surface_{KeinonenRatio} = p_{00} + p_{10} \cdot V + p_{01} \cdot h + p_{20} \cdot V^2 + p_{11} \cdot V \cdot h + p_{02} \cdot h^2 \qquad \text{Eq. 10-23}$$

The coefficients are given in table 10-8.

| Coefficient | Estimated value | Lower 95% confidence bound | Higher 95%confident bound |
|---|---|---|---|
| $P_{00}$ | 3.846 | 3.739 | 3.953 |
| $P_{10}$ | -1.689 | -1.771 | -1.607 |
| $P_{01}$ | -1.667 | -1.814 | -1.52 |
| $P_{20}$ | 0.2383 | 0.2204 | 0.2562 |
| $P_{11}$ | 0.2472 | 0.2013 | 0.2932 |
| $P_{02}$ | 0.2919 | 0.2447 | 0.3392 |

Table 10-8: values for coefficients in Keinonen ratio surface equation 10-23 with a 95% confidence bound.

The mean value of the Keinonen ratio:

$$P_{Keinonen} = \frac{The\ sum\ of\ all\ Keinonen\ ratios}{Total\ number\ of\ observations} = 0.87 \qquad \text{Eq. 10-24}$$

The mean value of Keinonen ratio is lower than the other two methods. Which mean using Keinonen's method to predict the resistance will in average be a conservative estimate.

From the residual plots it shows that Keinonen's method have a smaller scatter for lower speeds than the other two methods.

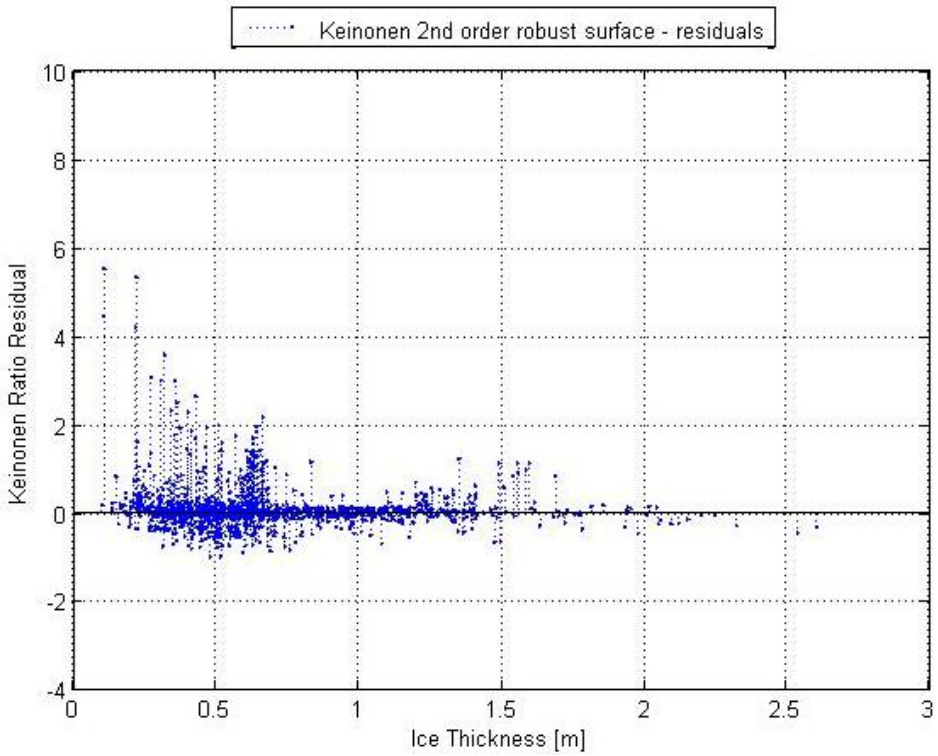


Figure 10-12: Keinonen ratio residuals plotted against ice thickness.

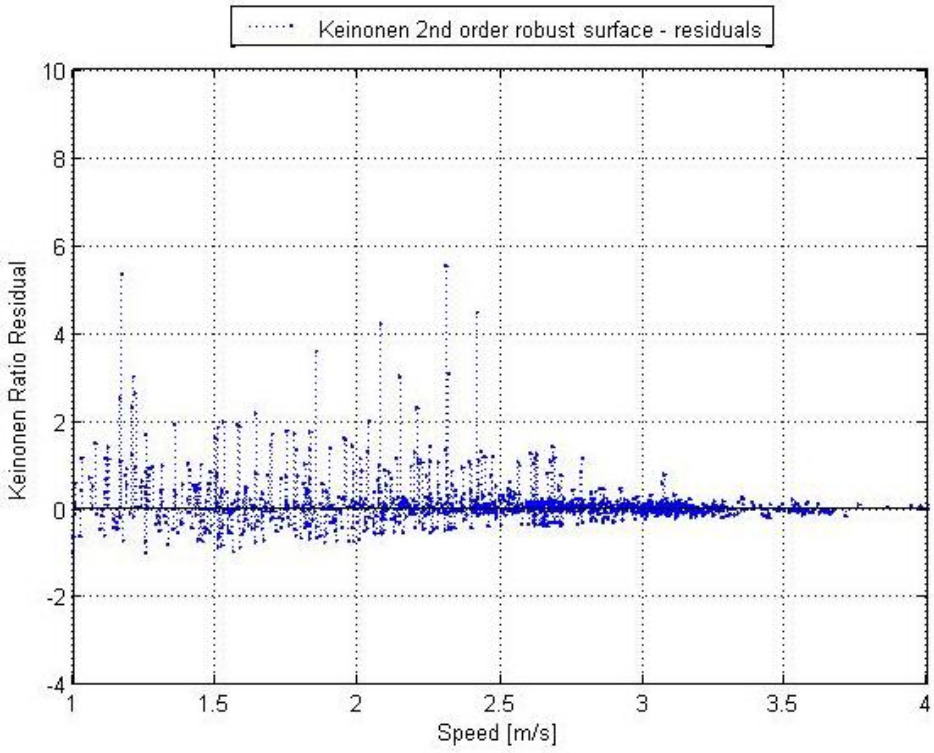


Figure 10-13: Keinonen ratio residuals plotted against ship speed.

## 10.7 Summary of section

It is seen that all three analytical methods gets similar surface fits and the goodness of fit values are around the same if it is assumed that open water resistance can be added to Lindqvist's method in the same way as Riska and Keinonen's method. For Riska and Keinonen's methods there is a much larger scatter in the ratios for low speeds which indicates that the fit is not very good for lower speeds. Keinonen's method seem to fit better than the other methods in low speed, but not good.

The fits seem to be good for higher speeds and ice thickness between 0,5m and 1,5 meter. The mean value will properly be overestimated due to the high values in the scatter of very low speeds.

## 10.8 Propeller efficiency

As described in chapter 8 the ice resistance will be overestimated for the full scale trial since the propeller efficiency is assumed to be 100%. It is more realistic to assume that the propeller efficiency will be lower than 100%. The effect of different propeller efficiencies is investigated. The surface fits and residuals fits from this investigation can be found in appendix C.

| Mean value of all the Ratios | | | | |
|---|---|---|---|---|
| **Propeller efficiency** | **Riska ratio** | **Lindqvist ratio without open water** | **Lindqvist ratio with open water** | **Keinonen ratio** |
| **100%** | 1,043 | 1,206 | 0,915 | 0,873 |
| **90%** | 0,938 | 1,086 | 0,824 | 0,768 |
| **80%** | 0,834 | 0,965 | 0,732 | 0,683 |
| **70%** | 0,729 | 0,843 | 0,640 | 0,597 |

Table 10-9: Mean value of all the ratios with different propeller efficiencies.

From table 10-9 the mean values for the different propeller efficiencies are plotted for all ratios including open water. The mean value of the ratios decreases as the propeller efficiency increases. The average value of the different ratios should not be over 1. If the value is over 1 it means that the analytical methods underestimate the estimated resistance from the measurements. Whit a propeller efficiency of 70% it is shown that the average value of the different ratios is getting very low which means the analytical methods overestimate the resistance a lot, hence using the analytical method for resistance prediction will be very over conservative in this case.

| Root mean squared value | | | | |
|---|---|---|---|---|
| **Propeller efficiency** | **Riska ratio** | **Lindqvist ratio without open water** | **Lindqvist ratio with open water** | **Keinonen ratio** |
| **100%** | 0,32 | 0,44 | 0,29 | 0,28 |
| **90%** | 0,29 | 0,39 | 0,26 | 0,24 |
| **80%** | 0,26 | 0,35 | 0,23 | 0,22 |
| **70%** | 0,22 | 0,30 | 0,20 | 0,19 |

Table 10-10: Root mean squared value of all the ratios with different propeller efficiencies.

Table 10-10 shows the root mean squared value of the different propeller efficiencies for all the ratios. The roots mean squared value increase as the propeller efficiency increase. Hence the root mean square value is better for lower propeller efficiency.

## 10.9 Dividing the data into groups

Due to the large scatter in the area for small speed it is interesting to look at data for some chosen speeds and ice thicknesses. To be able to fit the data to statistical distributions the data are divided into groups depending on ice thickness and speed. Minimum number of point in each group must exceed 20 observations to be able to get applicable data. 10-11 illustrates how the data are divided and how many points there are in each group. The cells marked with grey have to few observation points and will not be analysed here.

| | h =[0.0,0.5] | h =[0.5,1.0] | h =[1.0,1.5] | h =[1.5,2.0] | h =[2.0,2.5] | h =[2.5,3.0] |
|---|---|---|---|---|---|---|
| V =[0.0,0.7] | 41 | 39 | 17 | 6 | 2 | 0 |
| V =[0.7,1.3] | 21 | 36 | 44 | 22 | 2 | 2 |
| V =[1.3,2.0] | 37 | 105 | 59 | 13 | 8 | 0 |
| V =[2.0,2.7] | 119 | 163 | 74 | 9 | 2 | 0 |
| V =[2.7,3.3] | 222 | 188 | 28 | 2 | 0 | 0 |
| V =[3.3,4.0] | 54 | 31 | 10 | 0 | 0 | 0 |

**10-11: Dividing data into groups.**

## 10.10 Lognormal and Weibull distribution

The ratios of the different analytical methods described in chapter 10 are assumed to be lognormal distributed for each subgroup. By using built in MATLAB functions the mean value and standard deviation can be found. It is also assumed that a weibull distribution can model the data so a weibull line was fitted to the lognormal plots. To be perfectly weibull distributed the data points would follow the weibull line as illustrated on figure 10-14. To inspect if the lognormal distribution and weibull distribution can model the data a chi square test is done and residual plots are generated.

A lot of plots similar to the graph below are generated and attached in appendix D.

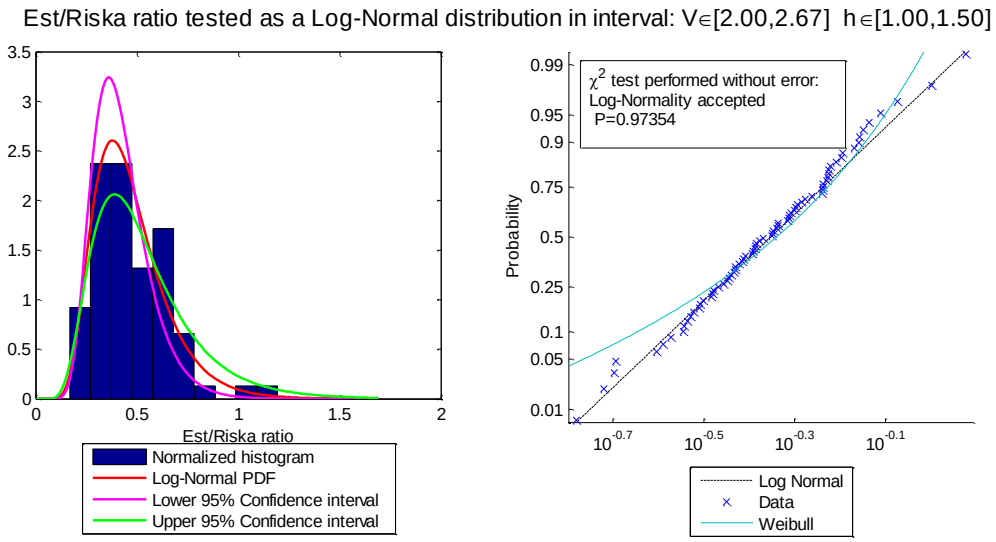


Figure 10-14: Lognormal distribution and weibull distribution for Riska ratio.

### 10.10.1 Chi square test

This is a goodness of fit test used to determine if the difference between the expected frequencies and the observed frequencies is significant in one or more categories.

$$X^2 = \frac{(O-E)^2}{E} \qquad \text{Eq. 10-25}$$

$O$ = observed frequency in each category
$E$ = expected frequency in each category
$X^2$= Chi-square

A short summary of the steps in a chi-square test:

- Observed frequencies are defined in one column and called O.
- The expected frequencies are founds and put in a column called E.
- The formula is used to find the chi square value.
- Calculate the degrees of freedom.
- Use the chi square table to find the relevant value.
- If the chi square value is equal to or greater than the table value, reject the hypothesis.

For more information on this test see [27].

The results from the chi square tests from all the ratios are given below. Table 10-12 to 10-14 represent the results from chi square test of the lognormal distribution and table 10-15 to 10-17 represent the results from the test done at the weibull distribution. The grey fields had too few points and are not considered. The red fields are values rejected by the hypothesis.

**Chi square test of the different ratios fitted to lognormal distribution:**

| | h =[0.0,0.5] | h =[0.5,1.0] | h =[1.0,1.5] | h =[1.5,2.0] | h =[2.0,2.5] | h =[2.5,3.0] |
|---|---|---|---|---|---|---|
| V =[0.0,0.7] | 0.00027 | 0.00094 | To few points | To few points | To few points | To few points |
| V =[0.7,1.3] | 0.15244 | 0.05343 | 0.60286 | 0.00002 | To few points | To few points |
| V =[1.3,2.0] | 0.02396 | 0.26571 | 0.03514 | To few points | To few points | To few points |
| V =[2.0,2.7] | 0.08205 | 0.00000 | 0.97354 | To few points | To few points | To few points |
| V =[2.7,3.3] | 0.04882 | 0.00020 | 0.15064 | To few points | To few points | To few points |
| V =[3.3,4.0] | 0.06197 | 0.00064 | To few points | To few points | To few points | To few points |

Table 10-12: Results from Chi square test of Riska ratio fitted to lognormal distribution.

| | h =[0.0,0.5] | h =[0.5,1.0] | h =[1.0,1.5] | h =[1.5,2.0] | h =[2.0,2.5] | h =[2.5,3.0] |
|---|---|---|---|---|---|---|
| V =[0.0,0.7] | 0.00007 | 0.00152 | To few points | To few points | To few points | To few points |
| V =[0.7,1.3] | 0.15244 | 0.04601 | 0.71400 | 0.00002 | To few points | To few points |
| V =[1.3,2.0] | 0.35063 | 0.33867 | 0.08944 | To few points | To few points | To few points |
| V =[2.0,2.7] | 0.06187 | 0.00000 | 0.32881 | To few points | To few points | To few points |
| V =[2.7,3.3] | 0.22558 | 0.00068 | 0.75148 | To few points | To few points | To few points |
| V =[3.3,4.0] | 0.06197 | 0.13389 | To few points | To few points | To few points | To few points |

Table 10-13: Results from Chi square test of Lindqvist ratio fitted to lognormal distribution.

| | h =[0.0,0.5] | h =[0.5,1.0] | h =[1.0,1.5] | h =[1.5,2.0] | h =[2.0,2.5] | h =[2.5,3.0] |
|---|---|---|---|---|---|---|
| V =[0.0,0.7] | 0.00027 | 0.00041 | To few points | To few points | To few points | To few points |
| V =[0.7,1.3] | 0.15244 | 0.01367 | 0.49833 | 0.00018 | To few points | To few points |
| V =[1.3,2.0] | 0.08397 | 0.31932 | 0.08944 | To few points | To few points | To few points |
| V =[2.0,2.7] | 0.01840 | 0.00000 | 0.96181 | To few points | To few points | To few points |
| V =[2.7,3.3] | 0.00830 | 0.00201 | 0.43980 | To few points | To few points | To few points |
| V =[3.3,4.0] | 0.17358 | 0.11319 | To few points | To few points | To few points | To few points |

Table 10-14: Results from Chi square test of Keinonen ratio fitted to lognormal distribution.

From the Chi square test is shown that the lognormal distribution does not describe the data very well in some cases and good in others. The distribution is well fitted for all data with ice thickness between 1 and 1.5 meters except one.

**Chi square test of the different ratios fitted to Weibull distribution:**

| | h =[0.0,0.5] | h =[0.5,1.0] | h =[1.0,1.5] | h =[1.5,2.0] | h =[2.0,2.5] | h =[2.5,3.0] |
|---|---|---|---|---|---|---|
| V =[0.0,0.7] | 0.00001 | 0.00000 | To few points | To few points | To few points | To few points |
| V =[0.7,1.3] | 0.09371 | 0.11161 | 0.76963 | 0.15730 | To few points | To few points |
| V =[1.3,2.0] | 0.01735 | 0.04445 | 0.47242 | To few points | To few points | To few points |
| V =[2.0,2.7] | 0.00005 | 0.00000 | 0.30355 | To few points | To few points | To few points |
| V =[2.7,3.3] | 0.01182 | 0.00000 | 0.62858 | To few points | To few points | To few points |
| V =[3.3,4.0] | 0.02026 | 0.11319 | To few points | To few points | To few points | To few points |

Table 10-15: Results from Chi square test of Riska ratio fitted to Weibull distribution.

| | h =[0.0,0.5] | h =[0.5,1.0] | h =[1.0,1.5] | h =[1.5,2.0] | h =[2.0,2.5] | h =[2.5,3.0] |
|---|---|---|---|---|---|---|
| V =[0.0,0.7] | 0.00004 | 0.00000 | To few points | To few points | To few points | To few points |
| V =[0.7,1.3] | 0.46922 | 0.34303 | 0.65802 | 0.15730 | To few points | To few points |
| V =[1.3,2.0] | 0.02396 | 0.08514 | 0.40120 | To few points | To few points | To few points |
| V =[2.0,2.7] | 0.00000 | 0.00000 | 0.64203 | To few points | To few points | To few points |
| V =[2.7,3.3] | 0.00000 | 0.00000 | 0.10540 | To few points | To few points | To few points |
| V =[3.3,4.0] | 0.00242 | 0.35352 | To few points | To few points | To few points | To few points |

Table 10-16: Results from Chi square test of Lindqvist ratio fitted to Weibull distribution.

| | h =[0.0,0.5] | h =[0.5,1.0] | h =[1.0,1.5] | h =[1.5,2.0] | h =[2.0,2.5] | h =[2.5,3.0] |
|---|---|---|---|---|---|---|
| V =[0.0,0.7] | 0.00005 | 0.00001 | To few points | To few points | To few points | To few points |
| V =[0.7,1.3] | 0.46922 | 0.22765 | 0.49833 | 0.07873 | To few points | To few points |
| V =[1.3,2.0] | 0.01735 | 0.02224 | 0.51040 | To few points | To few points | To few points |
| V =[2.0,2.7] | 0.00000 | 0.00000 | 0.64203 | To few points | To few points | To few points |
| V =[2.7,3.3] | 0.00304 | 0.00000 | 0.30772 | To few points | To few points | To few points |
| V =[3.3,4.0] | 0.00121 | 0.18653 | To few points | To few points | To few points | To few points |

Table 10-17: Results from Chi square test of Keinonen ratio fitted to Weibull distribution.

The Chi square test performed on different groups of data. The distribution describes some of the data good and other poorly as for the lognormal distribution. For all three ratios it is shown that all cases of ice thickness over 1 meter is described well by a Weibull distribution.

### 10.10.2 Residual plots

Residual plots for the statistical distributions are plotted for all ratios on the next figures. Both Lognormal and Weibull are plotted. From the residual plots it is easy to investigate how well the distributions fit the model.

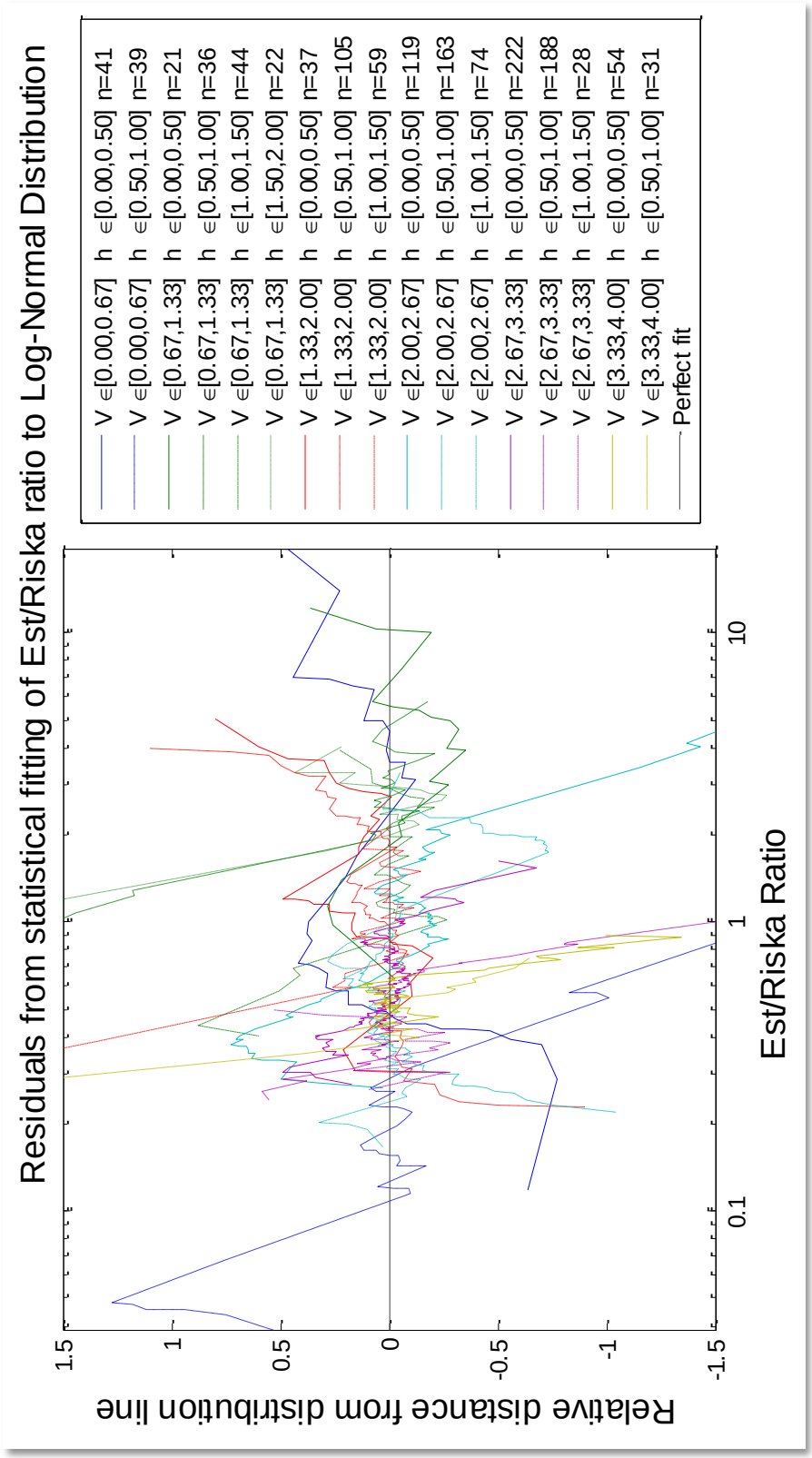


Figure 10-15: Residual curve from statistical fitting of Riska ratio to Lognormal Distribution.

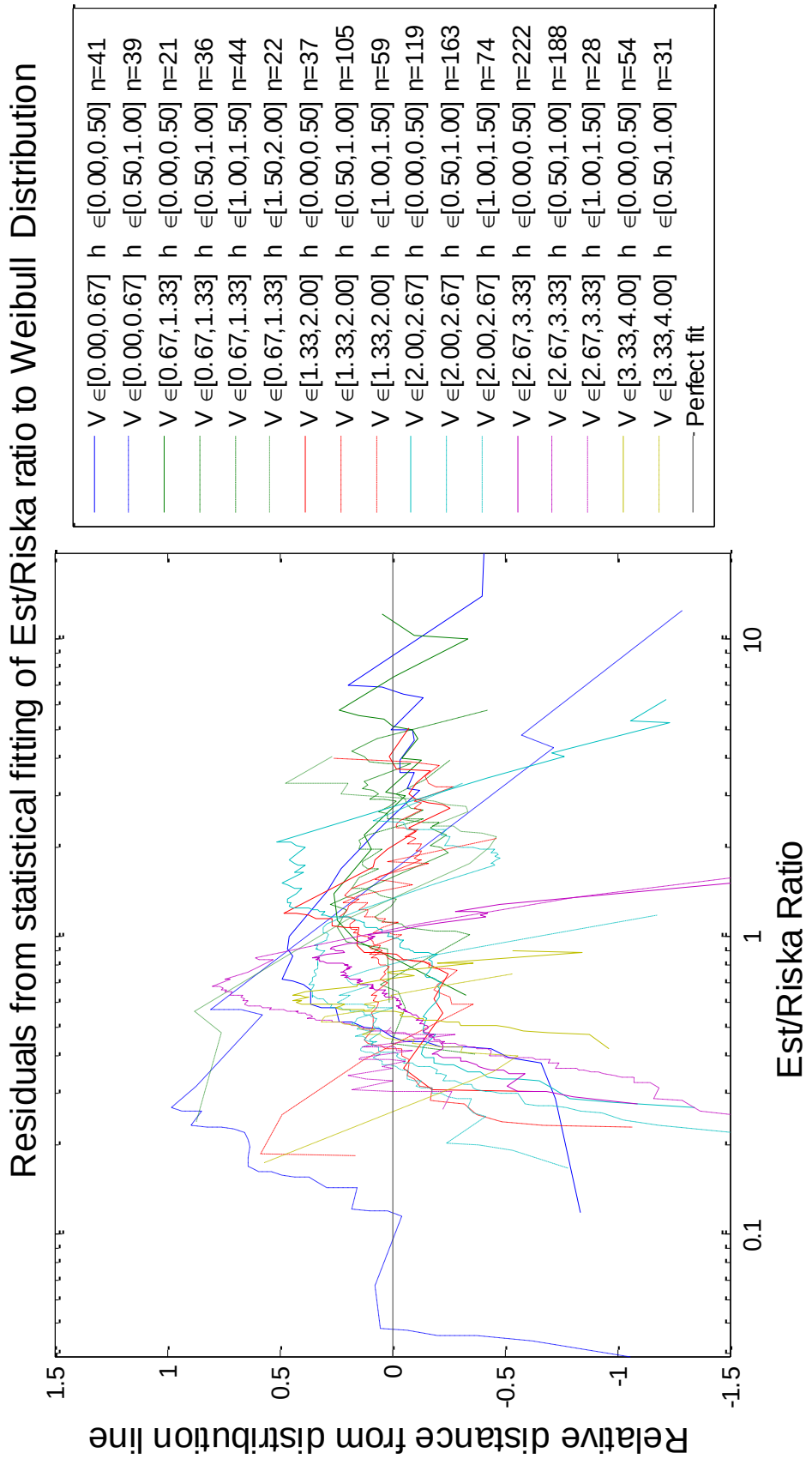


Figure 10-16: Residual curve from statistical fitting of Riska ratio to Weibull Distribution.

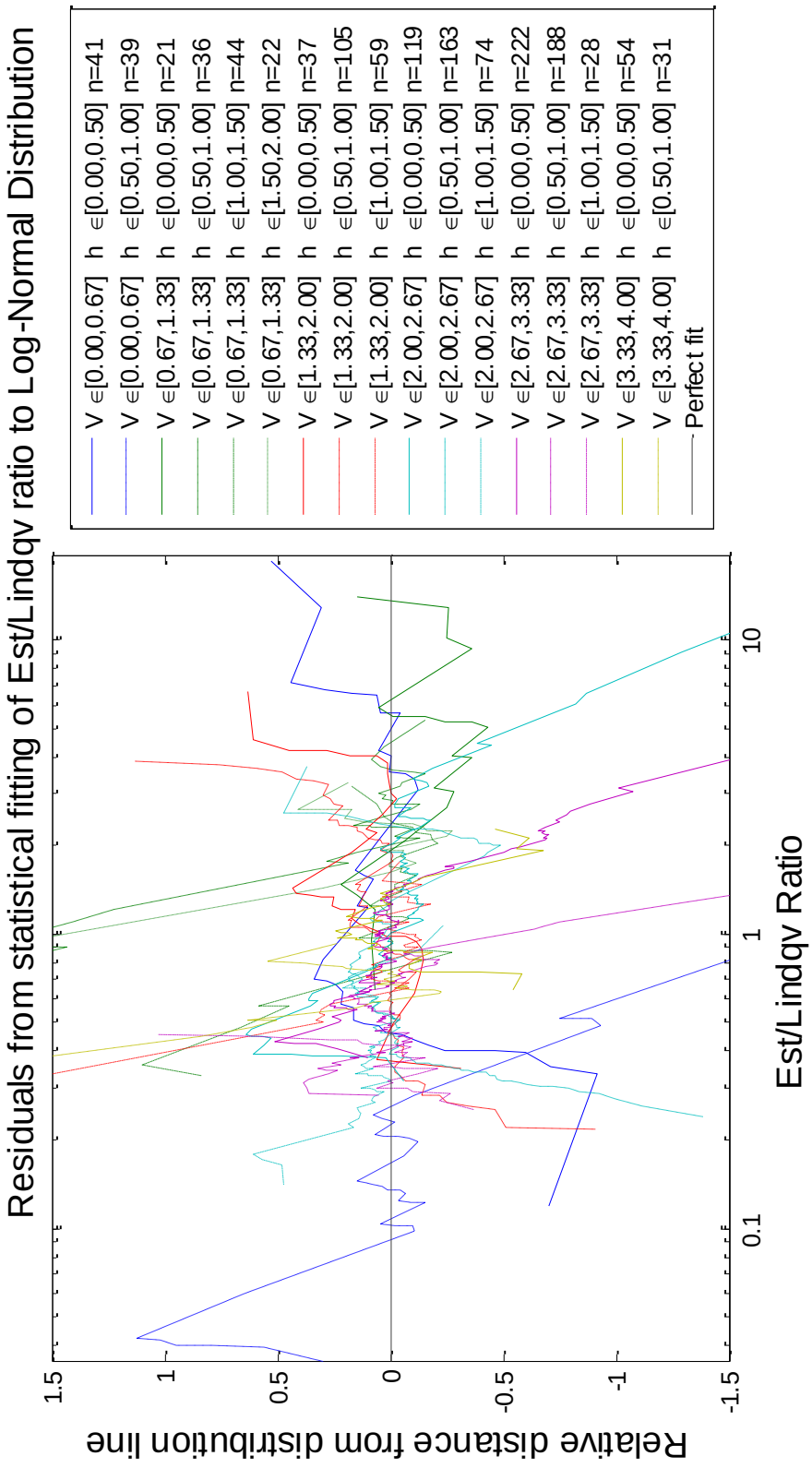


Figure 10-17: Residual curve from statistical fitting of Lindqvist ratio to Lognormal Distribution.

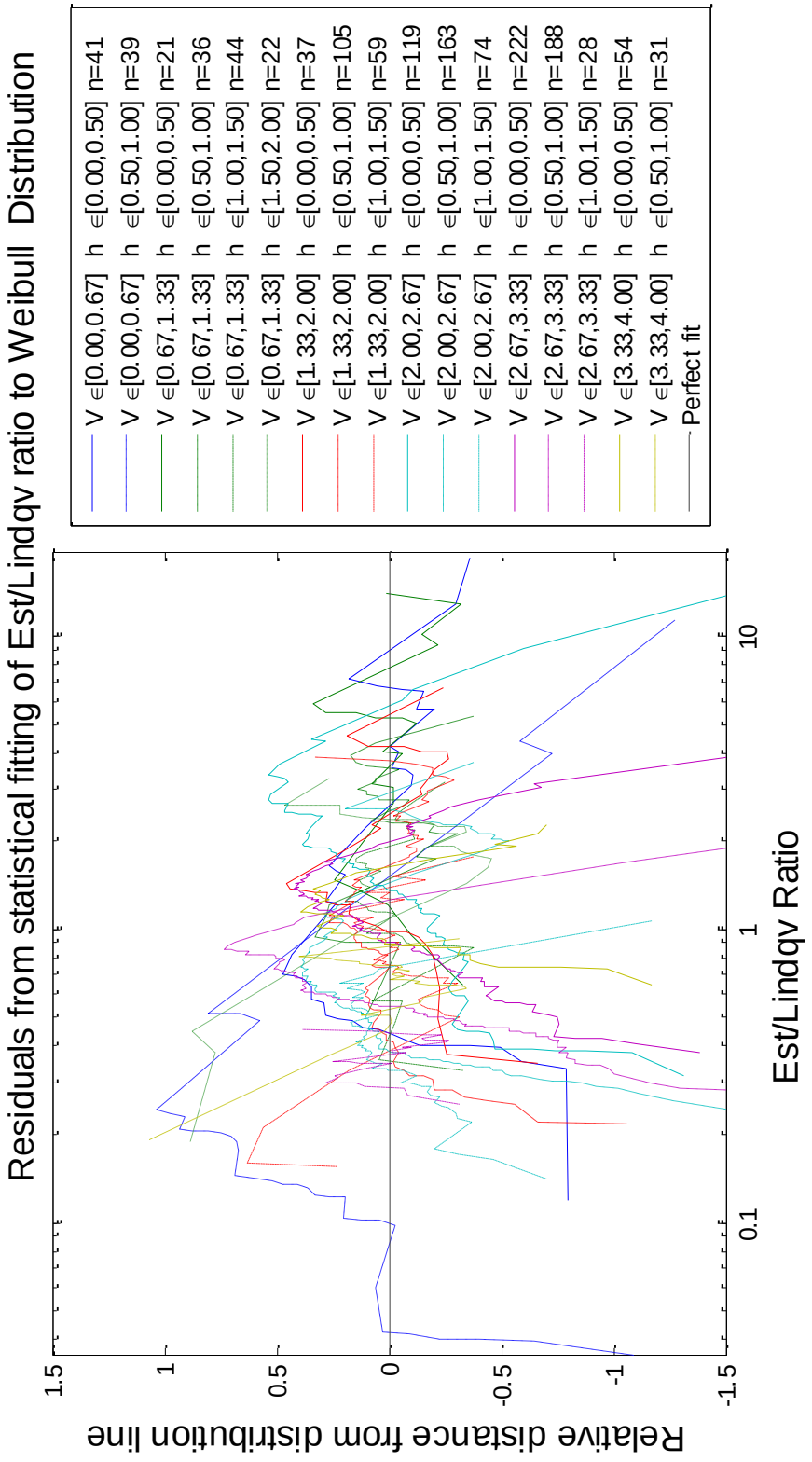


Figure 10-18: Residual curve from statistical fitting of Lindqvist ratio to Weibull Distribution.

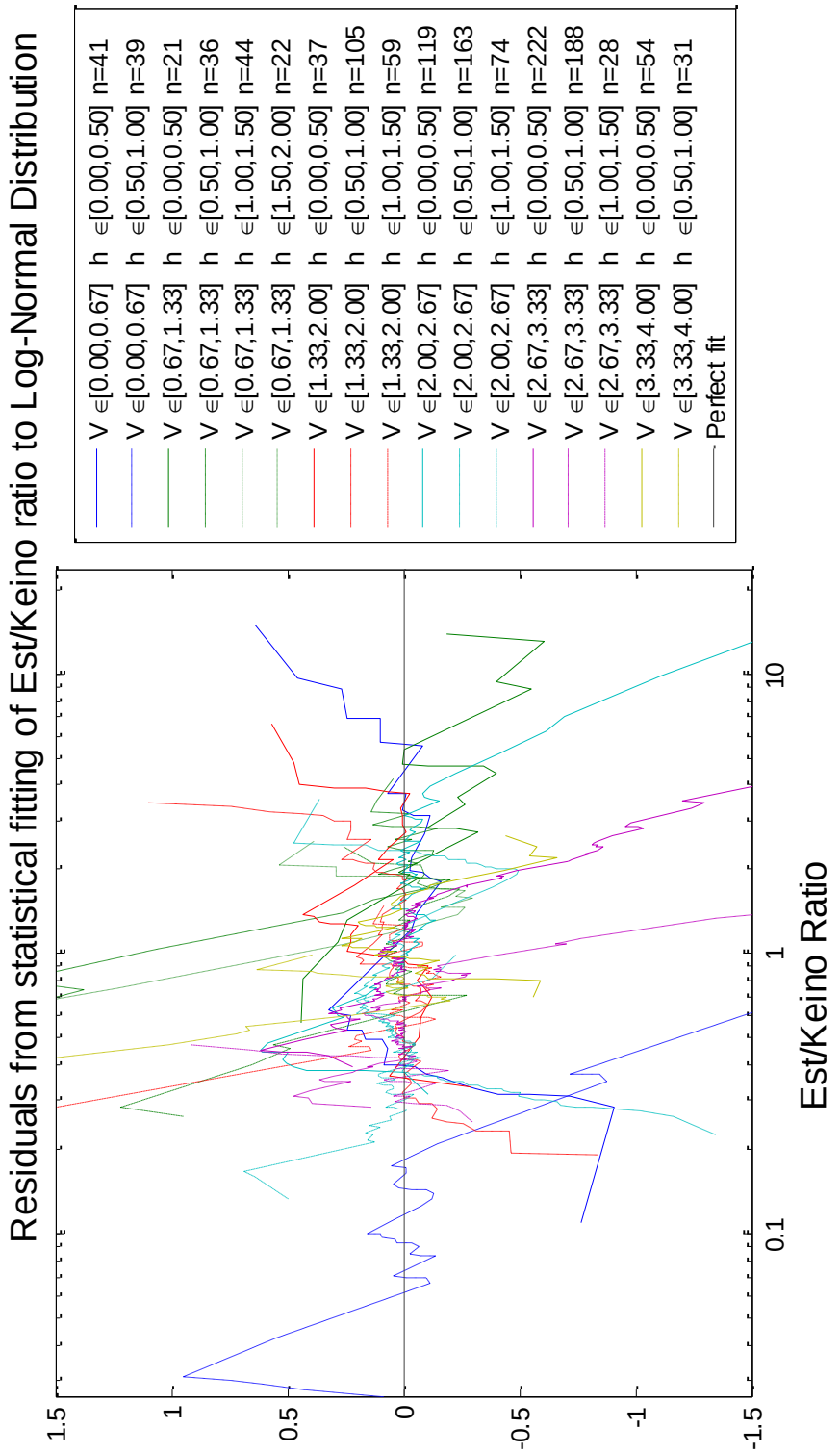


Figure 10-19: Residual curve from statistical fitting of Keinonen ratio to Lognormal Distribution,

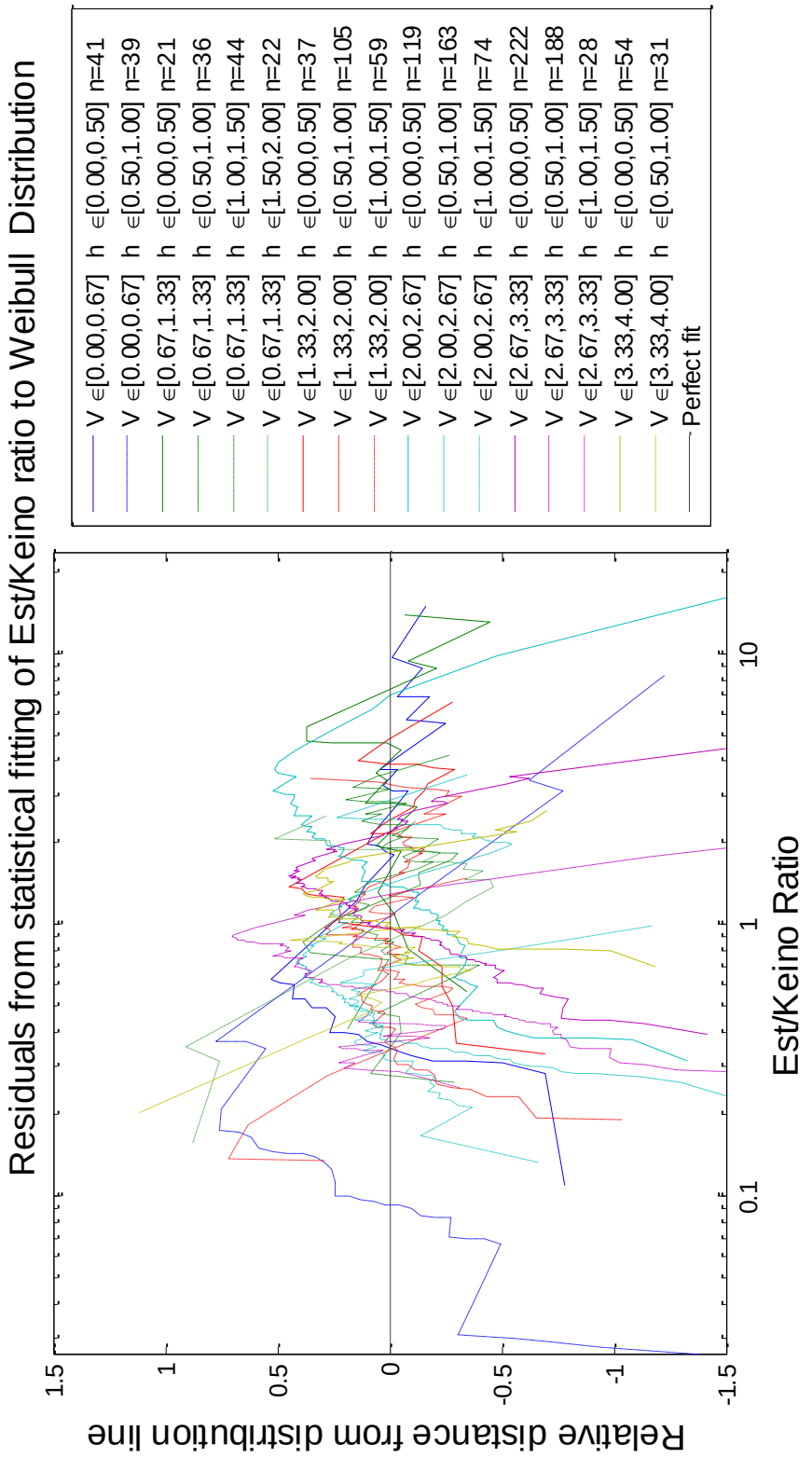


Figure 10-20: Residual curve from statistical fitting of Keinonen ratio to Weibull Distribution,

## 10.11 Idealized data

Abdillah Suyuthi is a Phd student at NTNU and has worked with the same raw data that is used in this thesis. In the full scale trial Kv Svalbard operated in unstable ice conditions. It is not easy to find a huge area to perform level ice trials. Therefore the data used in this thesis are not of high quality due to very varying ice thickness, areas with brash ice and large change in temperature. Suyuthi has chosen to investigate some selected time intervals where ice thickness and power out is steady over a time period of approximately 30 seconds.

Data points around three different ice thicknesses where obtained, 0.55 m, 1.05m and 1.55m. Due to few data points a linear fit is more suitable. The results are shown for Riska ratio in the graphs below.

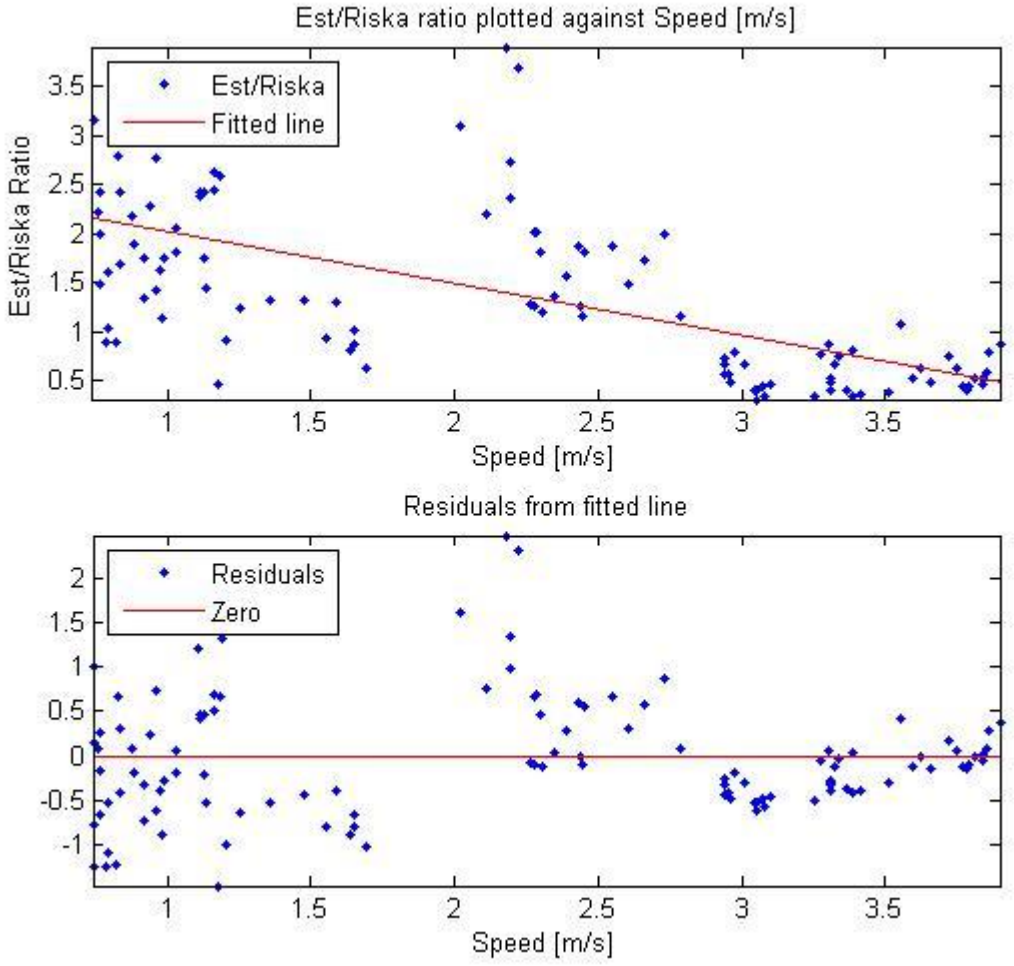


Figure 10-21: Riska ratio plotted against speed for idealized data.

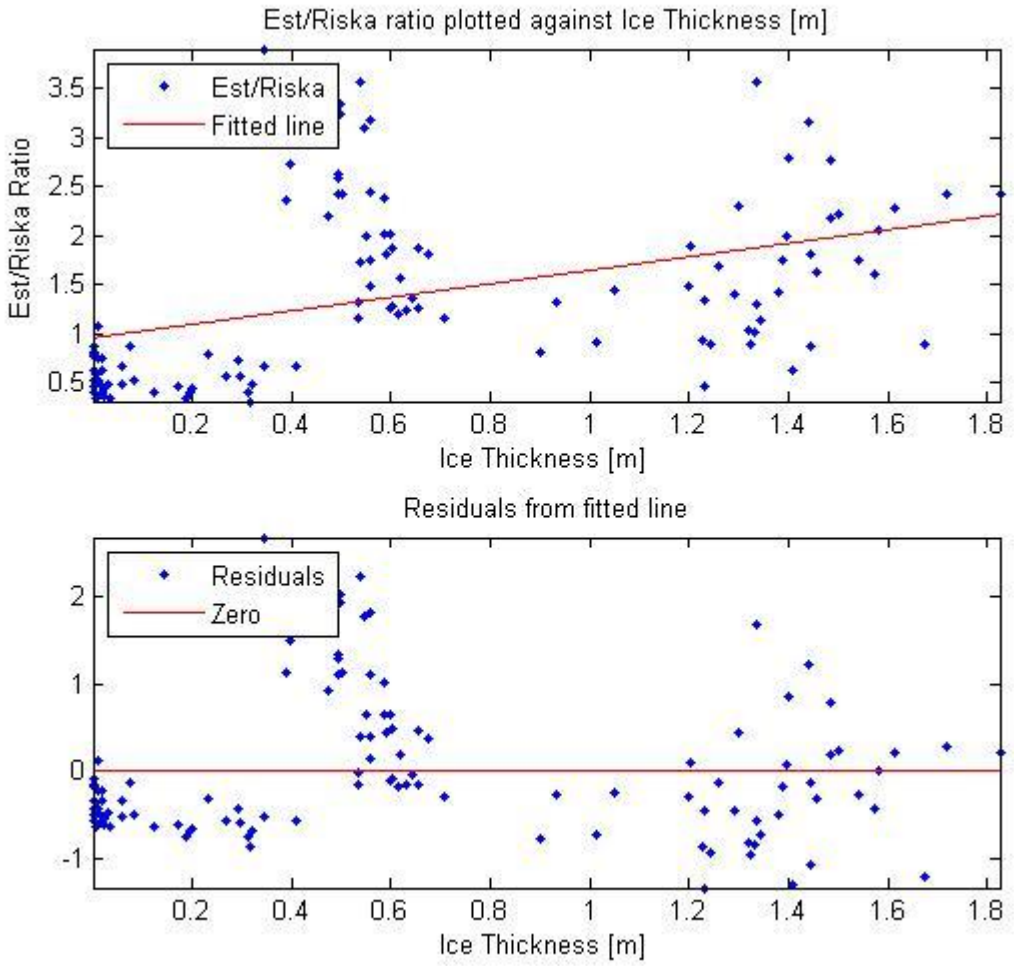


Figure 10-22: Riska ratio plotted against ice thickness for idealized data.

The results show that there is still a larger scatter, but not as huge scatter as for the other data. The data points are due to a few selected ice thicknesses concentrated in three areas.

# 11 Discussion and conclusion

## 11.1 Parameter sensitivity

The three different analytical methods have very different input parameter. Riska's method differs from the other methods since a lot of the ice properties are included in the estimated constant that work as input in the method. This makes it difficult to investigate the sensitivity of different ice properties in Riska's method. Keinonen is the only method depending on the temperature and it is shown that change in temperature influence the resistance significantly. The temperature is assumed to be constant in the calculations to simplify the calculations, but in the trials it varies from approximately plus 5 to minus 15 degrees. This will probably have some influence on the results.

## 11.2 Data used

The raw data obtained from the full scale trial with KV Svalbard are overall not good quality data. During the trial most of the ice where brash ice i.e. broken ice. In this thesis all ice is assumed to be level ice which is a large simplification. Many of the ice parameters, for example brine volume and density, will vary in different operating conditions due to change in temperature and types of ice. To simplify the calculations it is assume that the ice parameters, except ice thickness and vessel speed, are constant this may cause inaccurate results of the resistance.

Some idealized data was also investigated i.e. selected time intervals where ice thickness and the outgoing power is steady over a time period of approximately 30 seconds. This data had much fewer data points and only three different ice thicknesses where investigated. The scatter is lower but there was still a larger scatter than expected in the ratios. It should be noted that this results was fitted with a linear model due to very few data points. It would be interesting to investigate idealized data whit more data points and a larger interval of ice thickness.

## 11.3 Statistical results

From the statistical data it is seen that the analytical method behave quite similar. Lindqvist's method differs from the other two since there is no information on how the open water resistance should be taken into account for this method. Both Riska's method and Keinonen's method assume that the total resistance in ice can be super positioned by adding open water resistance to the ice resistance. If it is assumed that Lindqvist's method can calculate the total resistance in the same way, the results of the surface fit become significantly better and more similar to the other two methods.

For small speeds it is seen that the surface fit is rather poor for Riska and Lindqvist's methods, the scatter of data points here are large. However for larger speeds the fit seems to be better for all methods.

It is assumed in the calculations that the propeller efficiency is 100%. This is a rather large simplifications and it is more realistic to assume a lower value. To investigate the influence on the results different propeller efficiency where tested. These results illustrated that with decreasing propeller efficiency the analytical method became more conservative. Hence the analytical methods over predicted the resistance compared to the estimated resistance.

Due to the large scatter in the area of low speed the data was divided in subgroup to investigate specified intervals of ice thickness and speed. From the lognormal distributions it is seen that some intervals fits the distribution well and other fit the distribution poorly. When fitting the data to the weibull distribution the fit is good for ice thicknesses over 1 meter. For lower ice thickness the fit is in general poor. Other statistical distribution should be tested.

## 11.4 Conclusion

Which analytical method that predict the ice resistance best is hard to say. Because of many simplifications when calculating the measured resistance, the quality of these results needs improvement. All the analytical methods predict the resistance as a function of speed best. The dependence of ice thickness is very inaccurate and seems to fit best for thicknesses between 0.5m and 1.5m.

# 12 Further work

During the calculations in this thesis a number of simplifications in the calculations have been done due to lack of information. To improve the data used to calculate the resistance from full scale trials there are several points that should be investigated:

- Obtain data from a more steady ice condition and use data from areas without brash ice.
- Obtain of the propeller curves to avoid large simplifications in resistance calculations.
- The open water resistance should take into account wind and waves that will affect the resistance. In addition the open water resistance should be calculated from different speeds.
- Calculate the resistance with as a function of more input parameters, as for example temperature and flexural strength.

It would also be interesting to compare the analytical method and the estimated resistance form measurements with numerical methods of calculating the ice resistance.

# 13 References

[1] Ahlenius, H (2007) *Arctic sea routes - Northern sea route and Northwest Passage* [Internet], UNEP/GRID-Arendal, Available from: <http://maps.grida.no/go/graphic/arctic-sea-routes-northern-sea-route-and-northwest-passage> [Downloaded 20.october 2011]

[2] Forsvaret (2011) *Kystvaktens fartøy KV Svalbard* Available from: <http://forsvaret.no/om-forsvaret/utstyrsfakta/Sider/sjo.aspx>[Downloaded 14.november 2011]

[3] Furnes, Gunnar (2011) *Ice1- Lecture notes.* NTNU

[4] Frankenstein, G, Garner, R (1967) *Short note – Equations for determining brine volume of sea ice from -0,5$^{o}$ to – 22,0$^{o}$.* U.S. Army Cold Region Research and Engineering Labaratory, Hanover, New Hampshire, U.S.A.

[5] Ice ridge [Internet] Available from: <http://kaldtklima.net/node/233>[Downloaded 6.october 2011]

[6] Keinonen, A, Browne, R.P, Revill, C.R., Bayly, I.M (1991) *Ice Performance Prediction* . AKAC, Calgary, Alberta, Canada.

[7] Keinonen, A, Browne, R.P, Revill, C.R., Reynolds, A (1996) *Icebreaker characteristics synthesis.* AKAC, Calgary, Alberta, Canada.

[8] Leira, B, Børsheim, L, Espeland, Ø & Amdahl, J (2009) *Ice-load estimation for a ship hull based on continuous response monitoring.* NTNU, Trondheim, Norway.

[9] Lindqvist, Gustav (1989) *A straight forward method for calculation of ice resistance of ships.*

[10] Lubbad, R & Løseth, S (2010) *A numerical model for real-time simulation of ship–ice interaction*. NTNU

[11] Martio, Jussi (2007) *Numerical Simulation of Vessel`s Manoeuvring Performance in Uniform Ice.* Helsinki University of Technology

[12] Mike Usher (2005)*Pressure ridge in sea-ice* [Internet], Antarctica Travel Picture Gallery, Available from: <http://www.coolantarctica.com/gallery/travel/antarctica0032.html>[Downloaded 17.november 2011]

[13] Mæjlender-Larsen, M (2008) *Ice load monitoring (ILM),* Maritime Technology and Production center. [Internet] Available from: <http://www.tekna.no/ikbViewer/Content/34342/Mejl%E6nder-Larsen%20Morten.pdf>[Downloaded 5.october 2011]

[14] Mæjlender-Larsen, M (2007) *Sea Ice Observations on KV Svalbard-ILM,* Det norske Veritas.

[15] Riska, Kaj (2011) *Ice 2- Lecture notes.* NTNU

[16] Sand, Bjørnar (2008) N*onlinear finite element simulations of ice forces on offshore structures.* Lulea University of Technology

[17] Skår, Torstein (2011) *Ice induced resistance of ship hulls.* NTNU

[18] Su, B, Riska, K & Moan,T (2010) *A numerical method for the prediction of ship performance in level ice.* NTNU, Trondheim, Norway.

[19] Suyuthi, A, Leira, B. J. & Riska, K (2011) *Full Scale Measurement on Level Ice Resistance of Icebreaker.* Trondheim, Norway.

[20] The mathworks (1994-2012) *Matlab 2009b Help.* [Internet] Available from: < http://www.mathworks.se/>

[21] Timco, G. W. & Brien, S. O. (1994) *Flexural strength equation for sea ice.* National Research Council, Ottawa, Canada.

[22] Timco, G.W. & Weeks, W.F. (2010) *A review of the engineering properties of sea ice.* National Research Council, Ottawa, Canada.

[23] Valkonnen, J, Cammaert,G & Meljænder-Larsen, M, *Field Program for Simulation of Station-keeping Conditions for Arctic Drilling and Production Vessels.* DNV Maritime

[24] European Commision (2012) *Safeice-Increasing the safety of Icebound Shipping* [Internet] Available from: <http://ec.europa.eu/research/transport/projects/items/safeice_en.htm> [Downloaded 10.april 2012]

[25] Pfaffling, A. & Mejlænder-Larsen, M (2007) *Sea Ice Observations on KV Svalbard- Ice load monitoring project (ILM).* Det Norske Veritas (DNV)

[26] Pfaffling, A. &Haas, Dr C. (2007) *Ship-borne sea ice thickness electromagnetic measurements.* Det Norske Veritas (DNV), Høivik, Norway.

[27] Maben, A.F, *Chi square test.* [Internet] Available from: < http://www.enviroliteracy.org/pdf/materials/1210.pdf> [Downloaded 12.may 2012]

# Appendix A Calculations in MATLAB

The MATLAB program used has been developed by Torstein Skår on figure A-1 and A-2 there are two flow charts made by Skår that illustrates how the program work. A third analytical method has been added and the needed modification of the program has been done by the author.

The script is built up around a main file that reads in all the information from an input file. In the input file several things must be defined:

1. Time length for statistical analysis of raw data
2. Filename for data selection
3. Filename for resistance calculation
4. Data selection method (data selected from raw data or data selected by Suyuthi)
5. Which plots you want (scatter plot, surface fit, lognormal etc.)

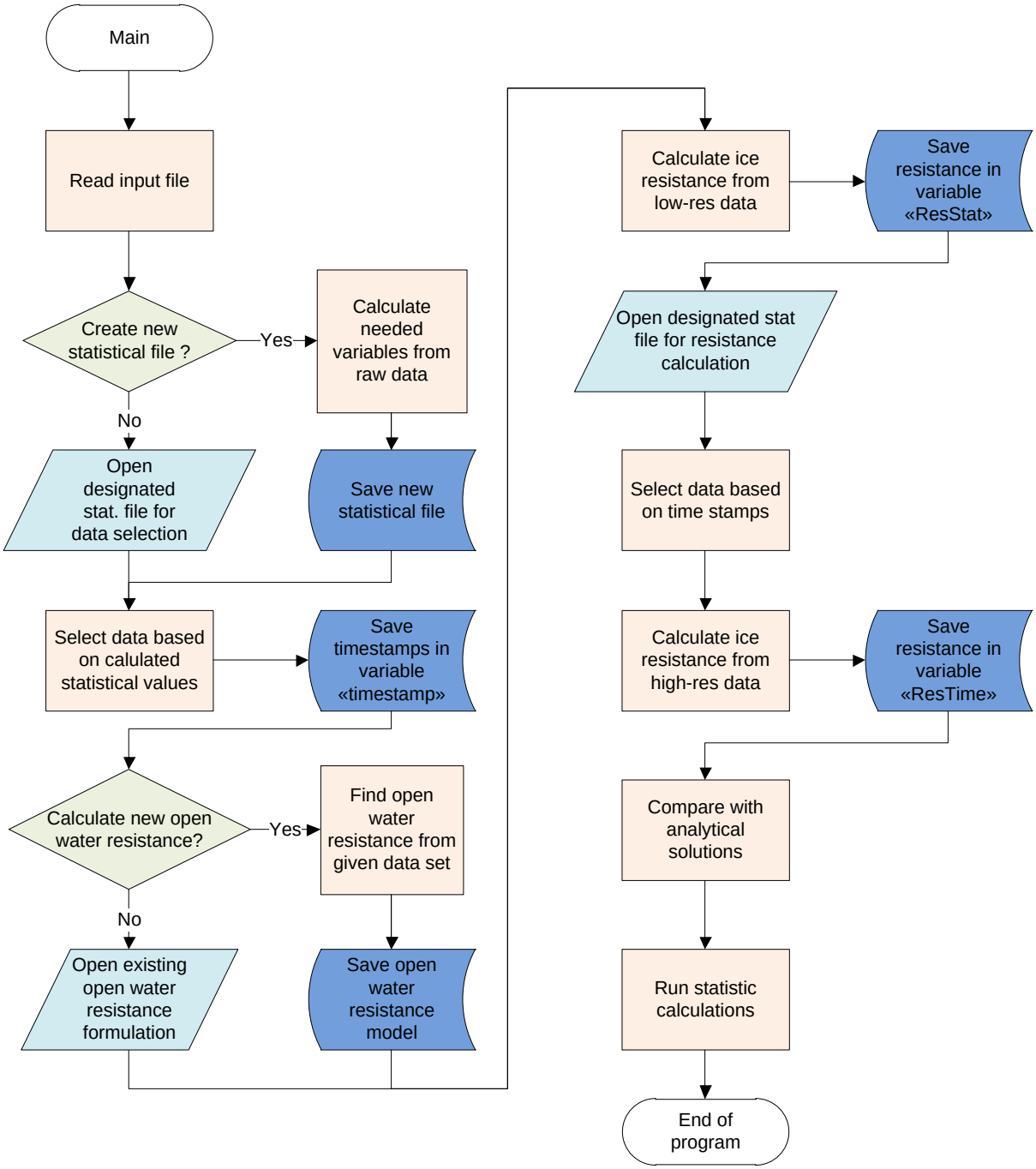


**Figure A-0-1: Flow chart on how the MATLAB program work [17]**

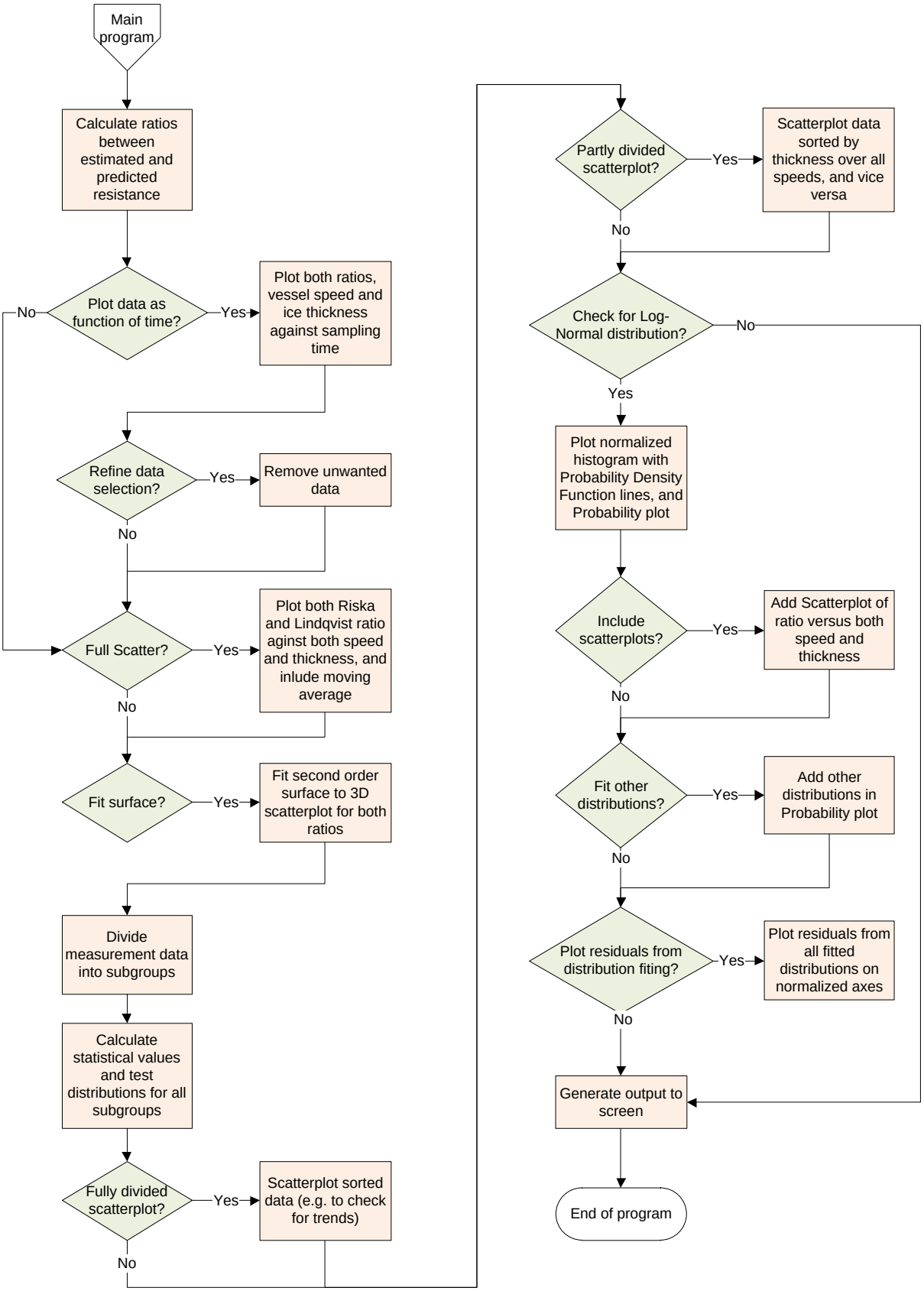


**Figure A-0-2: Flow chart on how the statistical calculation part in MATLAB works. [17]**

# Appendix B Sensitivity plot

## B.1 Flexural strength

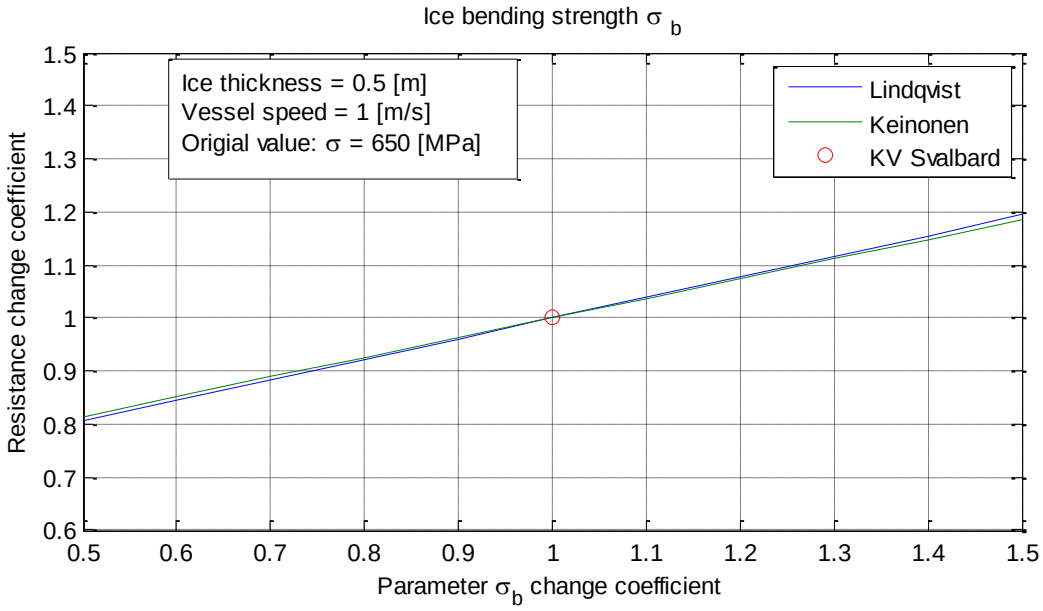


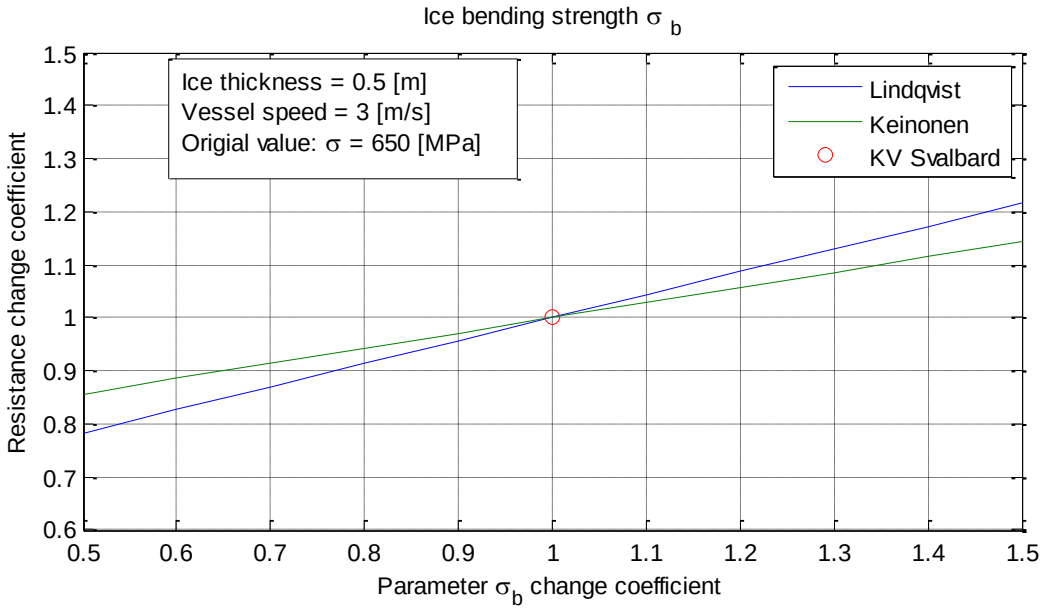

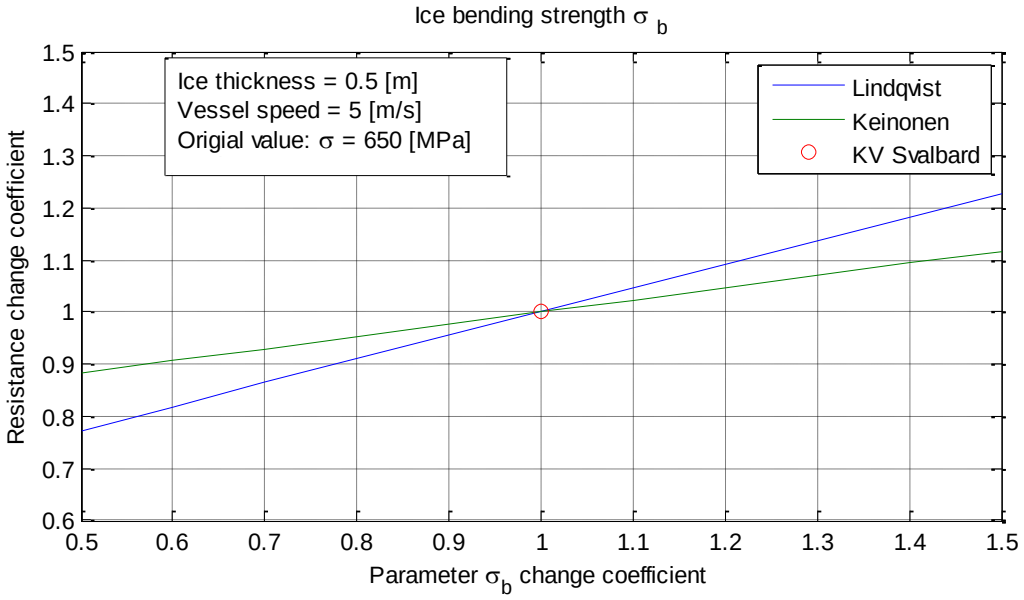
Ice bending strength σ b
Ice thickness = 0.5 [m]
Vessel speed = 5 [m/s]
Origial value: σ = 650 [MPa]
Lindqvist
Keinonen
KV Svalbard
Resistance change coefficient
Parameter σb change coefficient
1.5
1.4
1.3
1.2
1.1
1
0.9
0.8
0.7
0.6
0.5
0.6
0.7
0.8
0.9
1
1.1
1.2
1.3
1.4
1.5

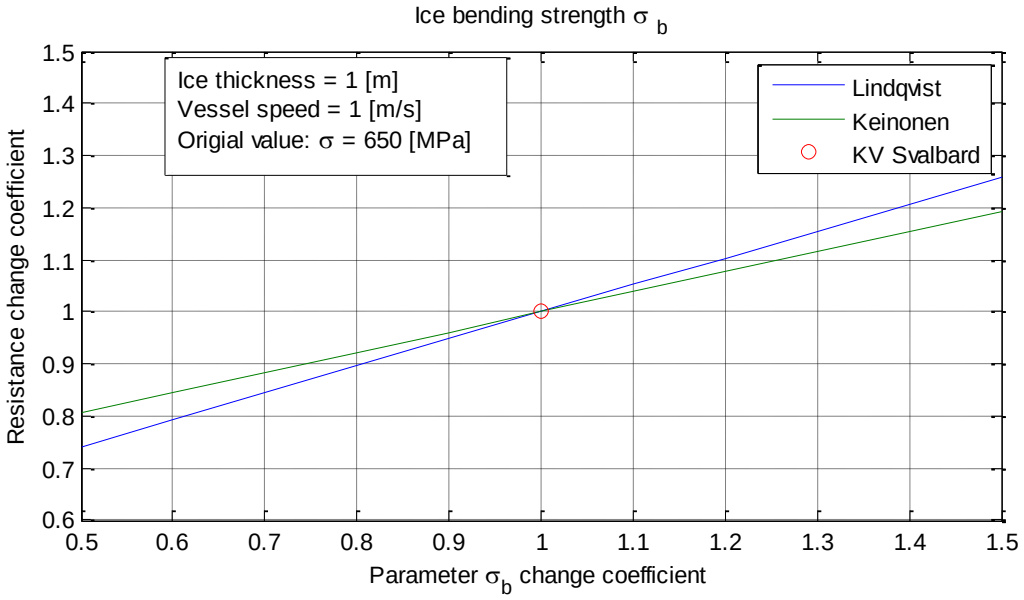
Ice bending strength σ b
Ice thickness = 1 [m]
Vessel speed = 1 [m/s]
Origial value: σ = 650 [MPa]
Lindqvist
Keinonen
KV Svalbard
Resistance change coefficient
Parameter σb change coefficient
1.5
1.4
1.3
1.2
1.1
1
0.9
0.8
0.7
0.6
0.5
0.6
0.7
0.8
0.9
1
1.1
1.2
1.3
1.4
1.5

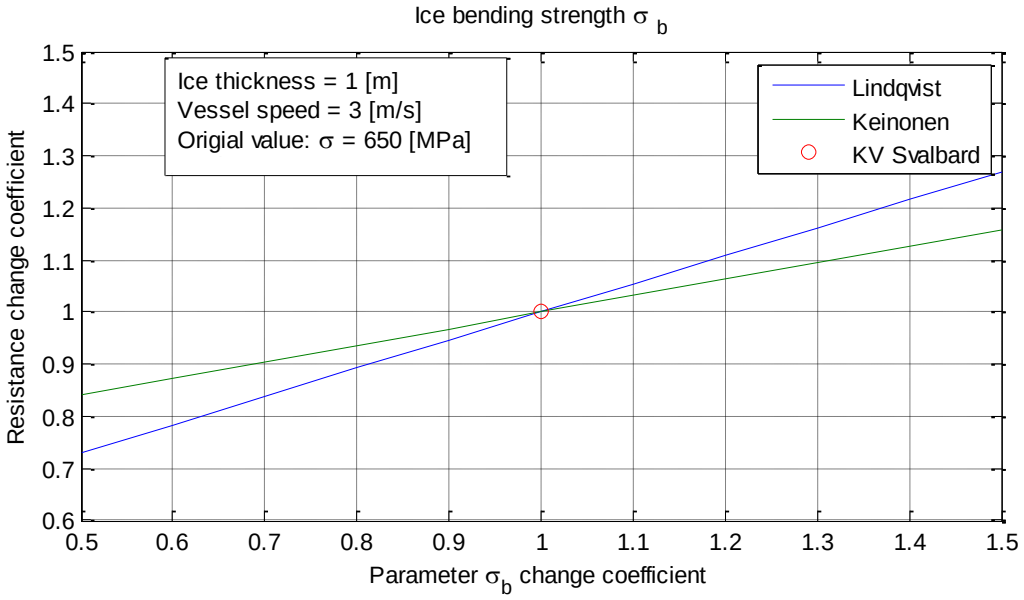
Ice bending strength σ b
Ice thickness = 1 [m]
Vessel speed = 3 [m/s]
Origial value: σ = 650 [MPa]
Lindqvist
Keinonen
KV Svalbard
Resistance change coefficient
Parameter σb change coefficient
1.5
1.4
1.3
1.2
1.1
1
0.9
0.8
0.7
0.6
0.5
0.6
0.7
0.8
0.9
1
1.1
1.2
1.3
1.4
1.5

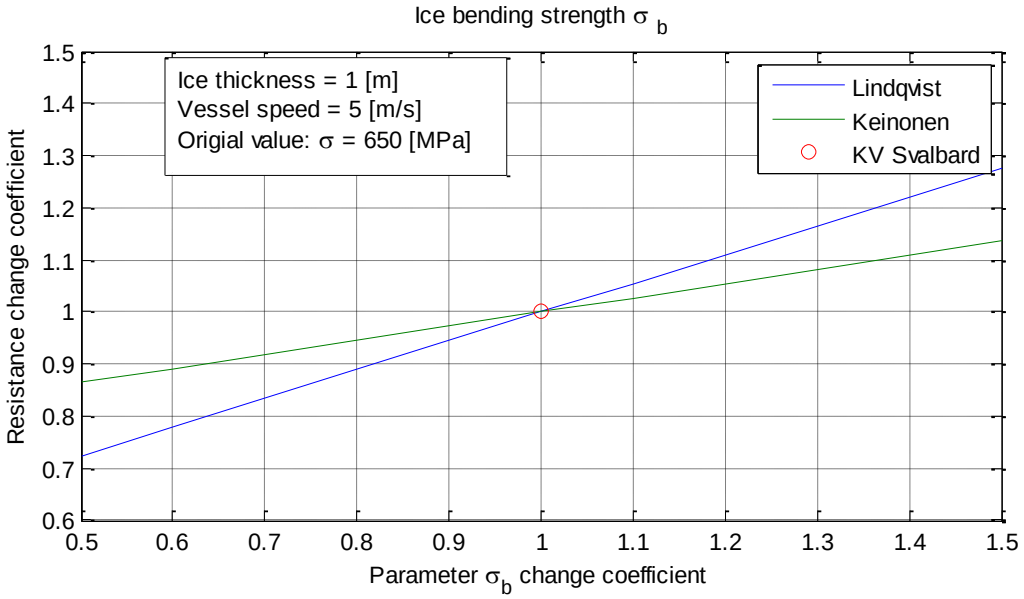
Ice bending strength σ b
Ice thickness = 1 [m]
Vessel speed = 5 [m/s]
Origial value: σ = 650 [MPa]
Lindqvist
Keinonen
KV Svalbard
Resistance change coefficient
Parameter σb change coefficient
1.5
1.4
1.3
1.2
1.1
1
0.9
0.8
0.7
0.6
0.5
0.6
0.7
0.8
0.9
1
1.1
1.2
1.3
1.4
1.5

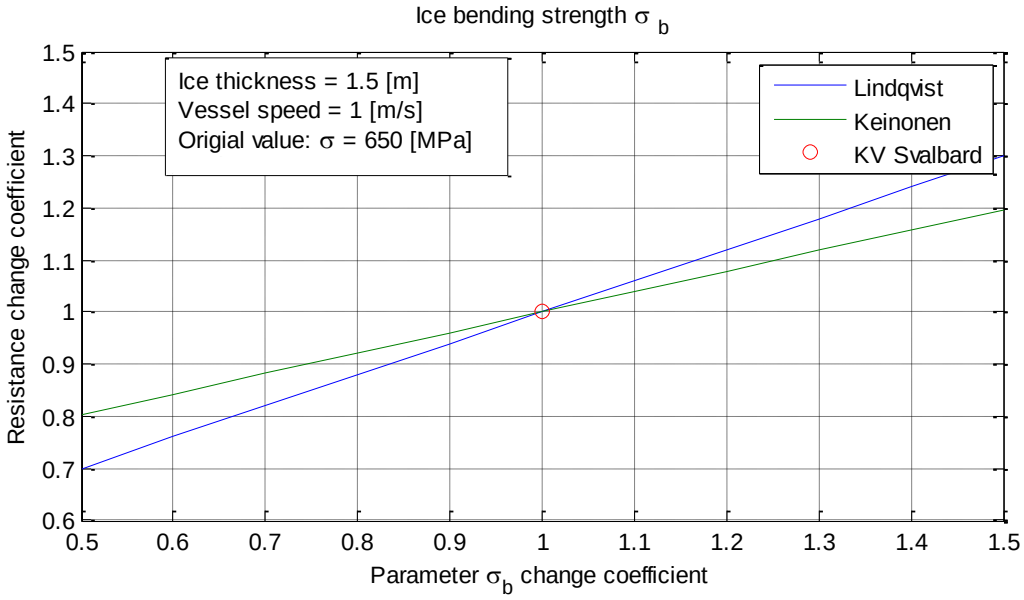
Ice bending strength σ b
Ice thickness = 1.5 [m]
Vessel speed = 1 [m/s]
Origial value: σ = 650 [MPa]
Lindqvist
Keinonen
KV Svalbard
Resistance change coefficient
Parameter σb change coefficient
0.5 0.6 0.7 0.8 0.9 1 1.1 1.2 1.3 1.4 1.5
0.6 0.7 0.8 0.9 1 1.1 1.2 1.3 1.4 1.5

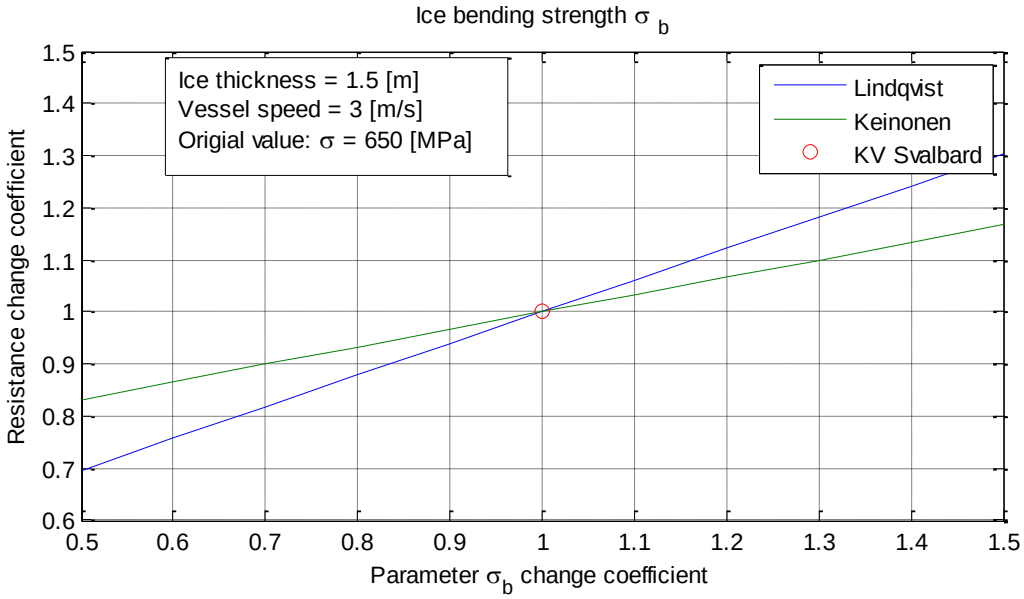
Ice bending strength σ b
Ice thickness = 1.5 [m]
Vessel speed = 3 [m/s]
Origial value: σ = 650 [MPa]
Lindqvist
Keinonen
KV Svalbard
Resistance change coefficient
Parameter σb change coefficient
0.5 0.6 0.7 0.8 0.9 1 1.1 1.2 1.3 1.4 1.5
0.6 0.7 0.8 0.9 1 1.1 1.2 1.3 1.4 1.5

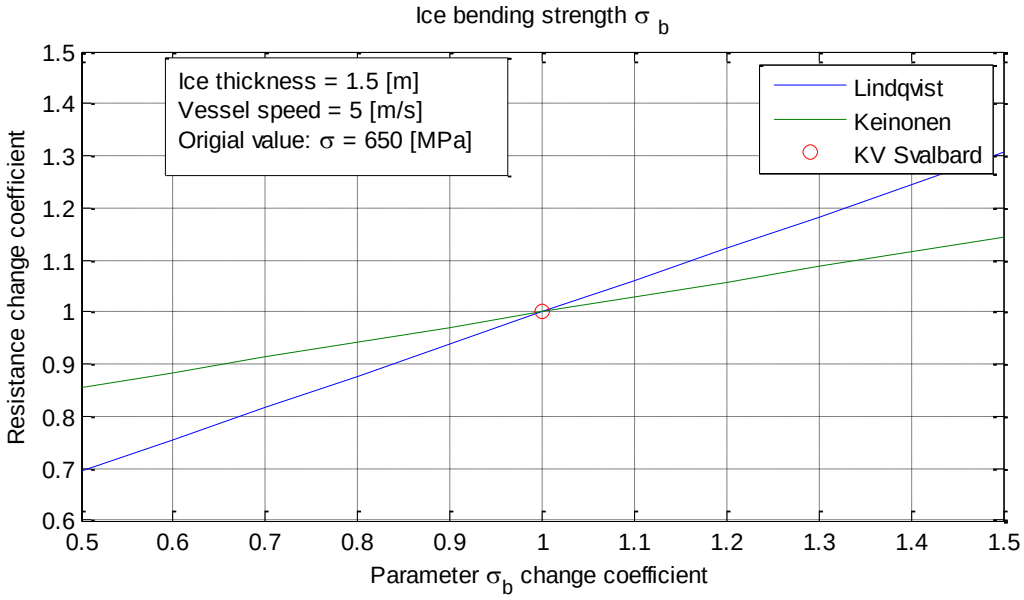


## B.2 Stem angle (bow angle)

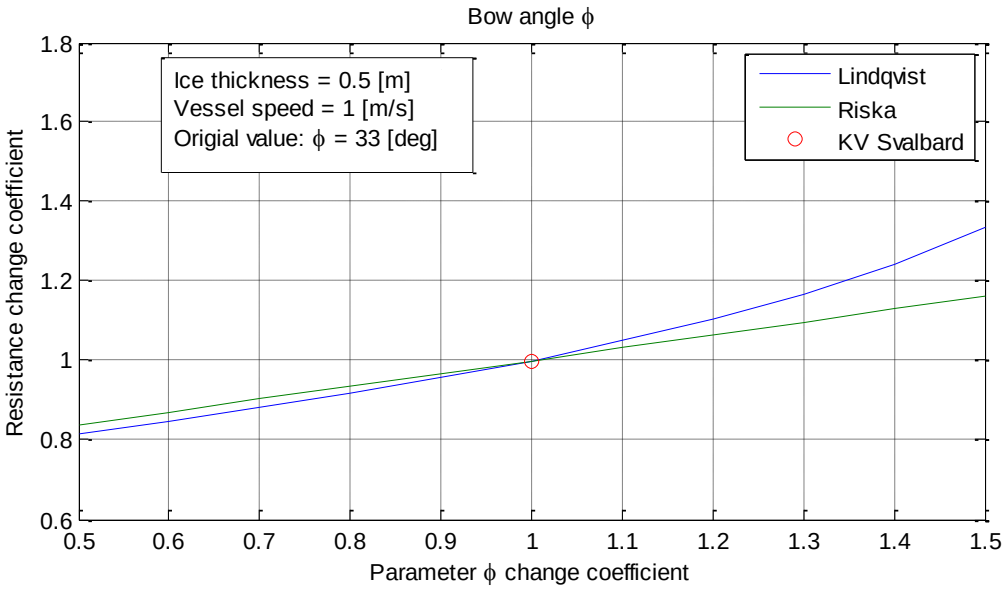

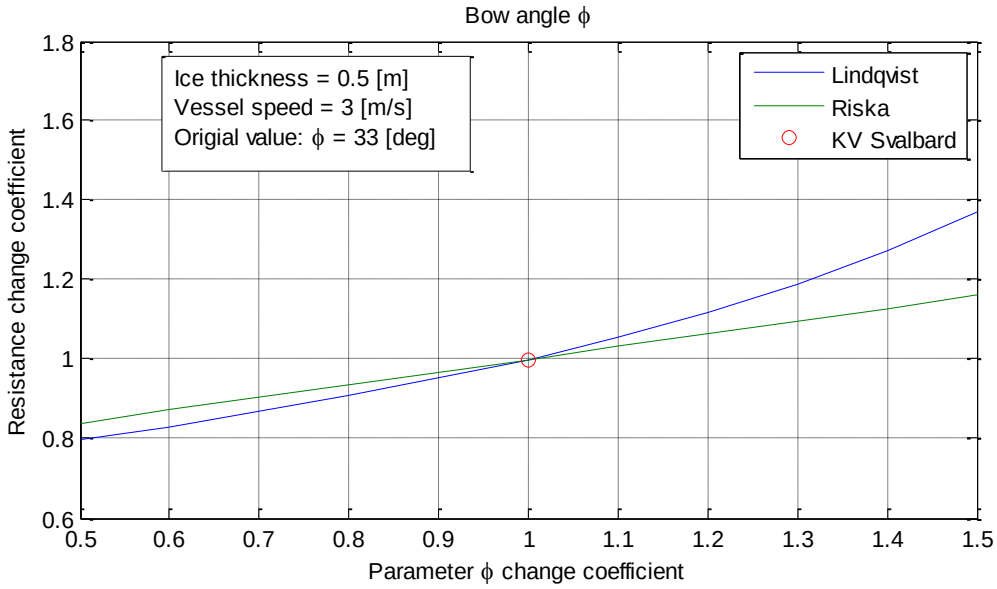
Bow angle ϕ
Ice thickness = 0.5 [m]
Vessel speed = 3 [m/s]
Origial value: ϕ = 33 [deg]
Lindqvist
Riska
KV Svalbard
Resistance change coefficient
Parameter ϕ change coefficient

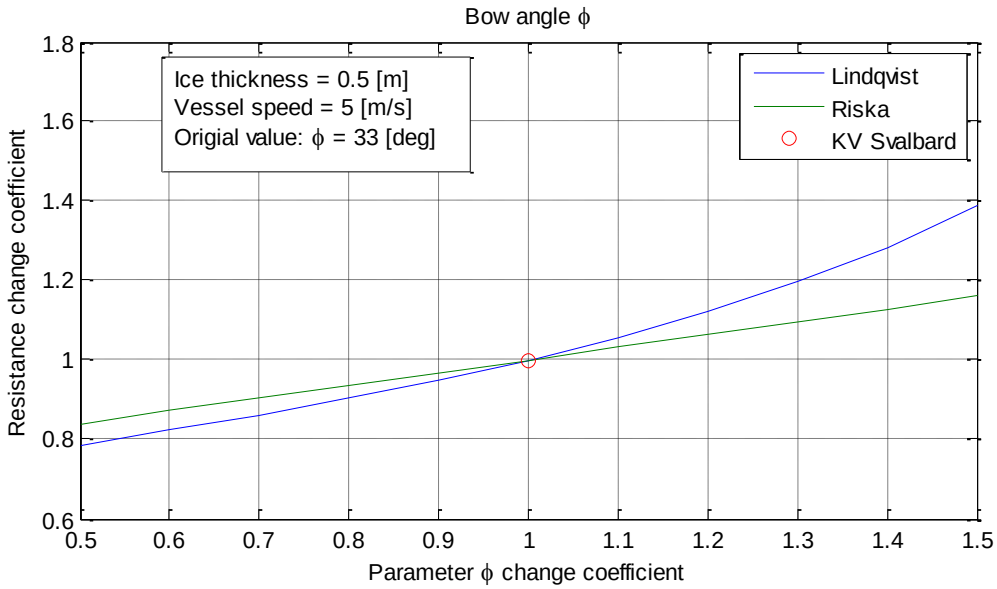
Bow angle ϕ
Ice thickness = 0.5 [m]
Vessel speed = 5 [m/s]
Origial value: ϕ = 33 [deg]
Lindqvist
Riska
KV Svalbard
Resistance change coefficient
Parameter ϕ change coefficient

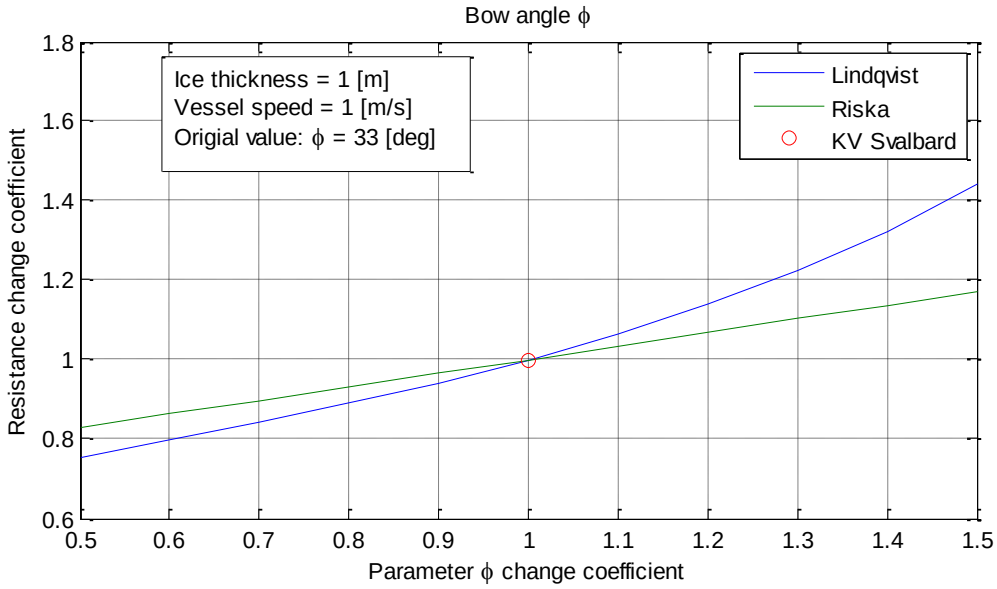
Bow angle ϕ
Ice thickness = 1 [m]
Vessel speed = 1 [m/s]
Origial value: ϕ = 33 [deg]
Lindqvist
Riska
KV Svalbard
Resistance change coefficient
Parameter ϕ change coefficient

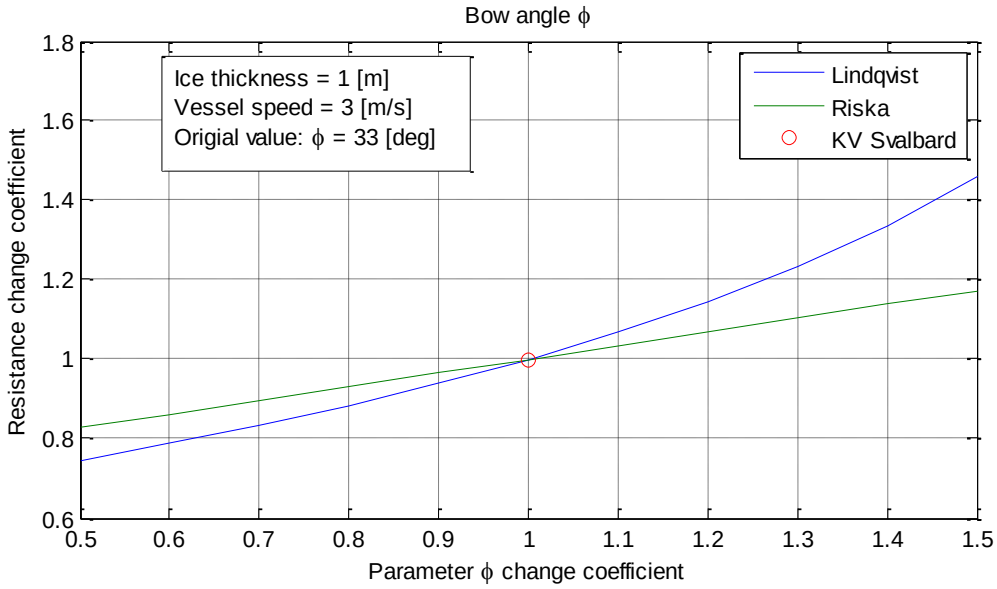
Bow angle ϕ
Ice thickness = 1 [m]
Vessel speed = 3 [m/s]
Origial value: ϕ = 33 [deg]
Lindqvist
Riska
KV Svalbard
Resistance change coefficient
Parameter ϕ change coefficient

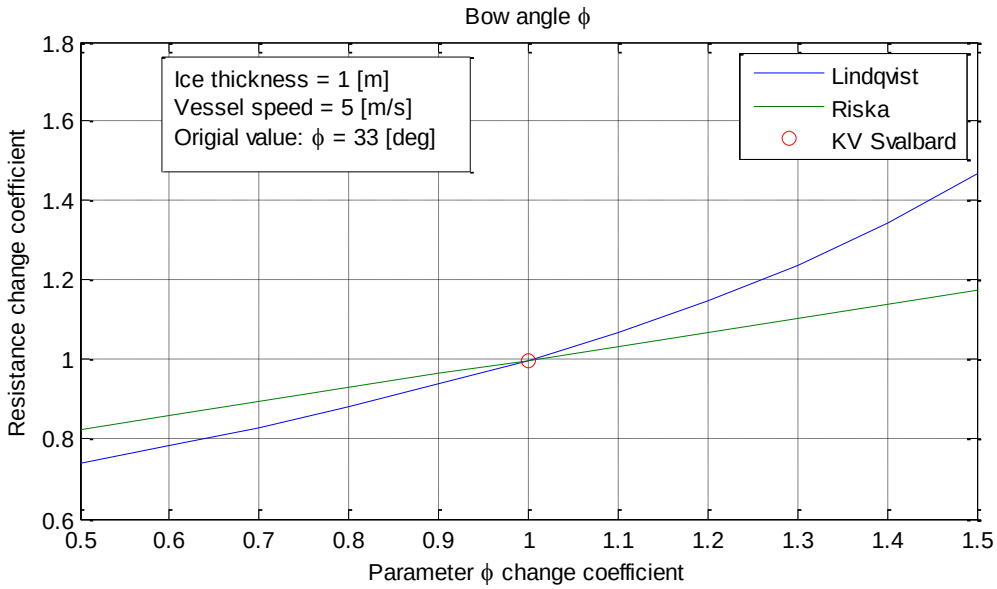
Bow angle ϕ
Ice thickness = 1 [m]
Vessel speed = 5 [m/s]
Origial value: ϕ = 33 [deg]
Lindqvist
Riska
KV Svalbard
Resistance change coefficient
Parameter ϕ change coefficient

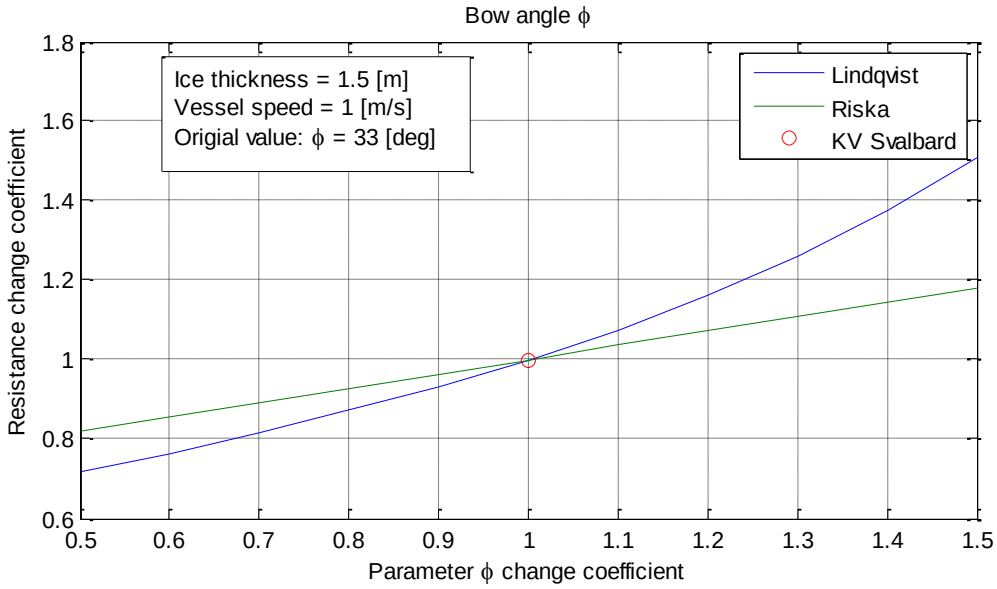
Bow angle ϕ
Ice thickness = 1.5 [m]
Vessel speed = 1 [m/s]
Origial value: ϕ = 33 [deg]
Lindqvist
Riska
KV Svalbard
Resistance change coefficient
Parameter ϕ change coefficient

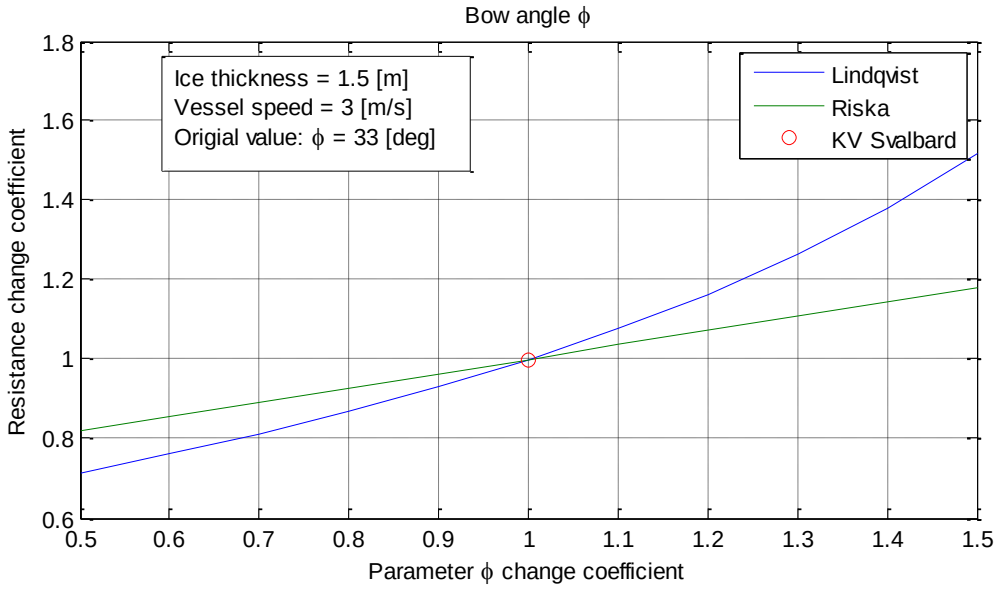
Bow angle ϕ
Ice thickness = 1.5 [m]
Vessel speed = 3 [m/s]
Origial value: ϕ = 33 [deg]
Lindqvist
Riska
KV Svalbard
Resistance change coefficient
Parameter ϕ change coefficient
1.8
1.6
1.4
1.2
1
0.8
0.6
0.5
0.6
0.7
0.8
0.9
1
1.1
1.2
1.3
1.4
1.5

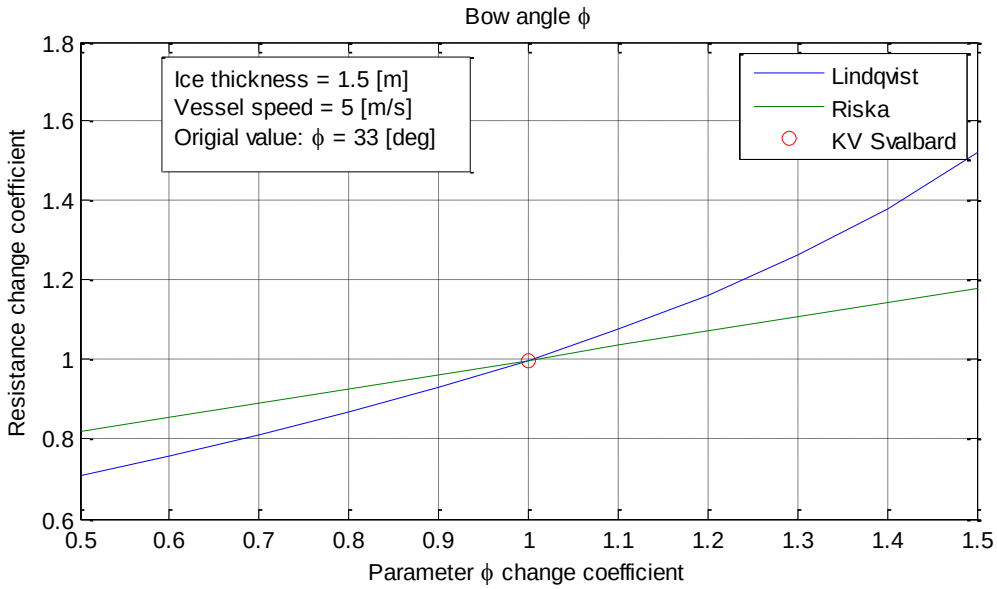
Bow angle ϕ
Ice thickness = 1.5 [m]
Vessel speed = 5 [m/s]
Origial value: ϕ = 33 [deg]
Lindqvist
Riska
KV Svalbard
Resistance change coefficient
Parameter ϕ change coefficient
1.8
1.6
1.4
1.2
1
0.8
0.6
0.5
0.6
0.7
0.8
0.9
1
1.1
1.2
1.3
1.4
1.5

## B.3 Temperature

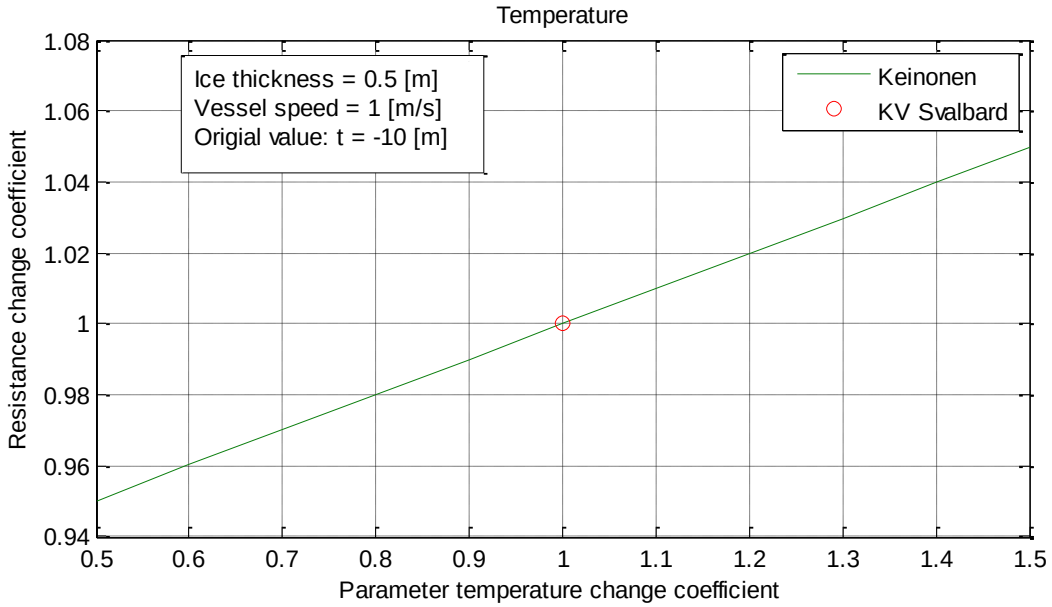


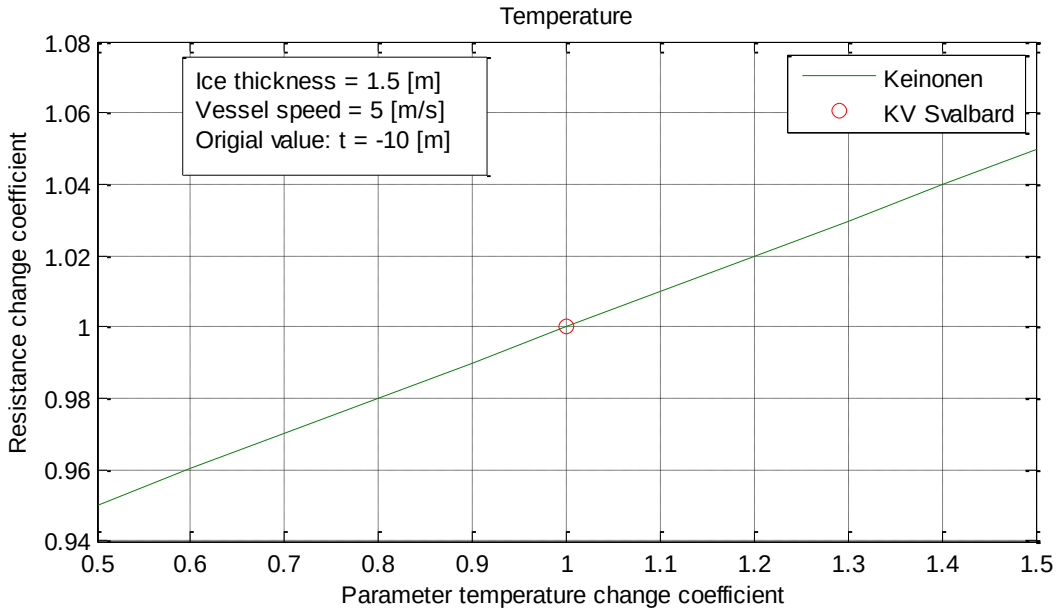

## B.3 Friction

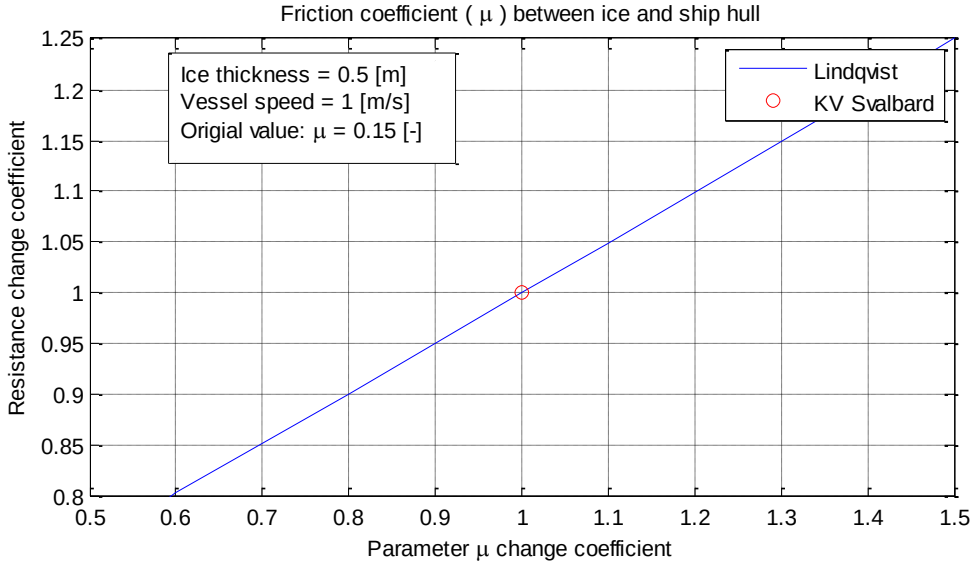
Friction coefficient ( μ ) between ice and ship hull
Ice thickness = 0.5 [m]
Vessel speed = 1 [m/s]
Origial value: μ = 0.15 [-]
Lindqvist
KV Svalbard
Resistance change coefficient
Parameter μ change coefficient

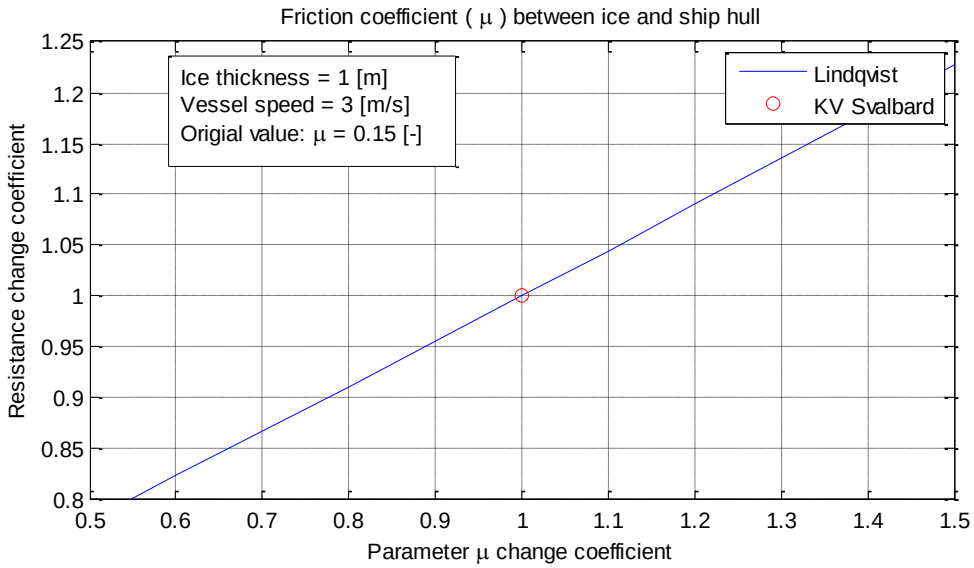
Friction coefficient ( μ ) between ice and ship hull
Ice thickness = 1 [m]
Vessel speed = 3 [m/s]
Origial value: μ = 0.15 [-]
Lindqvist
KV Svalbard
Resistance change coefficient
Parameter μ change coefficient

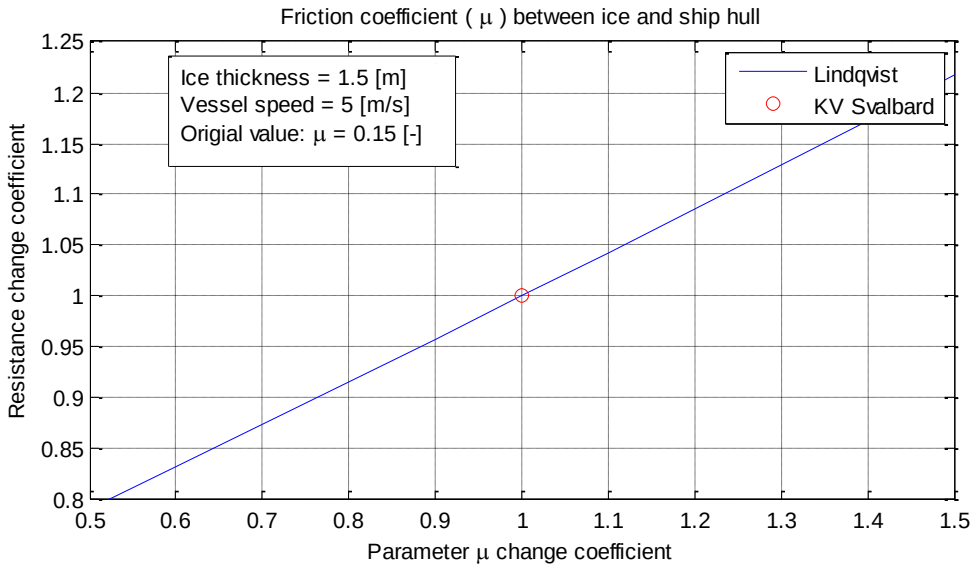
Friction coefficient ( μ ) between ice and ship hull
Ice thickness = 1.5 [m]
Vessel speed = 5 [m/s]
Origial value: μ = 0.15 [-]
Lindqvist
KV Svalbard
Resistance change coefficient
Parameter μ change coefficient

## B.4 Waterline entrance angle

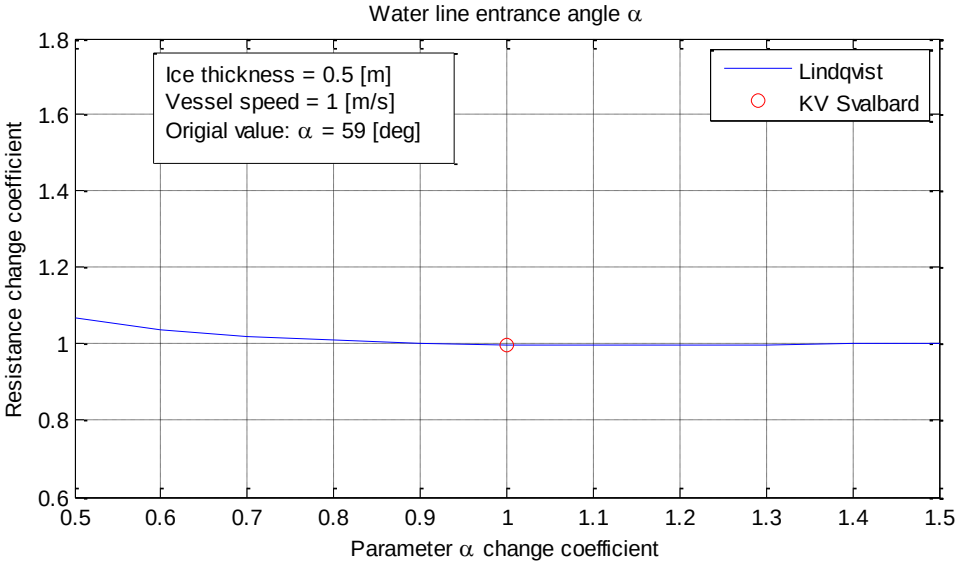


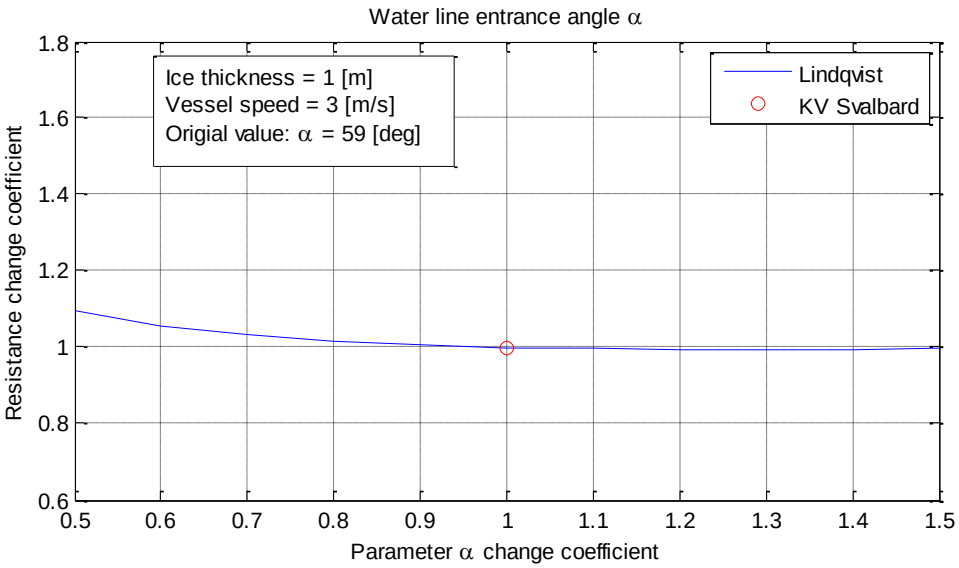


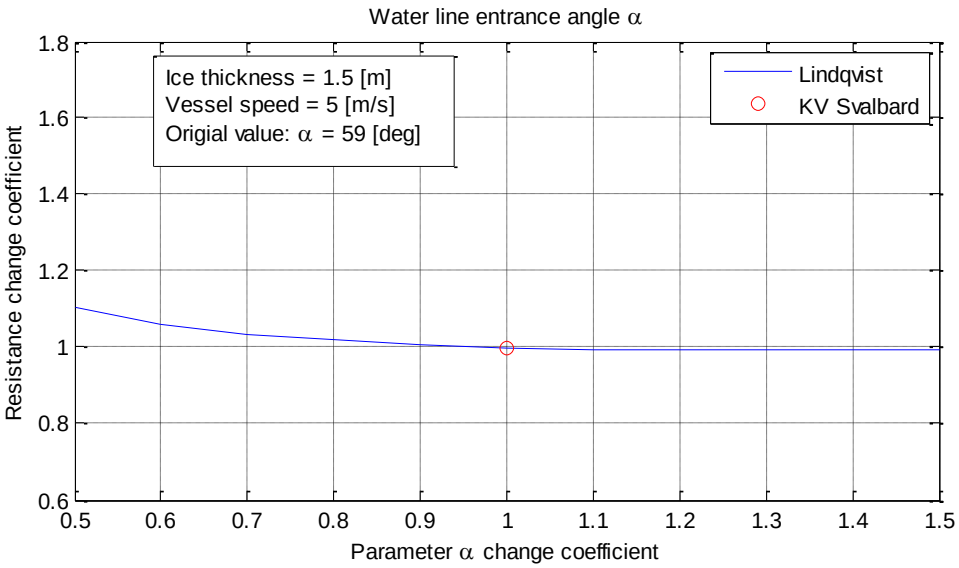

## B.5 Lpar

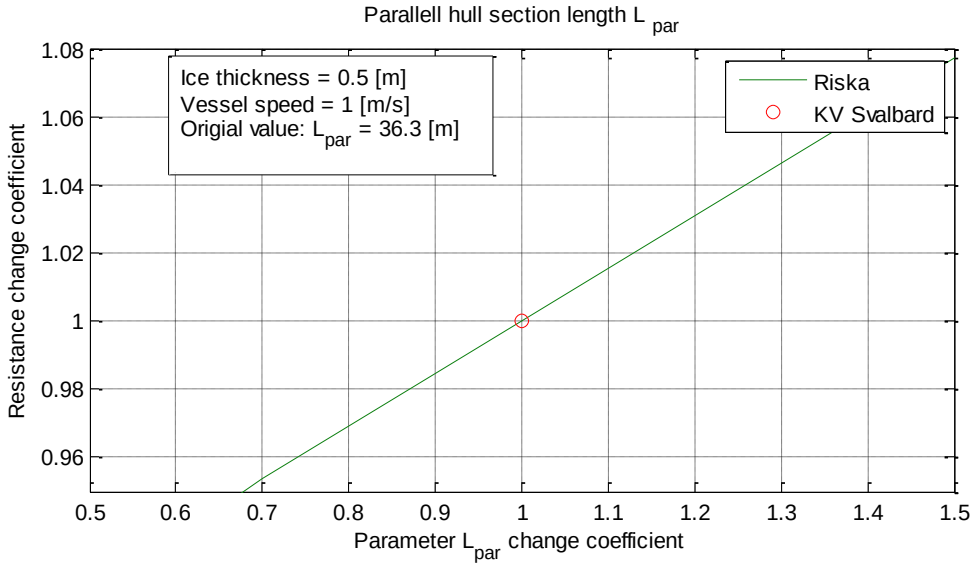
Parallell hull section length L par
Ice thickness = 0.5 [m]
Vessel speed = 1 [m/s]
Origial value: L par = 36.3 [m]
Riska
KV Svalbard
Resistance change coefficient
Parameter L par change coefficient
1.08
1.06
1.04
1.02
1
0.98
0.96
0.5
0.6
0.7
0.8
0.9
1
1.1
1.2
1.3
1.4
1.5

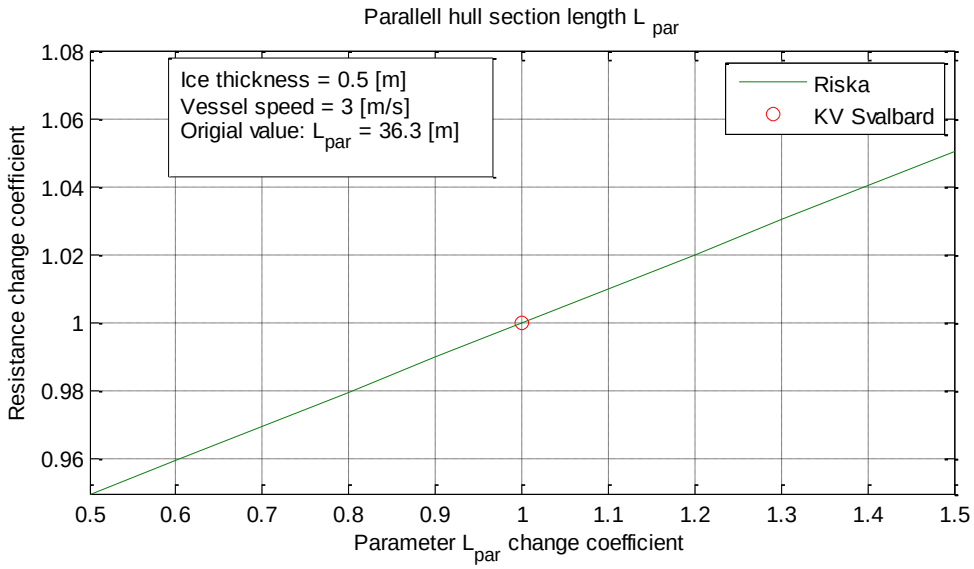
Parallell hull section length L par
Ice thickness = 0.5 [m]
Vessel speed = 3 [m/s]
Origial value: L par = 36.3 [m]
Riska
KV Svalbard
Resistance change coefficient
Parameter L par change coefficient
1.08
1.06
1.04
1.02
1
0.98
0.96
0.5
0.6
0.7
0.8
0.9
1
1.1
1.2
1.3
1.4
1.5

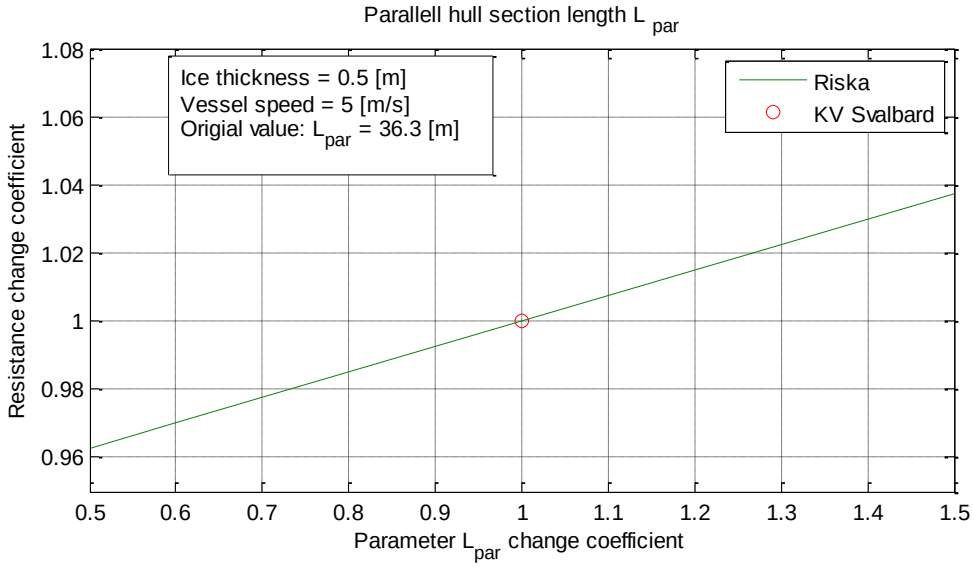
Parallell hull section length L par
Ice thickness = 0.5 [m]
Vessel speed = 5 [m/s]
Origial value: L par = 36.3 [m]
Riska
KV Svalbard
Resistance change coefficient
Parameter L par change coefficient
1.08
1.06
1.04
1.02
1
0.98
0.96
0.5
0.6
0.7
0.8
0.9
1
1.1
1.2
1.3
1.4
1.5

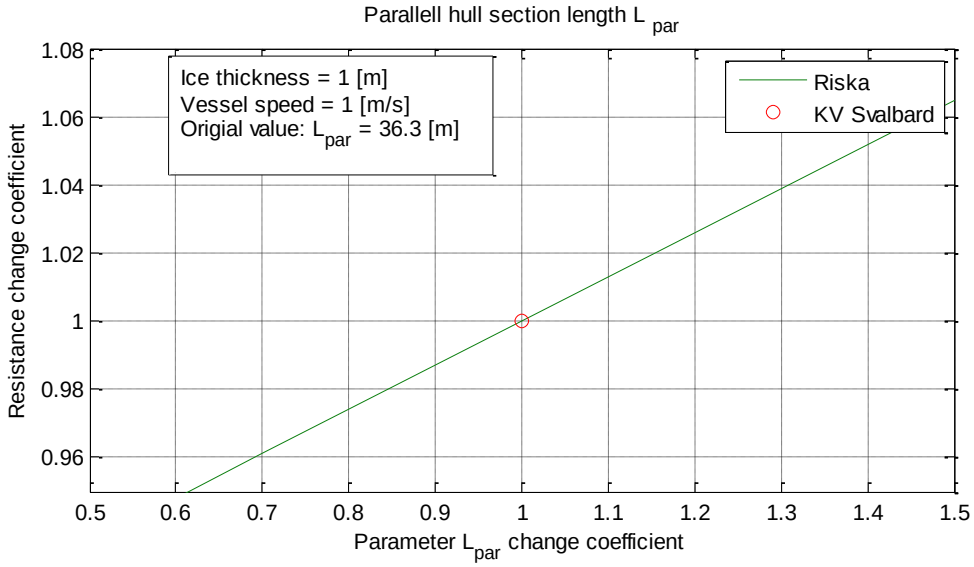
Parallell hull section length L par
Ice thickness = 1 [m]
Vessel speed = 1 [m/s]
Origial value: L par = 36.3 [m]
Riska
KV Svalbard
Resistance change coefficient
Parameter L par change coefficient
1.08
1.06
1.04
1.02
1
0.98
0.96
0.5
0.6
0.7
0.8
0.9
1
1.1
1.2
1.3
1.4
1.5

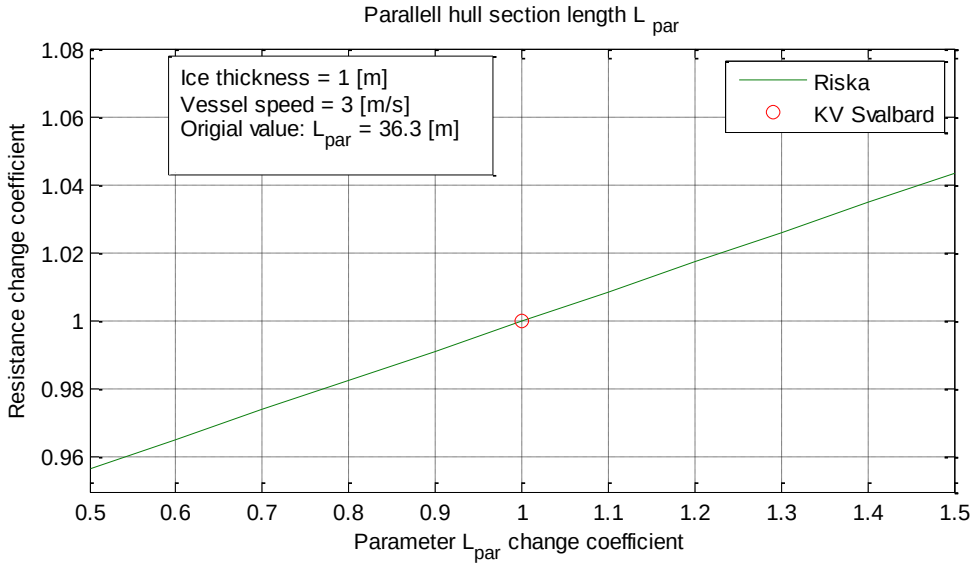
Parallell hull section length L par
Ice thickness = 1 [m]
Vessel speed = 3 [m/s]
Origial value: L par = 36.3 [m]
Riska
KV Svalbard
Resistance change coefficient
Parameter L par change coefficient
1.08
1.06
1.04
1.02
1
0.98
0.96
0.5
0.6
0.7
0.8
0.9
1
1.1
1.2
1.3
1.4
1.5

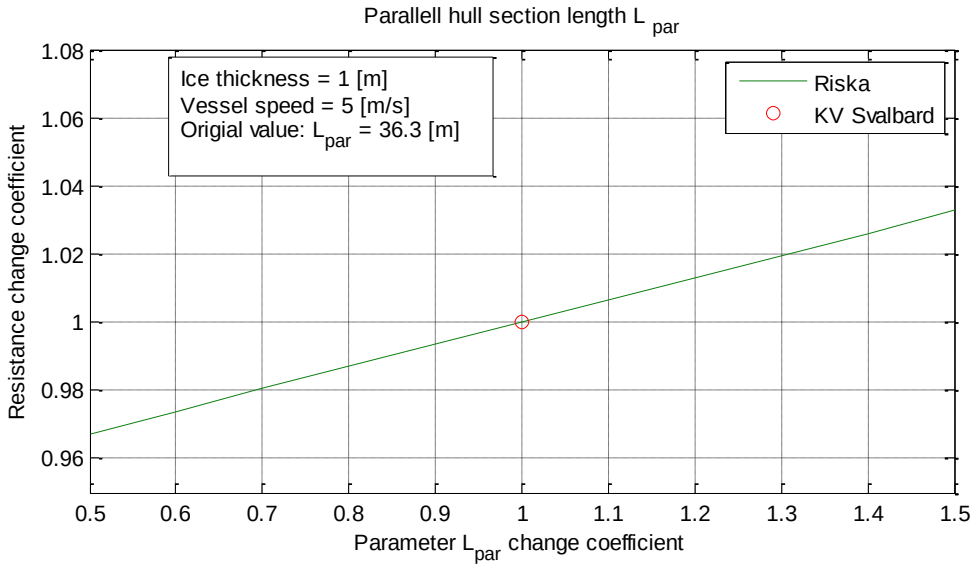
Parallell hull section length L par
Ice thickness = 1 [m]
Vessel speed = 5 [m/s]
Origial value: L par = 36.3 [m]
Riska
KV Svalbard
Resistance change coefficient
Parameter L par change coefficient
1.08
1.06
1.04
1.02
1
0.98
0.96
0.5
0.6
0.7
0.8
0.9
1
1.1
1.2
1.3
1.4
1.5

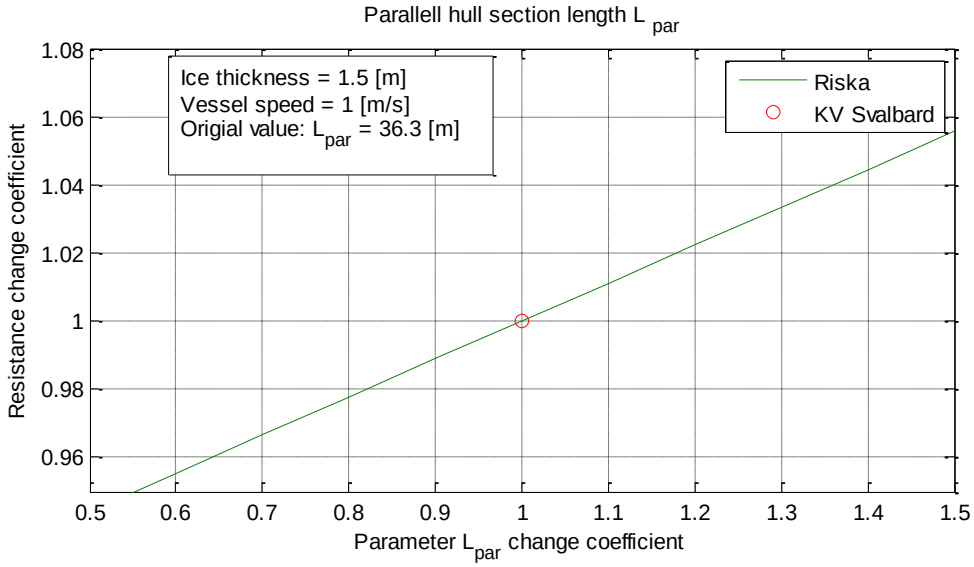
Parallell hull section length L par
Ice thickness = 1.5 [m]
Vessel speed = 1 [m/s]
Origial value: L par = 36.3 [m]
Riska
KV Svalbard
Resistance change coefficient
Parameter L par change coefficient
1.08
1.06
1.04
1.02
1
0.98
0.96
0.5
0.6
0.7
0.8
0.9
1
1.1
1.2
1.3
1.4
1.5

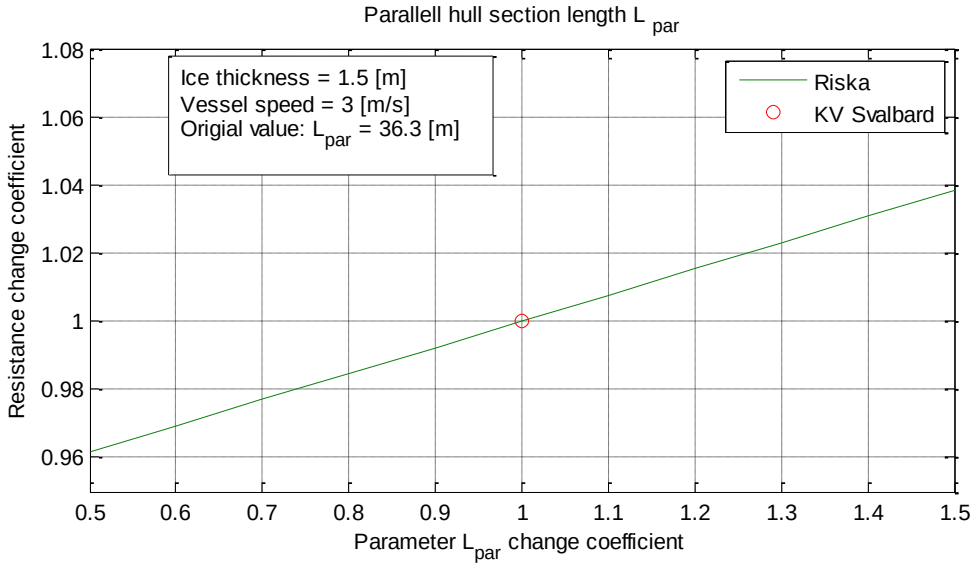
Parallell hull section length L par
Ice thickness = 1.5 [m]
Vessel speed = 3 [m/s]
Origial value: L par = 36.3 [m]
Riska
KV Svalbard
Resistance change coefficient
Parameter L par change coefficient
1.08
1.06
1.04
1.02
1
0.98
0.96
0.5
0.6
0.7
0.8
0.9
1
1.1
1.2
1.3
1.4
1.5

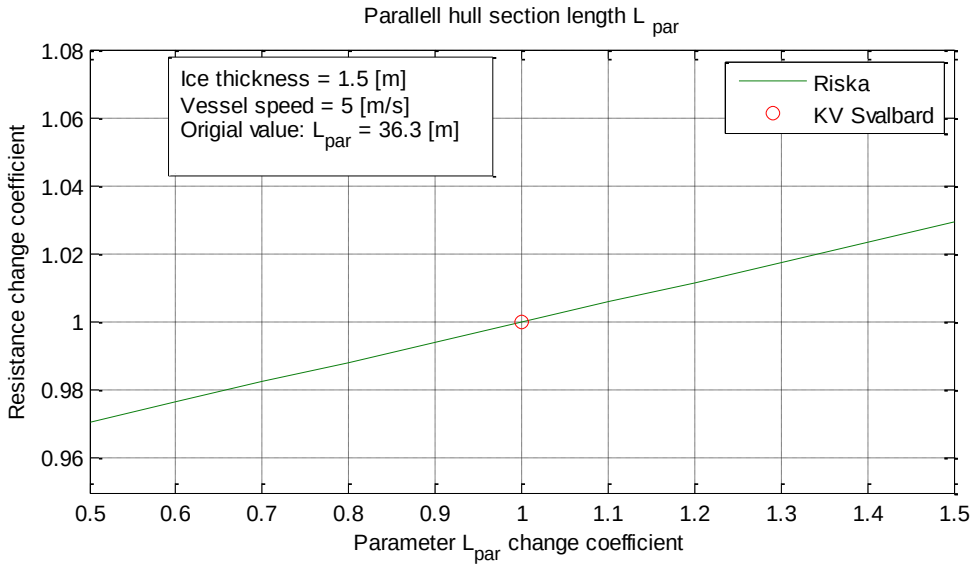
Parallell hull section length L par
Ice thickness = 1.5 [m]
Vessel speed = 5 [m/s]
Origial value: L par = 36.3 [m]
Riska
KV Svalbard
Resistance change coefficient
Parameter L par change coefficient
1.08
1.06
1.04
1.02
1
0.98
0.96
0.5
0.6
0.7
0.8
0.9
1
1.1
1.2
1.3
1.4
1.5

## B.6 Lbow

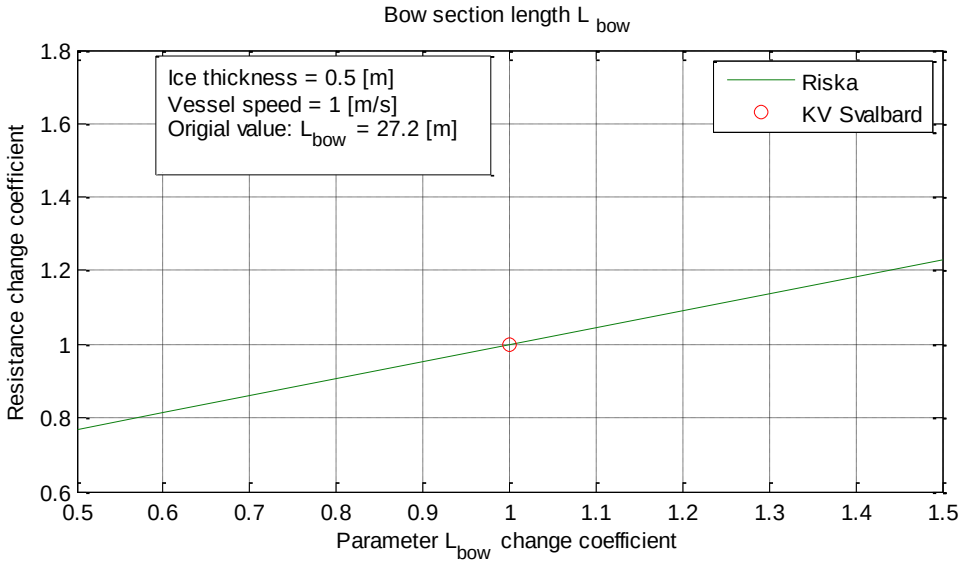
Bow section length L bow
Ice thickness = 0.5 [m]
Vessel speed = 1 [m/s]
Origial value: L bow = 27.2 [m]
Riska
KV Svalbard
Resistance change coefficient
Parameter L bow change coefficient
1.8
1.6
1.4
1.2
1
0.8
0.6
0.5
0.6
0.7
0.8
0.9
1
1.1
1.2
1.3
1.4
1.5

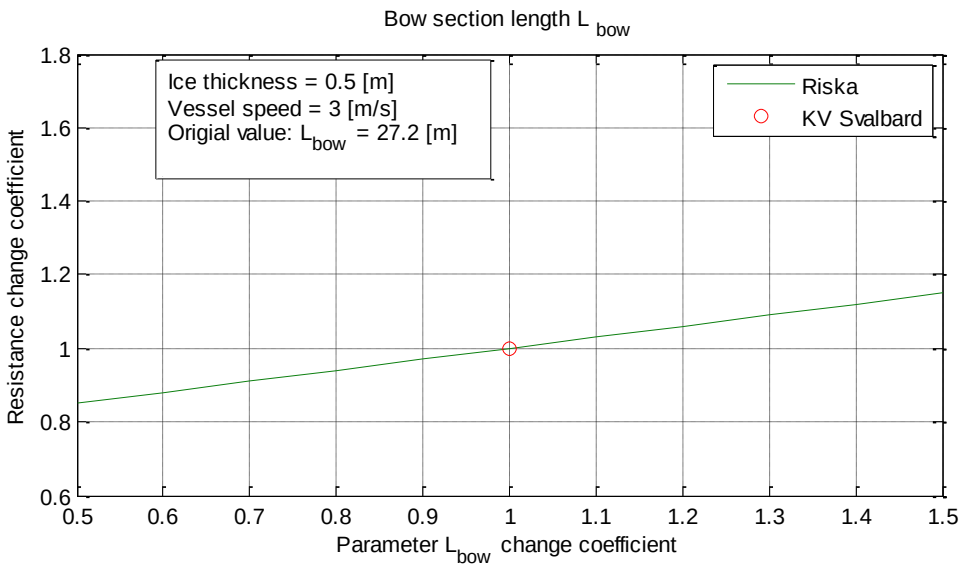
Bow section length L bow
Ice thickness = 0.5 [m]
Vessel speed = 3 [m/s]
Origial value: L bow = 27.2 [m]
Riska
KV Svalbard
Resistance change coefficient
Parameter L bow change coefficient
1.8
1.6
1.4
1.2
1
0.8
0.6
0.5
0.6
0.7
0.8
0.9
1
1.1
1.2
1.3
1.4
1.5

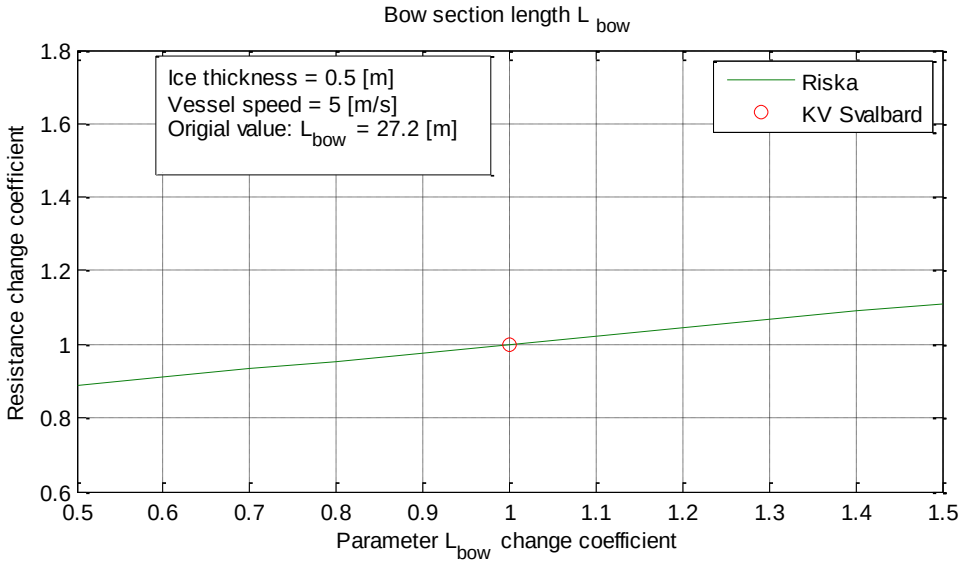
Bow section length L bow
Ice thickness = 0.5 [m]
Vessel speed = 5 [m/s]
Origial value: L bow = 27.2 [m]
Riska
KV Svalbard
Resistance change coefficient
Parameter L bow change coefficient
1.8
1.6
1.4
1.2
1
0.8
0.6
0.5
0.6
0.7
0.8
0.9
1
1.1
1.2
1.3
1.4
1.5

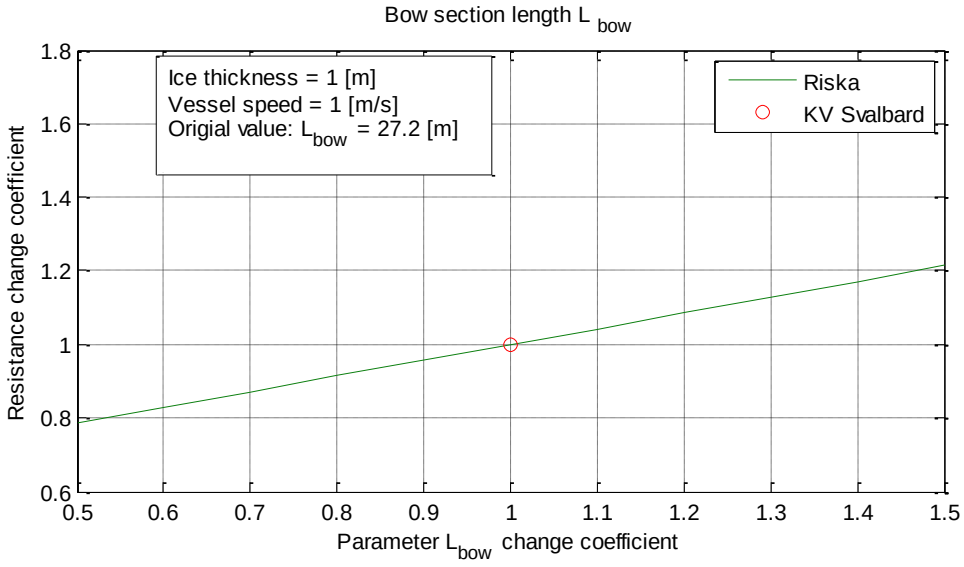
Bow section length L bow
Ice thickness = 1 [m]
Vessel speed = 1 [m/s]
Origial value: L_bow = 27.2 [m]
Riska
KV Svalbard
Resistance change coefficient
Parameter L_bow change coefficient
1.8
1.6
1.4
1.2
1
0.8
0.6
0.5
0.6
0.7
0.8
0.9
1
1.1
1.2
1.3
1.4
1.5

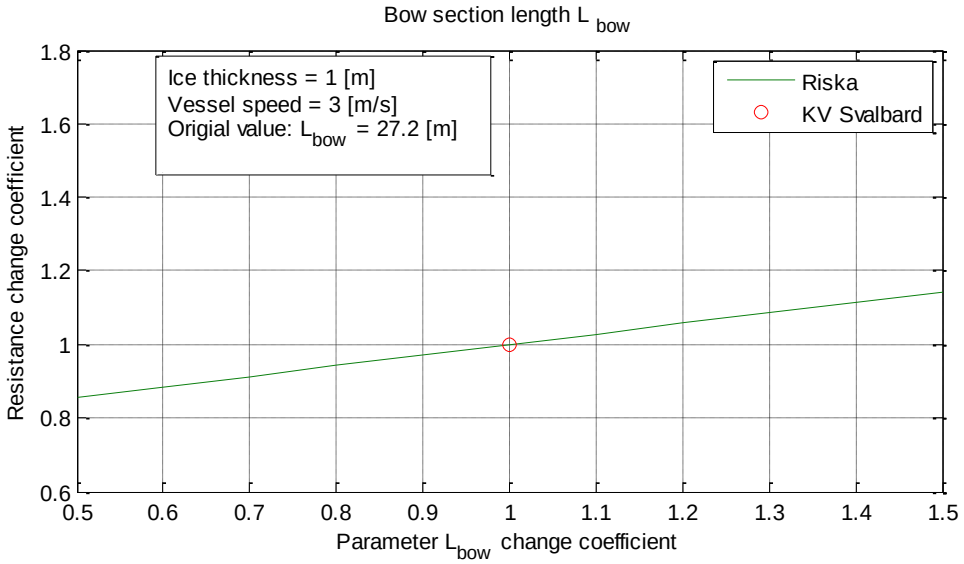
Bow section length L bow
Ice thickness = 1 [m]
Vessel speed = 3 [m/s]
Origial value: L_bow = 27.2 [m]
Riska
KV Svalbard
Resistance change coefficient
Parameter L_bow change coefficient
1.8
1.6
1.4
1.2
1
0.8
0.6
0.5
0.6
0.7
0.8
0.9
1
1.1
1.2
1.3
1.4
1.5

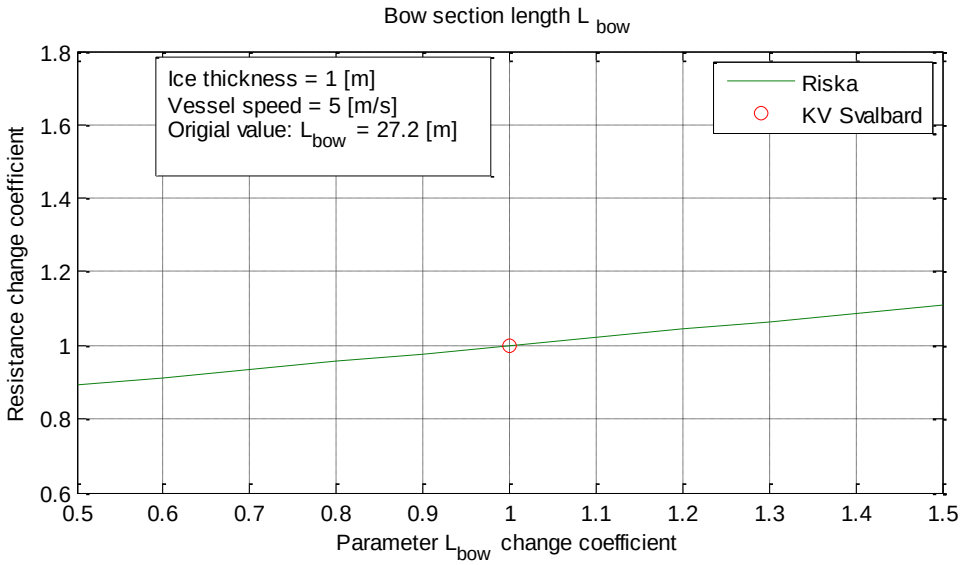
Bow section length L bow
Ice thickness = 1 [m]
Vessel speed = 5 [m/s]
Origial value: L_bow = 27.2 [m]
Riska
KV Svalbard
Resistance change coefficient
Parameter L_bow change coefficient
1.8
1.6
1.4
1.2
1
0.8
0.6
0.5
0.6
0.7
0.8
0.9
1
1.1
1.2
1.3
1.4
1.5

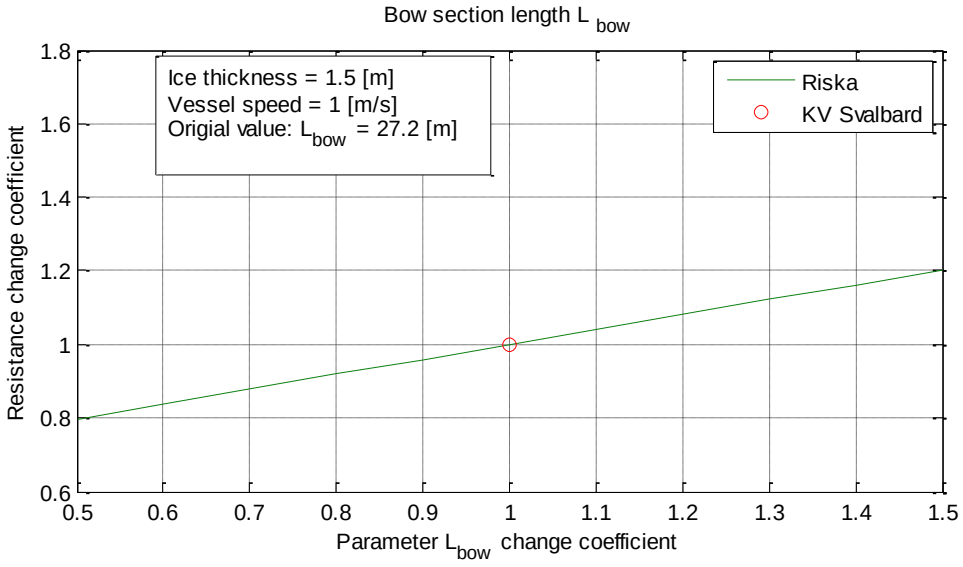
Bow section length L bow
Ice thickness = 1.5 [m]
Vessel speed = 1 [m/s]
Origial value: L_bow = 27.2 [m]
Riska
KV Svalbard
Resistance change coefficient
Parameter L_bow change coefficient
1.8
1.6
1.4
1.2
1
0.8
0.6
0.5
0.6
0.7
0.8
0.9
1
1.1
1.2
1.3
1.4
1.5

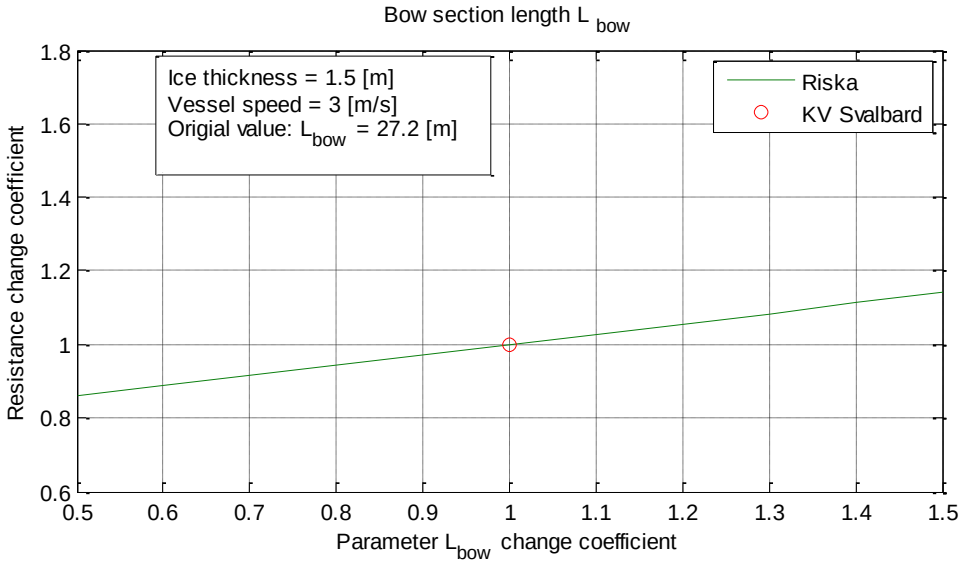
Bow section length L bow
Ice thickness = 1.5 [m]
Vessel speed = 3 [m/s]
Origial value: L_bow = 27.2 [m]
Riska
KV Svalbard
Resistance change coefficient
Parameter L_bow change coefficient
1.8
1.6
1.4
1.2
1
0.8
0.6
0.5
0.6
0.7
0.8
0.9
1
1.1
1.2
1.3
1.4
1.5

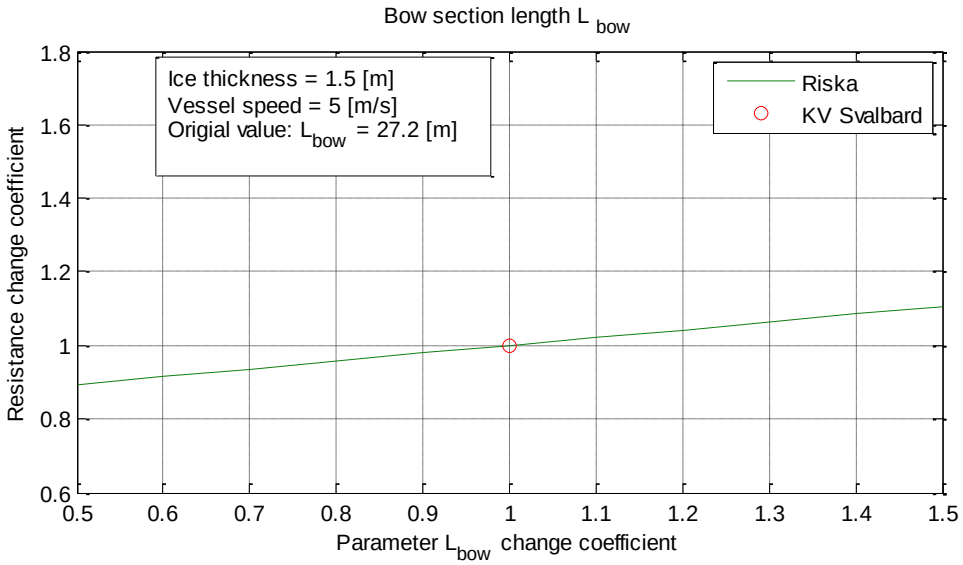
Bow section length L bow
Ice thickness = 1.5 [m]
Vessel speed = 5 [m/s]
Origial value: L_bow = 27.2 [m]
Riska
KV Svalbard
Resistance change coefficient
Parameter L_bow change coefficient
1.8
1.6
1.4
1.2
1
0.8
0.6
0.5
0.6
0.7
0.8
0.9
1
1.1
1.2
1.3
1.4
1.5

## B.7 Buttock angle

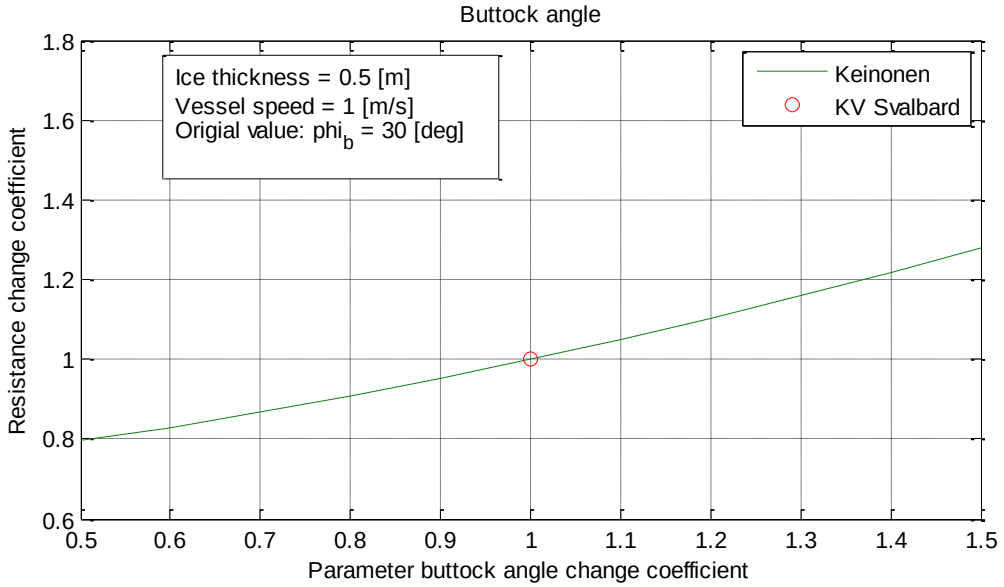


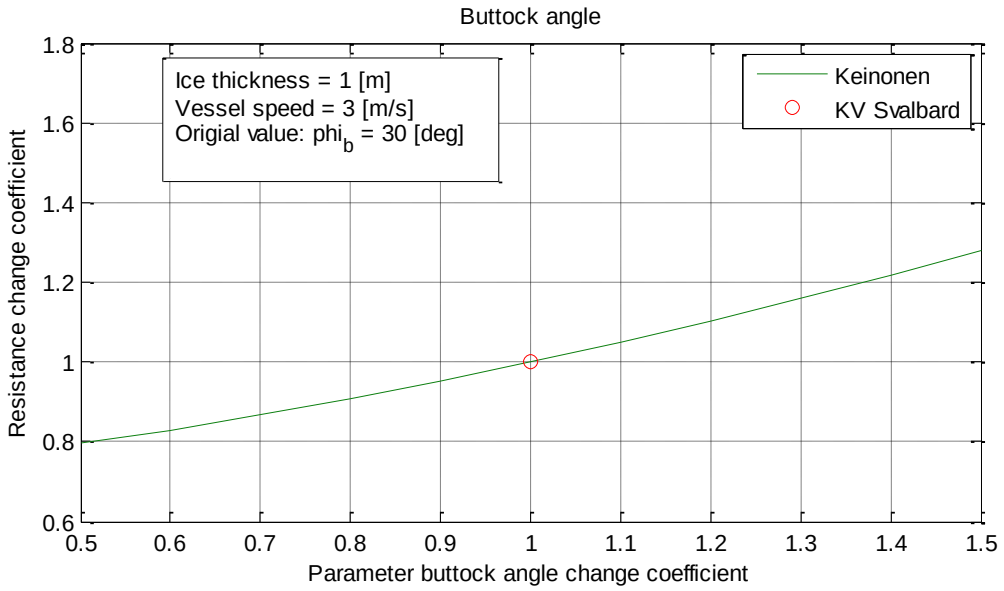

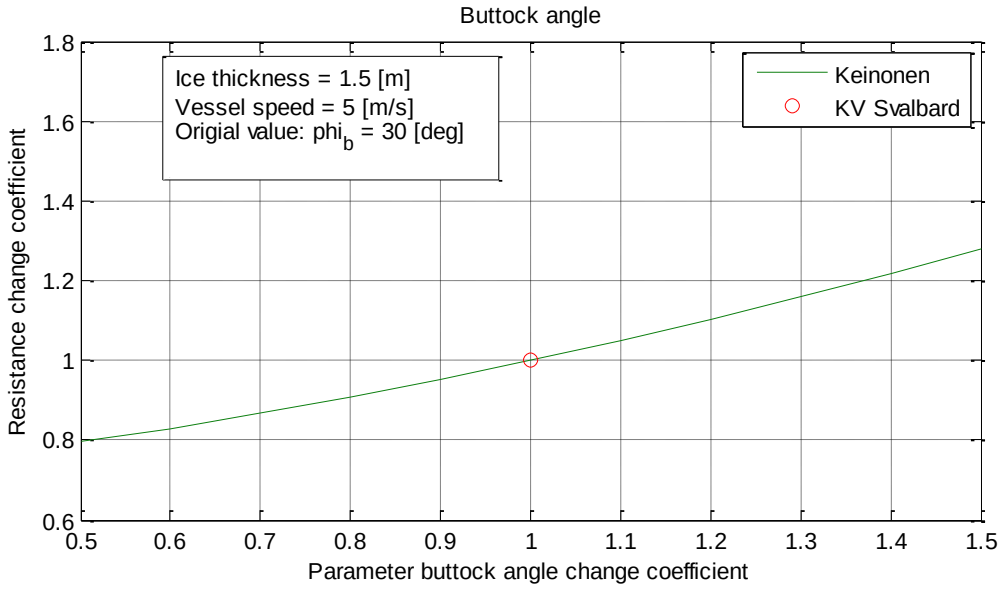
Buttock angle
Ice thickness = 1.5 [m]
Vessel speed = 5 [m/s]
Origial value: phi_b = 30 [deg]
Keinonen
KV Svalbard
Resistance change coefficient
Parameter buttock angle change coefficient
1.8
1.6
1.4
1.2
1
0.8
0.6
0.5
0.6
0.7
0.8
0.9
1
1.1
1.2
1.3
1.4
1.5

# Appendix C Surface and residual plot with different propeller efficiency

## C.1 Riska

**Propeller efficiency – 70%**

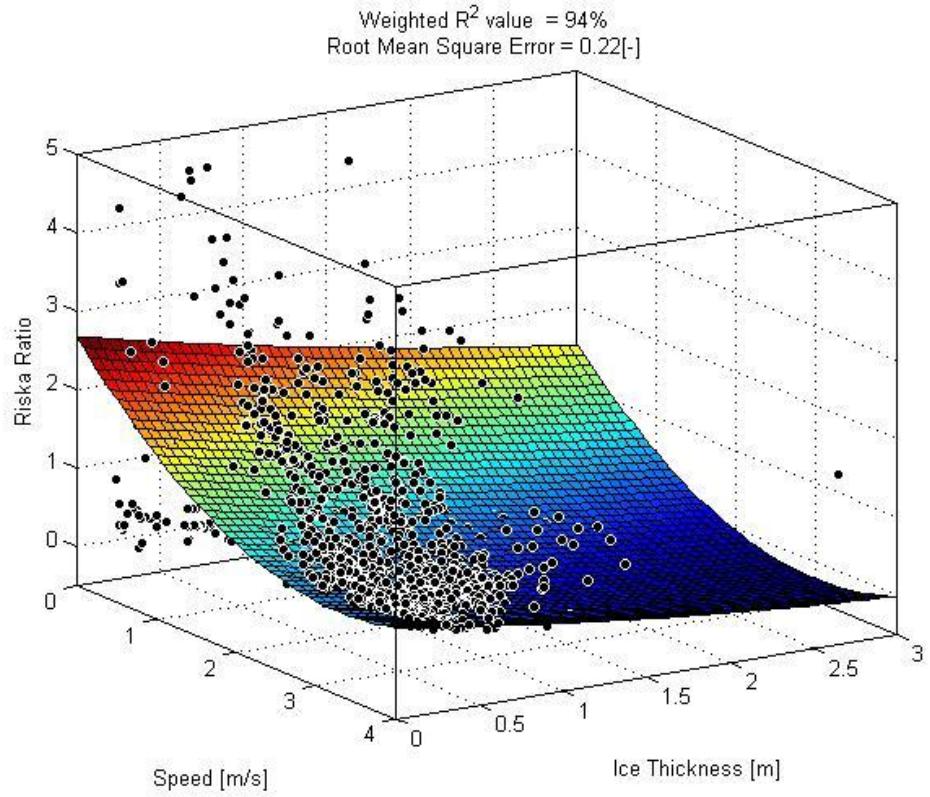


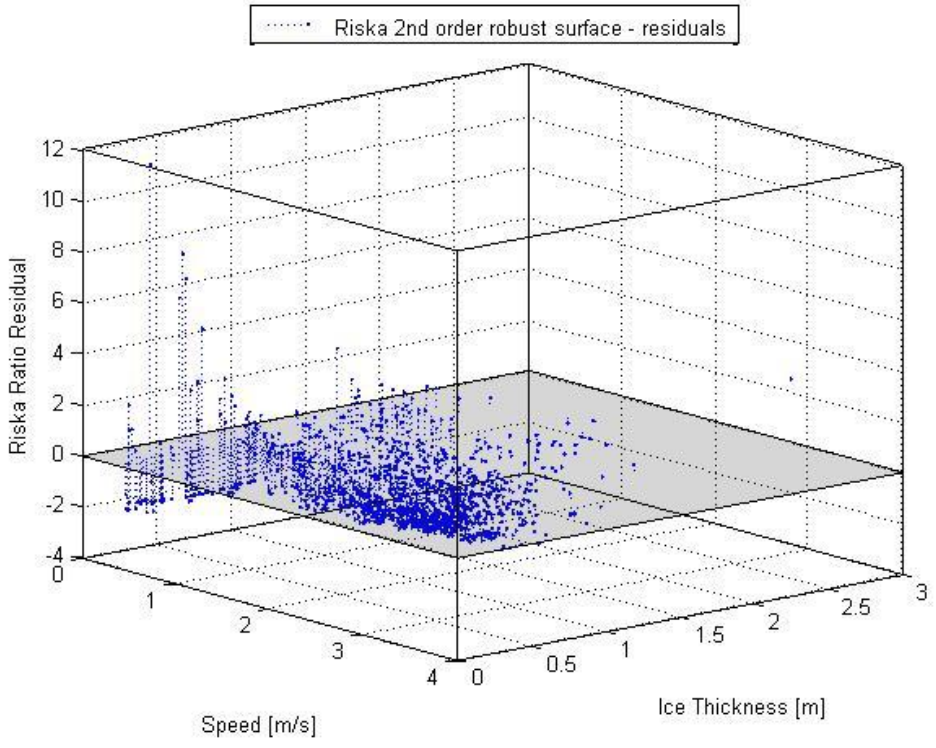

**Propeller efficiency – 80%**

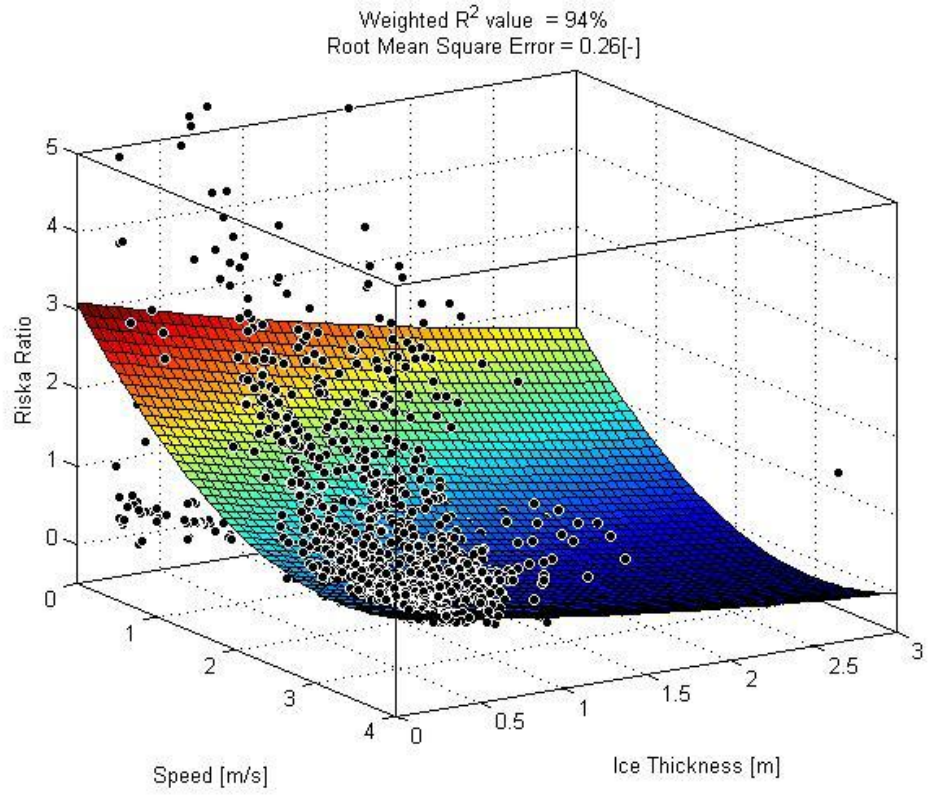


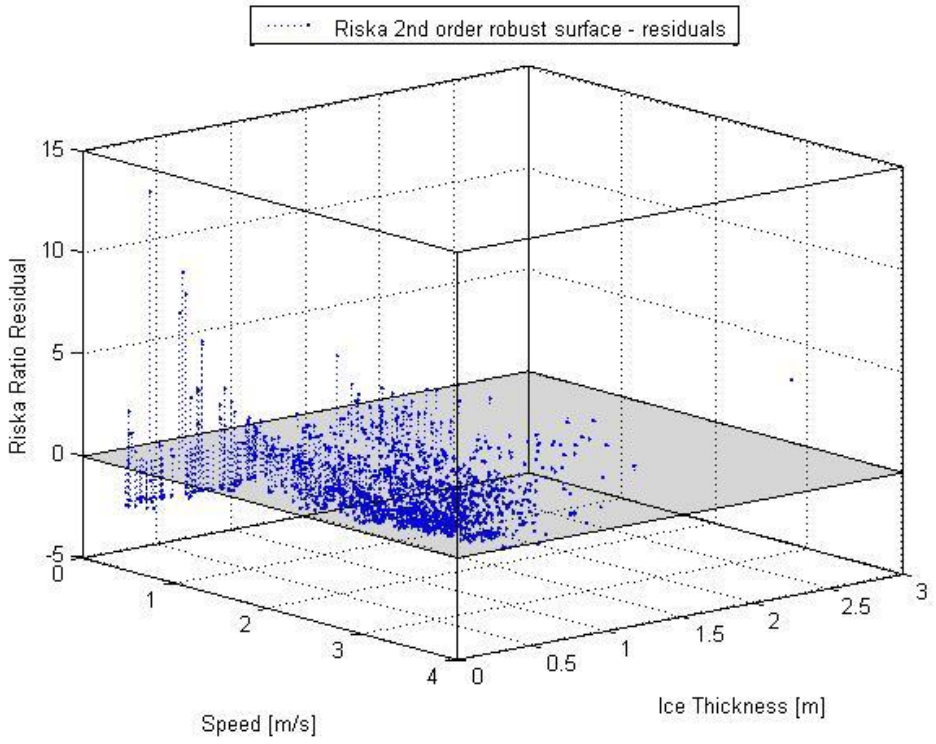

**Propeller efficiency - 90%**

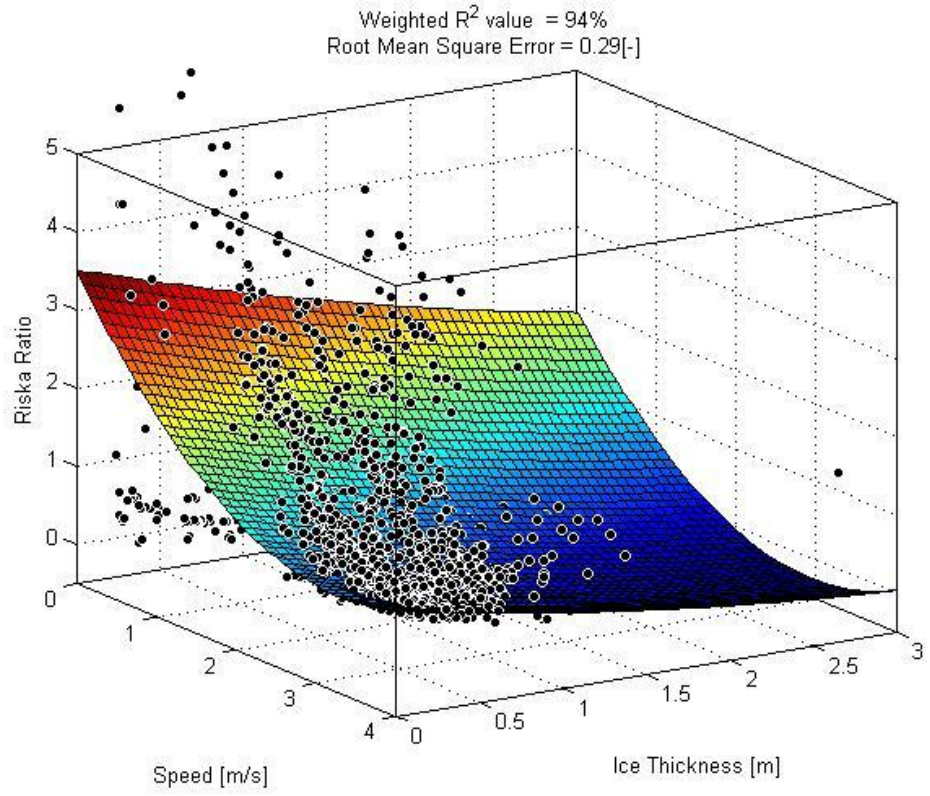


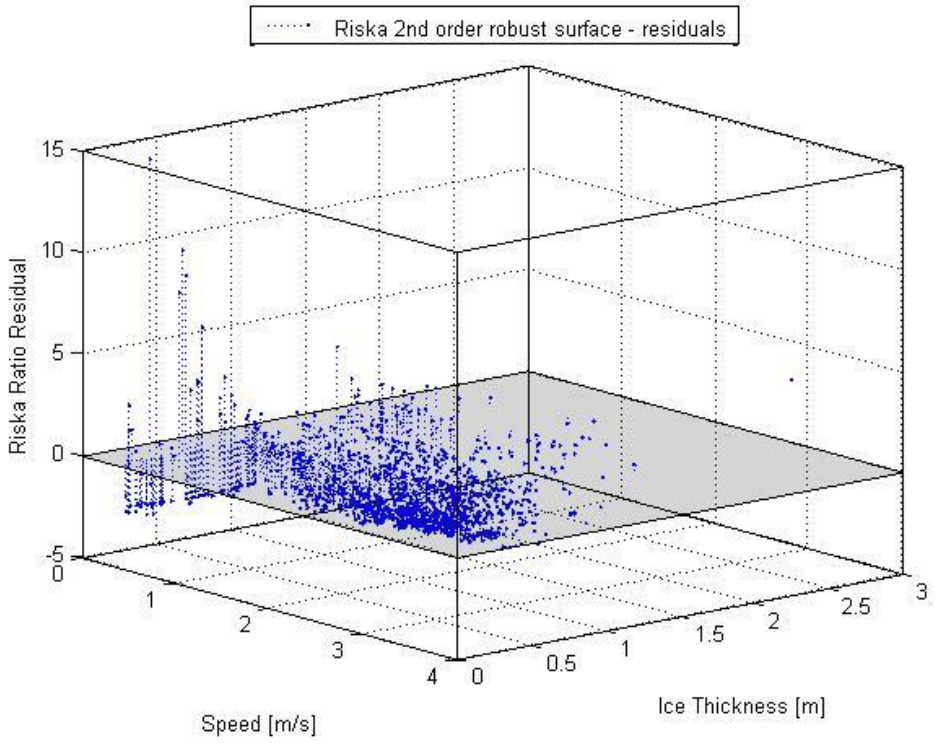

## C.2 Lindqvist without open water resistance

**Propeller efficiency – 70%**

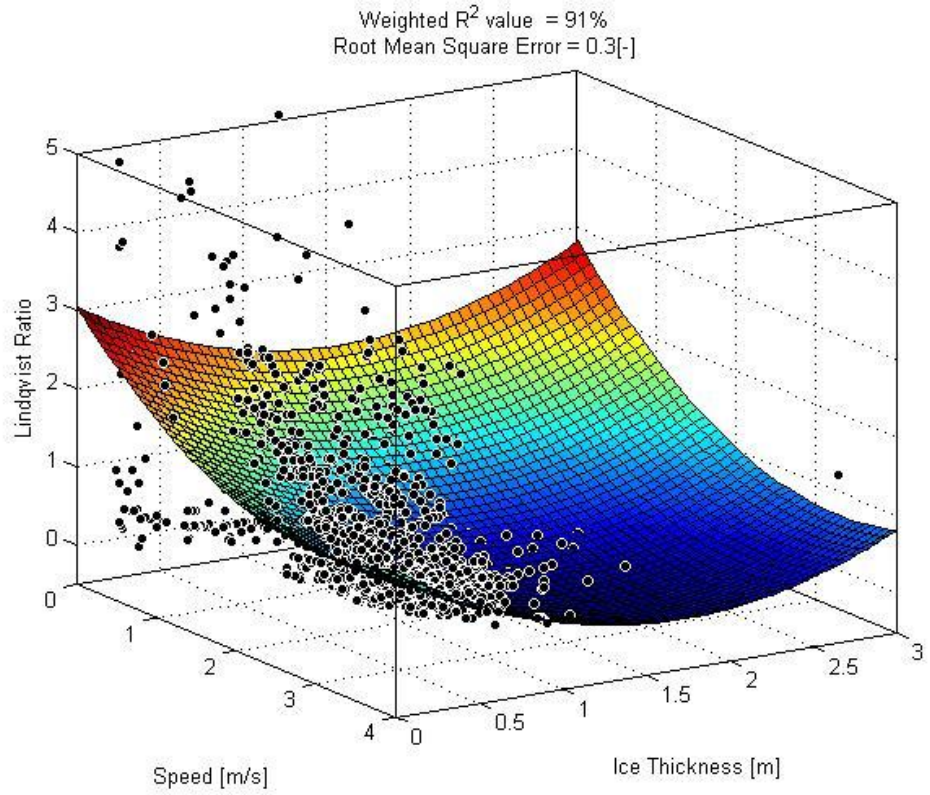


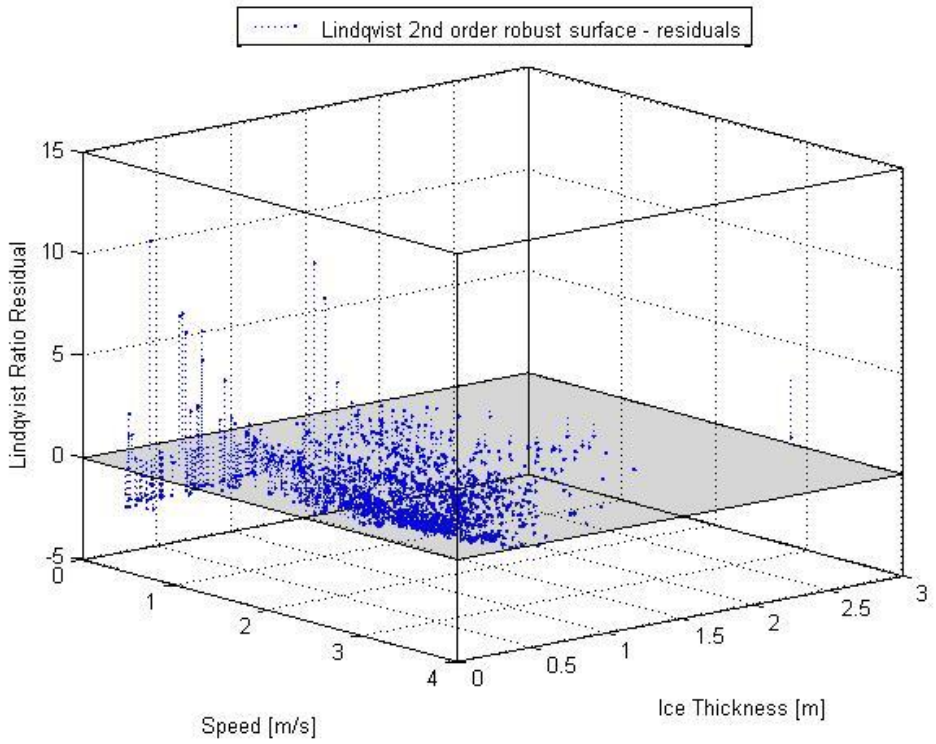

**Propeller efficiency - 80%**

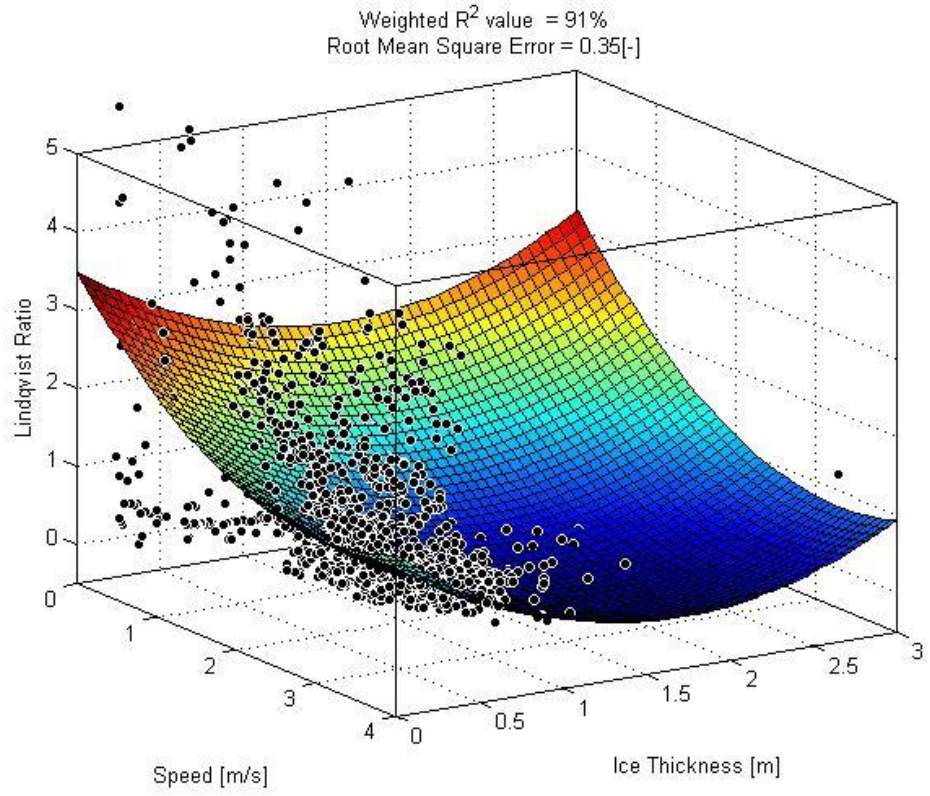


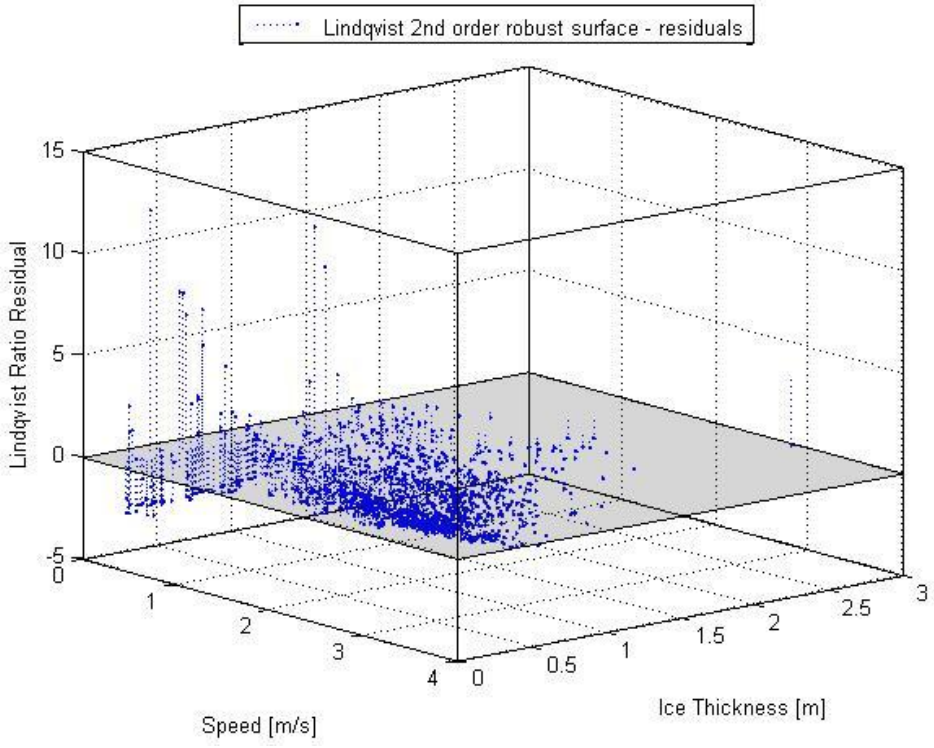

**Propeller efficiency - 90%**

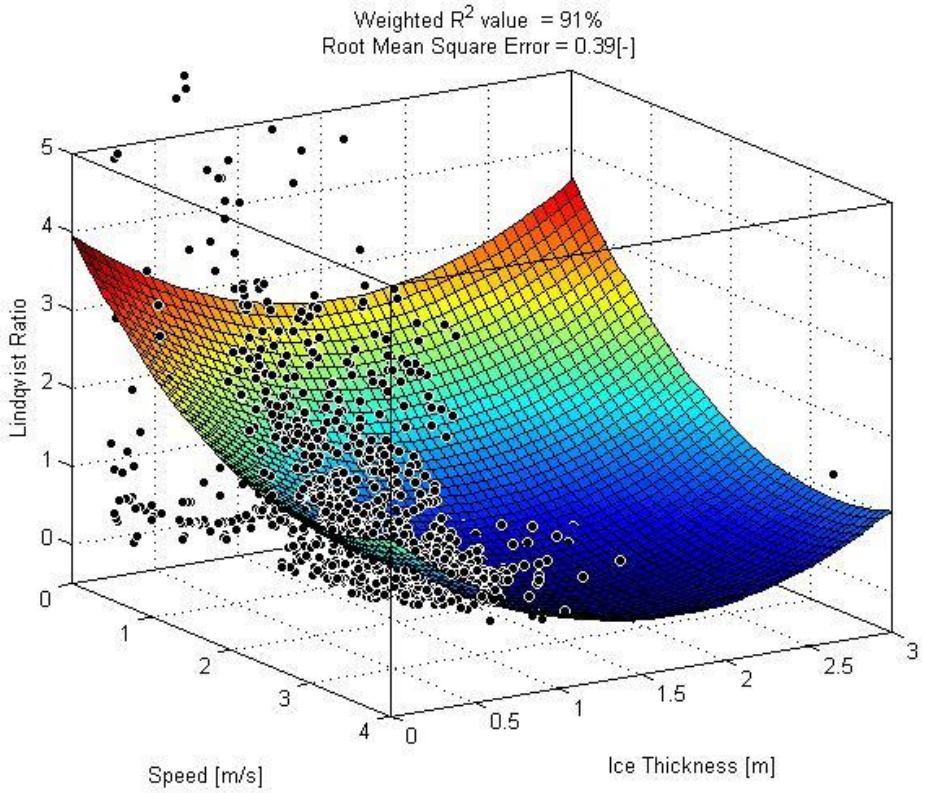


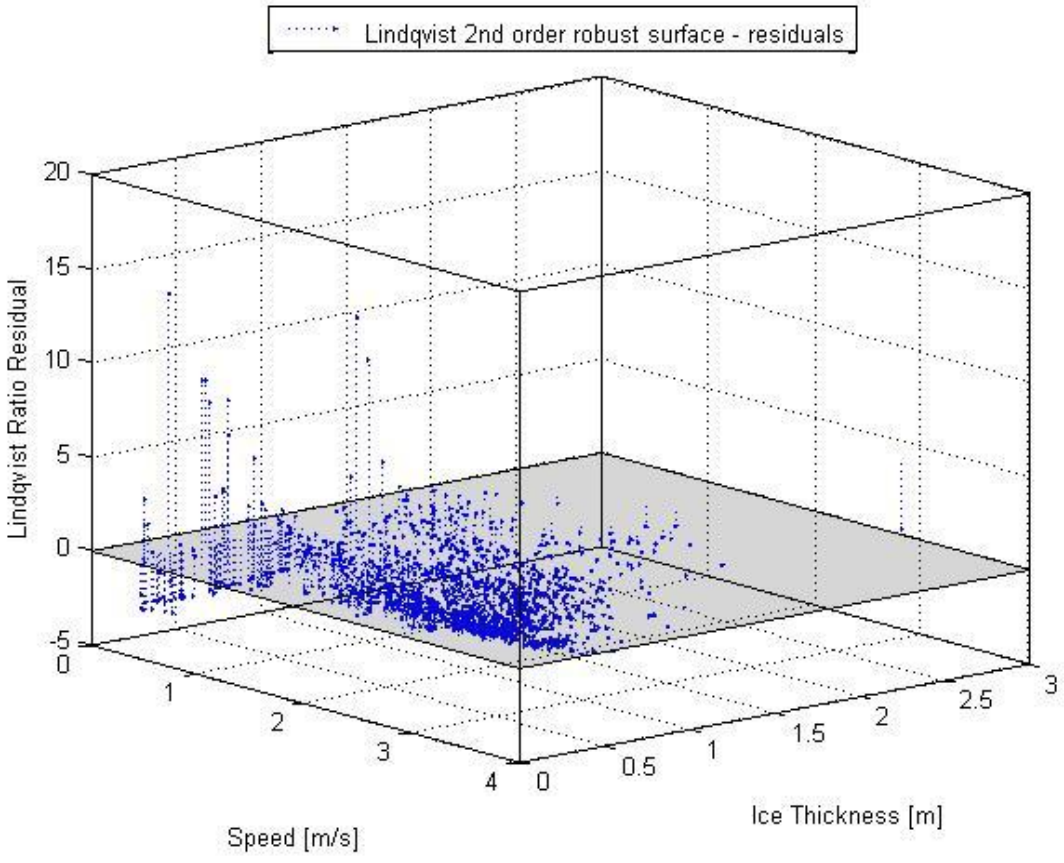

## C.3 Lindqvist with open water resistance

**Propeller efficiency – 70%**

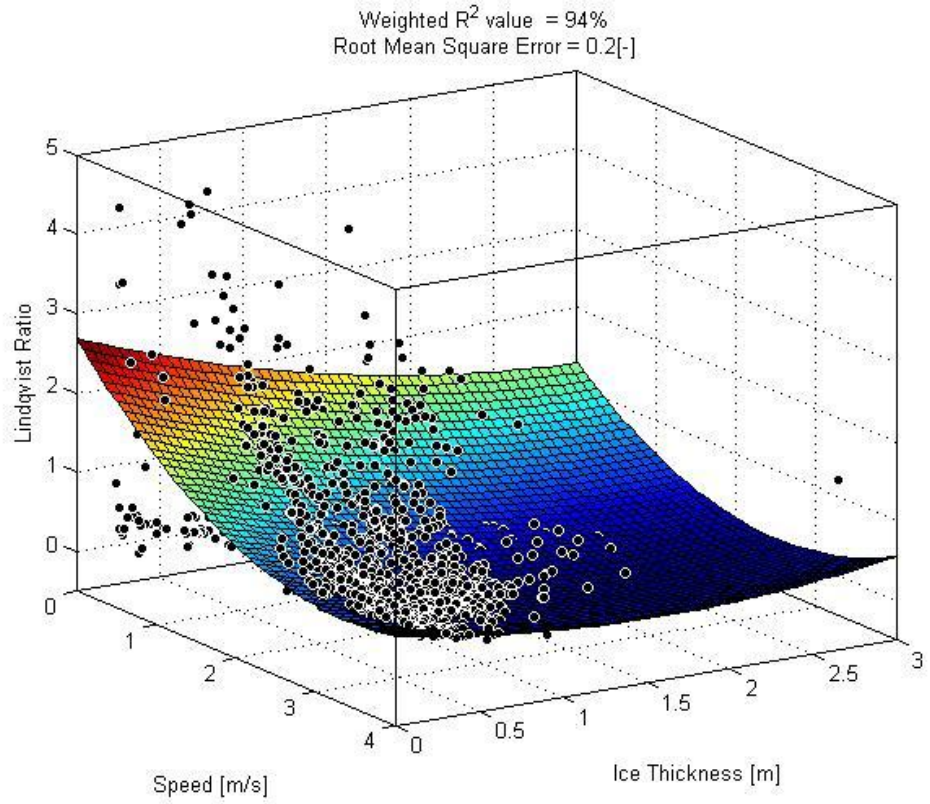


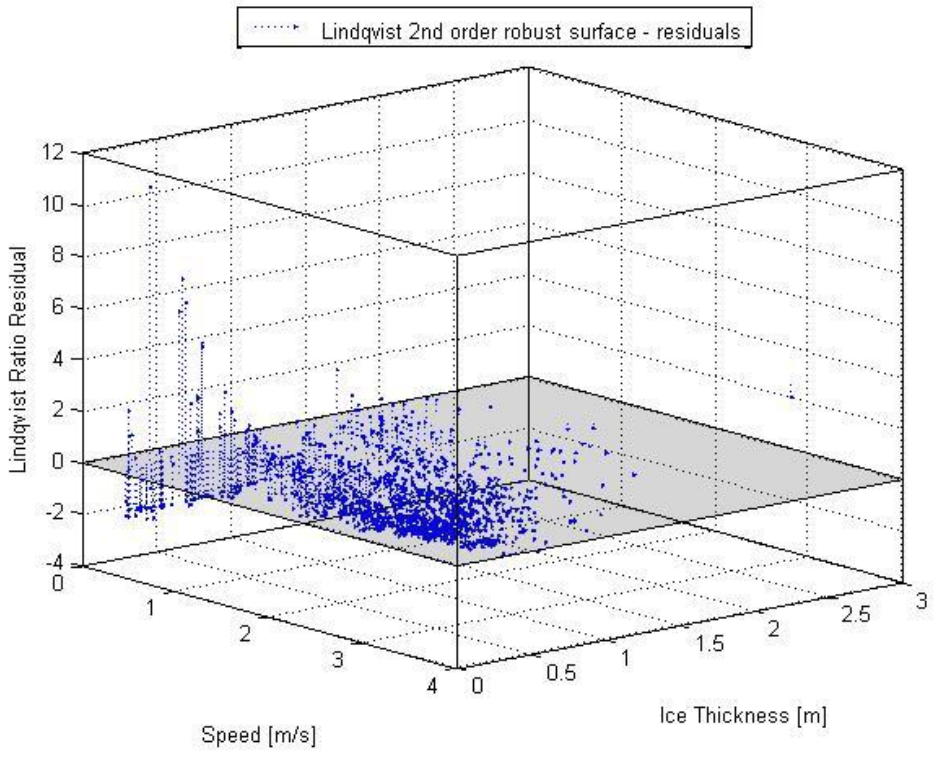

**Propeller efficiency – 80%**

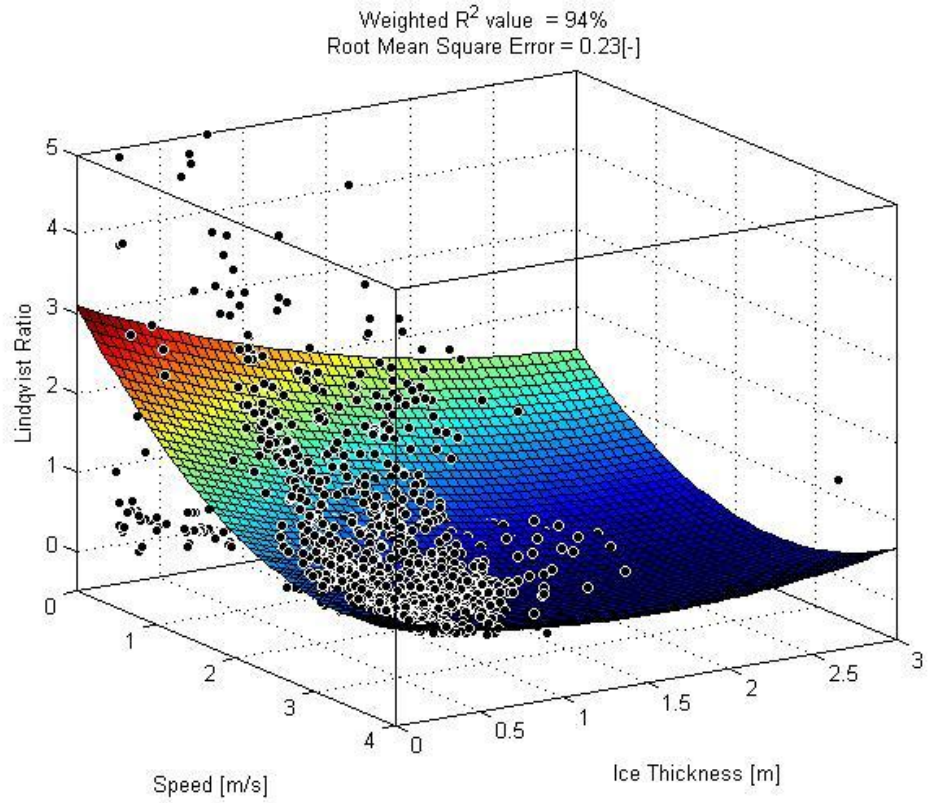


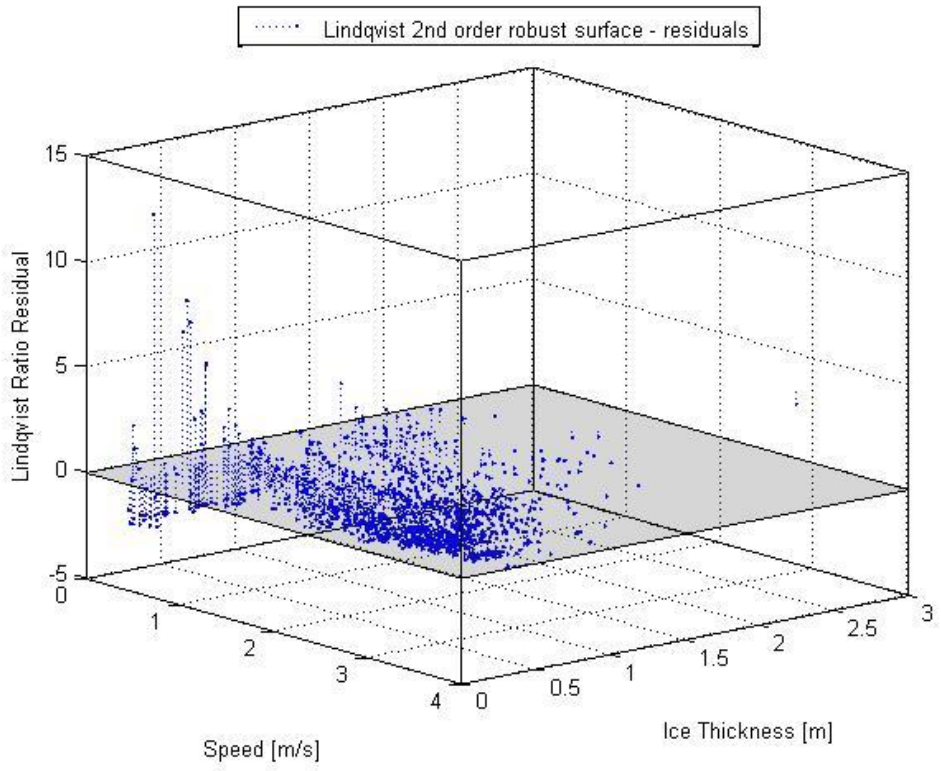

**Propeller efficiency – 90%**

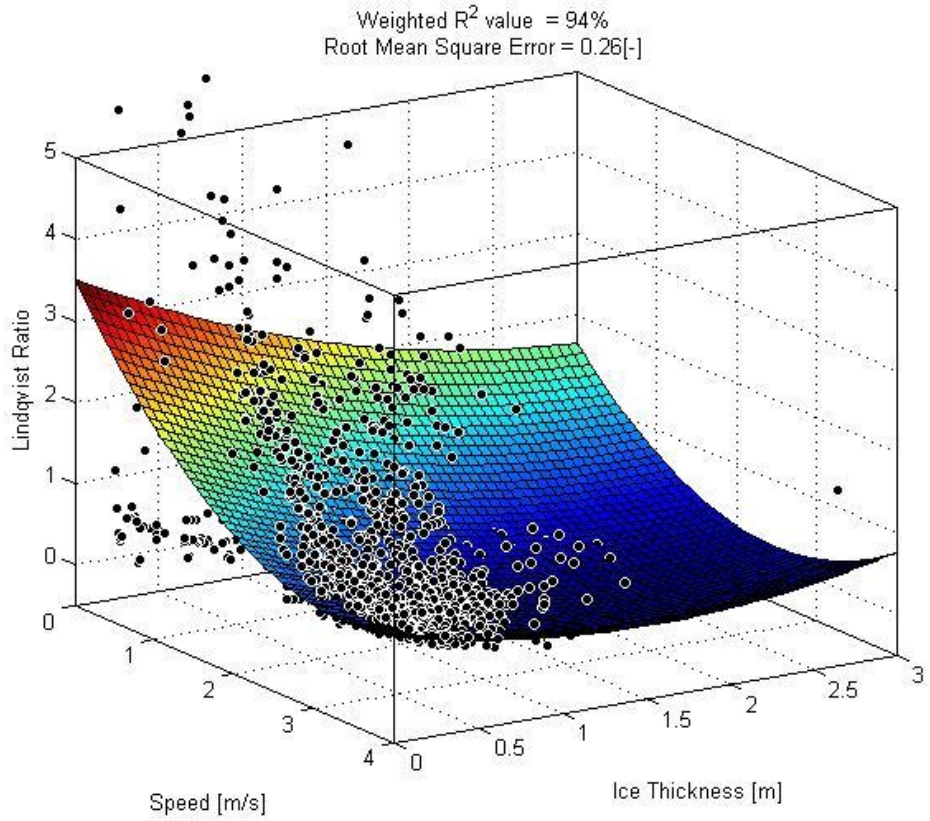


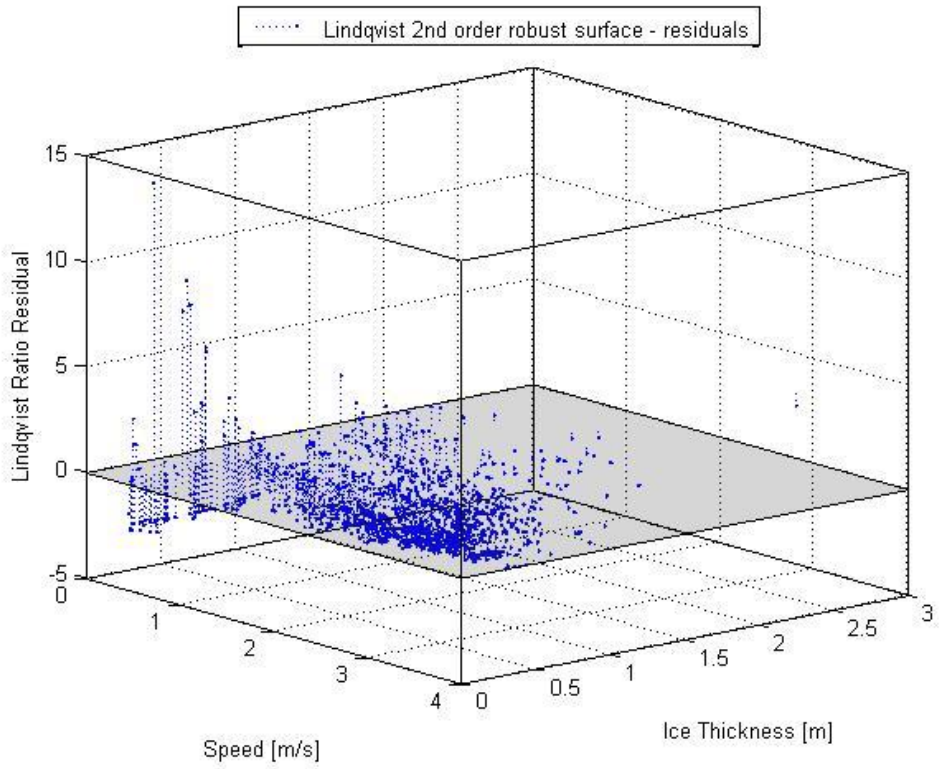

## C.4 Keinonen

**Propeller efficiency - 70%**

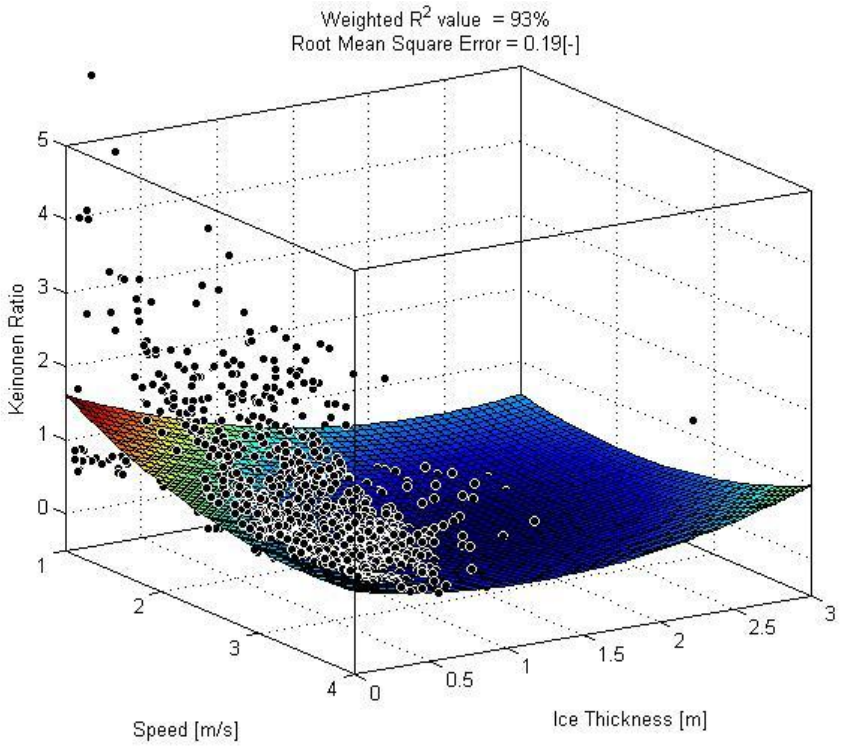


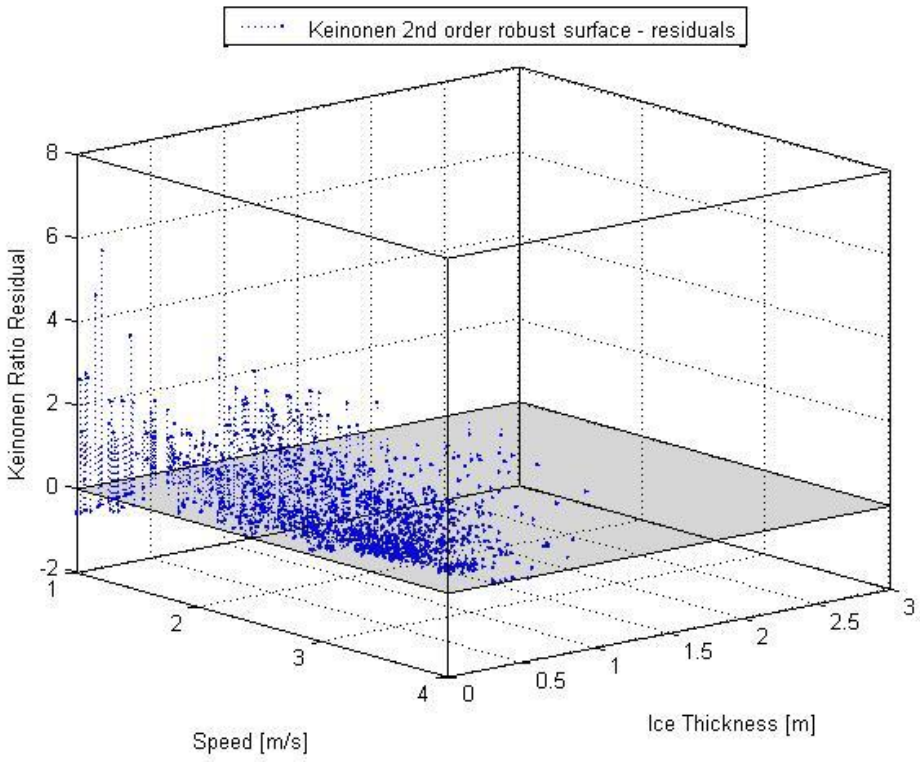

**Propeller efficiency - 80%**

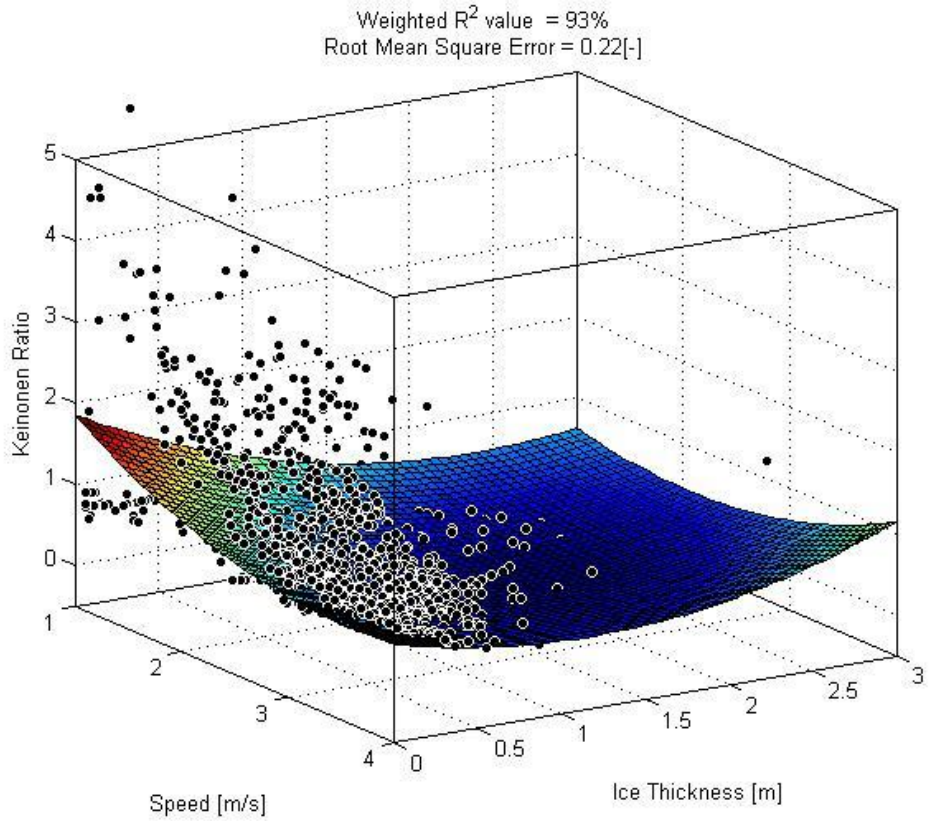


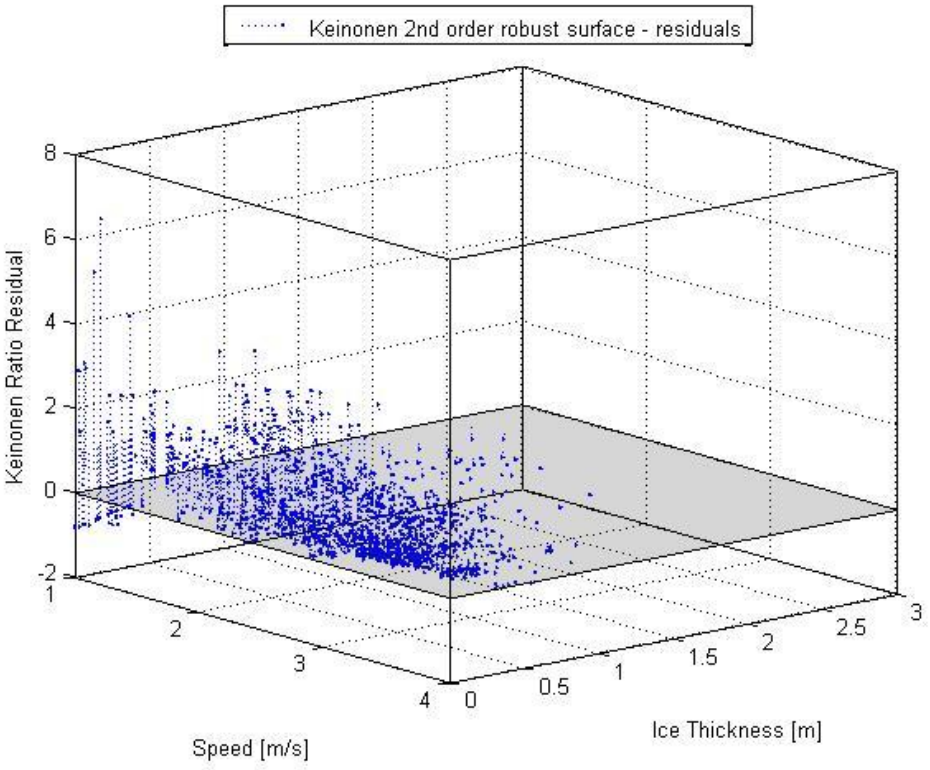

**Propeller efficiency - 90%**

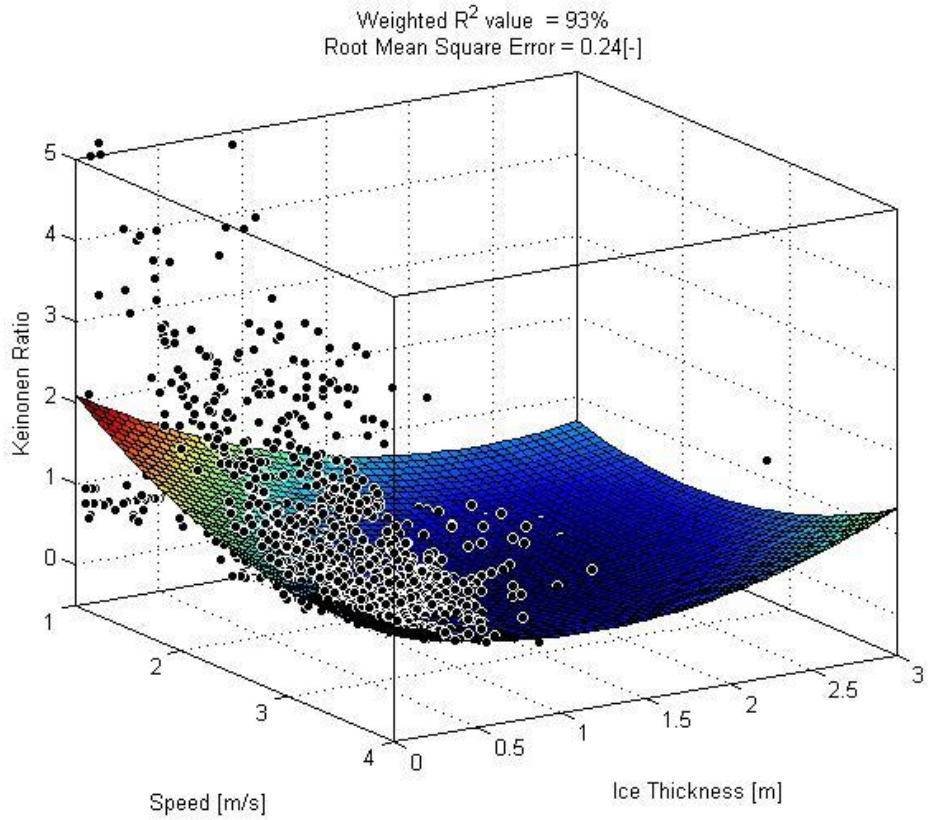


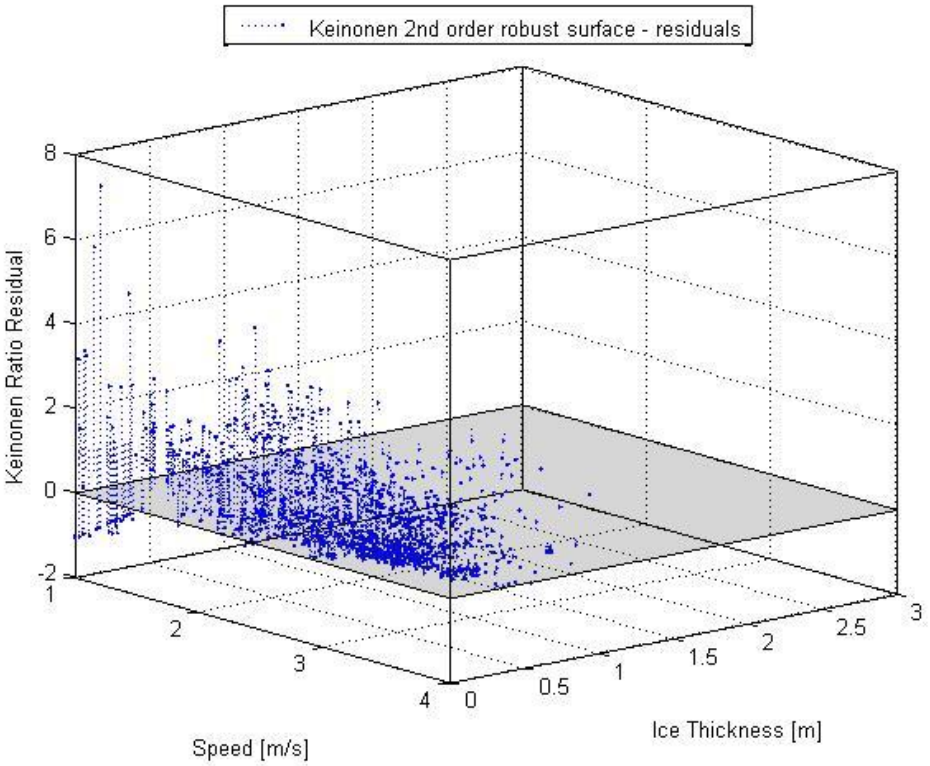

# Appendix D Lognormal distributions and Weibull distributions.

## D.1 Riska

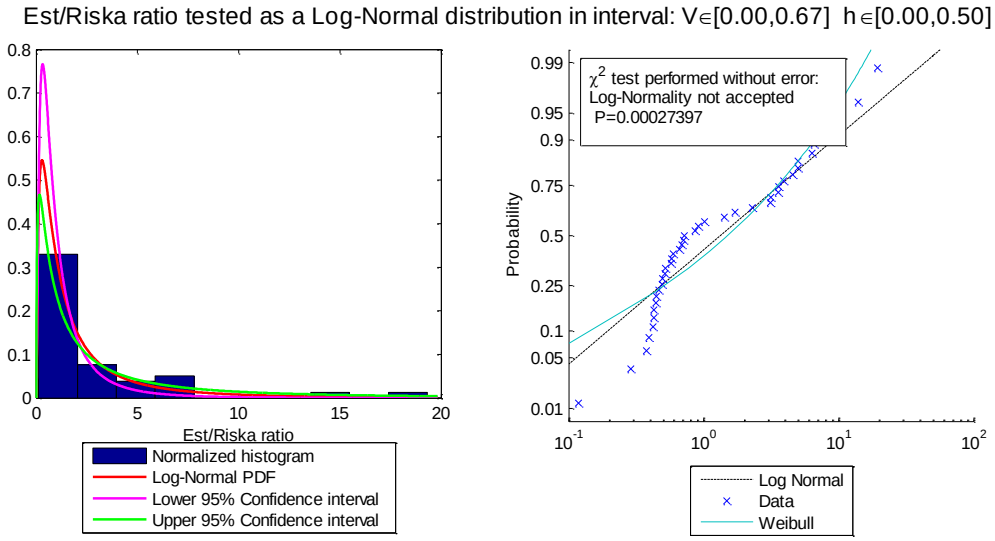


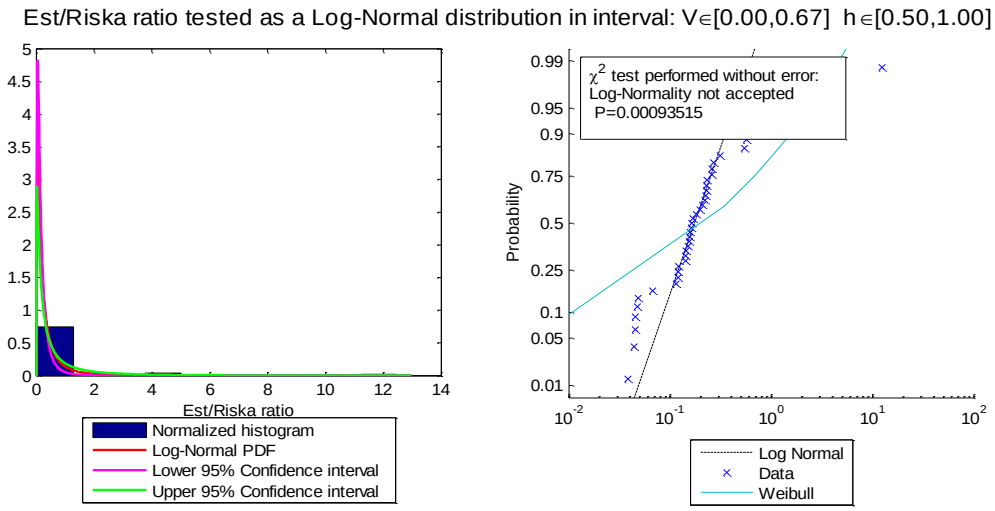

Est/Riska ratio tested as a Log-Normal distribution in interval: V∈[0.67,1.33] h∈[0.00,0.50]

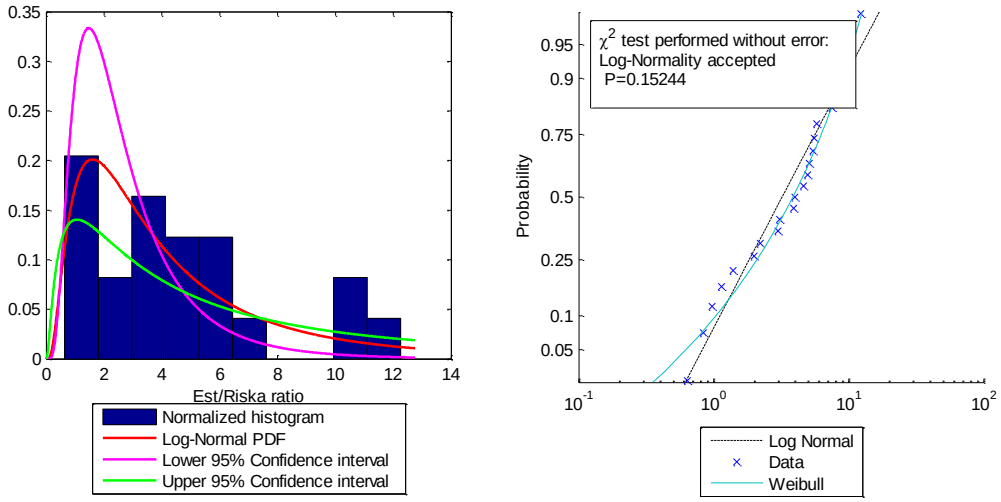


Est/Riska ratio tested as a Log-Normal distribution in interval: V∈[0.67,1.33] h∈[0.50,1.00]

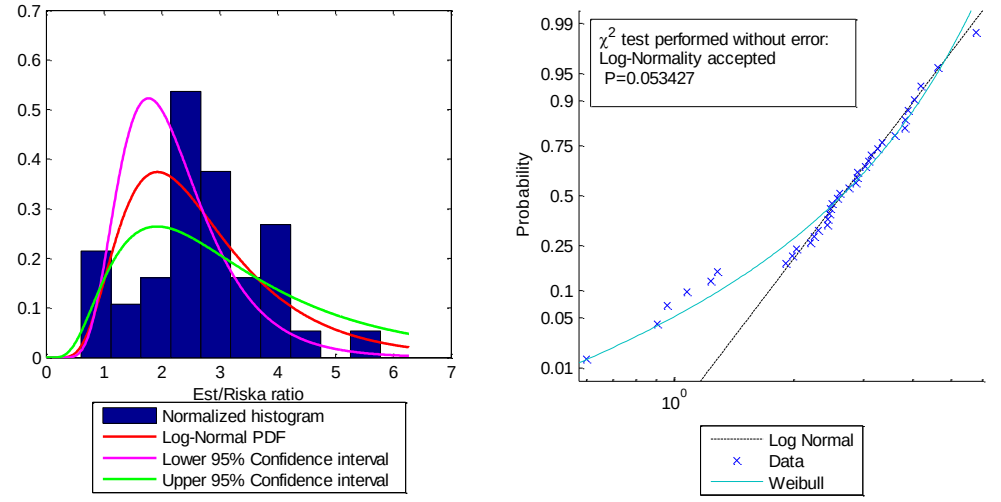


Est/Riska ratio tested as a Log-Normal distribution in interval: V∈[0.67,1.33] h∈[1.00,1.50]

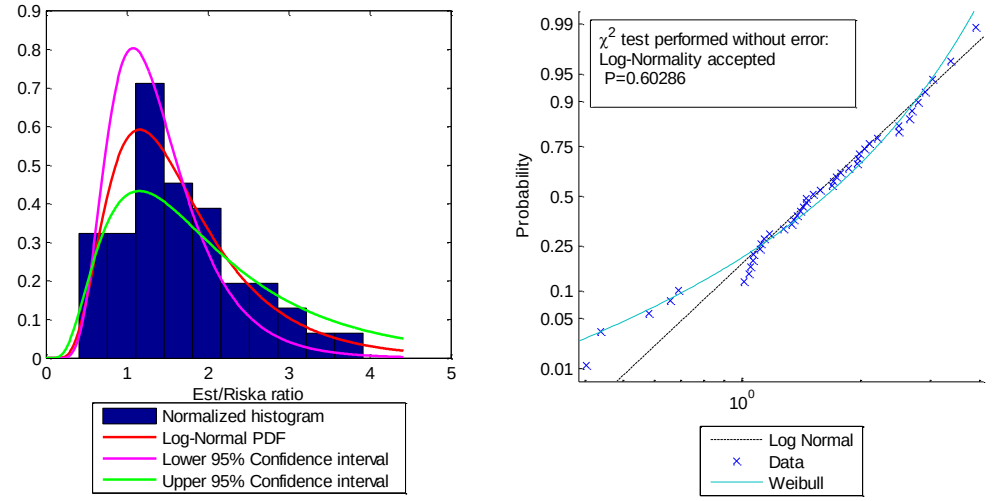

Est/Riska ratio tested as a Log-Normal distribution in interval: V∈[0.67,1.33] h∈[1.50,2.00]

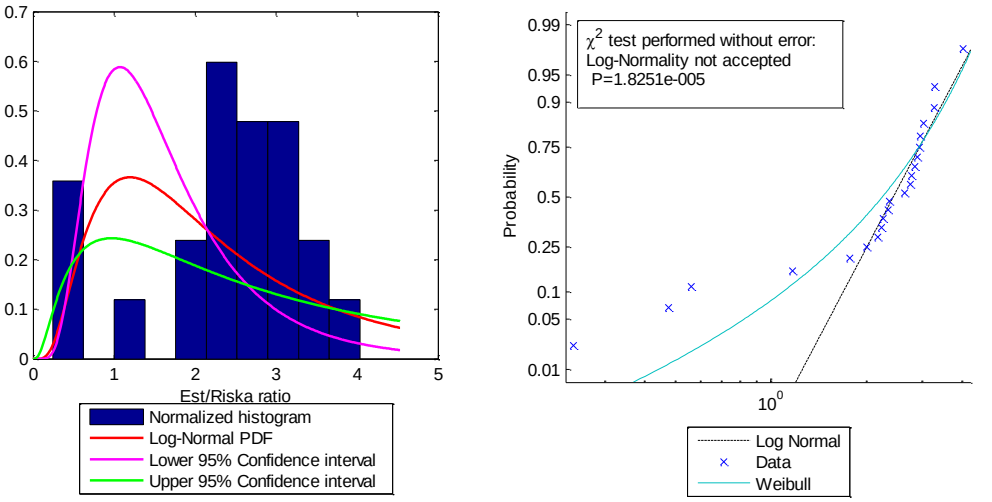


Est/Riska ratio tested as a Log-Normal distribution in interval: V∈[1.33,2.00] h∈[0.00,0.50]

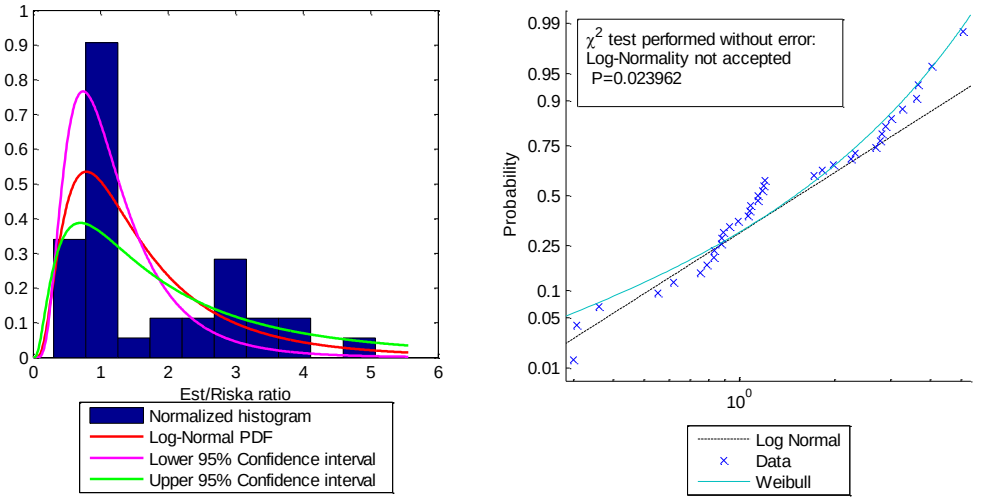


Est/Riska ratio tested as a Log-Normal distribution in interval: V∈[1.33,2.00] h∈[0.50,1.00]

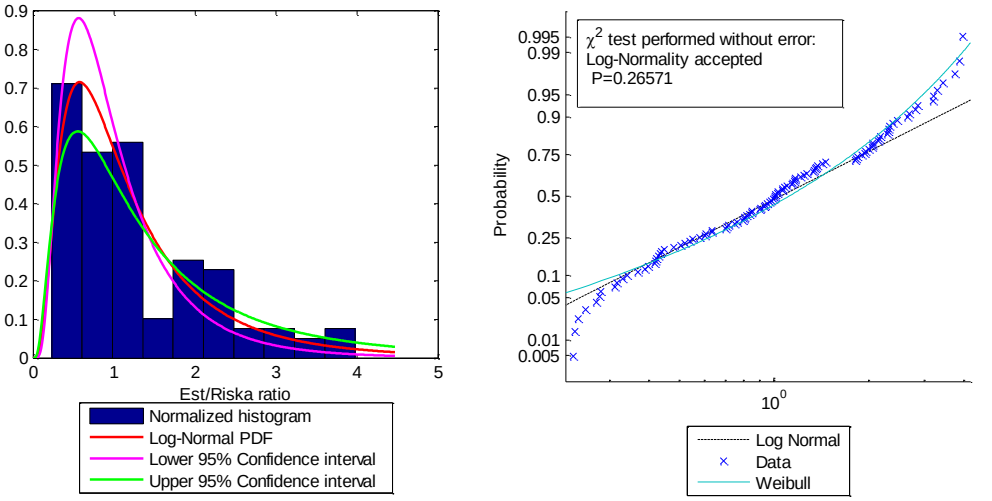

Est/Riska ratio tested as a Log-Normal distribution in interval: V∈[1.33,2.00] h∈[1.00,1.50]

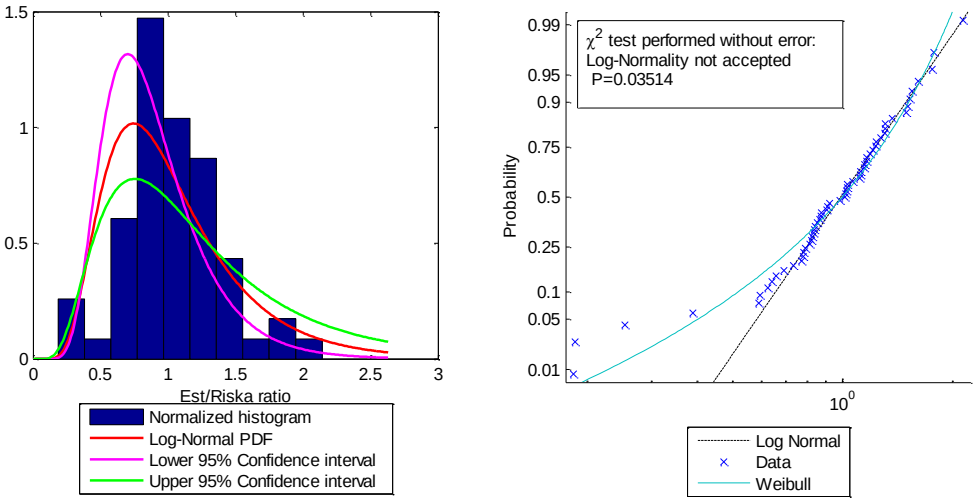


Est/Riska ratio tested as a Log-Normal distribution in interval: V∈[2.00,2.67] h∈[0.00,0.50]

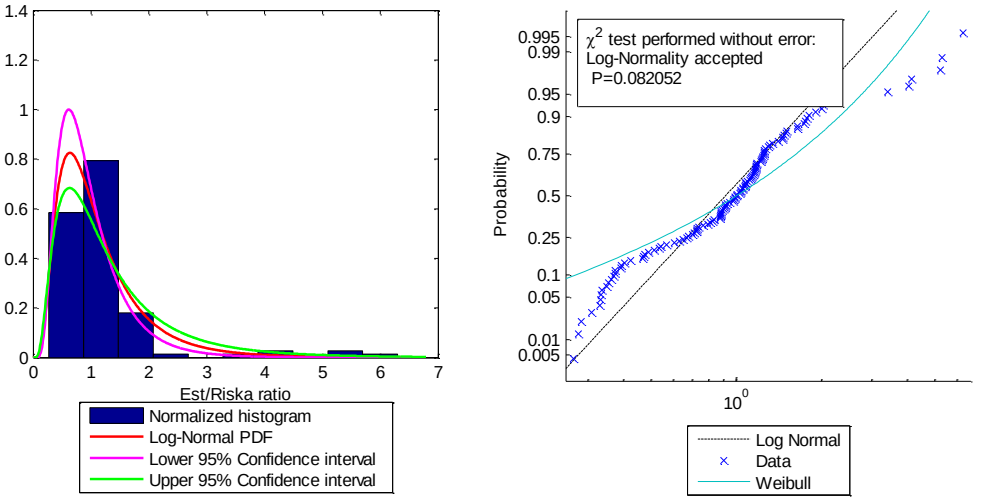


Est/Riska ratio tested as a Log-Normal distribution in interval: V∈[2.00,2.67] h∈[0.50,1.00]

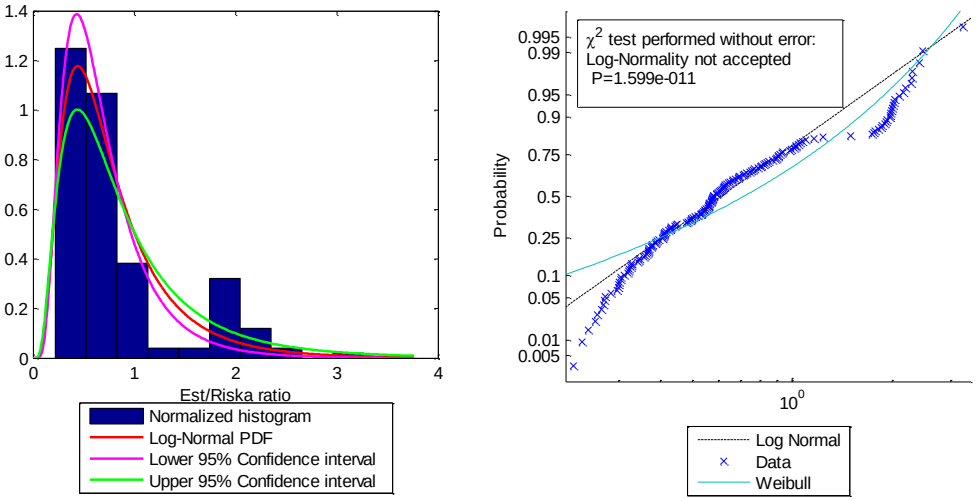

Est/Riska ratio tested as a Log-Normal distribution in interval: V∈[2.00,2.67] h∈[1.00,1.50]

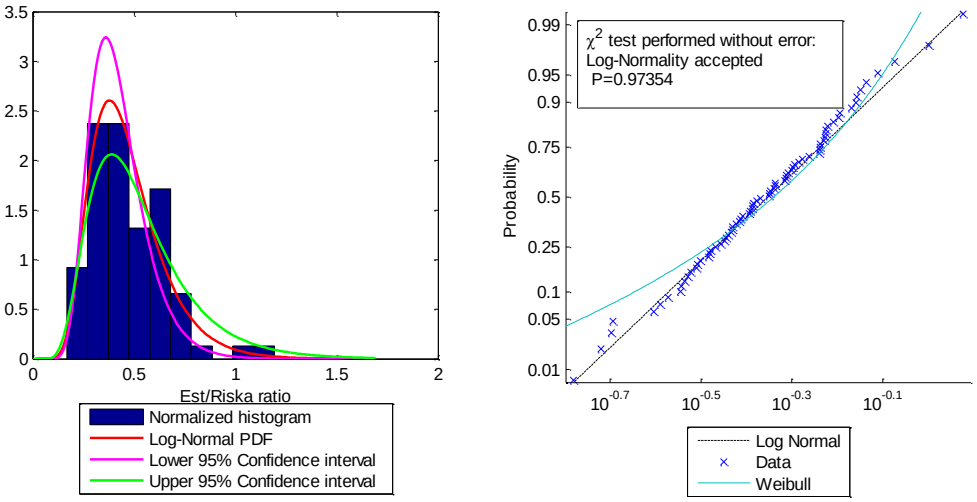


Est/Riska ratio tested as a Log-Normal distribution in interval: V∈[2.67,3.33] h∈[0.00,0.50]

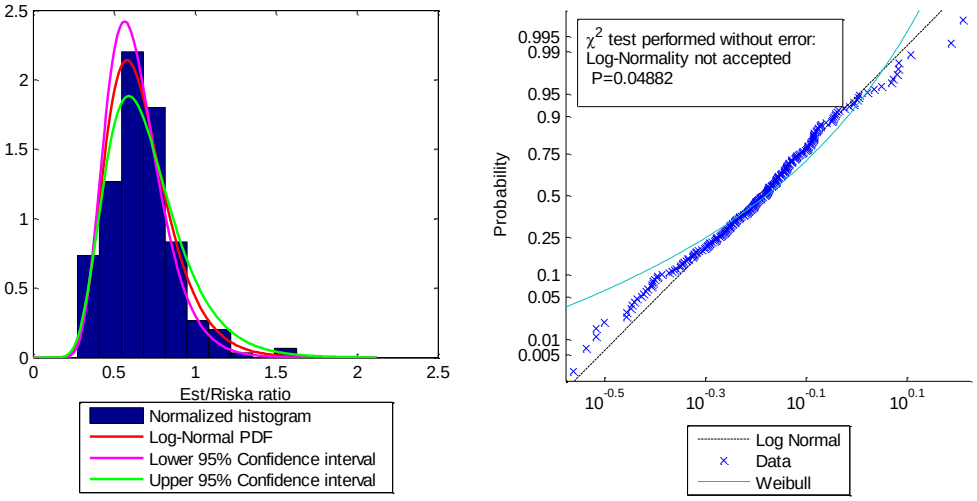


Est/Riska ratio tested as a Log-Normal distribution in interval: V∈[2.67,3.33] h∈[0.50,1.00]

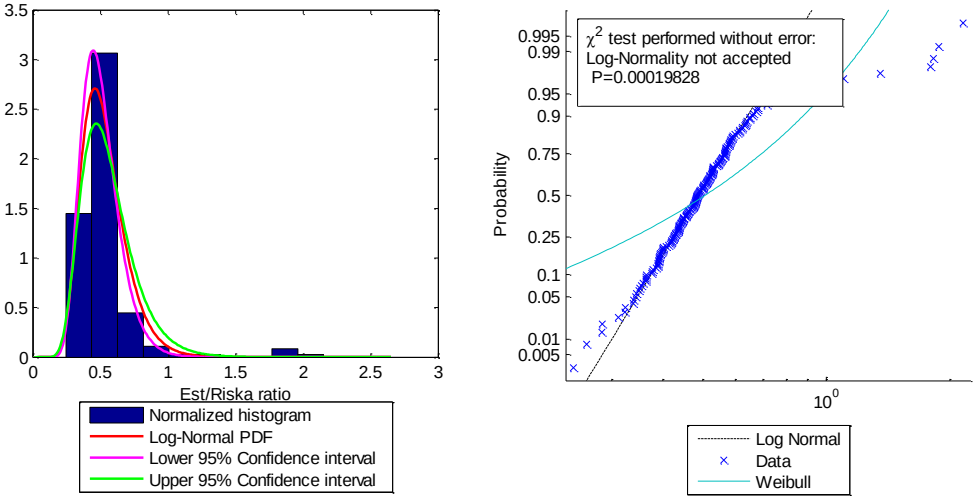

Est/Riska ratio tested as a Log-Normal distribution in interval: V∈[2.67,3.33] h∈[1.00,1.50]

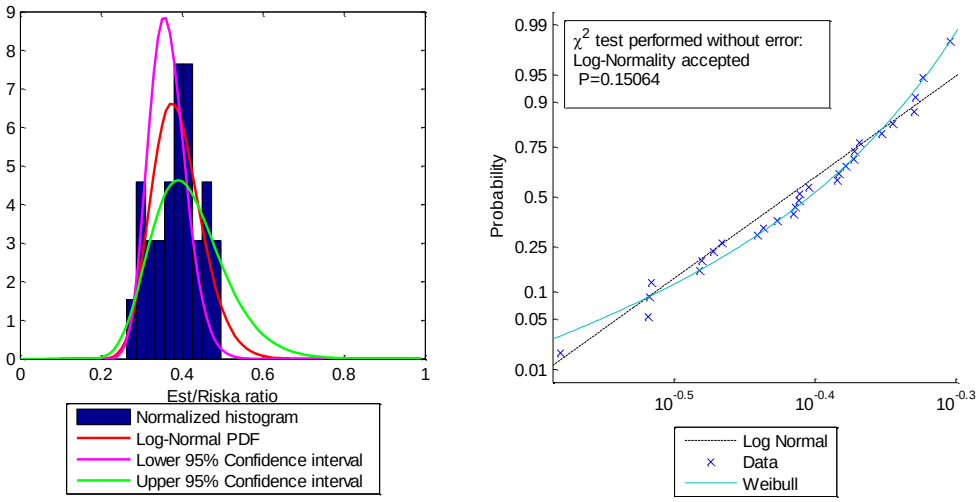


Est/Riska ratio tested as a Log-Normal distribution in interval: V∈[3.33,4.00] h∈[0.00,0.50]

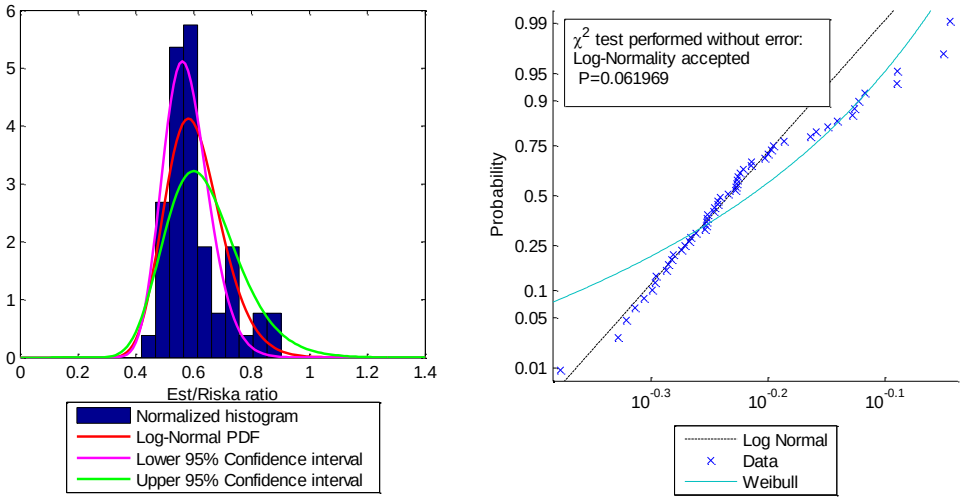


Est/Riska ratio tested as a Log-Normal distribution in interval: V∈[3.33,4.00] h∈[0.50,1.00]

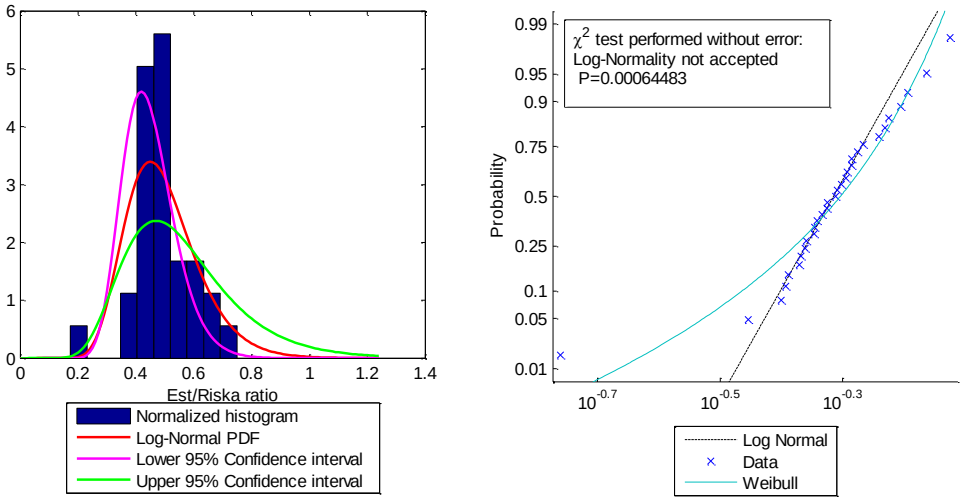

## D.2 Lindqvist

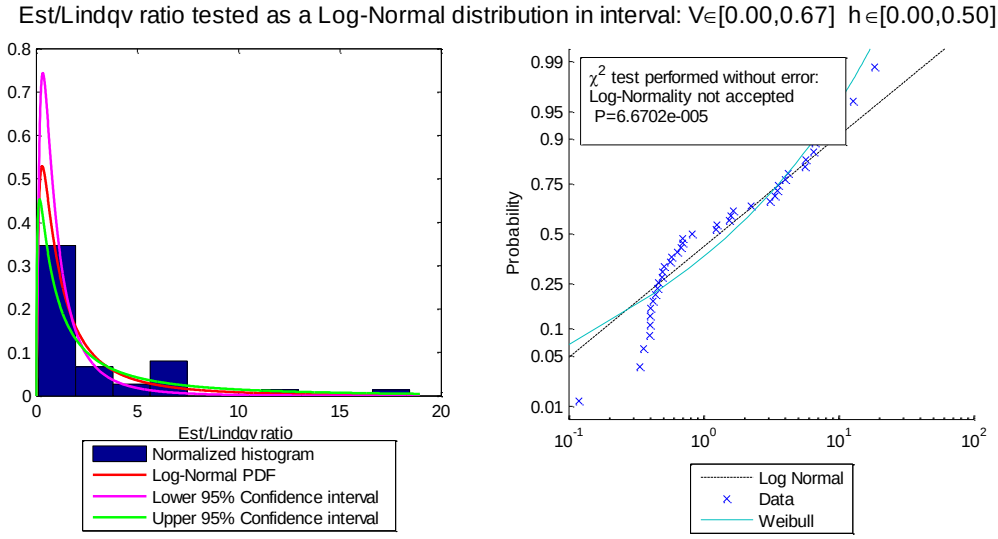


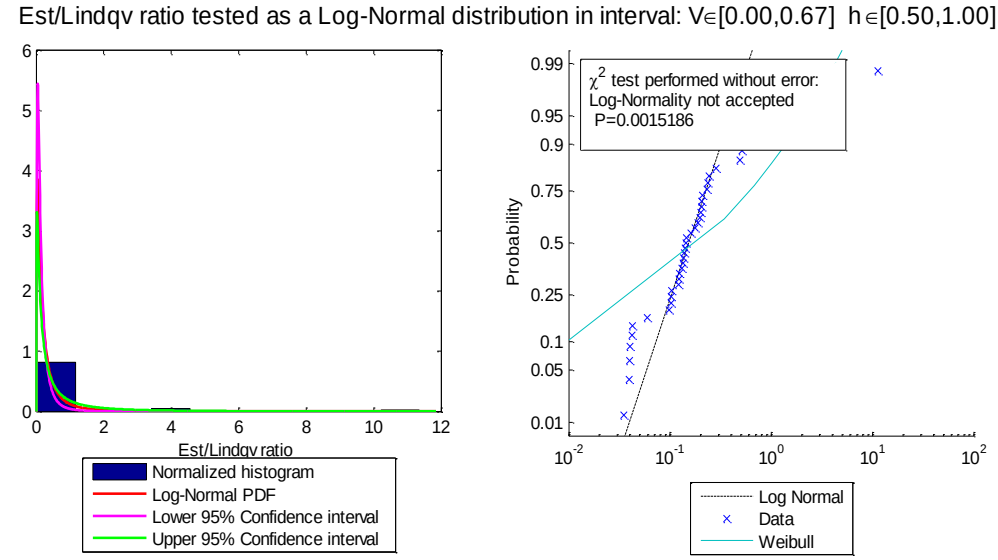

Est/Lindqv ratio tested as a Log-Normal distribution in interval: V∈[0.67,1.33] h∈[0.00,0.50]

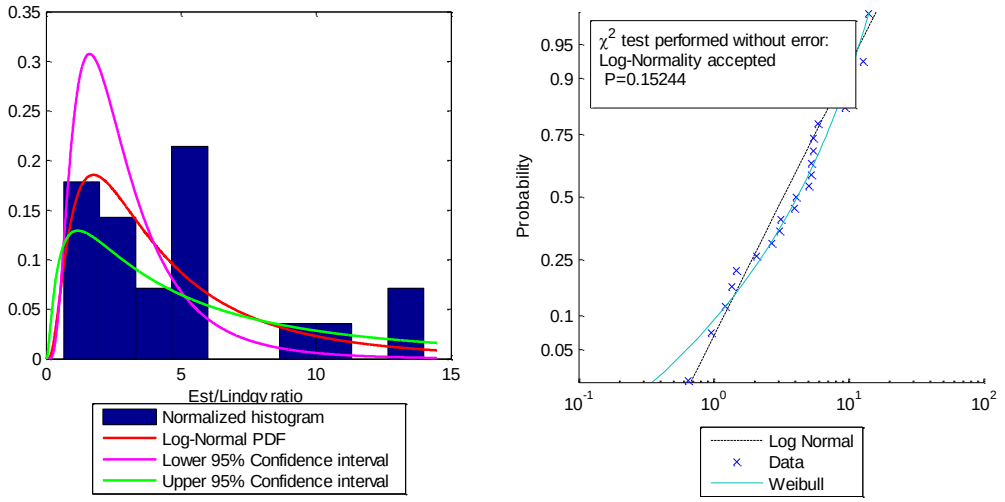


Est/Lindqv ratio tested as a Log-Normal distribution in interval: V∈[0.67,1.33] h∈[0.50,1.00]

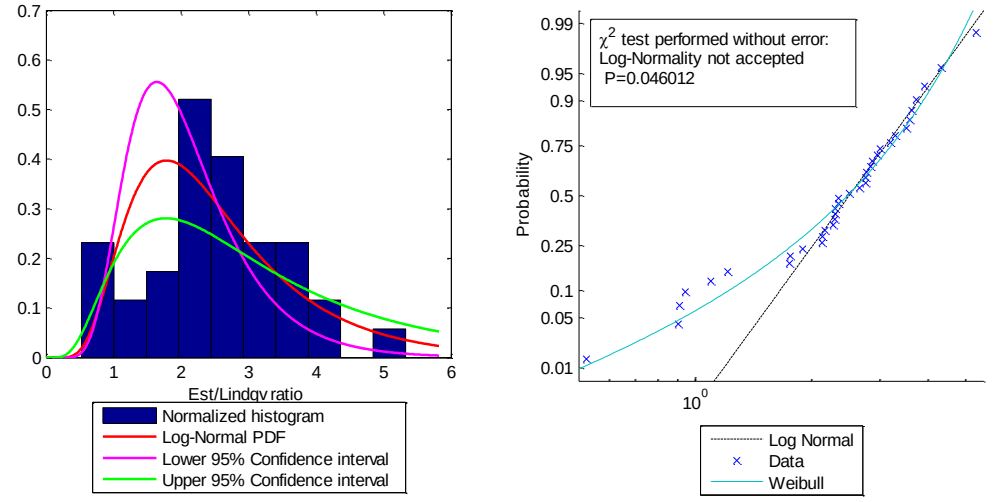


Est/Lindqv ratio tested as a Log-Normal distribution in interval: V∈[0.67,1.33] h∈[1.00,1.50]

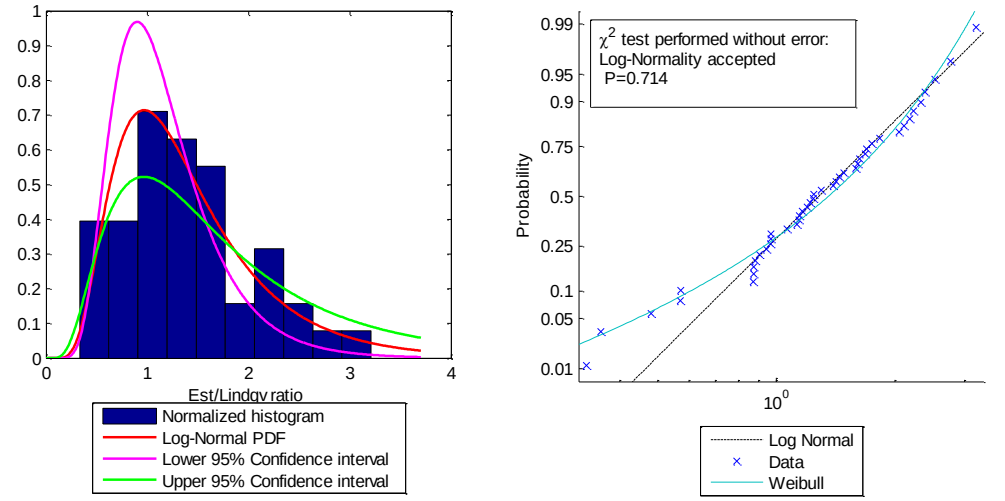

Est/Lindqv ratio tested as a Log-Normal distribution in interval: V∈[0.67,1.33] h∈[1.50,2.00]

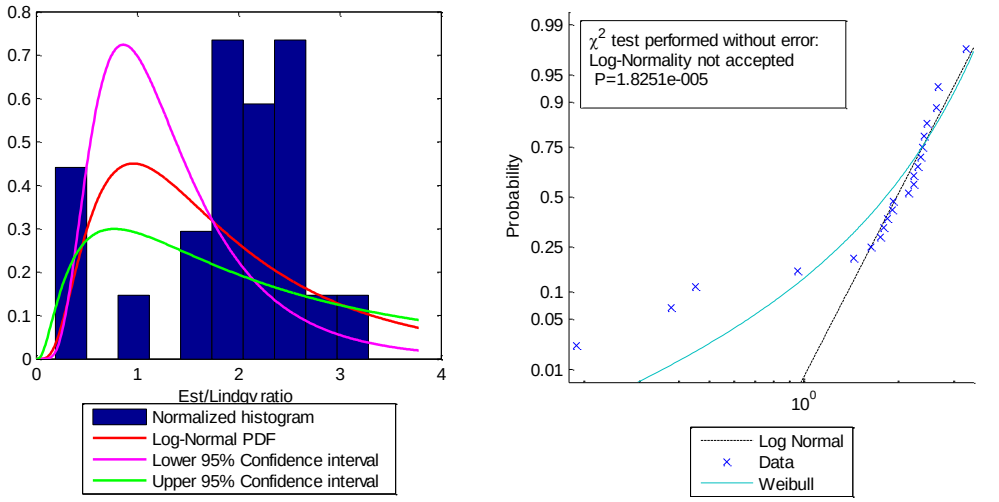


Est/Lindqv ratio tested as a Log-Normal distribution in interval: V∈[1.33,2.00] h∈[0.00,0.50]

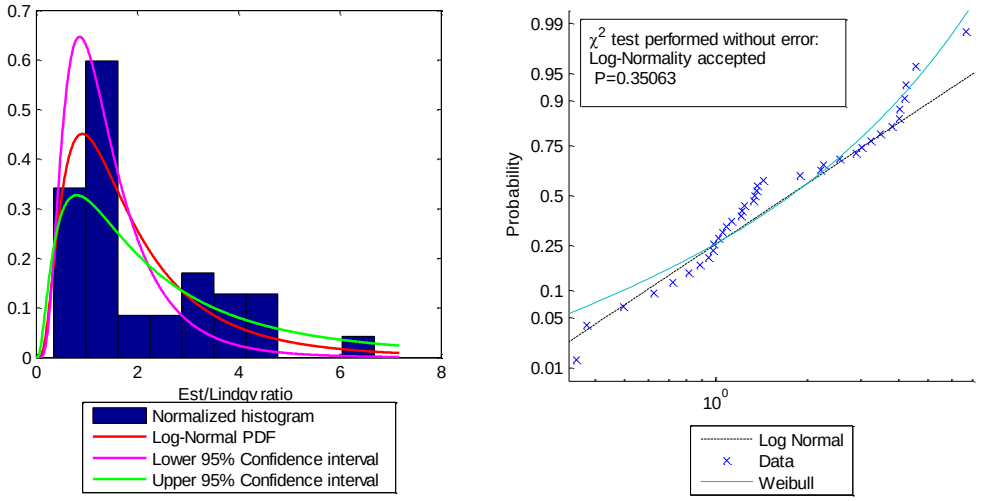


Est/Lindqv ratio tested as a Log-Normal distribution in interval: V∈[1.33,2.00] h∈[0.50,1.00]

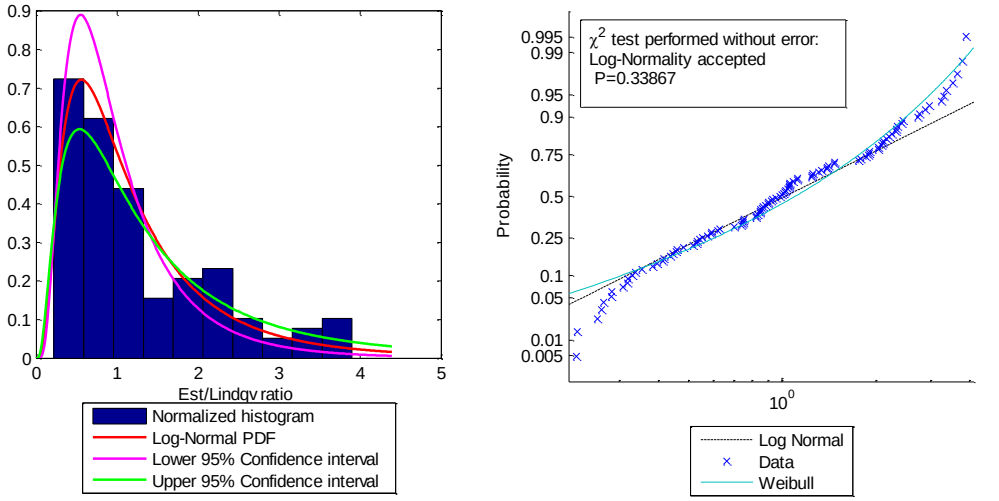

Est/Lindqv ratio tested as a Log-Normal distribution in interval: V∈[1.33,2.00] h∈[1.00,1.50]

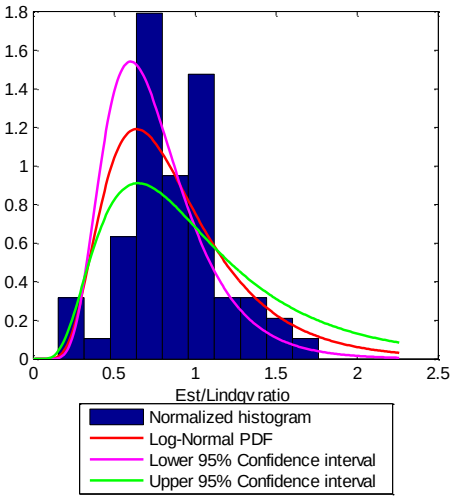


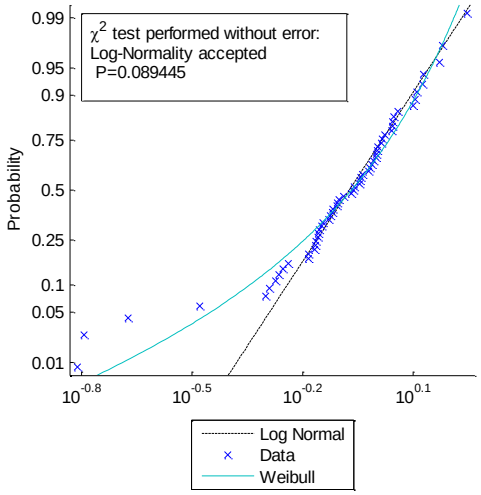


Est/Lindqv ratio tested as a Log-Normal distribution in interval: V∈[2.00,2.67] h∈[0.00,0.50]

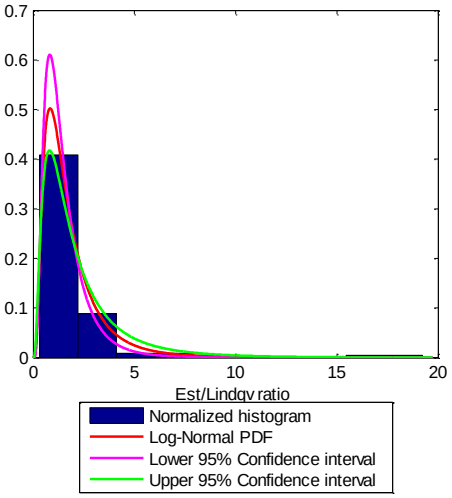


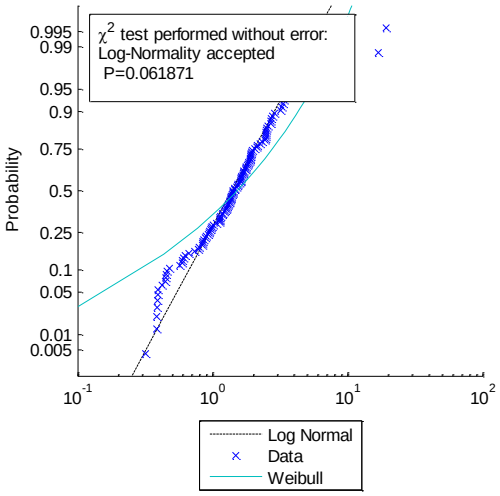


Est/Lindqv ratio tested as a Log-Normal distribution in interval: V∈[2.00,2.67] h∈[0.50,1.00]

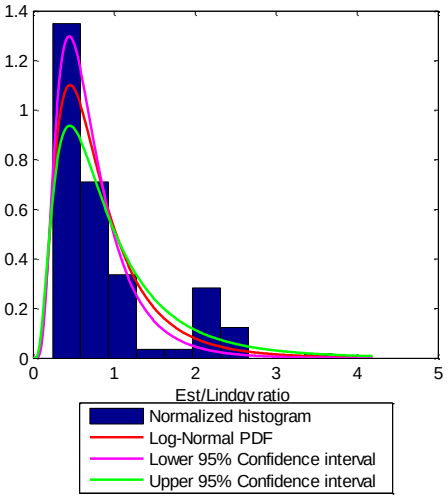


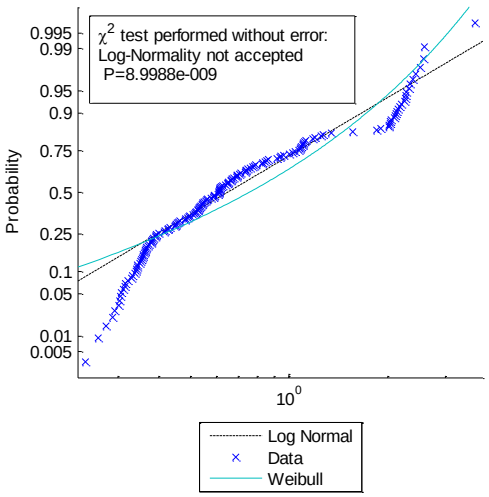

Est/Lindqv ratio tested as a Log-Normal distribution in interval: V∈[2.00,2.67] h∈[1.00,1.50]

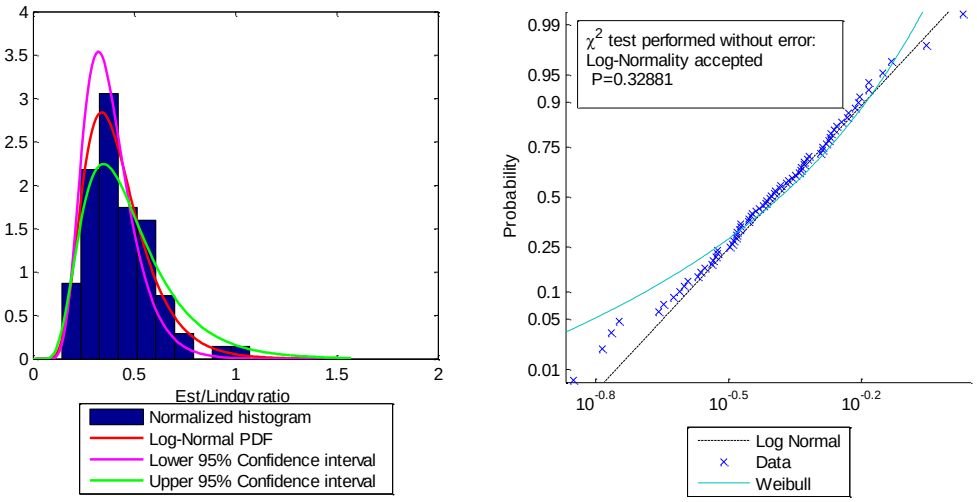


Est/Lindqv ratio tested as a Log-Normal distribution in interval: V∈[2.67,3.33] h∈[0.00,0.50]

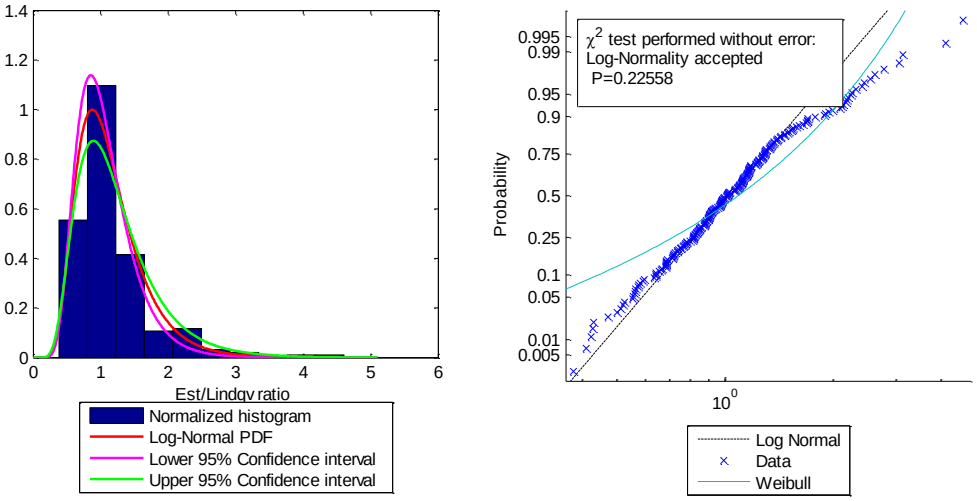


Est/Lindqv ratio tested as a Log-Normal distribution in interval: V∈[2.67,3.33] h∈[0.50,1.00]

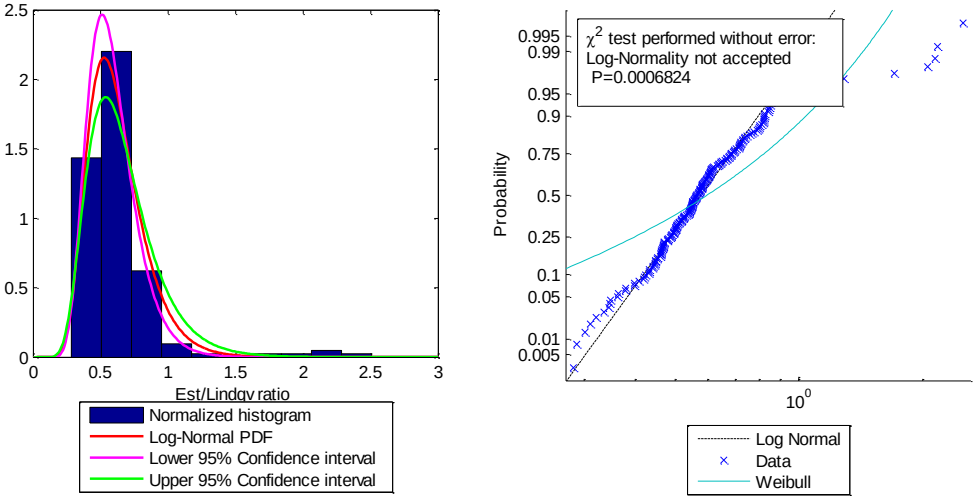

Est/Lindqv ratio tested as a Log-Normal distribution in interval: V∈[2.67,3.33] h∈[1.00,1.50]

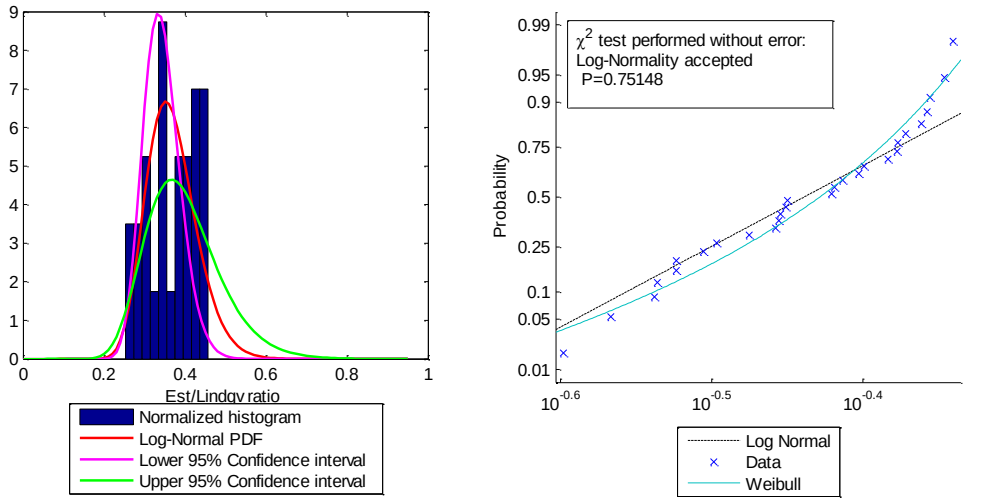


Est/Lindqv ratio tested as a Log-Normal distribution in interval: V∈[3.33,4.00] h∈[0.00,0.50]

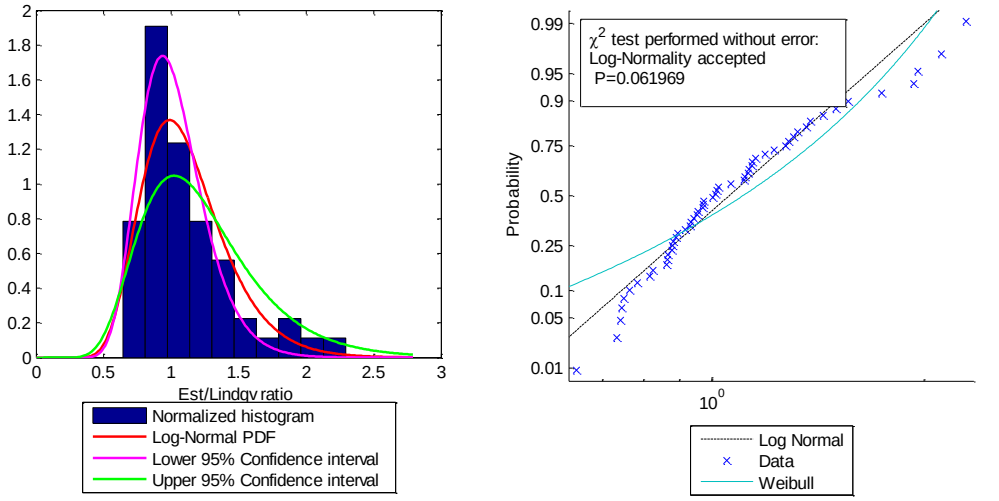


Est/Lindqv ratio tested as a Log-Normal distribution in interval: V∈[3.33,4.00] h∈[0.50,1.00]

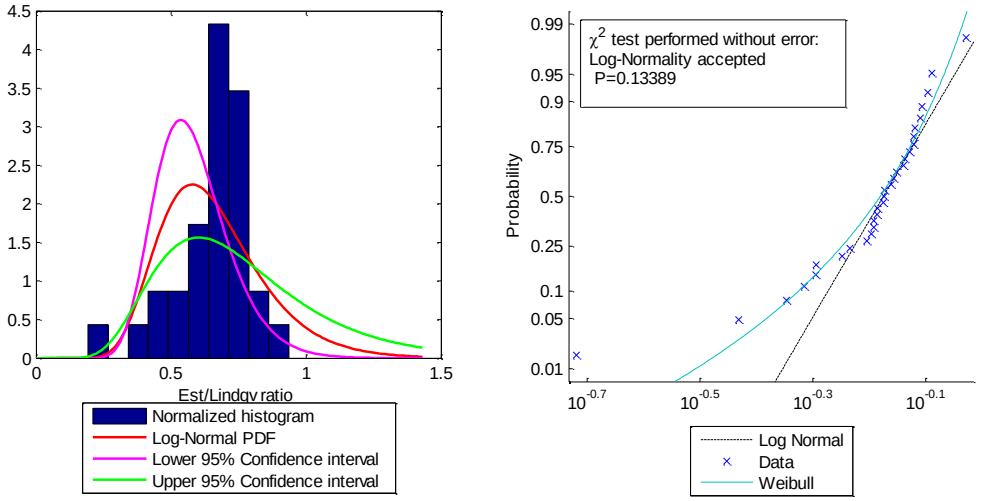

## D.3 Keinonen

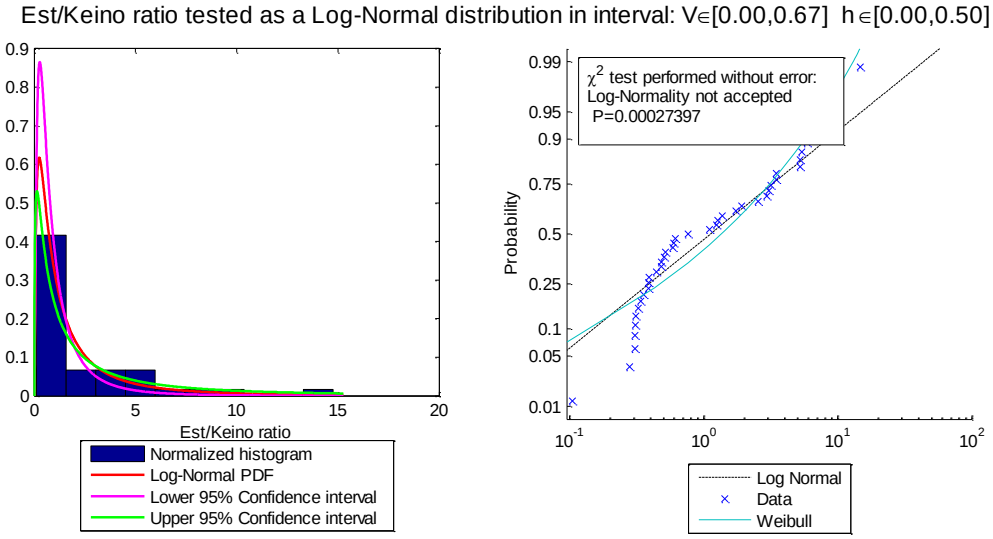
Est/Keino ratio tested as a Log-Normal distribution in interval: V∈[0.00,0.67] h∈[0.00,0.50]
Est/Keino ratio
Normalized histogram
Log-Normal PDF
Lower 95% Confidence interval
Upper 95% Confidence interval
χ2 test performed without error:
Log-Normality not accepted
P=0.00027397
Probability
Log Normal
Data
Weibull

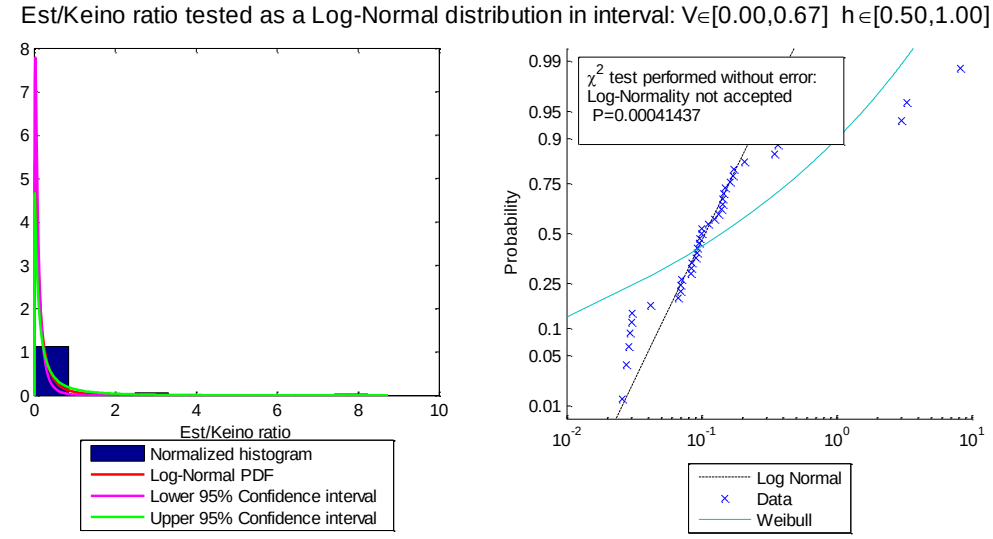
Est/Keino ratio tested as a Log-Normal distribution in interval: V∈[0.00,0.67] h∈[0.50,1.00]
Est/Keino ratio
Normalized histogram
Log-Normal PDF
Lower 95% Confidence interval
Upper 95% Confidence interval
χ2 test performed without error:
Log-Normality not accepted
P=0.00041437
Probability
Log Normal
Data
Weibull

Est/Keino ratio tested as a Log-Normal distribution in interval: V∈[0.67,1.33] h∈[0.00,0.50]

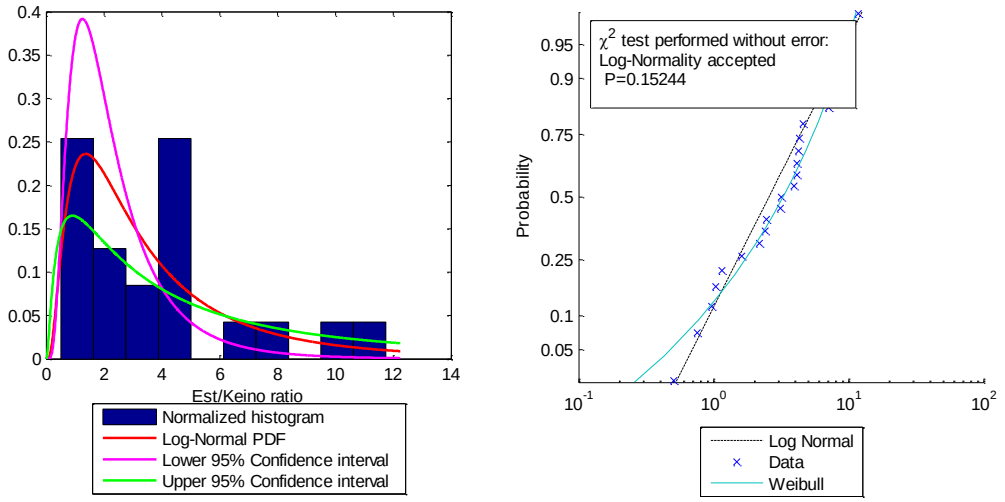


Est/Keino ratio tested as a Log-Normal distribution in interval: V∈[0.67,1.33] h∈[0.50,1.00]

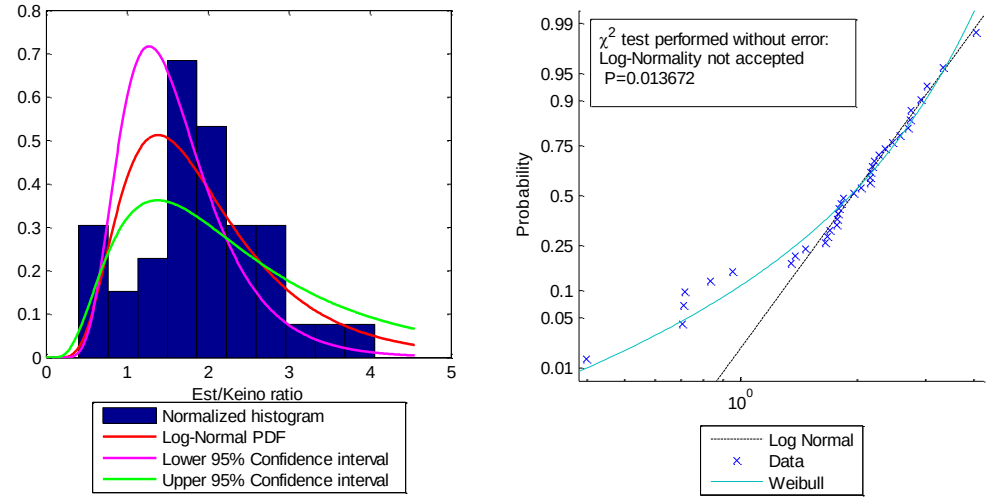


Est/Keino ratio tested as a Log-Normal distribution in interval: V∈[0.67,1.33] h∈[1.00,1.50]

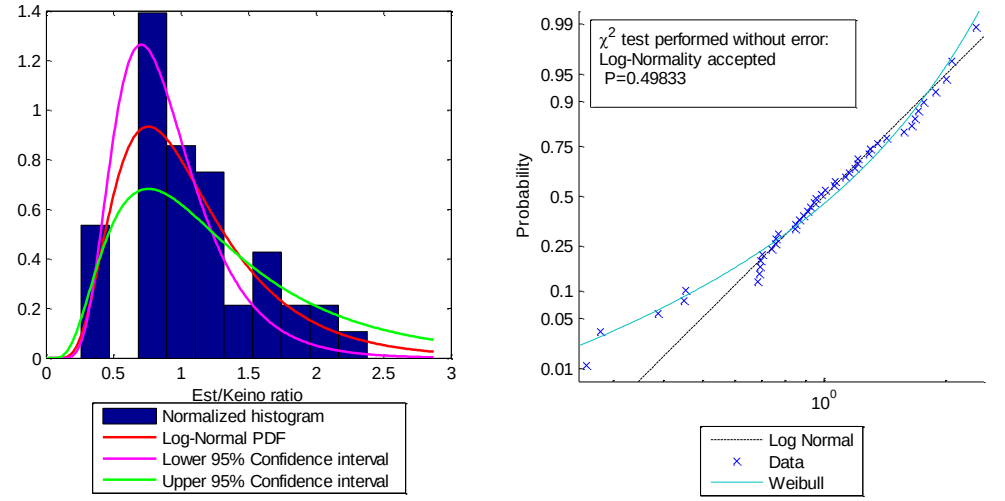

Est/Keino ratio tested as a Log-Normal distribution in interval: V∈[0.67,1.33] h∈[1.50,2.00]

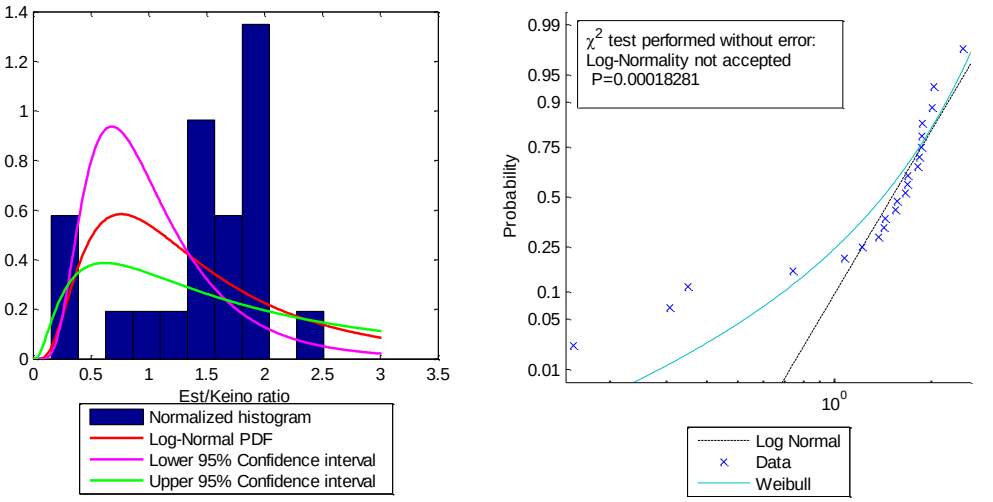


Est/Keino ratio tested as a Log-Normal distribution in interval: V∈[1.33,2.00] h∈[0.00,0.50]

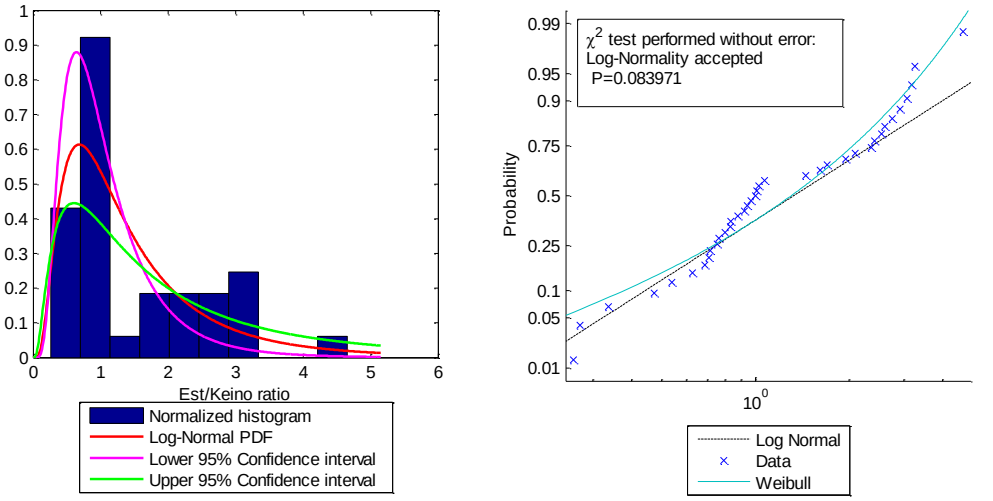


Est/Keino ratio tested as a Log-Normal distribution in interval: V∈[1.33,2.00] h∈[0.50,1.00]

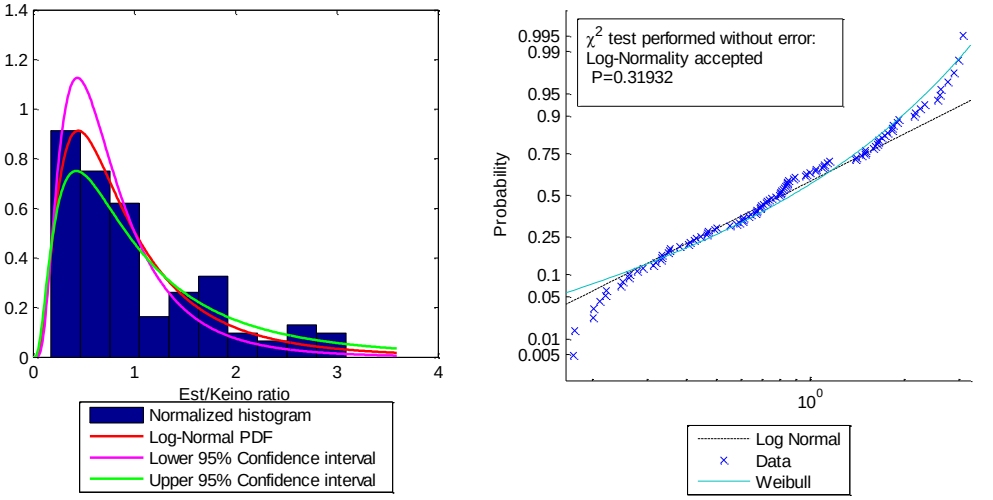

Est/Keino ratio tested as a Log-Normal distribution in interval: V∈[1.33,2.00] h∈[1.00,1.50]

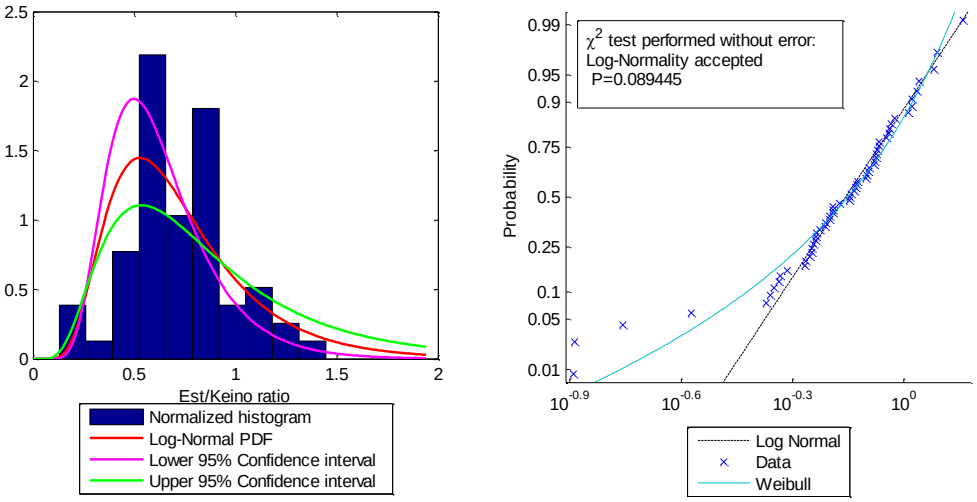


Est/Keino ratio tested as a Log-Normal distribution in interval: V∈[2.00,2.67] h∈[0.00,0.50]

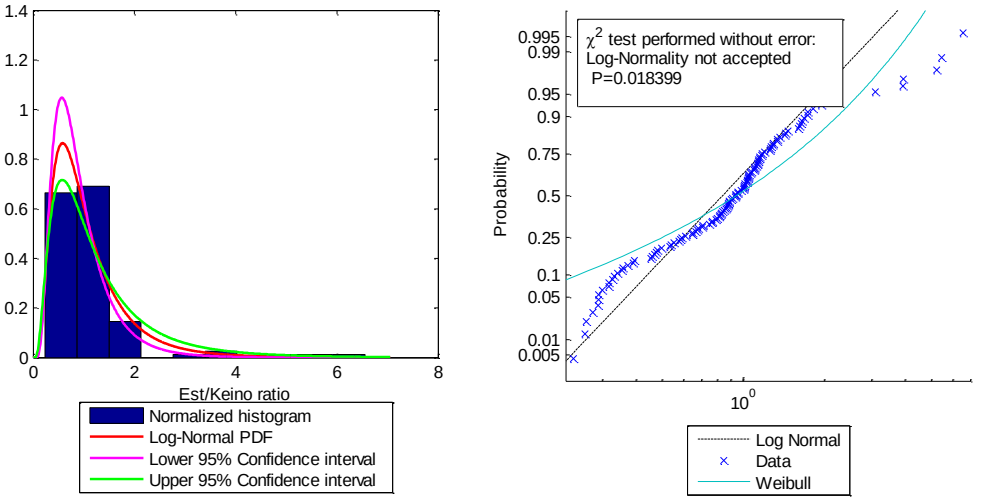


Est/Keino ratio tested as a Log-Normal distribution in interval: V∈[2.00,2.67] h∈[0.50,1.00]

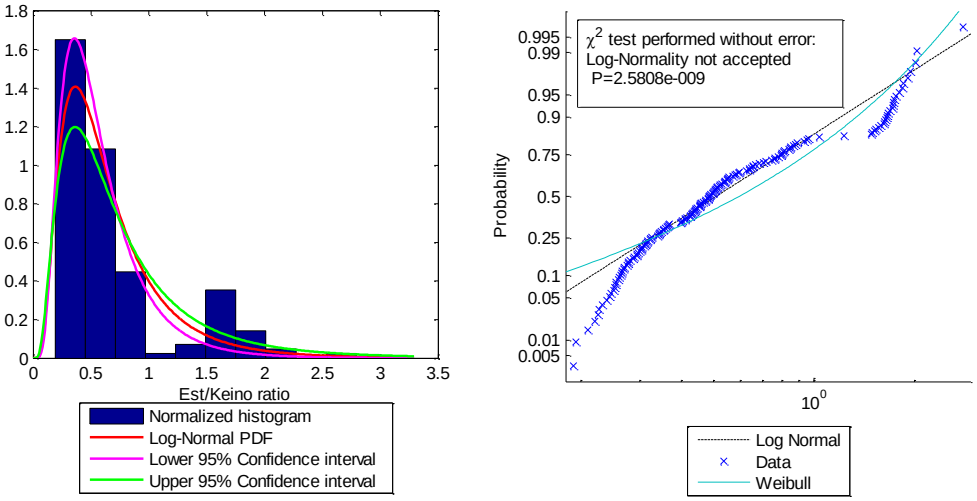

Est/Keino ratio tested as a Log-Normal distribution in interval: V∈[2.00,2.67] h∈[1.00,1.50]

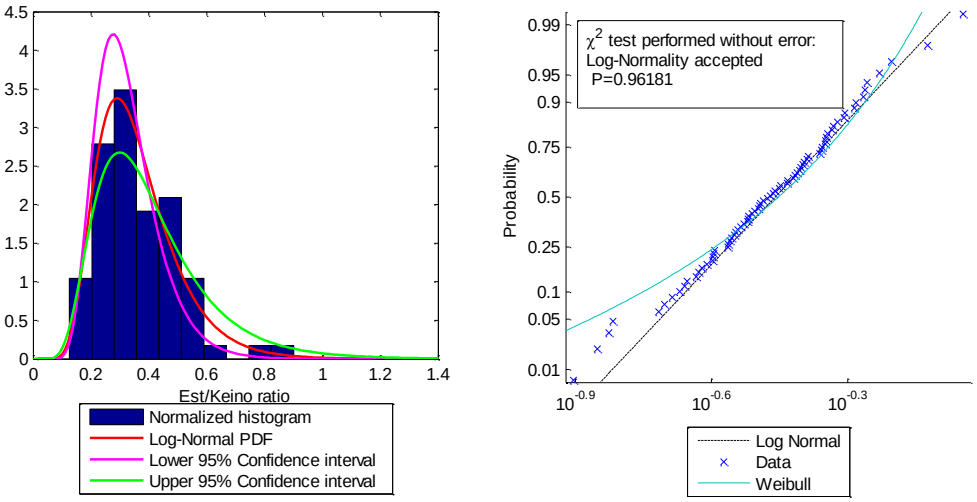


Est/Keino ratio tested as a Log-Normal distribution in interval: V∈[2.67,3.33] h∈[0.00,0.50]

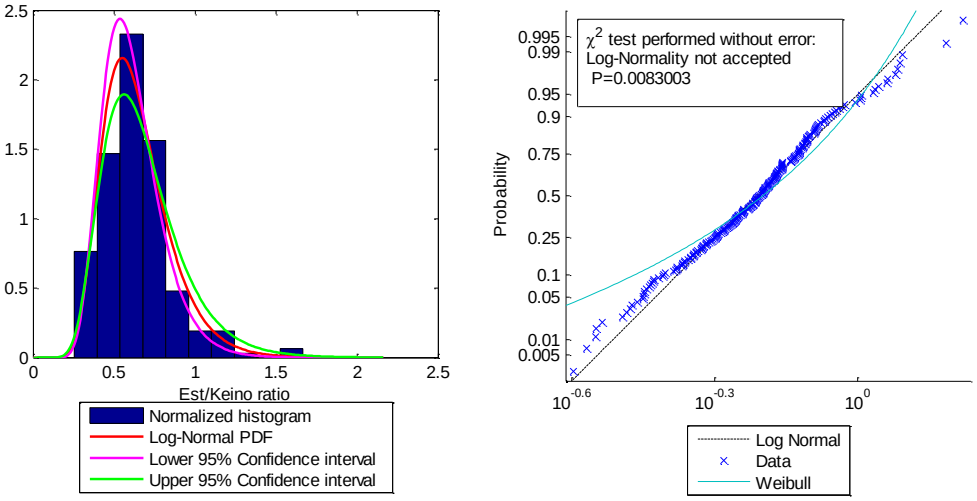


Est/Keino ratio tested as a Log-Normal distribution in interval: V∈[2.67,3.33] h∈[0.50,1.00]

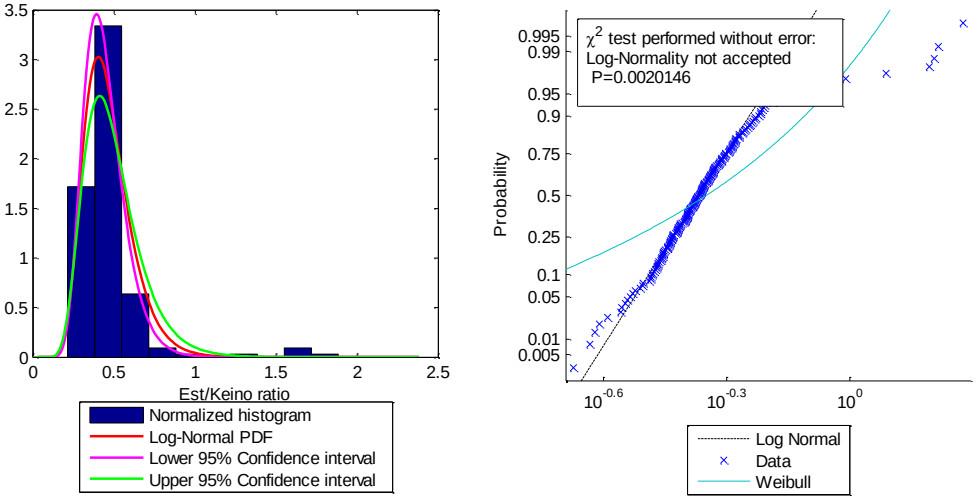

Est/Keino ratio tested as a Log-Normal distribution in interval: V∈[2.67,3.33] h∈[1.00,1.50]

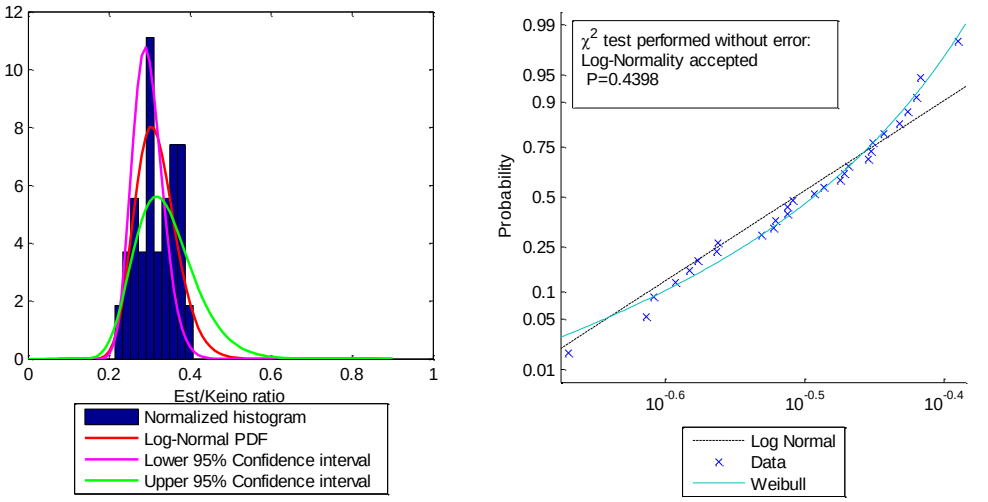


Est/Keino ratio tested as a Log-Normal distribution in interval: V∈[3.33,4.00] h∈[0.00,0.50]

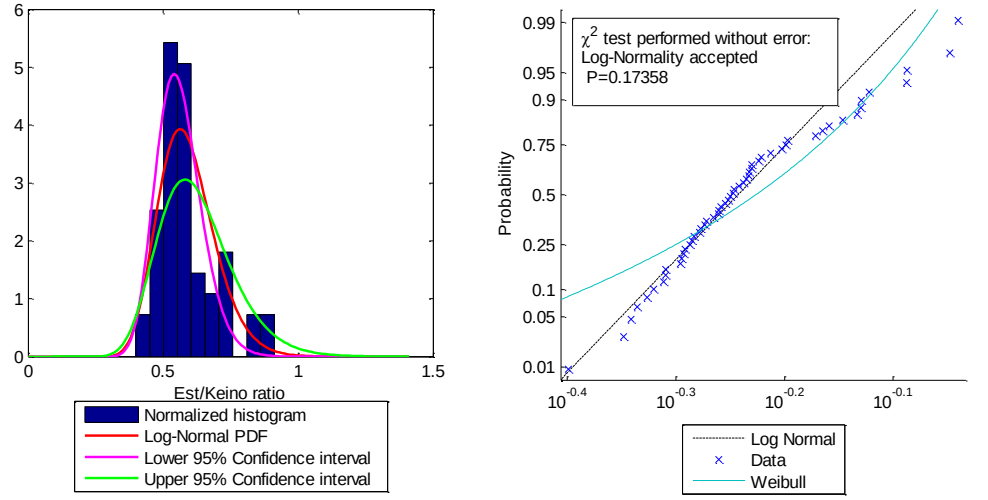


Est/Keino ratio tested as a Log-Normal distribution in interval: V∈[3.33,4.00] h∈[0.50,1.00]

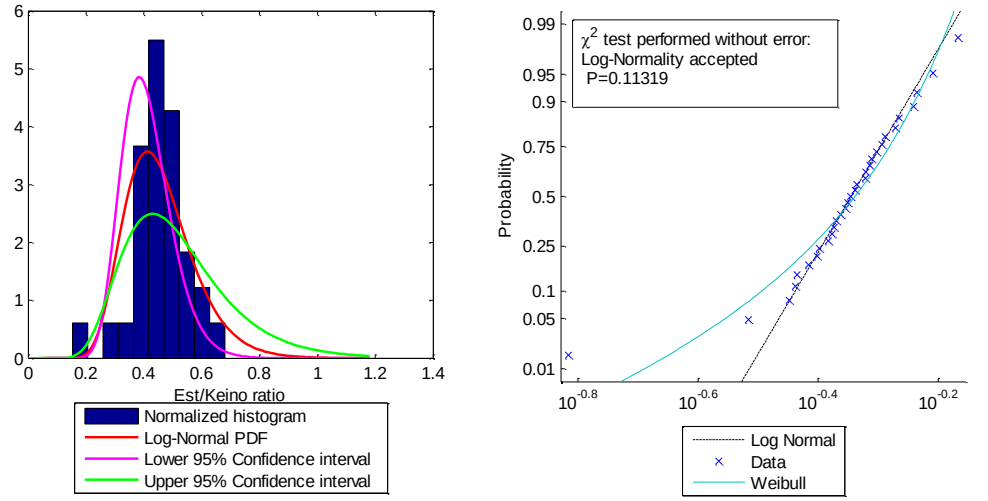

# Appendix E Ice observation data

| Date | Time | UTC | Position lat | lon | Wind spd | dir | T °C | Progress speed | ope. | Concentrations [%] floes | w.t. | nilas | Prevailing ice type conc1 | thick1 | type1 | floe1 | topo1 | snow1 | Secondary ice type conc2 | thick2 | type2 | floe2 | topo2 | snow2 | Comment |
|---|---|---|---|---|---|---|---|---|---|---|---|---|---|---|---|---|---|---|---|---|---|---|---|---|---|
| 22.03.07 | 11:10 | 10:10 | 77 | 5,62 | 19 | 138 | | 0 | | 90 | 2 | 5 | 90 | 60 | 60 | 600 | 761 | 5 | | | | | | | |
| | 12:04 | 11:04 | 77 | 13,48 | 19 | 123 | | 14 | 2 | 90 | 2 | 5 | 90 | 10 | 50 | 200 | 100 | 0 | | | | | | | some snowfall, sailing through refrozen polynya as seen on AMSRE ice map |
| | 13:07 | 12:07 | 77 | 25,32 | 20 | 7,28 | | 13 | 2 | 90 | 2 | 5 | 90 | 10 | 50 | 200 | 100 | 0 | | | | | | | sailing through open water |
| | 14:00 | 13:00 | 77 | 36,87 | 20 | 19,4 | | 16 | | 10 - | 2 | 5 | 10 | 10 | 10 | 100 | 100 | 0 | | | | | | | reached open water at end of ice obs |
| | 15:00 | 14:00 | 77 | 48,78 | 20 | 35,43 | | 0 | | 30 | 5 | 10 | 30 | 10 | 10 | 100 | 100 | 0 | | | | | | | on station |
| | 16:00 | 15:00 | 77 | 49,74 | 20 | 36,79 | | 0 | | 30 | 5 | 10 | 30 | 10 | 10 | 100 | 100 | 0 | | | | | | | on station |
| | 16:50 | 15:50 | 77 | 50,60 | 20 | 29,85 | | 0 | | 30 | 2 | 5 | 90 | 15 | 50 | 200 | 400 | 0 | | | | | | | |
| | 18:15 | 17:15 | 78 | 58,04 | 20 | 39,76 | | 13 | 2 | 80 | 2 | 5 | 90 | 15 | 50 | 200 | 400 | 0 | | | | | | | |
| | 19:05 | 18:05 | 78 | 5,71 | 20 | 39,9 | | 12 | 2 | 80 | 2 | 5 | 90 | 20 | 50 | 100 | 100 | 0 | | | | | | | |
| | 20:00 | 19:00 | 78 | 8,63 | 20 | 52,43 | | 0 | 3 | 100 | 0 | | 100 | 40 | 95 | 800 | 100 | 5 | | | | | | | Performing maneuver tests in fast ice, no photos due to darkness |
| 23.03.07 | 9:00 | 8:00 | 78 | 8,63 | 20 | 52,43 | | | | 100 | 0 | 0 | 100 | 40 | 95 | 800 | 100 | 5 | | | | | | | Still on fast ice station as evening before |
| | 10:00 | 9:00 | 78 | 8,63 | 20 | 52,43 | | | | 100 | 0 | 0 | 100 | 40 | 95 | 800 | 100 | 5 | | | | | | | still same station |
| | 11:00 | 10:00 | 78 | 7,66 | 20 | 49,05 | | | | 0 | 7 | 0 | 0 | | | | | | | | | | | | On CTD station just off the fast ice edge, left at ~10:30 |
| | 12:05 | 11:05 | 78 | 6,37 | 20 | 42,33 | | | | 40 | 7 | 5 | 35 | 10 | 50 | 600 | 200 | 0 | | | | | | | |
| | 13:10 | 12:10 | 78 | 6,01 | 20 | 41,15 | | | | 70 | 0 | 30 | 70 | 10 | 20 | 400 | 200 | 0 | | | | | | | |
| | 14:15 | 13:15 | 78 | 8,06 | 20 | 40,9 | | 1 | | 90 | 0 | 10 | 90 | 40 | 20 | 400 | 200 | 0 | 10 | 40 | 20 | 400 | 200 | 0 | Drifting with cake ice on CTD station |
| | 15:10 | 14:10 | 78 | 5,34 | 20 | 35,54 | | 1 | | 30 | 0 | 70 | 20 | 10 | 50 | 500 | 100 | 0 | | | | | | 0 | same as 14:00 |
| | 16:10 | 15:10 | 78 | 5,66 | 20 | 38,22 | | 1 | | 60 | 0 | 40 | 60 | 40 | 20 | 400 | 200 | 0 | | | | | | | same as 14:00 |
| | 17:04 | 16:04 | 78 | 4,79 | 20 | 36,01 | | 0,5 | | 80 | 0 | 20 | 60 | 20 | 50 | 500 | 100 | 0 | 10 | 40 | 20 | 400 | 200 | 0 | same as 14:00 |
| | 18:13 | 17:13 | 78 | 4,24 | 20 | 32,22 | | 2 | 3 | 90 | 0 | 10 | 90 | 20 | 20 | 200 | 200 | 0 | | | | | | | in transit between stations |
| 24.03.07 | 9:00 | 8:00 | 77 | 44,25 | 19 | 9,97 | | 10 | 3 | 80 | 3 | 0 | 80 | 50 | 50 | 600 | 501 | 0 | | | | | | | Several layers of cemented pancakes, rafted to 40-60 cm floes 9:00-15:00 |
| | 9:55 | 8:55 | 77 | 46,71 | 19 | 18,87 | | 11 | 1 | 40 | 5 | 10 | 40 | 50 | 50 | 700 | 501 | 0 | | | | | | | |
| | 11:05 | 10:05 | 77 | 50,36 | 19 | 31,31 | | 0 | 0 | 80 | 3 | 5 | 80 | 50 | 50 | 600 | 501 | 0 | | | | | | | |
| | 12:00 | 11:00 | 77 | 53,62 | 19 | 44,58 | | 0 | 0 | 80 | 3 | 5 | 80 | 50 | 50 | 600 | 501 | 0 | | | | | | | |
| | 13:00 | 12:00 | 77 | 54,83 | 20 | 4,07 | | 0 | 0 | 30 | 3 | 5 | 25 | 50 | 50 | 500 | 501 | 0 | | | | | | | |
| | 14:10 | 13:10 | 77 | 59,80 | 20 | 21,2 | | 12 | 3 | 100 | 0 | 0 | 50 | 50 | 50 | 600 | 200 | 0 | 50 | 20 | 20 | 500 | 200 | 0 | |
| | 15:00 | 14:00 | 78 | 1,94 | 20 | 22,07 | | 0 | 0 | 100 | 0 | 0 | 100 | 50 | 50 | 600 | 501 | 0 | | | | | | | |
| | 16:00 | 15:00 | 78 | 7,09 | 20 | 45,6 | | 0 | 0 | 100 | 0 | 0 | 100 | 70 | 50 | 800 | 551 | 0 | | | | | | | Ice is under pressure, heavily ridged |
| | 17:00 | 16:00 | 78 | 7,99 | 20 | 49,53 | | 3 | 4 | 100 | 0 | 0 | 100 | 80 | 50 | 800 | 571 | 0 | | | | | | | Got stuck with two engines, ~3kt with 4 engines at full load |
| 25.03.07 | 8:45 | 6:45 | 78 | 8,72 | 20 | 53,62 | | 7 | | 100 | 0 | 0 | 100 | 60 | 95 | 900 | 100 | 10 | | | | | | | |
| | 10:10 | 8:10 | 78 | 10,33 | 20 | 57,91 | | 14 | 306 | | 8,5 | 3 | 100 | 0 | 0 | 50 | 60 | 95 | 800 | 100 | 10 | 50 | 400 | 60 | 800 | 682 | 10 | Parked in front of rubble field |
| | 11:00 | 9:00 | 78 | 10,33 | 20 | 57,91 | | 11 | 323 | | 0 | 0 | 100 | 0 | 0 | 50 | 60 | 95 | 800 | 100 | 10 | 50 | 400 | 60 | 800 | 682 | 10 | |
| | 12:00 | 10:00 | 78 | 10,33 | 20 | 58,21 | | 12 | 315 | -5 | 0 | 4 | 100 | 0 | 0 | 100 | 400 | 60 | 800 | 682 | 10 | | | | | | | Beam test station onf fast ice |
| | 13:00 | 11:00 | 78 | 10,33 | 20 | 57,91 | | | | | 0 | 0 | 100 | 0 | 0 | 100 | 60 | 95 | 800 | 100 | 10 | | | | | | | |
| | 14:00 | 12:00 | 78 | 10,33 | 20 | 57,91 | | | | | 0 | 0 | 100 | 0 | 0 | 100 | 60 | 95 | 800 | 100 | 10 | | | | | | | |
| | 15:00 | 13:00 | 78 | 10,33 | 20 | 57,91 | | 7 | 320 | -5 | 0 | 0 | 100 | 0 | 0 | 100 | 60 | 95 | 800 | 100 | 10 | | | | | | | |
| | 16:00 | 14:00 | 78 | 10,33 | 20 | 57,91 | | 12 | 214 | -6 | 0 | 0 | 100 | 0 | 0 | 100 | 60 | 95 | 800 | 100 | 10 | | | | | | | leaving station at 16:15 |
| | 17:00 | 15:00 | 78 | 7,21 | 20 | 46,66 | | 6 | 100 | -5 | 9 | 2 | 30 | 4 | 50 | 30 | 150 | 60 | 700 | 581 | 0 | | | | | | | passing yesterdays, heavily ridged ex-polyinya ice |
| | 18:40 | 16:40 | 77 | 55,60 | 20 | 3,27 | | 8 | 120 | -6 | 8 | 2 | 90 | 3 | 10 | 90 | 50 | 60 | 600 | 811 | 10 | | | | | | | |
| | 20:10 | 18:10 | 77 | 42,81 | 19 | 21,81 | | 6 | 107 | -5 | 7 | 2 | 90 | 0 | 10 | 50 | 20 | 50 | 400 | 200 | 0 | 40 | 50 | 60 | 600 | 710 | 10 | |
| 26.03.07 | 13:00 | 11:00 | 76 | 54,71 | 22 | 49,21 | | | | | 10 | | 0 | | | | | | | | | | | | | |
| | 14:15 | 12:15 | 76 | 57,17 | 22 | 59,77 | | 20 | 22 | -5 | 9 | 2 | 50 | 20 | 90 | 300 | 200 | 0 | 40 | 40 | 60 | 400 | 701 | 10 | |
| | 15:15 | 13:15 | 77 | 4,13 | 23 | 25,98 | | 19 | 26 | -6 | 0 | 2 | 90 | 0 | 10Slush | 300 | 200 | 0 | 40 | 60 | 60 | 400 | 701 | 10 | Manoeuver tests |
| | 16:05 | 14:05 | 77 | 6,79 | 23 | 36,54 | | 22 | 35 | -7 | 12 | 2 | 90 | 2 | 20 | 90 | 300 | 200 | 0 | 40 | 60 | 60 | 400 | 701 | 10 | |
| | 17:05 | 15:05 | 77 | 14,40 | 23 | 57,09 | | 19 | 39 | -8 | 12 | 1 | 5 | 50 | 50 | 60 | 400 | 701 | 10 | | | | | | | Just passed edge between cake ice and polynya |
| | 18:50 | 16:50 | 77 | 30,02 | 24 | 42,27 | | 18 | 6 | -8 | 5 | 2 | 90 | 3 | 0 | 20 | 100 | 200 | 0 | 30 | 50 | 60 | 400 | 701 | 10 | |
| 27.03.07 | 9:15 | 7:15 | 78 | 0,53 | 25 | 26,45 | | 12 | 180 | -8 | 0 | 0 | 80 | 3 | 0 | 60 | 600 | 100 | 5 | 10 | 100 | 70 | 500 | 751 | 10 | Drifting with ice at .2 kt NNE |
| | 14:10 | 12:10 | | | | | | 6 | 180 | -6 | | | | | 10 | | | | | | | | | | | Still drifting, changed direction from N to S at 11:30, changed back to N at 17:30 TIDAL drift! |
| 28.03.07 | 9:30 | 7:30 | 78 | 0,13 | 25 | 21,09 | | 10 | 300 | -12 | 6 | 3 | 90 | 2 | 10 | 90 | 60 | 60 | 600 | 721 | 10 | | | | | | | Left Ice station |
| | 10:05 | 8:05 | 78 | 2,54 | 25 | 27,47 | | 10 | 311 | -13 | 6 | 3 | 100 | 1 | 0 | 100 | 60 | 60 | 700 | 711 | 10 | | | | | | | |
| | 11:05 | 9:05 | 78 | 4,40 | 25 | 37,66 | | 10 | 330 | -14 | 0 | 0 | 100 | 1 | 0 | 60 | 40 | 60 | 700 | 100 | 10 | 40 | 60 | 60 | 500 | 721 | 10 | Photos biased, as ship is braking vast floe into tiny pieces |
| | 12:00 | 10:00 | 78 | 4,34 | 25 | 53,27 | | 5 | 338 | -15 | 0 | 3 | 90 | 1 | 0 | 90 | 50 | 60 | 700 | 741 | 10 | | | | | | | |
| | 12:45 | 10:45 | 77 | 57,55 | 25 | 54,71 | | 6 | 260 | | 11 | 2 | 100 | 1 | 0 | 60 | 60 | 60 | 400 | 741 | 10 | 40 | 30 | 90 | 300 | 741 | 5 | |
| | 14:35 | 12:35 | 77 | 46,96 | 26 | 4,72 | | 2 | 213 | -11 | 10 | 2 | 100 | 1 | 0 | 90 | 40 | 60 | 400 | 810 | 10 | 10 | 20 | 90 | 300 | 200 | 0 | |
| | 19:20 | 17:20 | 77 | 2,33 | 25 | 48,49 | | 9 | 125 | -8 | 10 | 2 | 100 | 1 | 0 | 60 | 50 | 60 | 400 | 821 | 10 | 40 | 20 | 90 | 300 | 200 | 0 | |
| | 20:30 | 18:30 | 76 | 49,57 | 25 | 47,26 | | 12 | 120 | -6 | 12 | 2 | 30 | 1 | 50 | 30 | 30 | 60 | 100 | 200 | 10 | | | | | | | Passed from 30% cake + 50% Pancakes into 80% pancake at given latitude, end of obs |